Stellenbosch University

Department of Industrial Engineering

Thermal Management of Moulds and Dies – A Contribution to Improved Design and Manufacture of Tooling for Injection Moulding

A. A. Moammer

Dissertation presented for the degree of Doctor of Philosophy at Stellenbosch University

Promotor: Prof Dimitar Dimitrov

Co-Promotors: Prof Thomas Harms

: Dr Andre van der Merwe

Faculty of Engineering

Department of Industrial Engineering

Department of Mechanical and Mechatronic Engineering

March 2011

DECLARATION

By submitting this dissertation electronically, I declare that the entirety of the work contained therein is my own, original work, that I am the sole author thereof (save to the extent explicitly otherwise stated), that reproduction and publication thereof by Stellenbosch University will not infringe any third party rights and that I have not previously in its entirety or in part submitted it for obtaining any qualification.

Signature: .... Date: .... ”

ACKNOWLEDGEMENTS

In the name of Allah, the Beneficent, the Merciful

I thank Allah (God), who gave me the ability and health to complete this study.

The completion of my Doctor degree and the study is the result of many people's assistance and encouragement. I wish to express my sincere gratitude to all of them.

I would like to express my appreciation to the Principals and lecturers of the Stellenbosch University for making it possible for me to gather information leading to the conclusion of the study.

I wish to express my sincere gratitude to my supervisors, Prof Dimitri Dimitrov, Prof Thomas Harms and Dr Andre van der Merwe whom have provided me with invaluable advice and support for this project. Their example as professors, advisors will stay with me forever.

I appreciate the warmth, encouragement and the support I have received from the staff of Industrial Engineering Department at the Stellenbosch University.

Special thanks go to Rapid Product Development Laboratory especially Mr Philip Hugo and to Institute of Advanced Tooling in the Western Cape especially Mr Kassiem Omer. Also special thanks to USABCO company of South Africa.

I would like to thank my family for their patience and support and the many sacrifices made by them in sustaining both their spirits and mine throughout these expatriate years.

Finally, I appreciate the help and support I have received from the Centre for Research and Technological Studies (Polymer Research Branch) in Libya.

SYNOPSIS

Injection moulding of polymer components is subject to ever increasing demands for improved part quality and production rate. It is widely recognised that the mould cooling strategy employed is crucial to achieving these goals. A brief overview of injection moulding units and different types of injection moulds is given.

The modern Additive Manufacturing (AM) technology for processing metal powders such as Direct Metal Laser Sintering (DMLS) and Selective Laser Melting (SLM) offers almost full freedom to the mould designer. Some of these modern manufacturing methods based on metal powders, which are able to produce complex cooling channels are analysed.

A drastic change has entered the mould design domain - shifting the paradigm from design for manufacture to manufacture for design. In combination with suitable AM methods the concept of surface cooling moulds can now be efficiently implemented.

This study presents a new approach of predicting the minimum cooling time required for the produced part. Different cooling layouts are analysed taking the heat transfer into consideration. The lumped heat capacity method is implemented in this research in order to determine the minimum cooling cycle time required.

A new approach was developed to determine the most suitable cooling layout configuration, such as conventional cooling, conformal cooling or surface cooling, required for a moulded part based on its characteristics such as shape complexity, space available for the cooling layout, part quality requirements, production volume, and product life cycle.

A mould cooling design process including simulation, reverse engineering and manufacturing of the mould insert was implemented in this study.

In order to validate the generic model developed during the course of this research comparative experiments were carried out to determine the difference in performance of injection moulding using conventional or surface cooling methods. The experimental results showed a significant improvement in part quality produced with reduced cycle times using the surface cooling method.

Opsomming

‘Injection Moulding’ van polimeer komponente word al meer gedruk vir verbeterde kwaliteit en vinniger produksie tyd. Dit is orals bekend dat die gietvorm afkoeling strategie ‘n groot rol speel om hierdie twee doelwitte te bereik. Eers word ‘n kort oorslag gegee van ‘Injection Moulding’ eenhede en van verskillende ‘Injection Moulding’ vorms.

Die moderne Aditatiewe Vervaardigingstegnologie vir die prosessering van metaal poeiers soos bv. Direkte Metaal Laser Sintering (DMLS) en Selektiewe Laser Smelting (SLM) bied basies volle vryheid ten opsigte van gietvorm ontwerp. Party van die moderne vervaadigings metodes, wat op metaal poeiers gebaseer is, wat komplekse koelings kanale kan produseer word geanaliseer.

Die ontwerpers arena het ‘n groot verandering ondergaan deurdat die fokus van ontwerp vir vervaardiging verskuif het na vervaardiging vir ontwerp. In kombinasie met toepaslike aditatiewe vervaardigings metodes kan oppervlak verkoeling nou effektief geïmplementeer word.

Hierdie studie bied a nuwe manier om die minimum verkoelings tyd benodig vir ‘n part te voorspel. Verskeie verkoelings uitlegte word geanaliseer waar hitte oordrag in ag geneem word. Die “lumped heat capacity” metode word gebruik om die minimum siklus tyd te bepaal.

‘n Nuwe benadering is ontwikkel om die mees geskikste verkoelings uitleg soos bv. konvensionele verkoeling, konvorme verkoeling of oppervlak verkoeling te bepaal vir ‘n spesifieke part gebaseer op die part se vorm kompleksiteit, spasie beskikbaar vir verkoelings kanale, kwaliteit vereistes en produk lewensiklus.

Die volgende is in die studie geïmplementeer: ‘n vorm verkoelings ontwerp proses met simulasie, ‘reverse engineering’ en vervaardiging van die vorm insetsel.

Om die generiese model te verifieer gedurende die studie is vergelykende eksperimente uitgevoer om die verskil in prestasie te bepaal tussen die gebruik van konvensionele en oppervlak verkoelings metodes. Die eksperimentele resultate het ‘n beduidende verbetering in part kwaliteit getoon met ‘n verkorte siklus tyd tydens die gebruik van die oppervlag verkoelings metode.

TABLE OF CONTENTS

LIST OF FIGURES

LIST OF TABLES

LIST OF ABBREVIATIONS

3D	Three Dimensional
AM	Additive Manufacturing
ANOVA	Analysis of Variance
CAD	Computer Aided Design
CAE	Computer Aided Engineering
CFD	Computational Fluid Dynamics
CMM	Coordinate Measuring Machine
CNC	Computer Numerical Control
DMLS	Direct Metal Laser Sintering
DOE	Design of Experiment
EBM	Electron Beam Melting
EDM	Electrical Discharge Machining
FEA	Finite Element Analysis
FVA	Finite Volume Analysis
HSC	High Speed Cutting
HSM	High Speed Machining
IGES	Initial Graphics Exchange Specification
IR	Infra Red camera
ITER	International Thermonuclear Experimental Reactor
MPA	Moldflow Part Adviser
PP	Polypropylene
RE	Reverse Engineering
RP	Rapid Prototyping
RT	Rapid Tooling
SLM	Selective Laser Melting
SM	Subtractive Manufacturing
3DP	Three-Dimensional Printing

LIST OF SYMBOLS

α	Thermal diffusivity coefficient of the polymer	mm^2/s
μ	Coolant dynamic viscosity	kg/m.s
ν	Kinematic viscosity	m^2/s
ρ_m, ρ_p, ρ_c	Densities of the mould, the plastic part, and the coolant, respectively	kg/mm^3
τ	Mould time constant	s
A	Area of the specimens	mm^2
A_c	Cross-section of the cooling channels	mm^2
A_s	Boundary surface area	mm^2
c_m, c_p, c_c	Specific heat of the mould, the moulded part, and the coolant, respectively	kJ/kg/°C
D	Cooling channel diameter	mm
DF	Degree of freedom	
F	F-test	
FR	Coolant flow rate	l/min
h, h_w	Heat transfer coefficients of mould and water, respectively	W/mm^2 °C
k_A, k_B	Thermal conductivities of materials A and B, respectively	W/°C
K_m	Thermal conductivity of the mould	W/°C
K-Type	Type of thermocouple	
L	Width	mm
l_m	Distance from cooling line to mould wall	mm
l_p	Half the plastic part thickness	mm
MS	Mean of sum of squares	
P_j	Full power of the injection moulding machine	W
p_j	Injection pressure for the moulded part	MPa
P-value	Significance level	
$\dot{Q}$	Heat flow	W/s
R	Thermal resistance	°C/W
R_e	Coolant Reynolds number	

S	Output solution of the decision matrix	
SS	Sum of squares	
t	Time	s
t_i	Time instant	s
t_c	Cooling cycle time	s
t_{cycle}	Cycle time	s
t_f	Injection time	s
T	Temperature	℃
T_c	Coolant temperature	℃
T_e	Polymer ejection temperature	℃
T_i	Temperature at location, *i*	℃
$\overline{T_m}$	Cycle averaged mould temperature at steady state operation	℃
T_m	Mould temperature	℃
T_m (t)	Cycle averaged mould temperature as a function of time	℃
T_{melt}	Polymer melt temperature	℃
T_{m0}	Initial mould temperature	℃
$T_{\infty 1}$, $T_{\infty 2}$	Temperatures of the surrounding media on the two sides	℃
ΔT_c	Coolant temperature difference	℃
ΔT_p	Moulded part temperature difference	℃
ΔT_{pc}	Temperature difference between the moulded part and the coolant	℃
V	Velocity	mm/s
V_S	Volume of the moulded part	mm^3
W	Cooling line pitch distance	mm
W_e	Weight of each variable	g
x	Coordinate distance centre plane of wall normal to the plate surface	
x	Any point in the specimen between 0 and L	
Y	Production hours	
Z	Criteria of moulded part	

1. INTRODUCTION

1.1 Problem Statement

The development of innovative products and their realisation by means of advanced manufacturing methods and process combinations is becoming increasingly a key issue in international competitiveness (Bernard and Fischer, 2002). Shorter product life cycle times demand rapid response and high levels of flexibility in the production of injection moulds.

Typical manufacturing sequences, however, including pre-milling, heat treatment, Electrical Discharge Machining (EDM), and manual finishing are usually associated with high lead times, high machining costs, and limited flexibility. Die and mould makers are therefore increasingly being compelled to utilise modern technologies in their production chains to satisfy their customers' requirements (Dimitrov et al., 2008).

A prime example that offers vast possibilities for substantial performance improvement is the plastic conversion in the packaging industry. According to the common practice, between sixty and ninety percent of the injection moulding cycle time of moulded plastic objects is used to cool the product in the mould to a temperature at which sufficient mechanical strength has been gained to release it from the mould without any substantial distortion (Rännar, 2003).

The main productivity increase, therefore, can be achieved by optimising the cooling cycle. The optimal cooling layout of a mould is usually presumed by the designer. He is, however, restricted to conventional manufacturing processes, such as drilling and EDM. The cooling design is normally influenced by the product geometry, and most often is not considered during the design process of the product itself.

Different cavities are formed differently, and the same type of cooling cannot be used on all moulds. There are certain areas of the mould that need more cooling than others, such as areas where the plastic material is particularly concentrated due to the specifics of the moulding process. These areas become very hot during operation and are the specific areas where adequate cooling must be ensured.

Conventionally, the layout of the cooling channels is done most often empirically, relying solely on the designer's experience. However, the designer is normally not responsible for the cooling performance of the mould, but only for the sturdiness and the mechanical reliability. Therefore he will usually design a mould that is mechanically sound, and then try to arrange the cooling layout accordingly.

Furthermore, traditional manufacturing processes do not allow the freeform fabrication of a cooling layout for production parts that have a complex shape (complicated part features). That is why, in many cases when attempting to reduce cycle time, warpage and non-uniform shrinkage, as a result of high thermal gradients caused by uneven cooling, take place. However, the emergence of Additive Manufacturing (AM) technologies such as Selective Laser Melting (SLM) has demonstrated significant advantages over conventional manufacturing process. The lessons and technologies learned from AM have the potential to redefine the traditional processes such as injection moulding, for short production cycles and superior part quality. Therefore, the problem statement for this research can be summarised as follows:

Currently the conventional manufacturing methods do not offer possibilities for significant cooling performance improvement. Related to this primary problem, the question arises whether AM techniques can substantially improve this situation based on economic criteria.

1.2 Research Objectives

The cooling cycle and cooling quality are affected by several factors, such as melt temperature of the polymer, mould temperature, coolant type, coolant flow rate, coolant temperature, and cooling configuration or layout. All these factors can be optimised except the cooling layout, which is restricted by the manufacturing limitation of complicated cooling configurations.

Conventional tool manufacturing makes use of straight-line cooling channels. This has the disadvantage that the cooling channels cannot, in most cases, follow the part geometry of complex features due to the use of limiting manufacturing methods, as in the example of drilling. This simple method of cooling does not possess the capability to uniformly cool the proposed part, thus limiting the cooling time to the cooling time required for the hottest/thickest area in the part.

In contrast, AM is a technique that can produce cooling channels in an injection moulding tool that closely follow the geometry of the part to be formed. Uniform cooling of a plastic injected part does not only dramatically improve its quality, but can also significantly reduce the total cycle time of the component.

The purpose of this study is therefore to:

- develop a generic model that can predict the acceptable minimum cooling cycle time, thus maximising the productivity and assuring the required quality
- establish a method to help the mould designer to evaluate the cooling layout required for each produced part, while ensuring that the mould cost remains competitive
- validate, experimentally, the proposed methodology of the mould cooling design
- investigate the benefit of implementing the surface cooling method over the conventional cooling method.

1.3 Research Approach

The research approach can be subdivided in the following three steps:

- Develop a generic model to predict the minimum cooling time possible (Chapter 3)

  During this step the influences of the cooling system configuration on the injection moulding process are analysed. In particular, certain aspects of the process such as cooling time and moulded part quality are highlighted. The goal is to develop a generic model to predict the minimum cooling time possible for such moulded part. The analysis approach taken is to give the mould designer an indication of an ideal, minimal cooling time for such moulded part, using a simplistic heat transfer analysis. This would provide a benchmark to compare cooling times derived from more complex heat transfer analysis, e.g. exhaustive numerical heat transfer calculations for complex geometries, or predictions using comprehensive commercial mould design software packages, or even measurements on existing parts. The method would therefore, will give an indication for the *potential* to increase the productivity, with, however, keeping in mind the quality requirements.

- Develop a cooling design evaluation model (Chapter 4)

  The second step aims at the development of a methodology to evaluate the moulded part based on its characteristics such as geometrical issues, quality perspective and cost-efficiencies. Thus the manufacturing process capabilities and costs were considered in the evaluation model. This evaluation model can help the mould designer to choose the best cooling layout for the moulded part to achieve the optimum cooling time.

- Experimental validation of the proposed methodology (Chapter 6)

  During the third step the proposed methodology is validated experimentally. It was implemented and investigated using an industrial case study. The results of the experiments included the analysis of the quality measurements and temperature behaviour of the moulded parts. The real life case study allowed to demonstrate successfully, how the approach proposed could be employed to optimise the production process.

2. OVERVIEW OF INJECTION MOULDS

Injection moulding is one of the most important processes used to manufacture plastic products. Today, more than one third of all thermoplastic materials are injection moulded, and more than half of all polymer processing equipment is for injection moulding. The injection moulding process is ideally suited to manufacture mass-produced parts of complex shapes that require precise dimensions (Rees, 2002).

An injection moulding system consists of the machine and the mould for converting the raw thermoplastic material, usually in the form of pellets, into a part of desired shape and configuration.

2.1 Injection Moulding Machine

An injection moulding machine consists basically of four different elements (Figure 2.1):

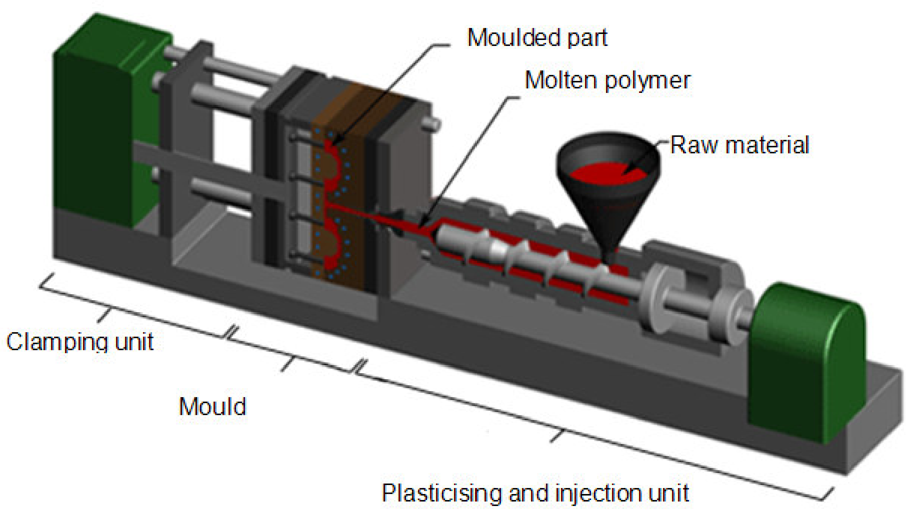

Figure 2.1: Schematic view of an injection moulding machine (CustomPartNet, 2007)

2.1.1 Injection unit

The injection unit has major tasks: to melt the pellets (polymer), to accumulate the melt in the screw chamber, to inject the melt into the mould (cavity), and to maintain the packing (holding) pressure during the cooling.

The injection units are usually rated with two numbers. The first is the shot capacity, defined as the maximum volume of polymer that can be displaced by one forward stroke of the injection plunger or screw. The second is the plasticising rate, which is the amount of material that can be plasticised into molten form by heating in the cylinder of the machine in a given time.

2.1.2 Clamping unit

The clamping unit has three functions: to open and close the mould halves, to eject the part, and to hold the mould closed with sufficient force to resist the melt pressure inside the mould as it is filled. Modern injection moulding machines use one of the three main clamping types: mechanical, hydraulic, or a combination of the two.

Mechanical toggle design

This design (Figure 2.2) utilises the mechanical advantage of a linkage to develop the force required to hold the mould during the injection of the material (Rees, 2002). Mechanical toggle clamps have very fast closing and opening action, and are lower in cost than other systems. However, the toggle mechanism only transmits its maximum closing force when the system is fully extended. The big disadvantage is that the clamp force is not precisely controlled; therefore these clamps are only used for smaller machines.

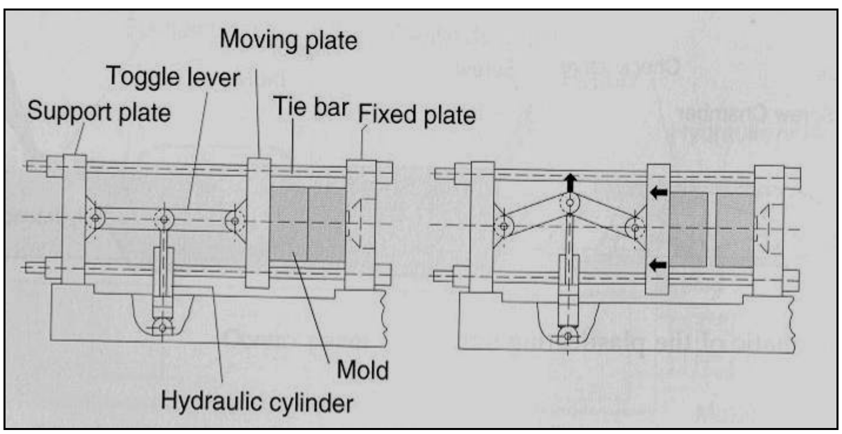

Figure 2.2: Generic mechanical toggle design (Osswald et al., 2002)

Hydraulic clamp units

The hydraulic system shown in Figure 2.3 uses hydraulic pressure to open and close the clamp and to develop the force required to hold the mould closed during the filling phase of the cycle (Rees, 2002). This type of design is characterised by long term reliability and precise control of the clamping force, but the process is relatively slow and expensive compared to the toggle clamp systems.

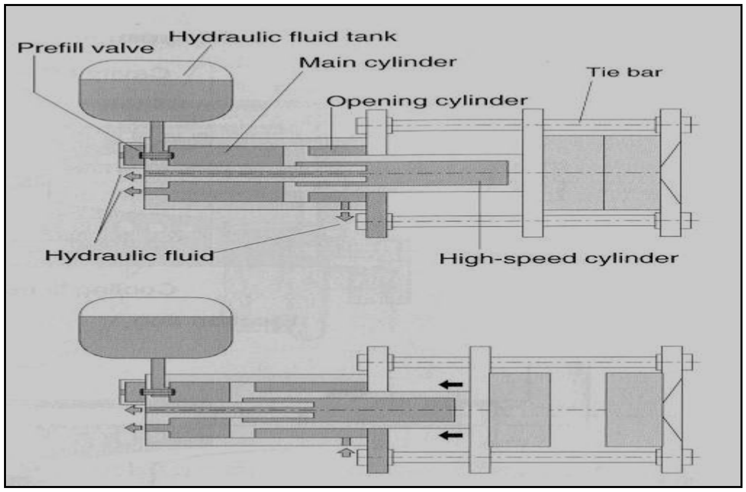

Figure 2.3: Generic hydraulic mould closing design (Osswald et al., 2002)

2.1.3 Mould

The mould is the central point of the injection moulding machine. Figure 2.4 shows the essential elements of an injection mould such as sprue, gate, runner, mould cavity, cooling system and ejector system.

Moulds for injection moulding are as varied in design, degree of complexity, and size as are the parts produced by them. The main objective of the mould is basically to form the desired shape of the plasticised polymer and then cool the moulded part.

In the injection mould the molten polymer is injected through the sprue. In multicavity moulds, the sprue feeds the polymer melt to a runner system, which leads into each mould cavity through a gate.

The core forms the inside configuration of the produced part and the cavity forms the outside of the produced part.

The most common types of moulds used in industry today are two-plate moulds, three-plate moulds, side-action moulds, and unscrewing moulds as explained below.

Two-plate mould type

A two-plate mould (Figure 2.4) consists of two active plates (cavity and core plates). Moulds of this type with a cold runner system, the sprue, runners and gates solidify with the part being moulded, and are ejected as a single connected item.

Today, most of the two-plate mould types use the hot runner system, which is essentially a heated extension of the machine nozzle built into the mould. The purpose is to dislodge off the often large plastic mass in the sprue that is slow to cool and also increases the moulding cycle.

The two-plate moulds have one parting line, and one opening direction. This type of moulds is capable of producing all kinds of parts that do not have an undercut, or inner and outer screw.

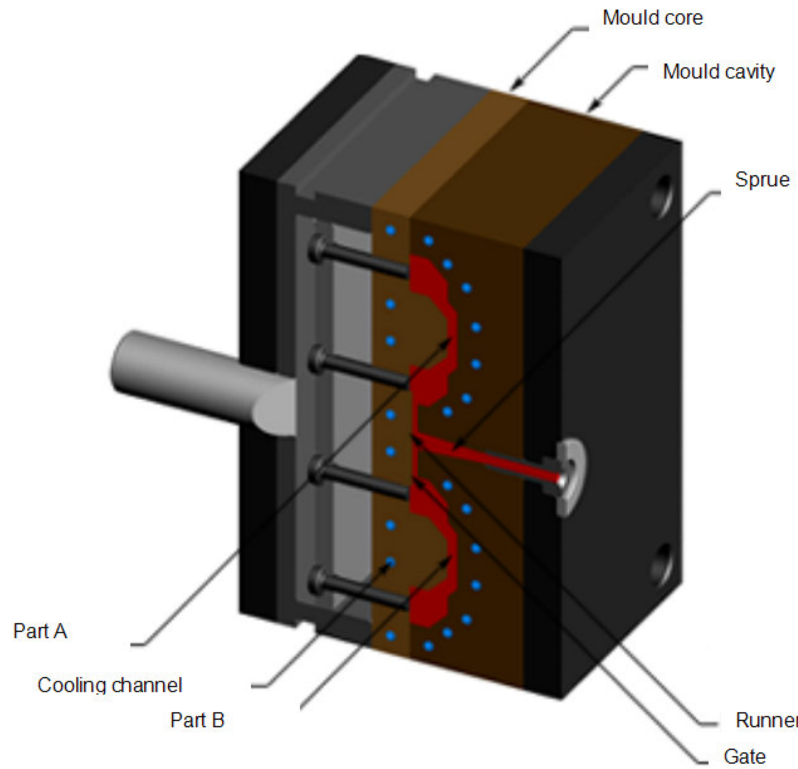

Figure 2.4: An injection two-plate mould (CustomPartNet, 2007)

Three-plate mould type

The three-plate mould (Figure 2.5) consists of

- stationary or runner plate, which contains the sprue and half of the runner
- middle or cavity plate, which contains the other half of the runner, the gates and cavities
- movable or core plate, which contains the cores and the ejector system.

The primary advantage of the three-plate mould with cold runner over the two-plate cold runner mould is that gating is now no longer limited to the perimeter of the part cavity. Another benefit of this type of mould is associated with the multicavity moulds, when the cavities can be positioned closer to each other, because there is no need to provide space between them for sprue and runners. Therefore, there is more space for other mould items such as ejector pins and cooling channels.

Slide mould type

The slide mould design (Figure 2.6) is similar to the two-plate mould but with slides and cam pins for additional lateral movement. The slide moulds are used in moulding components with undercuts or external threads.

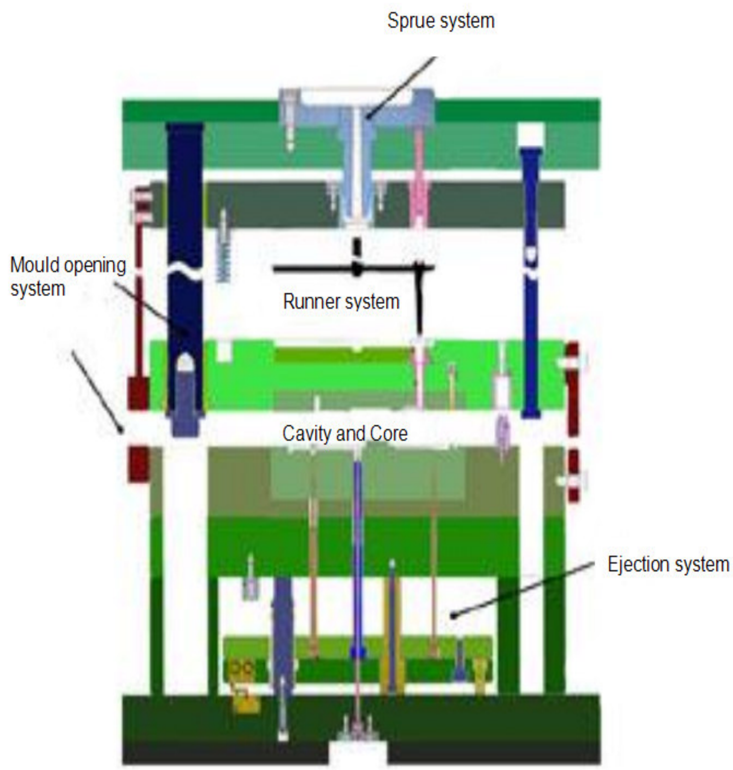

Figure 2.5: An injection three-plate mould (Sharon, 2009)

Split cavity mould type

Split cavity mould design (Figure 2.7) is similar to the two-plate mould but with a split cavity block for mouldings with undercuts or external threads.

Unscrewing mould type

The unscrewing mould is the most common method used to free the undercuts formed by internal or external threads. A gear rack moved by a hydraulic cylinder engages with a super gear attached to the threaded core pin (Pye, 2000).

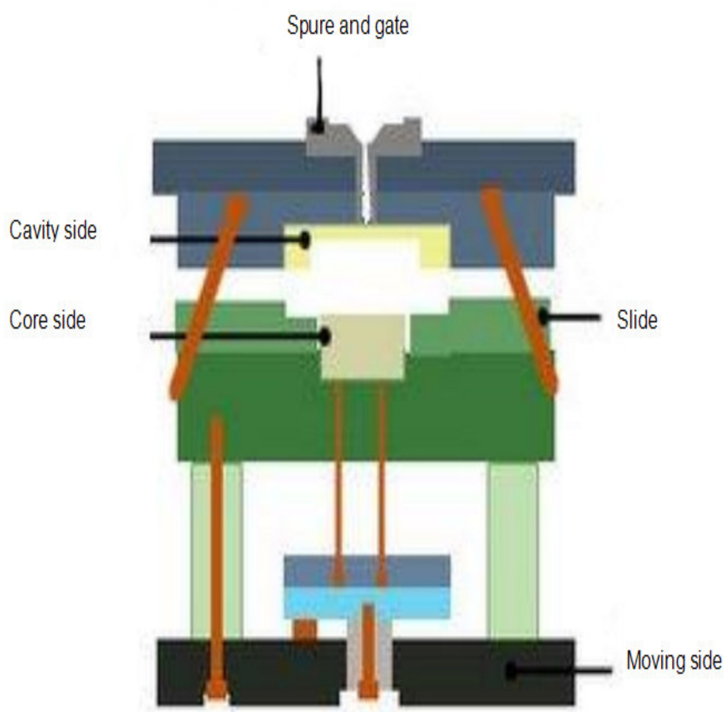

Figure 2.6: An injection slide mould (Sharon, 2009)

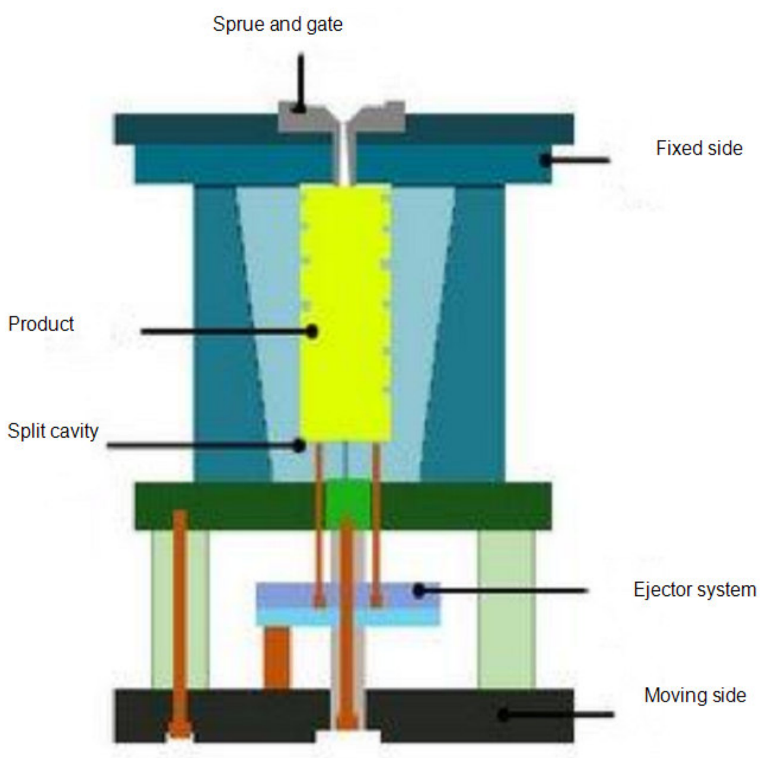

Figure 2.7: An injection split cavity mould (Sharon, 2009)

2.2 Cost of Moulded Part

Generally the cost of an injection moulded part is significantly affected by the production volume, and is closely related to the productivity achieved. Reducing the part cycle time leads to productivity improvement and delivery of the required production volume in a shorter time. This effectively means freeing up of additional production capacity.

The part cost is a function of direct costs, including material, direct labour, and mould or other tooling that is required to produce the parts. Indirect costs include the building expenses, equipment, and support staff.

In the case of production volume, an hourly rate is assigned to each of the injection moulding machines according to its cost. This is typically reflected by the size of the machine.

The main factors that influence the part cost are the following (Osswald et al., 2002):

2.2.1 Material cost

The cost of the moulded part depends on the part weight and the material cost:

Material cost per part = part weight (g) x material cost ($)

2.2.2 Production cost

The production cost depends on how many parts are produced per hour, the cost of the labour and the production cost.

Parts per hour = (3600/moulding cycle(s)) x number of cavities

Production cost per part = (machine rate cost ($/hour) + labour cost ($/hour))/(parts per hour)

2.2.3 Mould cost per part

The total mould cost must include the mould cost plus the interest rate. To determine the total cost per part, the total cost of the mould divided by the total production over the years for which the total mould cost will be amortised.

Tooling cost per part = total cost ($)/(annual production (parts/year) x number of years amortised)

Thus the total cost of the injection moulded part is:

Total cost = (material cost per part + production cost per part + tool cost per part) x production yield (%)

The production yield is defined as the percentage of acceptable quality parts produced in a given period of time relative to total production.

2.3 Mould Making Techniques

Injection moulds are made by many different processes and combinations. A steel cavity is normally preferred due to its durability. In order to manufacture the injection mould conventionally the designer must follow the rules of design for manufacturing.

The design for manufacture is particularly important for moulded parts because the cost and quality of the parts manufactured are highly geometry dependent. Moulding processes such as injection moulding are extremely flexible and can be used to manufacture products with a wide range of styled or aerodynamic curved shapes.

The limitations of moulding processes are mostly due to the behaviour of the molten material as it fills and cools in the mould. The mould cooling requirements for example, make specific demands on the designer, and a complicated geometrical part with a complicated cooling channel layout may be impossible to manufacture with subtractive manufacturing technologies.

However, the AM technologies, which create parts in a layered way, have given designers an opportunity to produce complex parts even with complicated cooling channel layouts. Many Rapid Prototyping (RP) and Rapid Tooling (RT) technologies based on layer-by-layer manufacturing have been developed in the last decade (Levy et al., 2003, Rännar et al., 2007, Ryder et al., 2002).

Today, the greatest opportunities and efforts are in the direct manufacture of long-term consistent metal parts. The competitive advantage of this technology is geometrical freedom.

Some issues related to this technology are materials limitation, accuracy, advanced Computer Aided Design (CAD) software, and high production cost comparing to the SM technology (Levy et al., 2003).

Therefore, the designer is no longer restricted by the same rules of design for manufacturing by taking the capability of the following possibilities into consideration:

2.3.1 Subtractive manufacturing technologies

Subtractive Manufacturing (SM) means that material is removed from a solid block of metal. The SM processes usually used to manufacture moulds include the following:

- Conventional milling and drilling/boring
- Computer Numerical Control (CNC) milling and drilling/boring
    - Normal (3,4 and 5 axis)
    - High Speed Machining (3, 4 & 5 axis)
- Electrical Discharge Machining (EDM)

    - Spark erosion
    - Wire cutting
- Turning
    - Conventional
    - CNC

High Performance/High Speed Machining (HPM/HSM)

With the HPM/HSM methods it is relatively quick to produce a mould. HSM produces a good quality product with a high accuracy. High performance milling is especially effective, because it can be used to cut into hardened materials; cutting inserts for cutting tooling steel of up to 65 Rockwell are available (Voha, 2005). Previously much slower spark eroding process was used.

The advantage of HSM is particularly the good surface finish, thus reducing the hand finishing required in polishing the cavity/core.

The major disadvantages of SM are that an area must be reachable in order to be machined. Thus drilled holes must be straight and undercuts kept within the machining capability limits. Here the 5-axis machining brings a particular advantage.

Electrical Discharge Machining

Electrical discharge machining is a reproducing subtractive process, which uses the material removing effect of short, successive electric discharges in a dielectric fluid (hydrocarbons) that is electrically conductive, but has a fairly low high flash point to prevent combustion that would otherwise set the machine alight. The fluid also has the function of flushing away the burnt carbon deposits to prevent electrical arcing.

This technique can be used to machine a work piece with complex geometric shape, the smallest of internal radii, and deep grooves (slots). The machine has variable settings to produce different rates of material removal, for rough to smooth surface finishes. Through judicious selection of the process parameters, far greater removal can be made to occur at the work piece than at the tool, allowing the process to be economically viable.

The EDM machine produces a pulsing current that gradually erodes the metal, to produce the corresponding shape of the electrode. Once the required depth is obtained, the machine automatically comes to rest. The electrode is retracted and the work piece can be removed for the next process.

Many factors affect the time taken to remove material by the EDM process, for example:

- The volume of material to be removed

- The complexity of the shape to be achieved
- The required surface finish
- The choice of machine settings used by the machine operator
- The availability of both rougher and finisher electrodes.

Good surface quality of the injection moulds is required; therefore, several electrodes are used for roughing and finishing the cavity walls. It is possible to achieve a surface smoothness to within an accuracy of 1 µm or less, with roughness heights of 0.1 µm (Menges et al., 2000).

2.3.2 Additive manufacturing technologies

The additive manufacturing technology provides a viable alternative to SM processes and metal casting for some applications. Various AM technologies are used to produce metal parts and tooling. The competitive advantage of AM technology is geometrical freedom. AM technology is applied in a wide variety of industries, from aerospace and motorsports to medical implants and dentistry (Ding et al., 2004, Gibbons and Hansell, 2005, Khainga et al., 2001, King and Tansey, 2002, King and Tansey, 2003, Morrow et al., 2007, ÓDonnchadha and Tansey, 2004, Simchi, 2006, Simchi et al., 2003, Zhang et al., 2003, Zhong et al., 2004, Zhu et al., 2003).

Additive manufacturing technologies allow for the greatest flexibility when designing the cooling of a mould. The advantage achieved is that the cooling channels can be incorporated into the 3D model as it is built. Some of the AM technologies used in mould manufacturing are the following (Wohlers, 2009):

- 3D Printing (3DP)
- Electron Beam Melting (EBM)
- Direct Metal Laser Sintering (DMLS)
- Selective Laser Melting (SLM)
- LaserCusing

3D Printing (ProMetal)

The 3D printing process is continuously building up material, layer by layer, until a complete model (green part) is obtained. However, the green part is still easily broken for direct use and requires two further operations, burning out the polymeric binder and infiltrating with an alloy to achieve a dense part. It is reported that injection moulds has been made from stainless steel powder (316L) using 3D printing process (Sachs et al., 2000). When using the 3DP technique, the installation of conformal cooling channels lead to reduced cooling times, and thus also cycle times.

The manufacturing of conformal cooling with 3DP presents several challenges. The loose powder within the channels must be removed. This presents a constraint on the length and diameter of the channels as well as a challenge in determining the point of completion of the powder removal operation. Porosity can also present challenges. There are also some issues associated with the material's properties, such as hardness and toughness (Xu, 1999).

Electron Beam Melting

The EBM system was developed by Arcam (Mumtaz et al., 2008). The EBM machine reads in data from a three-dimensional CAD model and lays down successive layers of powdered material, and in this way builds up the model. The method is similar to laser sintering in that it fuses metal powder to form objects. However, the EBM permits the direct fabrication of metal powder to 100% solidity (non porous) (Wohlers, 2007).

The EBM technology can be used to manufacture parts by melting metal powder using an electron beam in a high vacuum. Unlike some metal sintering techniques, the parts are void free, and extremely strong. The surface of the parts is relatively rough and may require finishing by CNC machining or another method, depending upon the intended application. Different materials can be processed, such as titanium, cobalt-chrome and other.

The EBM technology can be used to make injection moulds with conformal cooling channels. A minimum channel width of 5 mm and curvature radius of 10 mm are recommended in order to obtain cooling channels that can be cleaned fairly easy (Rännar et al., 2007, Villalon, 2005) Figure 2.8 shows a part produced by EBM with different widths of cooling channels.

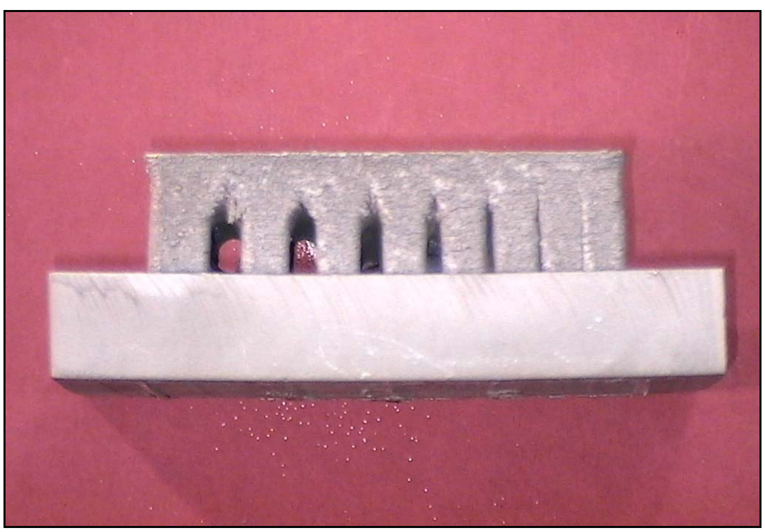

Figure 2.8: Example – a part produced by EBM (Villalon, 2005)

Direct Metal Laser Sintering

This method uses a polymer coated metal powder, which is melted together in the shape of the CAD model, using a laser beam. The heat from the laser melts the polymer and forms the bond between the powder particles. The part is then sintered in an oven and an infiltrant such as bronze is used to ensure that the density of the piece reaches 100%. Some finishing operations will typically be necessary in order to ensure that the surface quality meets the requirements. Figure 2.9 shows as an example a tool insert produced by the DMLS method with conformal cooling channels.

There are few advantages of the DMLS process over more traditional methods, including:

- The ability to create multiple parts simultaneously in one manufacturing run
- Operation of the machine unattended 24 hours a day
- The ability to create conformal cooling lines in the tool.

However, there are also some disadvantages including:

- Requirement for post processing such as polishing and infiltration with a low melting bronze alloy
- Limitation of producing different cooling channels shapes
- Difficulty of removal of the powder from small cooling channels.

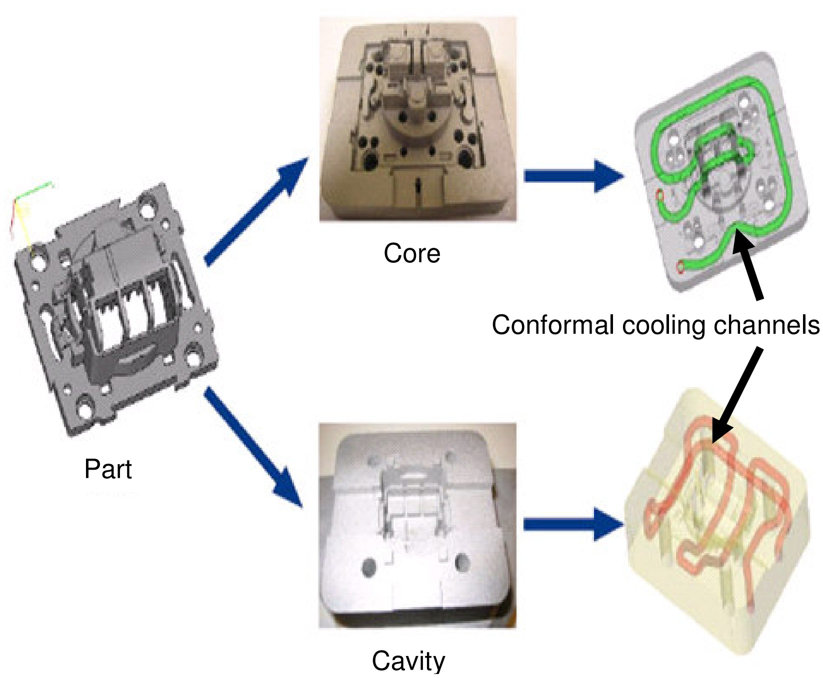

Figure 2.9: DMLS insert with conformal cooling channels (EOS, 2009)

Selective Laser Melting

The SLM method has been presented by a number of authors (Abe et al., 2001, Kruth et al., 2007, Matsumoto et al., 2002, Mumtaz et al., 2008, Osakada and Shiomi, 2006, Kruth et al., 2005). This process uses a high energy laser to melt the powder particles together. The part then reaches almost a 100% dense microstructure without additional infiltration being required.

The SLM process has the possibility to process standard materials, e.g. stainless steel 316L, 17-4PH and others, hot work steel (1.2709, 1.2344), titanium, different aluminium and cobalt-and nickel-based alloys (Brinksmeier et al., 2010).

The layer thickness resulting from this process is about 30 – 50 µm, which ensures a relatively good surface finish with little layering effect. For mirror finish parts, however, additional surface preparation is still required.

During the process the metal powder (e.g. stainless steel 1.4404) is locally melted by an intensive infrared laser beam that traces the layer geometry. It is possible to build the finest details, like thin vertical walls of less than 100 µm thickness. Directly after the production process the manufactured parts show a surface roughness of approximately 10–30 µm.

Performance and limitations of the SLM technology for fabrication of elements of cooling systems in International Thermonuclear Experimental Reactor (ITER) installations were analysed (Yadroitsev et al., 2007). The study showed the possibility of using SLM technology for creating complex shapes. One of the principle criteria is the accuracy of fabrication with respect to the desired dimensions of the final product. Conformal cooling channels can be positioned as close as 0.5 mm to the cavity surface (SLM, 2008).

LaserCusing

This technology has been developed by the German company Concept Laser. The term **C**using is a combination of the words ‘fusing’ and the name of the process developer **C**oncept Laser GmbH. In this process, like the SLM, LaserCusing completely melts a steel powder (e.g. stainless steel powder) layer-by-layer to produce a 100% component density. A specially developed exposure strategy allows the generation of solid material and large-volume components without any deformation. A variable focus diameter laser guarantees a rapid component construction despite even the most filigree of cavities and very sharp contours. A patented surface post-treatment process applied directly after the construction process ensures the highest surface quality and hardness. Several moulds for injection moulding and die casting have already been realised using this technology, showing excellent results.

Of particular interest is the surface cooling concept, assuring the manufacture of mould inserts with contour equivalent mould surface. The typical surface cooling geometry has a honeycomb structure, as shown in Figure 2.10 which closely follows the cavity surface at a depth of approximately 2.5 mm (LaserCusing, 2009).

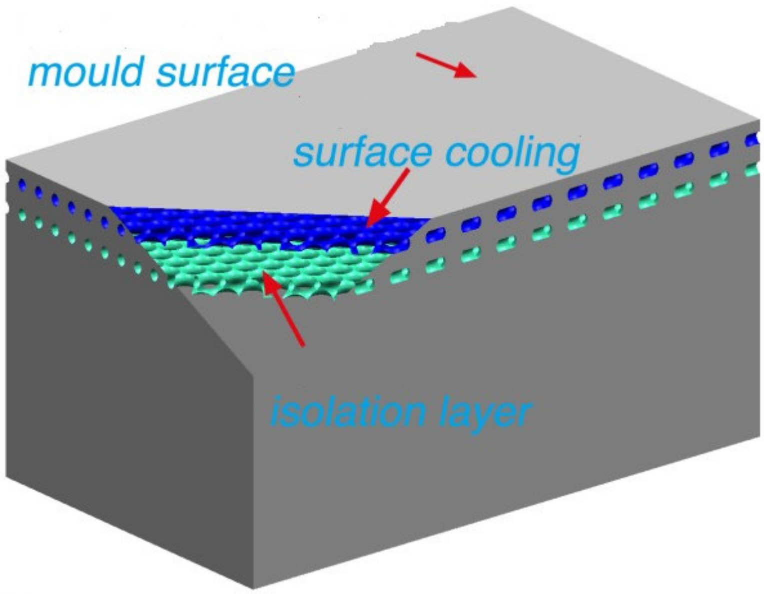

Figure 2.10: Honeycomb cooling structure (LaserCusing, 2009)

2.4 Conclusion

This chapter comprised an overview of injection moulds, including injection moulding machine, cost of moulded part, and mould making techniques. The mould making techniques were classified as SM and AM. The main advantage of the AM technologies is the freedom to create complex geometries, however, the SM technologies has the capability to produce massive parts with high speed. An appropriate combination of these two types of process can lead to best results in mould manufacture. Some benefits of AM and SM are summarised below:

AM technologies	SM Technologies
1. Freedom to create complex geometries	1. High production speed for massive parts
2. Excellent material properties	2. High surface quality and precision
3. Variable material composition	3. All machinable materials
4. Minimal material consumption	4. Common technology

3. THEORETICAL CONSIDERATIONS AND APPARATUS

3.1 Injection Moulding Cycle

The point of departure of the following considerations is the injection moulding cycle. The main steps involved in this cycle are the following:

- Closing the mould
- Moving injection unit forward (plunger or screw)
- Inject the hot molten plastic into the cavity (filling)
- Keep the mould closed and under pressure until the plastic has solidified sufficiently for ejection (packing)
- Moving injection unit backward (plunger or screw)
- Plasticise the material for next shot
- Open the mould
- Eject the finished part.

In time terms, these steps are illustrated in Figure 3.1. The injection cycle begins when the mould closes, this is followed by the injection of the material in its molten state into the mould cavity, and subjection to rapid cooling from the mould wall on the one hand and internal shear heating on the other. The polymer melt then undergoes solidification under the high packing and holding pressure of the injection system. Once the part is sufficiently cool the mould is opened and the part is ejected. The machine is then reset for the next cycle to begin.

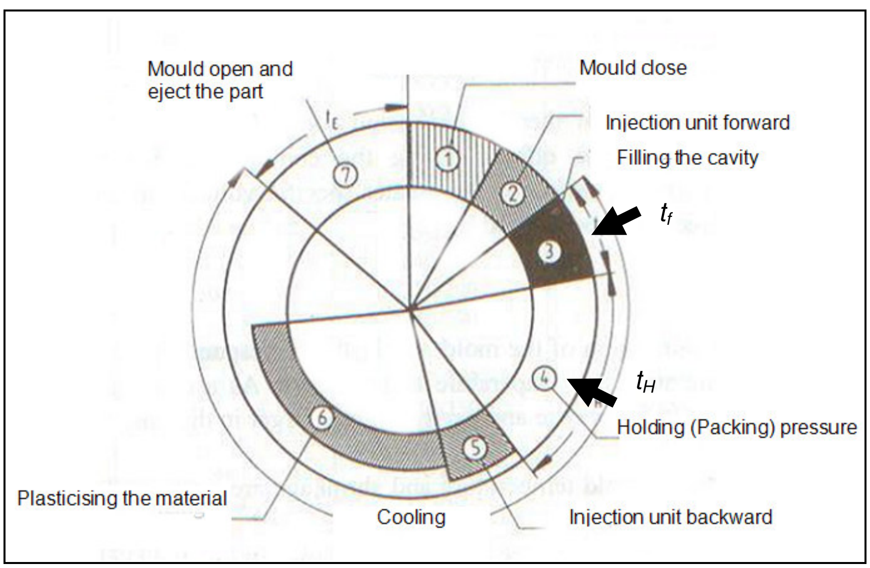

Figure 3.1: Injection moulding cycle (Osswald et al., 2002)

On the pressure/time axes, the moulding cycle can be effectively divided into three separate stages (Figure 3.2): injection (filling) stage, cooling stage and mould ejection and resting stage.

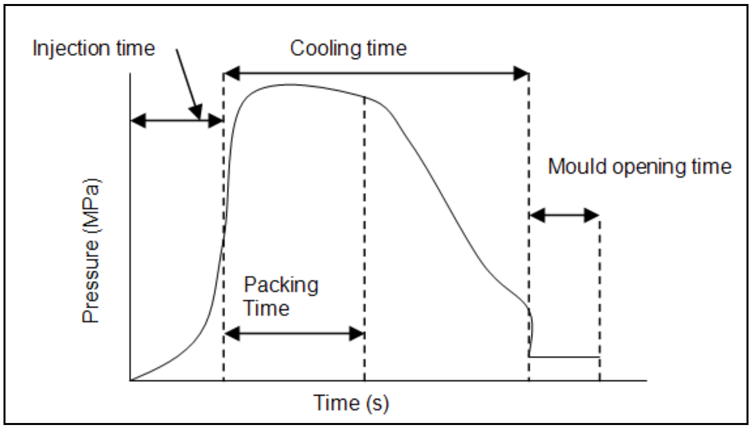

Figure 3.2: Mould cycle stages (Boothroyd et al., 2002)

3.1.1 Injection (filling) stage

In this stage the plastic material is first heated to the molten state and plasticised before the filling process. Under high pressure, the screw plunges forward to inject the plastic into the mould. The plastic flows through the nozzle and into the sprue, and then into the mould cavity.

The packing phase begins when the filling of the mould cavity is complete. This involves further application of pressure to the material in an attempt to pack more material into the cavity, in order to ensure uniform shrinkage, and consequently reduce component warpage.

Figure 3.3 shows the difference between the end of the filling phase (left image) and the end of the packing phase (right image). At the end of the packing phase (right image) there are more polymer chains.

Figure 3.3: Illustration of the end of the filling and packing phases (Moldflow, 2005)

The estimation of the injection time requires an extremely difficult analysis of the polymer flow as it flows through the runners, gates and the cavity. Boothroyd et al. (2002) estimated the injection time (t_f) as shown in the equation (3.1):

$$t_f = 2V\, P_j \,/\, p_j \qquad (3.1)$$

where V is the volume of the molten polymer (m^3), P_j is the full power of the injection moulding machine (Watt) and p_j is the recommended injection pressure for the moulded polymer (N/m^2).

In general, the typical injection time is 1–10% of the total cycle time, depending on the wall thickness of the part and the injection unit power of the machine.

3.1.2 Cooling stage

Cooling starts after the first rapid filling of the cavity and continues during packing (Figure 3.2). Normally the number of injection cycles per hour is used as an indicator of the mould's performance. During the cooling time the machine does not move, the mould is in a closed state, and the part is in the solidification phase. The part must be then cooled to a temperature at which it will have sufficient structural strength to be ejected. If, however, the required product quality is not met or is inconsistent, the simplest way of improving it would be to increase the cooling time, thus increasing the total cycle time, but leading to a decrease in productivity.

In practice, the time spent on cooling can easily reach 60% and comprise as much as 90% of the total cycle time. Obviously, if this time can be reduced it will add directly to the production capacity of the machine.

The injection moulding machine can be seen as a production system, in which the mould is one of its subsystems. Among its various tasks, the injection mould acts as a heat exchanger (Beaumont et al., 2002). A number of factors directly influence its efficiency in this task, the most important being the mould material, coolant, coolant temperature, and cooling configuration. Depending on the component to be produced as well as on certain related conditions, the tool designer selects the appropriate mould material, coolant, and suitable coolant temperature. These choices are pre-determined in many cases. Of these four factors only the cooling configuration is subjective, and can vary substantially depending on the mould designer's experience and capabilities, as well as on available manufacturing methods.

3.1.3 Mould ejection and resetting stage

During this stage the mould is opened, the part is ejected, and the mould is closed again for the next cycle to begin. Although it is economical to have quick opening and closing of the mould, rapid movement may cause undue strain on the equipment, and when mould faces come into contact at speed the edges of the cavities can be damaged.

The closing and the ejection times can last from a fraction of second to a few seconds, depending on the size of mould and machine. The adequate time for the mould ejection must allow the part to fall free of the moving side of the mould, which depends on the part dimension. After resetting, the mould is closed and locked, thus completing one cycle.

3.2 Heat Flow

3.2.1 General

The injection mould temperature, usually already specified by the raw material manufacturer, should be reached as quickly as possible at the start of production, remain constant over a long period, and be the same at all points of the cavity surface (Dimitrov et al., 2008).

Mould cooling analysis and optimisation are receiving considerable attention. Comprehensive studies were undertaken to predict the temperature behaviour for the mould and the part during the cooling stage (Li et al., 2005, Nylund and Meinander, 2005, Park and Kwon, 1998, Smith et al., 2008, Tang et al., 1997, Tang et al., 2006, Weidenfeller et al., 2005). There are many factors that have to be considered when calculating the optimum cooling design in order to reduce the cycle time and obtain high part quality, such as:

- The temperature difference between the inlet and outlet water
- The volume flow of the water
- The thermal properties of the moulded part
- The type of runner system (hot or cold)
- The shape of the cooling channel.

The heat flow in a mould system is characterised by two main phenomena: conduction and convection. Heat conduction is the transfer of energy from the more energetic particles of a substance to the adjacent particles (Çengel and Yunus, 2003), thus the transfer of energy in a medium, typically in the mould material or in the plastic being cooled.

Convection is the mode of heat transfer between a solid (the mould) and an adjacent fluid (cooling water) or gas, which is in motion (flowing). Convection combines the effects of conduction and motion.

3.2.2 Conduction

Conduction is the transfer of energy from the energetic particles of a substance to the adjacent, less energetic ones as a result of interactions between the particles. The rate of heat conduction

$\dot{Q}$ through a medium depends on the geometry of the medium, its thickness, the material of the medium, and the temperature difference across the medium (Figure 3.4).

The type of material used to manufacture a mould greatly influences the cooling time. Taking steel as an example, its thermal conductivity is much lower than that of aluminium. This means that steel will conduct less heat (measured in Watt) than aluminium under the same conditions.

One might then ask: why do we not manufacture all moulds from a metal with a very high thermal conductivity? Steel is a much stronger material than aluminium; it can tolerate a high injection pressure and hence guarantee many more cycles than a softer or weaker material. A softer material can nonetheless be used in low volume production. The type of material used to manufacture the product influences the cooling as much as the mould material. Each plastic has a specific thermal conductivity and heat capacity, which influences the heat flow, and which in turn influences the cycle time.

There is also a boundary layer between the mould and the coolant. This boundary layer is influenced by several factors: the velocity, water turbulence and the scale build up on the surface in the water channels are the most important.

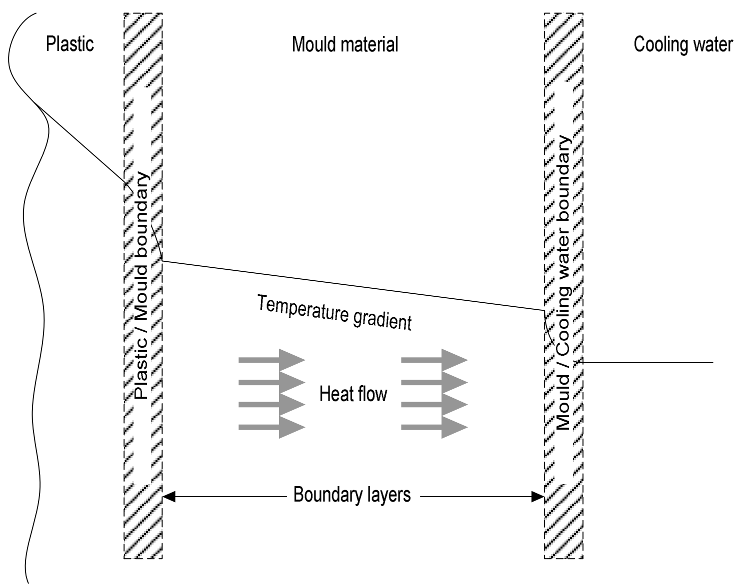

Figure 3.4: Heat flow in a mould across boundary layers (Çengel and Yunus, 2003)

3.2.3 Surface boundary conditions

A surface cannot store any energy because it does not have any thickness or mass. Therefore, if two surfaces are in contact they will have the same temperature at the point of contact (Figure 3.5).

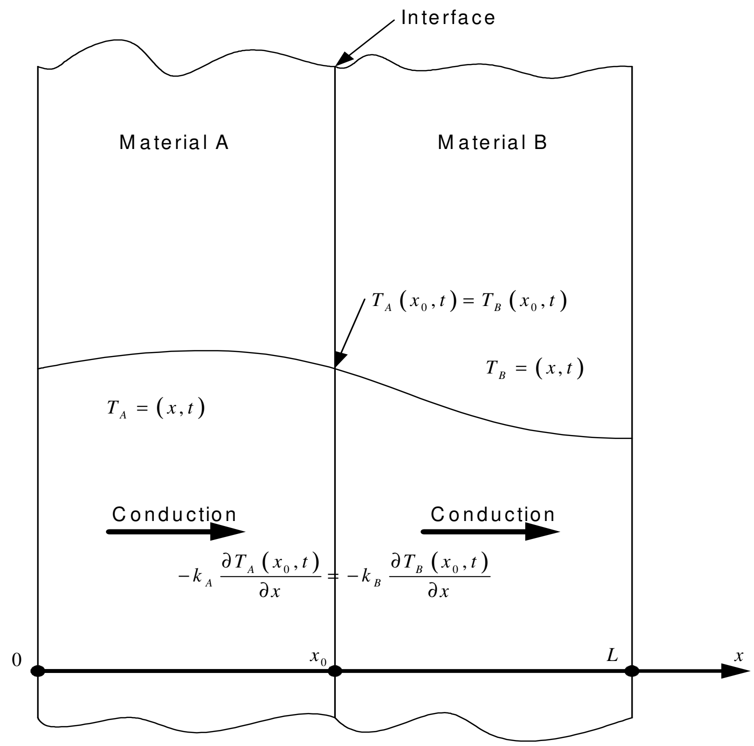

Figure 3.5: Interface boundary condition (Çengel and Yunus, 2003)

The values of k_A and k_B are the thermal conductivities of materials A and B, respectively, where $T_A(x_0,t)$ is the temperature of specimen A at distance x_0 at time t, and $T_B(x_0,t)$ is the temperature of specimen B at distance x_0 and time t. L is the total width of the combined specimen.

3.2.4 Convection

Convection is probably the most common boundary condition found in practice, since most heat transfer surfaces are exposed to the environment. The convection boundary is based on the surface energy balance expressed as follows (Çengel and Yunus, 2003):

$$\left\{\begin{array}{c}\text{Heat conduction at the surface in} \\ \text{a selected direction.}\end{array}\right\} = \left\{\begin{array}{c}\text{Heat convection at the surface in the} \\ \text{same direction.}\end{array}\right\}$$

According to Cengel and Yunus (2003) the heat flow through a plate can be expressed by equations (3.2) and (3.3), as shown in Figure 3.6:

$$-k.\frac{\partial T(0,t)}{\partial x} = h_1[T_{\infty 1} - T(0,t)] \tag{3.2}$$

$$-k.\frac{\partial T(L,t)}{\partial x} = h_2[T(L,t) - T_{\infty 2}] \tag{3.3}$$

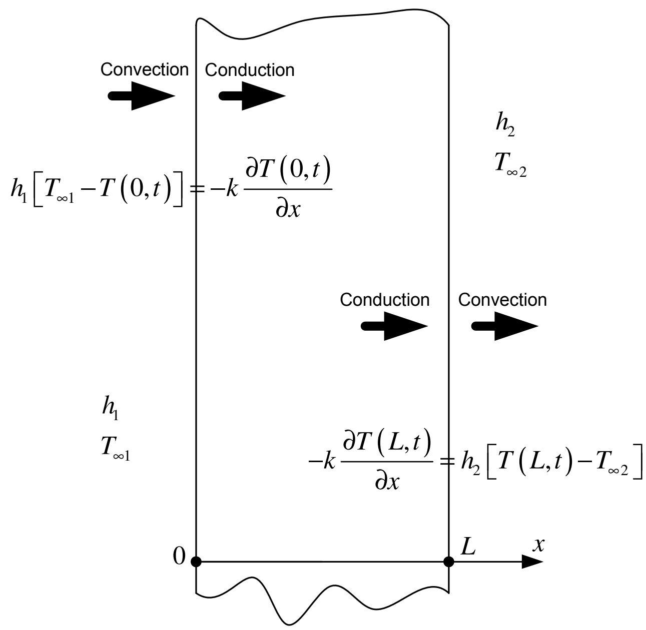

Figure 3.6: Convection boundary condition on two surfaces (Çengel and Yunus, 2003)

where h_1 and h_2 are heat transfer coefficients, and $T_{\infty 1}$ and $T_{\infty 2}$ are temperatures of the surrounding mediums on the two sides of the plate. The thermal conductivity of the specimen is given by *k*. L is the width of the specimen, x is any point in the specimen between 0 and L, and t_i is an instant in time.

3.2.5 Thermal resistance network

The heat flowing in a mould from the mould cavity to the cooling channels can be seen as one-dimensional. The temperature difference between the plastic and the water is the greatest; therefore the heat will flow in a straight line along the shortest route between these two entities. The heat flow can be described as shown in Figure 3.7.

Explained in words it means:

$$\left\{\begin{array}{c}\text{Rate of heat}\\ \text{convection into}\\ \text{the wall}\end{array}\right\} = \left\{\begin{array}{c}\text{Rate of heat}\\ \text{conduction}\\ \text{through the wall}\end{array}\right\} = \left\{\begin{array}{c}\text{Rate of heat}\\ \text{convection}\\ \text{from the wall}\end{array}\right\}$$

The heat flow is given by $\dot{Q}$ and equation (3.4) gives the total heat that will flow (Figure 3.7). The values of R represent thermal resistance, L is the width and A is the area of the specimens. The values of *k* represent the conductivity coefficient and the values of *h* represent the convection coefficient of the different specimens.

$$\dot{Q}=h_1A\left(T_{\infty 1}-T_1\right)=k_1A\frac{T_1-T_2}{L_1}=k_2A\frac{T_3-T_2}{L_2}=h_2A\left(T_3-T_{\infty 2}\right) \tag{3.4}$$

This equation can be rearranged to specifically show the influence of the thermal resistance factor on the heat flow (Figure 3.7):

$$\dot{Q} = \frac{(T_{\infty 1} - T_1)}{R_{conv,1}} = \frac{T_1 - T_2}{R_{plastic}} = \frac{T_2 - T_3}{R_{mould}} = \frac{T_3 - T_{\infty 2}}{R_{conv,1}} \quad (3.5)$$

If $\dot{Q}$ is known then the heat flow equation can be generalised as shown in equation (3.6), where T_i is temperature at location *I,* and $R_{total,i\text{-}j}$ is the total thermal resistance between locations *i* and *j* (Çengel and Yunus, 2003):

$$\dot{Q} = \frac{T_i - T_j}{R_{total,i-j}} \quad (3.6)$$

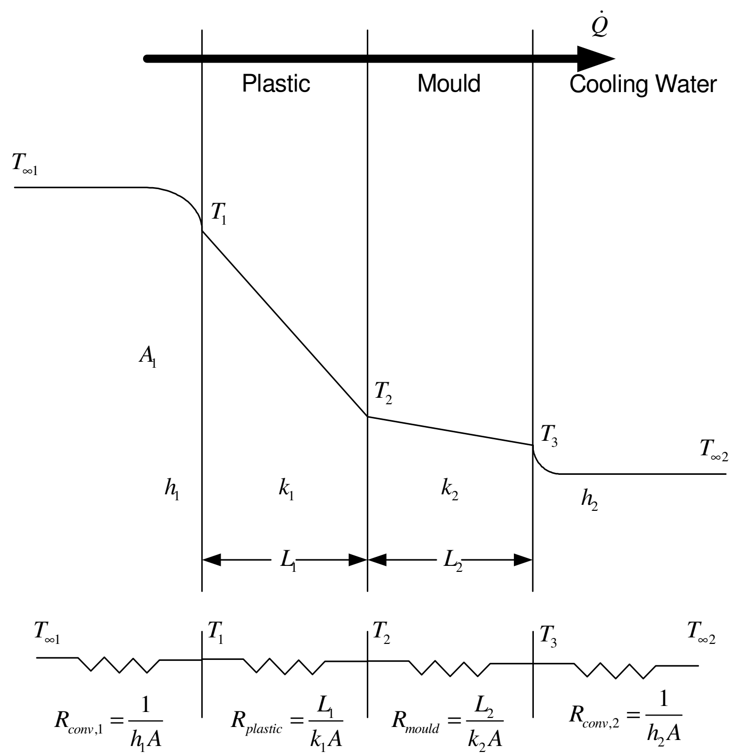

Figure 3.7: The thermal resistance network (Çengel and Yunus, 2003)

3.3 Cooling System Configuration

The cooling system configuration – layout and geometry of the cooling channels strongly influences the cooling behaviour of the mould, and present a vast area for design optimisation. One can distinguish between:

- Optimal layout of the cooling lines, which includes

  - length of the cooling channels (minimum pressure drop) – depending on the part geometry as well as on inlet and outlet location
  - distance of the cooling lines from the mould cavity surface – depending on the mould material, the size and shape of the cooling channels, as well as the cavity pressure
- Optimal geometry of the cooling lines, which includes the diameter of the cooling channels, their shape (cross section), as well as the surface roughness.

3.3.1 Conventional cooling layouts

The conventional cooling channels are typically drilled straight holes around the tool cavity, allowing coolant to circulate through the injection mould, removing the heat by conduction and convection. Ejector pins, parting planes, etc. make it impossible to gain the optimal cooling effect, and the methods to improve the cooling, such as baffles and bubblers, are rather time consuming. The worst situation arises when complex parts may need extra post-mould cooling in a custom-fit jig. This operation is costly, both in lead-time and man-hours.

Traditionally, calculation of the cooling time is based on the assumption that the cooling in the mould takes place almost entirely by heat conduction. That is because, during the injection moulding cycle, the polymer is injected into the mould cavity with a polymer melt temperature of T_{melt}, then the mould is held at a constant temperature of T_m, and then the heat transfers into the cooling channels across the wall thickness l_m of the mould. The variation in temperature across the wall thickness and over time, is described by one-dimensional heat conduction according to equation (3.7):

$$\partial T/\partial t = \alpha \, \partial T^2/\partial x^2 \qquad (3.7)$$

where x is the coordinate distance centre plane of the wall normal to the plate surface (mm), T is the temperature (℃), t is time (s) and α is the thermal diffusivity coefficient (mm^2/s).

With boundary condition $T(0) = T_m$, and $T(t_c) = T_e$, thus the cooling time t_c is given by equation (3.8) (Boothroyd et al., 2002):

$$t_c = \frac{l_m^{\,2}}{\pi^2 \alpha} \log_e \frac{4(T_{melt} - T_m)}{\pi (T_e - T_m)} \qquad (3.8)$$

where T_e is the recommended ejection temperature.

The cooling configuration includes the spacing, geometry and layout of cooling lines. This in turn defines to a large extent further influencing factors, such as coolant efficiency and pressure drop. Thus the mould cooling configuration design represents a wide area for optimisation of the cooling behaviour, leading to an improved thermal management of the mould subsystem, and hence a better process economics without significant capital expenditure.

3.3.2 Conformal cooling layouts

Xu (1999) reported, that if, however, the cooling lines are placed very close and conformal to the mould surface, the steady state condition is reached much sooner than if the cooling lines are placed far from the mould surface (Figure 3.8).

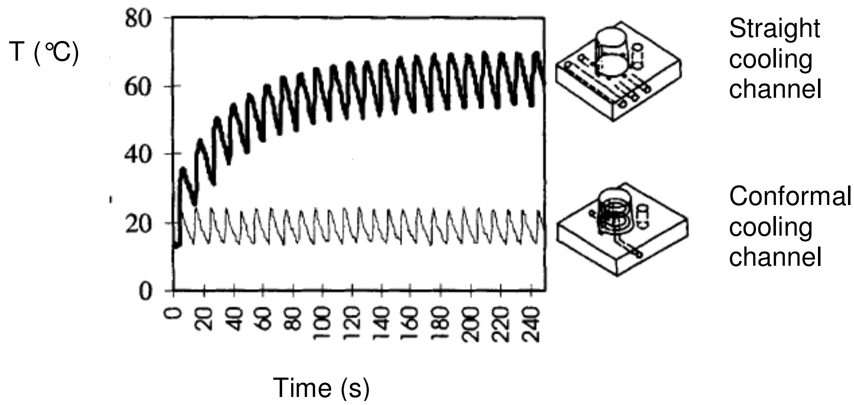

Figure 3.8: Comparison of mould surface temperature histories for a straight cooling channel and a conformal cooling channel (Xu, 1999)

The derived the energy balance equation for the active portion of a mould, namely the portion between the mould surface and the cooling lines (water):

$$\rho_m c_m l_m \frac{dT_m(t)}{dt} + \frac{h\pi D K_m}{2K_m W + h\pi D l_m}\left(T_m(t) - T_c\right) = \frac{\rho_p c_p l_p \left(T_{melt} - T_e\right)}{t_{cycle}} \qquad (3.9)$$

where: ρ_m and ρ_p are the densities of the mould and the plastic part; c_m and c_p are the specific heats capacities of the mould and the plastic part; l_m is the distance from cooling line to mould wall; l_p is half the plastic part thickness; T_m (t) is the cycle averaged mould temperature as a function of time; *h* is the heat transfer coefficient between mould and coolant; D is the cooling channel diameter; K_m is the thermal conductivity of the mould; W is the cooling line pitch distance; T_c is the coolant temperature; T_{melt} is the plastic melt processing temperature; T_e is the plastic ejection temperature, and t_{cycle} is the injection cycle time.

This differential equation describes the dynamic response of the cycle's average mould temperature during successive injections. Its first term reflects the thermal state of the tool and the accumulation of heat as the mould temperature increases. The second part represents the transfer of heat by conduction through the mould and then through convection into the coolant.

The right-hand side of equation (3.9) captures the source of the heat, which is the hot plastic. Its solution leads to equation (3.10), namely:

$$T_m(t) = \overline{T}_m + (T_{m0} - \overline{T}_m)^{e^{-t/\tau}} \tag{3.10}$$

where $\overline{T_m}$ is the cycle averaged mould temperature at steady state operation; T_{m0} is the initial mould temperature and τ is the time constant of the mould or the time the mould needs to reach its steady state condition. The solution of this equation for τ leads to the simplified form:

$$\tau = \frac{\rho_m c_m l_m^2}{K_m} \tag{3.11}$$

This equation is of enormous practical importance. It shows, in a simple expression, the most influential variables in the tooling heat transfer problem and their relationship: the thermal diffusivity of the mould is characterised by the ratio $K_m/(\rho_m c_m)$, and the fact that the time constant is proportional to the square of the distance between the mould surface and the cooling lines. Therefore, while the mould material properties are important, the cooling layout and configuration are even more important.

Finally, the conformal cooling condition of a mould can be formulated mathematically as the requirement that the mould time constant is less than one injection cycle (Xu et al., 2001), or:

$$\tau < t_{cycle} \tag{3.12}$$

The meeting of this condition reflects the base for the appropriate thermal management of a mould due to the fact that the temperature of the mould surface is always close to the temperature of the coolant.

Various studies confirm that this approach leads to a better mould performance represented by cycle time reduction and improved product quality (Au and Yu, 2006, Au and Yu, 2007, Bester, 2006, Dalgarno and Stewart, 2001, Dimla et al., 2005, Ferreira and Mateus, 2003, Gloinn et al., 2007, Moammer, 2007, Norwood et al., 2004, Rännar, 2003, Sachs et al., 2000, Saifullah and Masood, 2007, Smith et al., 2008, Sun et al., 2002, Villalon, 2005).

3.3.3 Surface cooling layouts

The new design approach for mould cooling systems, now possible to be realised, leads to considerations of new means to determine the cooling cycle time required to cool the molten part within the injection mould.

The wall between the molten part and the cooling surface has a very small thickness (1.5–2.5 mm) (LaserCusing, 2009). It is therefore assumed that the wall of the mould between the molten part and the cooling channels has the same temperature T_m of the molten part, with conductivity k, and is cooled convectively, with convective heat transfer coefficient *h*, by a coolant of temperature T_c.

The initial analysis of surface cooling method is essentially inspired by the classical lumped heat capacity method, as described by Rolle (2000). It is assumed that the wall is a good conductor of heat, so good that the heat conduction can occur over an infinitesimal temperature gradient. One can thus say that the wall temperature of the cooling surface is uniform. For the transient condition, the small wall of the mould, and the temperature without temperature gradient, is only a function of time (Rolle, 2000):

$$T(x,y,z,t) = T(t) \quad (k \rightarrow \infty \text{, or very small heat conduction system}) \tag{3.13}$$

Assuming that the irregular shape of the mould surface shown on Figure 3.9 is surrounded by cooling channels all over (cooling surface), then the energy balance for the system is:

$$\dot{Q}_{boundary} = -\frac{dE}{dt} \tag{3.14}$$

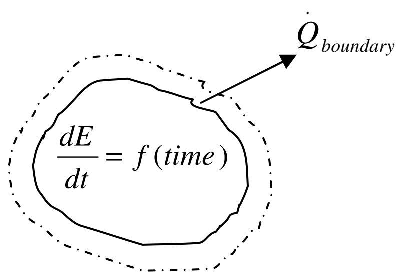

Figure 3.9: Irregular shape of molten part

The negative sign in the rate of energy change term, dE/dt, reflects that the part is losing energy. Equation (3.14) describes the heating or cooling processes of lumped heat capacity systems (Rolle, 2000).

The cooling surface configuration provides a networking system that transfers heat from the hot surface to the coolant. The performance of the thermal management is based on the heat transfer coefficient *h* which is related to the heat flux per unit area $\dot{Q}$ from the hot surface,

$$\dot{Q}_{boundary} = hA_s[T(t) - T_c] \tag{3.15}$$

where A_s is the boundary surface area.

The energy rate change is

$$\frac{dE}{dt} = \rho_p V_s c_p \frac{dT(t)}{dt} \tag{3.16}$$

where V_s is the part volume, and ρ_p is the part density.

Equation (3.15) then becomes

$$hA_s[T(t) - T_c] = -\rho_p V_s c_p \frac{dT(t)}{dt} \tag{3.17}$$

From the substitution $\theta(t) = T(t) - T_c$ with $\frac{d\theta(t)}{dt} = \frac{dT(t)}{dt}$ equation (3.15) is transformed to

$$hA_s\theta(t) = -\rho_p V_s c_p \frac{d\theta(t)}{dt} \tag{3.18}$$

for $t \geq 0$ and $T(0) = T_m$ the temperature of the molten plastic, i.e. $\theta(0) = T_m - T_c$

Separating variables $\int_{\theta_i}^{\theta} \frac{d\theta(t)}{\theta(t)} = -\frac{hA_s}{\rho_p V_s c_p} \int_0^{t_c} dt$ and

integrating this equation gives $\ln \theta(t) - \ln \theta_i = -\frac{hA_s}{\rho_p V_s c_p} t_c$

With the time constant τ of the mould cooling surface defined by

$$\tau_{Cooling.surface} = \frac{\rho_p V_s c_p}{hA_s} \tag{3.19}$$

an idealised minimum cooling time can then be obtained from equation (3.20).

$$t_c = -\tau_{Cooling.surface} . \ln\left[\frac{T_e - T_c}{T_m - T_c}\right] \tag{3.20}$$

whereas T_e is the plastic ejection temperature. The time constant τ of the conformal cooling was determined based on the distance between the cooling channels and the cavity surface. It was also based on the mould material properties, such as conductivity, density, and specific heat. On the other hand, the time constant of the surface cooling layout ($\tau_{Cooling.surface}$) was determined based on volume, boundary surface area, and the polymer properties, such as the heat transfer coefficient, density, and the specific heat capacity transfer of the moulded part.

When using the surface cooling layout the assumption was made that the wall of the mould is a good conductor of heat because of the short distance between the molten plastic and the cooling channels (0.5–2.5 mm). The advantage is that the heat conduction can occur over an infinitesimal temperature gradient.

3.4 Coolant Parameters

3.4.1 Coolant temperature

The most common coolant is water. Water is used as heat transfer fluid in diverse heat exchange systems within the mould. Its high specific heat capacity and low cost make it a suitable heat-transfer medium. It is usually used with additives, like corrosion inhibitors and anti-freezes.

A disadvantage of using water is that it is somewhat corrosive, which can lead to blockage of the cooling channels while the mould is not in use.

The water temperature can directly influence the cooling of the mould: the lower the water temperature the shorter the cooling time. The water temperature, however, can not be reduced infinitely, since defects in the plastic will occur. If the water temperature is too low, dew drops will form in the mould, which can cause corrosion in the mould cavity and marks on the products. Determining the optimal temperature can be done by trial and error, but in most plastic conversion factories the water temperature is between 11 °C and 15 °C, throughout the plant.

There are three major temperature differences (ΔT) that can be identified, and must be taken into consideration (Figure 3.10).

The first temperature difference (ΔT_p) is that between the plastic melt temperature (injection temperature) and the ejection temperature for one cycle time. This temperature difference ΔT_p depends on the plastic properties (some of the most common injection moulding materials are shown in Table A1 in *Appendix A*), the features of the part, and the injection process parameters. For example, some parts with small cross-sections or passages may require that the plastic be heated to higher temperature to reduce its viscosity during mould filling.

The second temperature difference (ΔT_{pc}) represents the average temperature difference between the moulded part and the coolant. The greater this temperature difference ΔT_{pc} the greater the heat transfer rate between them. In the case of cooling a moulded part, the ΔT_{pc} decreases with time, i.e. as the heat is transferred from the moulded part to the coolant.

Finally, the third temperature difference (ΔT_c) of the cooling water from "in" to "out" occurs as the coolant flows through the mould and absorbs the heat from the moulded part. In general, the coolant temperature is the temperature required to cool the moulded part to the ejection temperature and also to keep the mould at the operation temperature of the part (mould temperature). For many general purpose moulds this temperature difference ΔT_c should be kept to not more than 5–6 ℃. A greater ΔT_c can result in uneven mould cooling and longer cycle times (Rees, 2002).

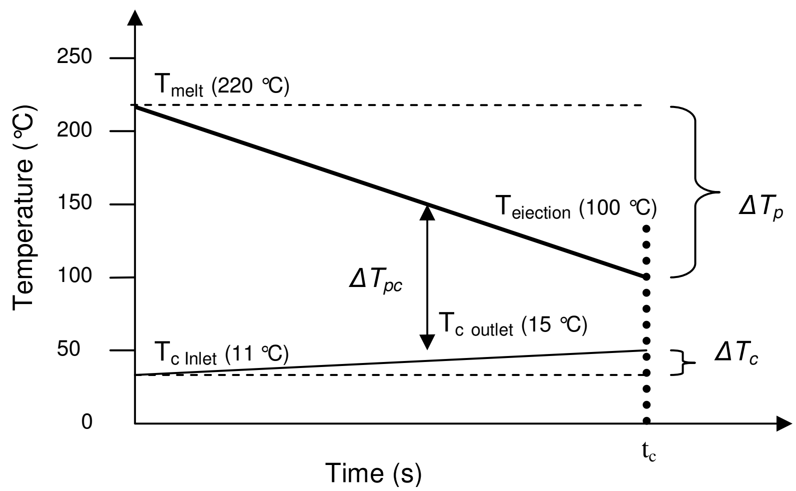

Figure 3.10: HDPE example of temperature differences

If water at 11–15 ℃ is continuously circulated there is often a metered water charge, so many companies have installed external water cooling towers to recirculate the warm water, returning it to the mould at an ambient temperature of about 30 ℃ (Osswald et al., 2002). Chilling is generally used with injection moulding to control the water temperature required for the mould. The flow is regulated to control the temperature at a strategic point in the mould and moulded part, depending on the material properties and geometry. A diagram of a typical cooling system for a mould is shown in Figure 3.11. Moulds, however, can become too cold. Then the incoming plastic melt prematurely solidifies before it can flow into the mould cavity, causing short moulding. Manual balanced flow regulators are therefore often used. They are usually used to control the water flow to each cooling channel.

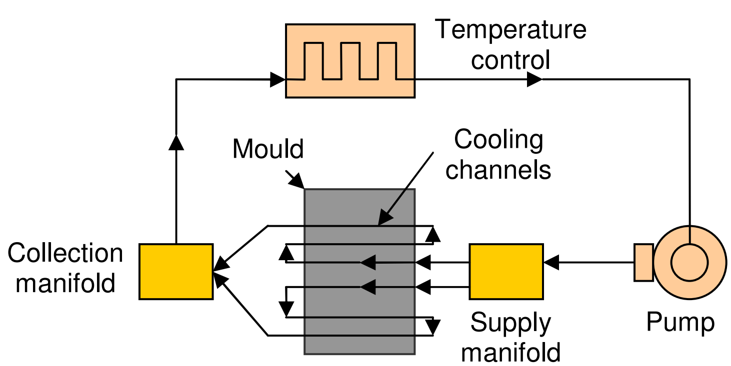

Figure 3.11: Typical cooling system for a mould

3.4.2 Coolant mass flow rate

There are many factors that affect the flow of the coolant through the mould as listed below:

- *Pressure differential*

  The difference pressure between the coolant inlet coming from the supply and the coolant outlet return must be high enough to provide a high flow rate.

- *Cross-section of channels*

  The flow rate is proportional to the square of the diameters. Cooling channels with a big diameter of 10 mm can pass roughly four times as much fluid as a channel with diameter of 5 mm. It is important to distribute sufficient cooling when it needed, to create uniform mould cooling.

- *Length of the channels and their layout*

  The effect of the channel lengths in small moulds can be ignored. What is important here is the change of direction of the flow which can reduce the coolant flow, depending on the diameter of the cooling channel.

- *Viscosity of the coolant*

  According to Rees (2002), the effect of the viscosity of the coolant can for practical purposes be usually ignored.

- *Condition of channels (deposits)*

  Deposits can affect the cooling efficiency by reducing the cross-section of the cooling channels, which thereby reduces the flow of coolant. Furthermore, the deposit usually has much lower heat conductivity than the mould material. This is of particular importance where small cooling channels are used (Rees, 2002).

- *Turbulence or laminar coolant flow*

  If the volume flow through the mould is very low (resulting in low flow velocity) the water will become warmer and thus less heat transfer will take place, causing an increase in the cooling time. On the other hand, if the flow is sufficient the water will not heat significantly, and then heat transfer can take place at a constant rate. There will be a certain truncation point for the flow volume in any mould. This happens at a point where the water will remove all the heat the mould and mould-fluid boundary layer can conduct to the water. Thus, the constraint in the heat conduction chain is the mould’s conductivity (Rees, 2002).

Turbulent flow greatly enhances convective heat transfer rates at the cost of increased friction losses. The intense mixing of the fluid in turbulent flow as a result of rapid fluctuations enhances heat and momentum transfer between fluid particles, which increases the friction force on the surface and the convection heat transfer rate. Figure 3.12 gives an idea of the difference between laminar and turbulent flow.

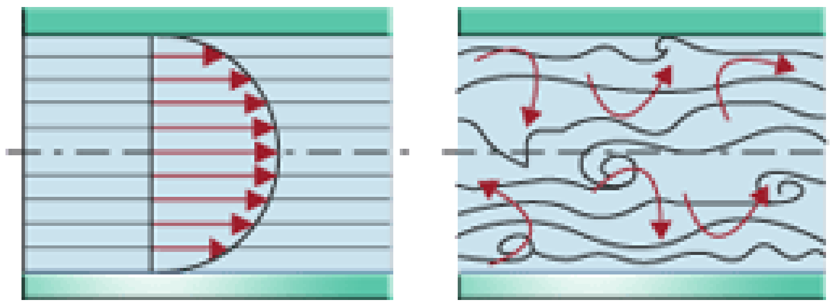

Figure 3.12: Laminar and turbulent flow (Shoemaker, 2006)

Both the friction and heat transfer coefficients reach maximum values when the flow becomes fully turbulent. Therefore it is necessary to use a larger pump to overcome the larger friction force accompanying the higher heat transfer rate. The flow rate should be high enough to achieve a Reynolds number (R_e) > 3,200, better yet, R_e > 10,000 (Rees, 2002). The Re can be calculated from equation (3.21).

$$R_e = \frac{D\ v\ \rho_c}{\mu} \qquad (3.21)$$

where D is the diameter of the cooling channel, v is the average velocity of the coolant, ρ_c is the density of the coolant, and μ is the dynamic viscosity of the coolant.

Determination of the coolant mass flow rate

The amount of heat that has to be removed can be calculated from the mass of the part and its specific heat at moulding temperature, allowing for the fact that the temperature of the mould when ejected will generally be well above ambient (Shoemaker, 2006).

The rate at which heat must be removed from the moulded part can be calculated from equation (3.22):

$$\dot{Q}_{part} = \rho_p V_S c_p \Delta T_p / t_c \qquad (3.22)$$

where t_c is the cooling cycle time, ρ_p is the part density, V_S is the moulded part volume, c_p is the specific heat of the moulded part, and ΔT_p is the temperature difference between the plastic melt temperature T_{melt} and the plastic ejection temperature T_e. ΔT_p can be calculated from equation (3.23):

$$\Delta T_p = (T_{melt} - T_e) \tag{3.23}$$

The energy balance equation applied to heat removal rates results in:

$$\dot{Q}_{part} = \dot{Q}_{coolant} \tag{3.24}$$

$$\dot{Q}_{coolant} = \dot{m} c_c \Delta T_c \tag{3.25}$$

$$\Delta T_c = (T_{out} - T_{in}) = 5 \text{ °C} \tag{3.26}$$

$$\dot{m} = \frac{\dot{Q}_{part}}{\Delta T_c c_c} \tag{3.27}$$

where c_c is the specific heat of the coolant, $\dot{m}$ is the coolant mass flow rate, and ΔT_c is the coolant temperature difference.

3.5 Conclusion

In order to design the cooling layout it is important to understand the basics of heat transfer, especially during the injection moulding cycle. The fact that interfacing surfaces are at the same temperature allows for useful calculations to be made about heat transfer flow from the plastic to the mould.

The use of the lumped heat capacity method to calculate the minimum cooling time possible to cool the moulded part provides the designer with a benchmark. This means that the designer can now provide, and quantify, strong motivation to use newly emerging AM techniques to reach an optimal cooling layout, ensuring minimum cooling cycle time, while simultaneously meeting quality requirements.

The designer must know that water flowing turbulently removes more heat from the mould than laminar flowing water. This is mostly caused by large near wall temperature gradients, and better heat transfer cross the flow. Thus the cooling mass flow rate at which heat must be removed from the moulded part at the minimum cooling time possible must be determined, and then circulated through the cooling channels accordingly to achieve the maximum cooling efficiency.

4. MOULD THERMAL MANAGEMENT EVALUATION MODEL

Injection moulding of polymer components is subject to ever increasing demands for part quality and production rates. It is widely recognised that the mould cooling strategy employed is crucial to achieving these goals. It has already been stated that uniform cooling channels, i.e. channels equidistant from the surface to be cooled, have an impact on the quality of the product as well as on the cycle time.

The emergence of the AM technologies now makes it possible to make the cooling channel configuration required for the mould. Figure 4.1 illustrates a proposed framework of the mould design.

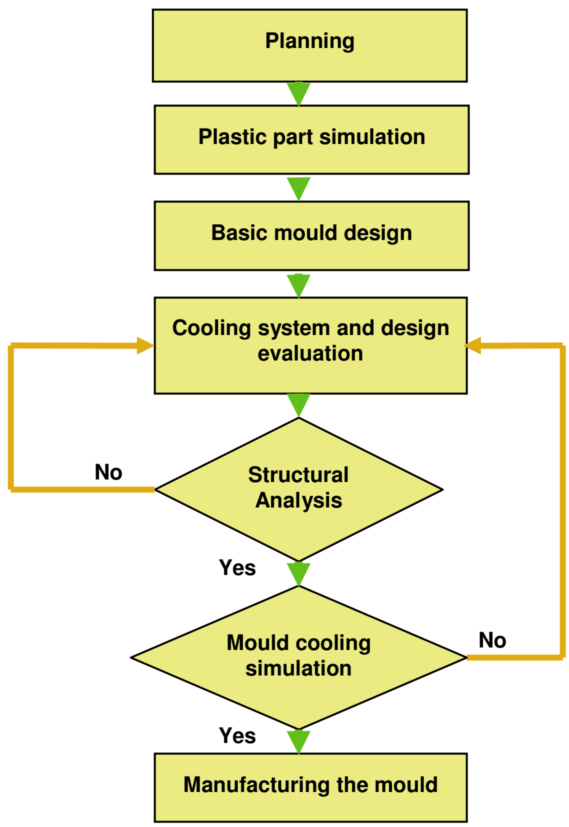

Figure 4.1: Proposed mould design process chain

4.1 Planning

In order to carry out adequate planning of the mould design, various questions should first be answered and factors considered, such as the following (Dalgarno and Stewart, 2001):

- Part complexity
- Machine parameters
- Number of mould cavities
- Moulded material
- Batch size
- Product lifespan
- Anticipated cycle time
- Function of the moulded product
- Product tolerances
- Moulded material shrinkage
- Product draft angles and split lines
- Runner system
- Gate and ejector locations
- Permissible gate size and shape
- The required part finish
- Mould engraving
- Mechanical moulded part removal
- Project lead time
- Project budget.

Answers to these questions help the designer to determine the customer's precise requirements, and also guide the designer in avoiding elementary mistakes.

4.2 Plastic Processing Analysis

In the past, before a scientific approach was introduced into the tooling development for plastic conversion, the design of the mould cooling system was largely left to the designer's experience. This involved using simple guidelines and mathematical expressions related to basic heat transfer issues (Li, 2001, Li et al., 2005, Lin, 2002, Menges et al., 2000, Pye, 2000). With the significant improvements of the capabilities of computer hardware and the associated fast development of the CAD and Computer Aided Engineering (CAE) systems, and the three-dimensional computer modelling in particular, the introduction and use of simulation as an analytical tool occurred rapidly in the mould design process (Figure 4.2).

There are various software packages available for the simulation of plastic processing. The most prominent area of development is injection moulding, followed by blow moulding to a lesser extent.

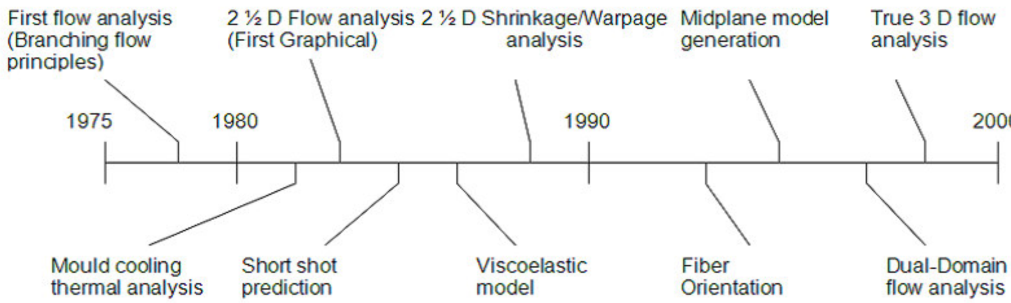

Figure 4.2: Milestones in injection moulding CAE development (Beaumont et al., 2002)

4.2.1 Plastic part simulation

Typical simulation packages for analysis of the moulded part are Simuflow (SIMUFLOW, 2010), Moldflow (Moldflow, 2005), Moldex3D (Moldex3D, 2005), Rem3D (Transvalor, 2006), and others. Their analytical capabilities are related mainly to the following issues (Jardan, 2002):

- Variable injection rates
- Shear stress calculation
- Automatic weld line interpretation
- Automatic gas entrapment interpretation
- Flow vectors
- Hot runners
- Programmable gate injection time
- Gate modelling
- Fully integrated mould filling, packing and cooling analysis
- Automatic runner balancing
- Recommended cooling layout
- Cycle time determination
- Differential (cavity/core) cooling effects.

The most widely used package is Moldflow. The Moldflow Part Adviser™ (Moldflow, 2005) module would be use to quickly check the manufacturability of a plastic part design early in the design process, when the cost of any change is still at its lowest. Users can get rapid feedback on how modifications to wall thickness, gate locations, material or geometry can affect the filling pattern, and pressure and temperature distributions in the part cavity. The analytical results and detailed design advice can be used to determine the optimum thickness of the part and gate locations, as well as to identify and eliminate cosmetic issues such as weld lines, air traps and sink marks.

4.2.2 Mould cooling simulation

When designing traditional cooling channels it is easy to predict what the water flow will be like and what the approximate heat convection will be between the channel wall and the water. However, with conformal and surface cooling layout it is not as easy.

The simulation capabilities of Moldflow are confined to channels. A typical cooling layout suggested by Moldflow for a cup-shaped component, for example, is shown in Figure 4.3.

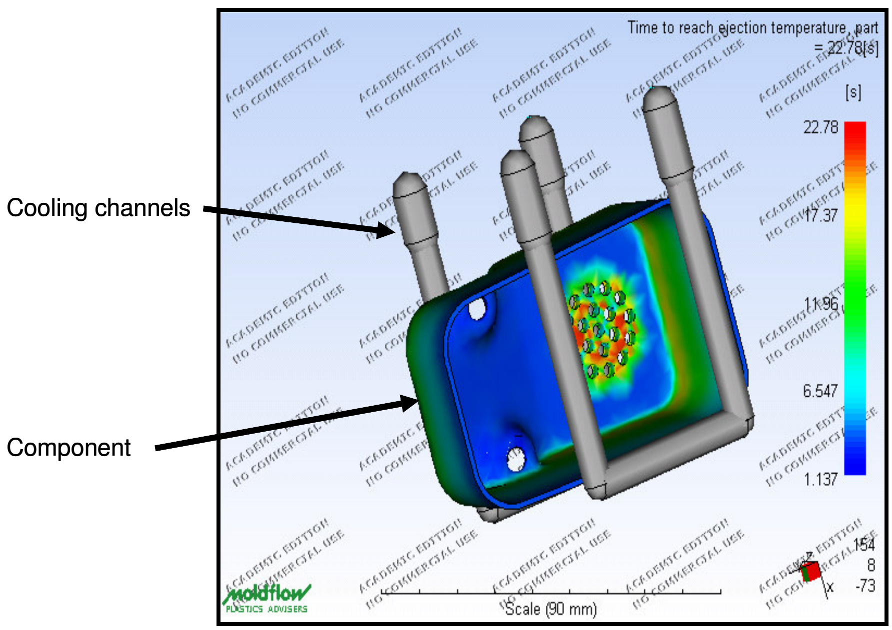

Figure 4.3: Typical Moldflow cooling layout

The cooling channels suggested by the Moldflow are straight, and the design can also include bubblers and baffles, which are typical of conventional machining. Moldflow allows the designer to import custom designed wireframe networks as Initial Graphics Exchange Specification (IGES) lines. These lines can be spirals or any other complex curve. The curves are then converted to round or half-round water channels, but still there is no option for flood or complex conformal cooling layouts.

Despite Moldflow being a powerful software tool for the analysis of injection moulding processes it is unable to accommodate the free design of the cooling channels such as results from surface cooling. Figure 4.4 shows cooling channels designed in such a way as to conform to the part surface. The Moldflow software fails to simulate this type of cooling channels. However, the Moldex3D was capable of simulating the complicated cooling layouts.

The Moldex3D is engineering simulation software. The simulation of the moldex3D is based on Finite Volume Analysis (FVA) and Computational Fluid Dynamics (CFD).

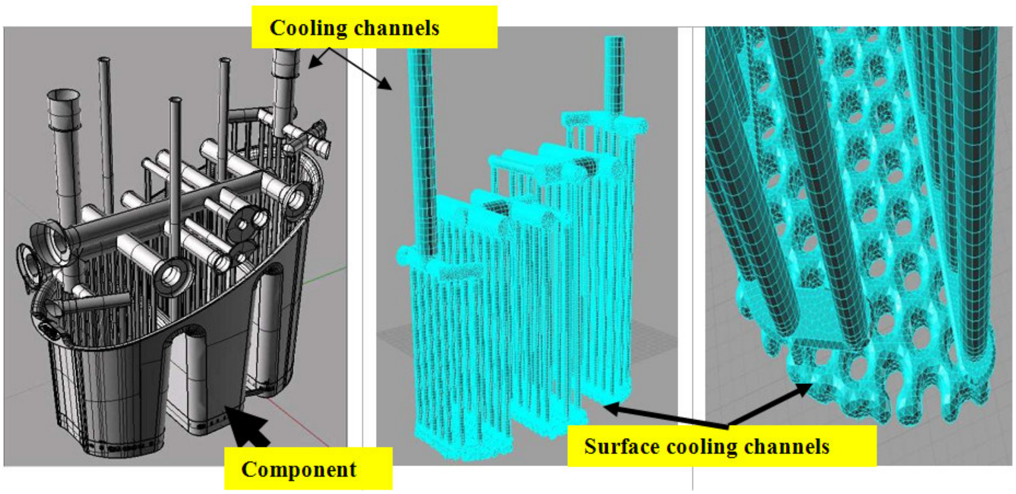

Figure 4.4: 3D models of surface cooling channels design

4.3 Basic Mould Design

The mould design can be simple or very complex, depending on the features of the moulded parts. Generally, the accepted design of the mould is associated with the mould capability to produce the part at minimum cost and with good quality.

The basic requirements of an injection mould are summarised below (Dimitrov et al., 2008). It must

- contain a core and cavity set that forms the features of the part
- deliver the molten plastic from the machine barrel to the forming cavity via a gate, runner system, and sprue
- act as a heat exchanger, which cools the part rapidly and uniformly
- be able to eject the part by the ejector system
- be able to resist the internal melt pressure, the compressive force from the moulding machine's clamp, and the pressure and forces acting during the injection moulding cycle.

The basic mould design includes the mould layout, moulding operation sequences, plastic shrinkage, mould surface tolerances, gates and runners, venting, ejection, and mould cooling. The mould cooling design and related considerations are discussed in the following section.

4.4 Cooling Systems

At this stage decisions need to be made on design aspects like the distance between the mould cavities, the position of leader pins, and the ejector system.

Design problems can occur due to many factors that influence the mould filling and mould cooling. Therefore, the designer has to take into consideration all the factors that may cause unacceptable cost or quality of the moulded parts before manufacturing the mould.

4.4.1 Cooling method

General cooling design considerations

There are certain restrictions that a mould designer has to take into account. These restrictions can be summarised in two broad areas:

- Mould manufacturability – this factor is determined by the manufacturing capabilities and available technologies, i.e. 5 axis milling, high speed cutting, EDM capabilities, adequate measuring equipment, etc.
- Economic viability of the mould design.

The workshop restrictions are however becoming less of a problem as a result of the introduction of the AM technologies. The modern AM machines can produce mould inserts, which can be used even for high-volume production (Figure 4.5).

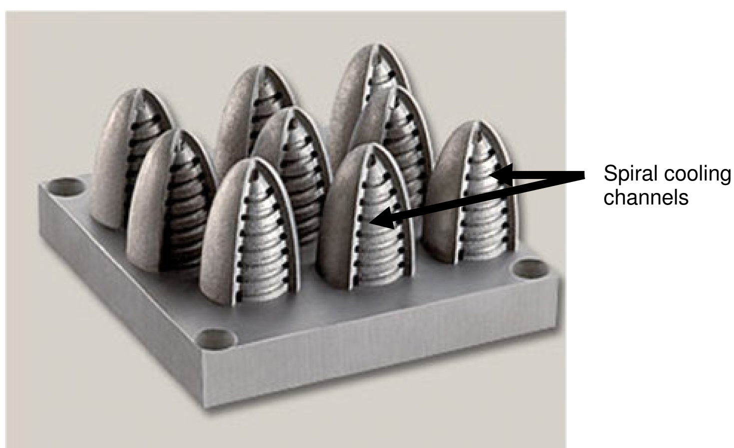

Figure 4.5: Mould insert with conformal spiral cooling (LaserCusing, 2009)

AM technologies are relatively new developments, to which only limited space is allocated in textbooks. Nevertheless, mould designers should be aware of the possibilities that these manufacturing methods offer. The most important advantage related to tool making is greater freedom of cooling layout design. As seen on the mould insert above, the cooling layout, although not difficult to design, is very difficult (or even impossible) to manufacture using conventional manufacturing methods.

In general, the cooling hardware is very well documented in the available textbooks; however, there is less focus on the cooling design. The textbooks describe only conventional cooling methods; they do not discuss alternatives such as conformal or surface cooling (Bester, 2006).

Although the textbook authors clearly have much design experience, it appears that they try and oversimplify the cooling of the moulds. Some of the examples given are very crude, and can be misleading. Bester (2006) extensively analysed common mistakes resulting from the oversimplification of cooling issues. Other authors have studied common errors in cycle time prediction (Stelson, 2003).

There is also some research being carried out on automatic cooling layout design using algorithms for the heuristic search for the best cooling layout (Li, 2001, Li et al., 2005, Lin, 2002). The process presented in those studies is however limited by the use of drilled channels. It might have the advantage of supplying a quick cooling design, but it will not solve the problem caused by cooling completely. It will only be effective if it could be developed to enable the use of AM technologies.

Conformal cooling method

Conformal cooling in itself is not a completely new concept; it has been used in many experiments and also in different applications. The basic principle of conformal cooling, in its simple form, is a cooling system in which the cooling channels follow the cavity being cooled at a constant distance. Figure 4.6 shows two different layouts used in the design of two specific injection moulding tools.

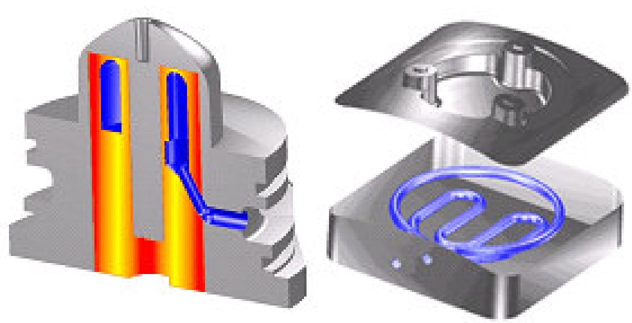

Figure 4.6: Conformal cooling channels in injection moulding tools (Bratt, 2010)

Since conformal cooling is a cooling layout where the water channels follow the mould cavity closely, it is obvious that different designs would satisfy this requirement.

A comprehensive methodology for the design of conformal cooling configurations has been developed by Xu, (1999). Six design rules are related to the design for the following:

- Conformal cooling condition
- Coolant pressure drop
- Coolant temperature uniformity
- Sufficient part cooling
- Uniform cooling
- Mould strength and deflection.

Based on these six design rules and relationships, as well as other physical constraints, suitable conformal cooling design windows can be constructed. Those design windows can be used by mould designers as guidelines to select appropriate mould parameters and cooling conditions. (Figure 4.7).

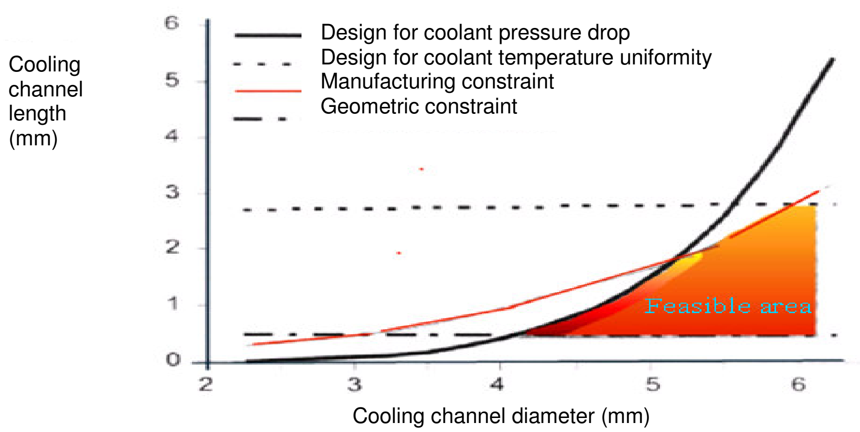

Figure 4.7: A conformal cooling design window of cooling channel diameter vs. cooling channel length (Xu, 1999)

Surface cooling method

Selective laser melting technology, such as the LaserCusing technique, has opened a new door to the mould designer for the design of an optimum cooling channel layout. Thus, cooling channels can completely conform as net channels to the cavity/core surface.

The cooling surface method, shown in Figure 4.8 is a more expensive method of cooling moulds. The cooling is in a honeycomb shape that closely follows the cavity surface at a depth of approximately 2.5 mm (LaserCusing, 2009), and it can be multi-layered, where the one layer can be used for cooling and the second layer for heating. This method is recommended for high volume-production and it provides excellent performance.

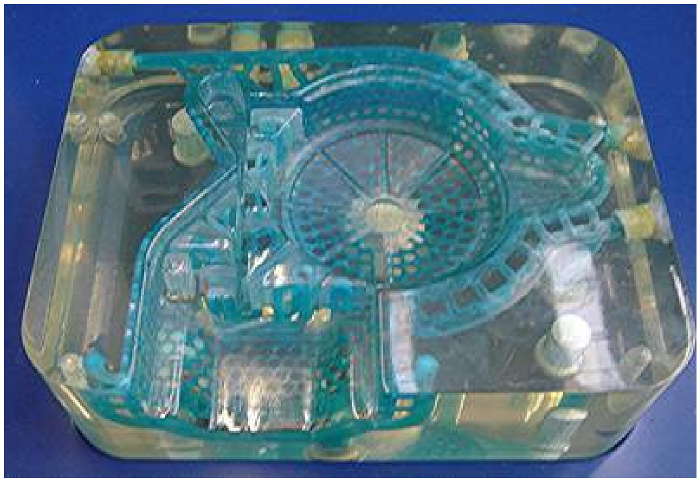

Figure 4.8: Surface cooling method (LaserCusing, 2009)

Au and Yu (2007) analysed various attempts to incorporate conformal cooling channels using different rapid tooling technologies. They found that the contemporary conformal cooling layout offers a near uniform cooling with consistent heat transfer. Therefore, they proposed a novel scaffold cooling method, which is very much like the surface cooling method, for the “design of a more conformal and hence more uniform cooling channel”.

Figure 4.9a shows the modelling of mould cavity surface and Figure 4.9b the cavity mould half with scaffolding elements inserted for uniform cooling.

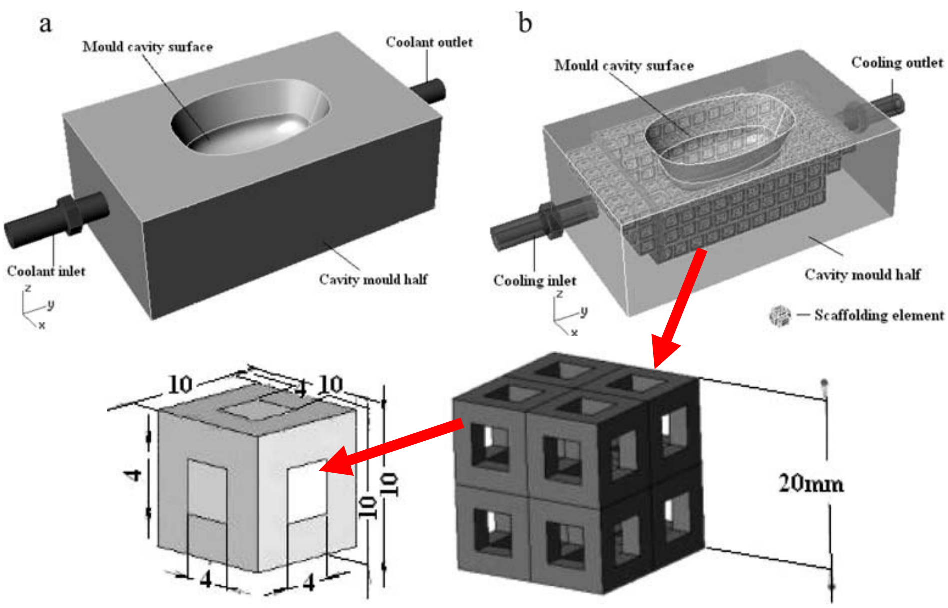

Figure 4.9: Cooling channels with a scaffold design (Au and Yu, 2007)

The CAD model for constructing the scaffolding architecture was examined and the cooling performances were validated by CAE and CFD analysis methods. However, no practical realisation or experimental validation has been reported.

Hybrid cooling method

The hybrid method was developed by LaserCusing to achieve maximum cooling performance at the lowest manufacturing cost. Usually the cooling problem occurs at the top of cores, where cooling channels must be closed to the cavity surface.

The hybrid tooling shown in Figure 4.10 is produced with a combination of conventional mould manufacture and LaserCusing. The base of the mould is manufactured using conventional methods such as milling or turning and then with the use of LaserCusing the top part of the mould is built on the machined part. Some finishing is done afterwards to ensure a good surface quality.

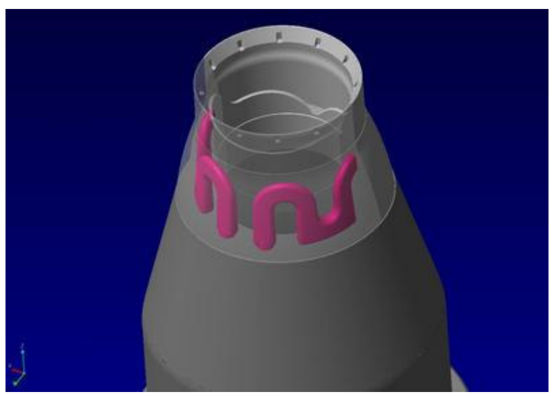

Figure 4.10: Hybrid tooling method (LaserCusing, 2009)

Combined surface and straight channel cooling is illustrated in Figure 4.11. The base of the mould core (Figure 4.11 (a)) is machined and the channels are drilled, after which the component is hardened. The top of the core is then grown on top of the machined part using LaserCusing technology (Figure 4.11 (b)). Thereafter the machining finishing operation takes place.

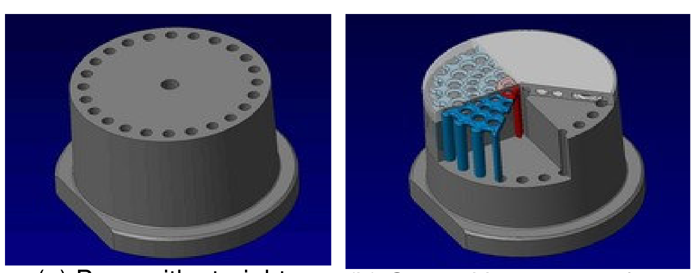

(a) Base with straight drilled holes

(b) Core with grown surface cooling channels

Figure 4.11: Combined surface and straight channels (LaserCusing, 2009)

4.4.2 Cooling design evaluation

A new methodology for designing the cooling channel layouts according to the moulded part considerations is described below. It represents an attempt to systematically apply a selection strategy to determine the most suitable mould cooling design based on the part characteristic from the mould cooling point view. These part characteristics include shape complexity, space available for the cooling channels layout, quality requirements, production volume, and product life cycle. To be specific, the five criteria are derived from different perspectives:

- 2 criteria from geometrical issues
  - Part complexity (Shape)
  - Space available for the cooling layout
- 1 criterion from a quality perspective
- 2 criteria from an organisational perspective
  - Production volume
  - Product life cycle

Part complexity

As a rule, the arrangement of the cooling channels must provide fairly good cooling into the mould. The designer must always bear in mind the basic requirements for proper, sufficient and equal coolant flow for all cavities/cores at a reasonable mould cost. Therefore, from the mould cooling point of view, the part complexity can be low, medium or high with regard to the manufacture of uniform cooling channels.

Each moulded part has its own shape characteristic features, such as different wall thickness, corners, curves, ribs and bosses, which can make the cooling channels very complicated in order to be uniform to the part surface. In the decision matrix below, the part geometry has been given the highest weighting because the mould manufacturability determines whether the mould will be expensive to produce or not with the suitable cooling layout.

- Low part complexity

  These parts are the flat-shaped parts. They are considered to be all those cavities and cores that are virtually identical and without contour (e.g. flat plates, test pieces, etc). They are easy to cool by straight (parallel or series) cooling channels, as shown in Figure 4.12. Any cooling arrangement (series, series-parallel or parallel cooling channels) must satisfy the requirement that the heat will be equally well removed from all sides of the moulded product. Cooling channels such as circular grooves are easily produced on a lathe or milling machine. Spirally grooved cooling channels can be produced on milling machine or on CNC equipment.

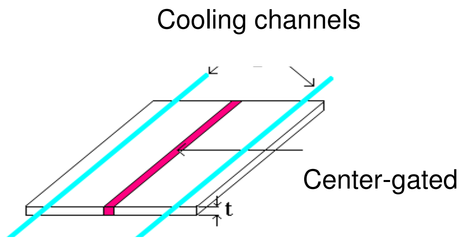

Figure 4.12: Flat part with straight cooling channels (Poli, 2001)

- Medium part complexity

  A typical medium complex part for cooling would be one that is cup-shaped, such as cups, closures, and cassettes, and whether round, oval or rectangular.

  These cup-shaped parts usually have features such as ribs, bosses, corners, varying cavity diameters, and different wall thickness, and thus require for uniform cooling channels that conform to the shape of the part.

  There are some general rules that the designer must take into consideration when designing the cooling inside the core, e.g. the area opposite the gate must always be properly cooled, to provide adequate cooling for the rest of the core.

  To obtain conformal cooling using conventional methods, the helical insert shown in Figure 4.13 is machined into the outside of the plug to obtain uniform cooling. The internal drilling through the core back plate and plug is positioned so that the coolant is directed from the inlet, through the centre of the helical insert, across the face of the plug, and to the outlet channel via the helical channel.

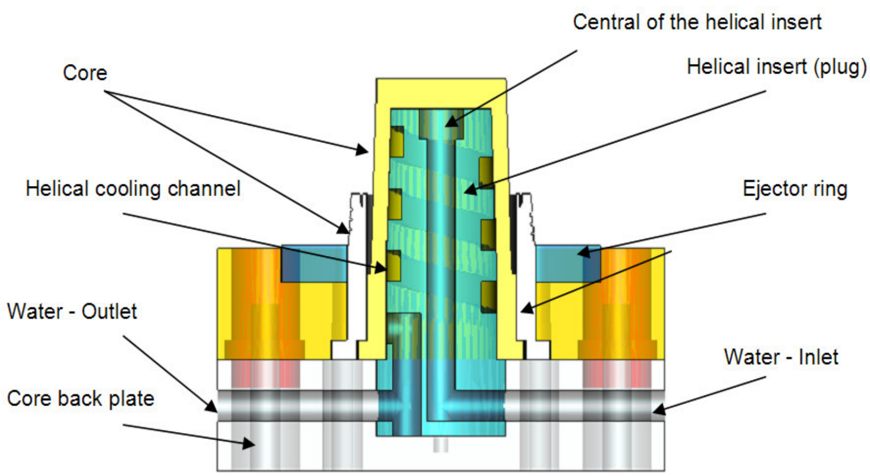

Figure 4.13: Spiral cooling channels in the core side

- High part complexity

  With the parts that required extensive heating/cooling systems as shown in Figure 4.14, and with parts that have uneven core diameters, the uniform cooling methods are impossible to be produced with the conventional methods. The only way to achieve the conformal cooling layout is to use the AM technologies.

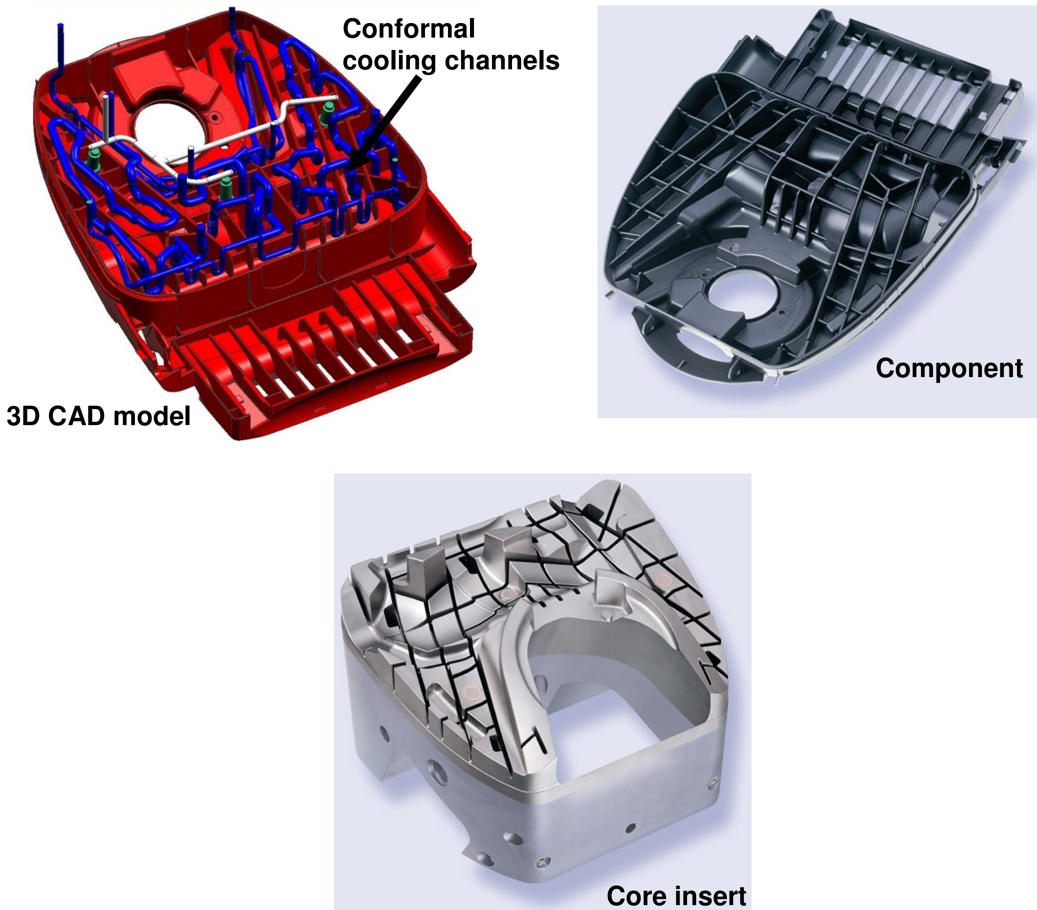

Figure 4.14: Conformal cooling channels produced by SLM-process (LaserCusing, 2009)

Space available for the cooling channels layout

Finding the best location for each channel of the cooling circuit, while also optimising the cooling performance, and avoiding interference with the other mould features, is not a simple task. Consider the example shown in Figure 4.15. There are many different components, such as screws used in the plates, ejector pins, slides, sub-inserts, and others, which have to be packed into the mould insert.

Thus, ideal cooling is impossible to achieve with conventional methods because of the possible restrictions outlined above. Moreover, the cost of the mould is affected by the complexity of the cooling layout.

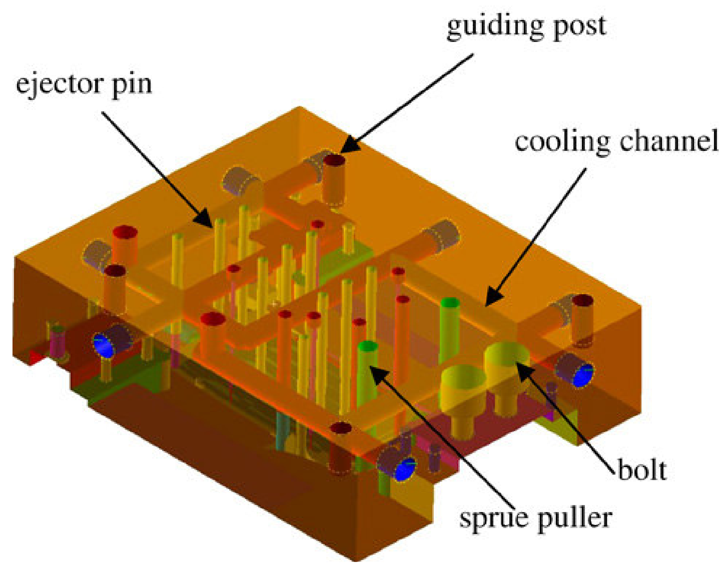

Figure 4.15: Space available for cooling channels layout in a mould (Li and Li, 2008)

The space available in the mould for the cooling channels layout is divided into wide, medium, and narrow.

- Wide space for the cooling channels layout

  Here wide space is considered when the mould maker can produce the cooling layout using the conventional methods. Thus the designer drills a cooling channel with diameters of 4, 8 or 10 mm following the mould cavity without any restriction.

- Medium space for the cooling channels layout

  Here the designer is restricted by the number of the mould items, thus the designer can not drill cooling channels that follow the shape of the cavity. However, there is a space available for cooling channels with 4, 8 or 10 mm cooling channels. The designer can use the SM to produce the conformal cooling channels if it is possible, otherwise the designer must use the AM technologies.

- Narrow space for the cooling channels layout

  When the space available for conformal cooling channels within the mould is very narrow (diameters < 3 mm), it is very difficult, if not impossible, to produce such cooling channels using the conventional methods. Conversely, it is easy to produce such cooling channels with AM techniques.

Part quality requirements

As it has been stated previously, the main point of the mould cooling is to cool the moulded product from the molten temperature to the ejection temperature at the minimum cycle time possible while meeting the quality requirements.

The cooling layout has a great influence on the part quality, such as appearance, non-uniform shrinkage (warpage), and functionality. Thus the cost of the mould is affected by the complexity of the cooling layout. Therefore, all parameters must be considered to decide what quality of cooling will be required, and at what cost.

Regarding the cost, the part quality is the third most important criterion in the decision matrix below.

The quality requirement is divided into three levels: low, medium and high, based on the product application.

- Low quality requirement

  This type of products includes plain containers, household wares, toys, and any utility product where the form itself does not mean too much as long as the product fulfils its intended function, whether alone or in an assembly. The designer must point out where shrinkage may distort the product.

- Medium quality requirement

  This type of products is the same as in utility products. However, approval is often difficult to obtain because these products may be required for their sales appearance.

- High quality requirement

  In this category of products the functionality of the product is the key requirement. The designer must therefore carefully consider the cooling layout in order to obtain high accuracy and appearance, if required. Examples of such products are computer hardware, cassette boxes, sunglasses, and structural components (automotive).

Production volume

The designer must always be aware of the actual requirements of the mould. It is very important to establish the volume production expected from the mould before commencing with design. Production volume is considered as the fourth most important variable from the cooling point of view. In fact, the better the cooling the more complicated and expensive it is to fabricate the mould, even with sophisticated equipment.

The cost of the mould must be competitive. It must be affordable for the customer, but it must also be designed and built based on the Cost-effectiveness analysis.

As an example, a comparison of cost per moulded part between the AM produced insert and the conventionally produced insert is shown in Figure 4.16. The AM cavity insert produced with conformal cooling channels was manufactured by means of DMLS at Central University of Technology, Bloemfontein, South Africa, at a cost of R 23,257.00. The cost of post processing of the conformal cavity insert was R 1,790.00.

Because the AM cavity insert is more expensive than the CNC cavity insert, a calculation in terms of production hours Y can be carried out to determine when the AM cavity insert will be amortised. For that purpose, a simplified equation (4.1) can be written as follows:

$$\text{Fixed cost} - \text{variable cost} = 0 \quad (4.1)$$

The production of the AM cavity insert is rounded off to 257 units/hour (cycle time of 14 sec), whereas that of the CNC cavity insert is rounded off to 189 units/hour (cycle time of 19 sec). The plastic material used for a single component costs R 0.50. The hourly rate of an applicable injection moulding machine is set to R 500 per hour.

$$25\,047.00 - (257 * 0.5\,Y) - 500\,Y = 1790 - (189 * 0.5\,Y) - 500\,Y$$

Then the production hours Y = 684 hours.

From this it can be seen that over a longer period of time (more than 684 hr) the AM insert becomes more economical to use.

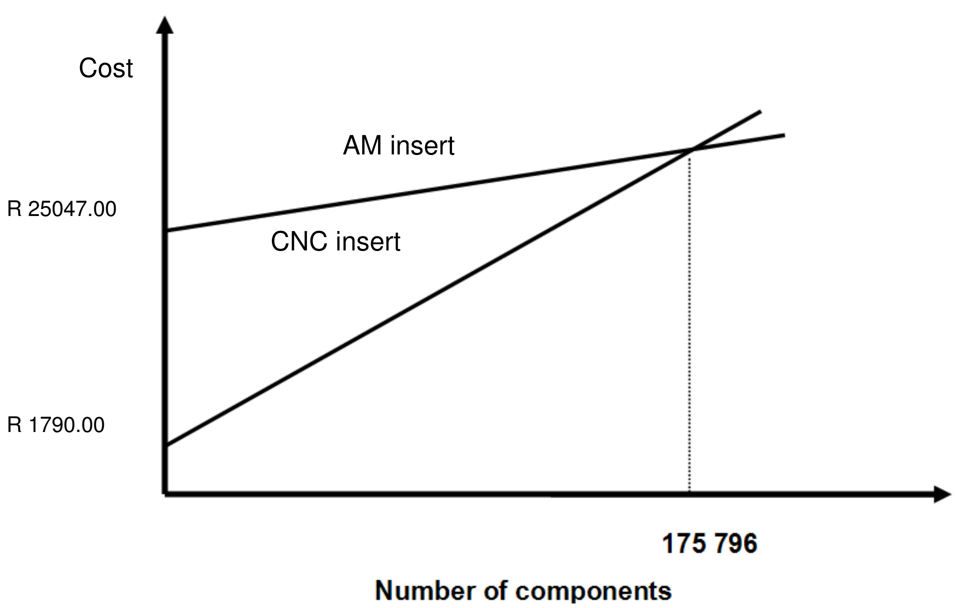

Figure 4.16: Break-even point calculated for the AM and CNC cavity inserts (Moammer, 2007)

The moulded part produced by AM insert costs less for high production volumes due to the short injection cycle time.

With regards to the above, the production volume is classified based on a designer's review in low, medium and high production volume.

- Low production volume

  Low product volume considers a mould for a limited production run, in the order of a few thousand or even up to ten thousand pieces per year. This may include an initial production run of a new product, for example to test its customer acceptance before committing to a high production. For low production, a simple mould, with little sophistication in cooling or ejection may be quite satisfactory.

- Medium production volume

  Medium production volume involves the moulding of products at the lowest possible cost. Typical quantities are between 10,000 and 100,000 pieces per year.

- High production volume

  The most important factor here is to produce the required quantities of product in the client's desired time. In order to achieve a high production volume, the best cooling method must be carefully considered. Here a high production volume is considered to be more than 100,000 pieces per year.

Product life cycle

Product life cycle defines the life of a product in the market with respect to commercial costs and sales measures. The product life cycle in this study is divided into three levels based on the position of the product in the market, as follows:

- Short product life cycle

  New product in the market: Customers are testing the product in this phase. It is quite possible that after an initial run changes to the product may be required. The cycle time may be long, so there is no need to create sufficient cooling layout with expensive manufacturing tools. In this phase the product life cycle considered as short with a period below 3 years in the market.

- Medium product life cycle

  Growing product in the market: Customers become more interested in the product, sales are increasing, and competitors are emerging. A reduction in the cycle time is recommended in order to keep the product price competitive. Therefore, all parameters pertaining to increasing the productivity must be considered. The product life cycle considered as medium with a period of 3–6 years in the market.

- Long product life cycle

  Known product in the market: The market has reached saturation and strong competition is found for the same product; the only way to survive is to keep the price as low as possible. Reduction of moulding cycle time is highly recommended as well as meeting the product quality requirements. The product life cycle in this case is typically between 6–20 years.

Decision matrix

The decision to choose one of the layouts (conventional, conformal or surface cooling layout) can be made after considering a number of important criteria (Z), as outlined above. The weighting (W_e) is arranged in descending order, from 5 to 1. The product of all the criteria is 15 because there are 5 criteria each consisting of 3 levels (5 x 3 = 15).

The first and most important criterion restricting the mould designer in designing a technically sound cooling layout for the moulded part is the manufacturing methods. Thus the part complexity weighting is 5/15.

The space available for optimising the cooling layout is weighted 4/15. The space available is also restricted by the manufacturing methods. Producing a proper cooling layout through a narrow mould space would increase the mould cost.

The quality requirement is the third most important criterion. The designer's aim is to cool the part in minimum cooling time while maintaining the quality requirements. Therefore the designer must determine the best cooling layout possible. Thus the quality requirements weighting is 3/15.

If the designer could manufacture the desirable cooling layout for such moulded parts, then the next consideration is to determine whether if it is worth manufacturing an expensive cooling layout from the production volume point of view. The production volume weighting is 2/15.

Another important criterion from the cost point of view is the product life cycle in the market. The designer must consider where the product is positioned in the market, and whether it is justified to increase the productivity by manufacturing an expensive cooling layout. The product life cycle weighting is 1/15.

The weighting of the five criteria above, was set after broader consultation with mould makers and designers.

The decision to choose the appropriate cooling channel layout for such a moulded part can be obtained from a decision matrix shown in Table 4.1.

Table 4.1: A decision matrix to determine the appropriate cooling method

Criteria (Z)	Weight (W_e)	Levels		
Part complexity	0.34	Low	Medium	High
		1	2	3
Space available for the cooling channels	0.26	Wide	Medium	Narrow
		1	2	3
Quality requirement	0.20	Low	Medium	High
		1	2	3
Production volume	0.14	Low	Medium	High
		1	2	3
Product life cycle	0.06	Short	Medium	Long
		1	2	3

The decision to choose the appropriate cooling channels for such a mould can be determined from Table 4.1, and equations (4.2) and (4.3)

$$S = \sum_{i=1}^{5} Z_{ij}.W_{e\,i} \qquad \text{Criteria } i = 1,\ldots, 5\text{; and level } j = 1, 2, 3 \qquad (4.2)$$

where S is the output solution of the decision matrix, and W_e is the weight of each variable. Thus:

$$\begin{aligned} &\text{Conventional cooling method} && 1 \le S < 2 \\ &\text{Conformal cooling method} && 2 \le S < 2.6 \\ &\text{Surface cooling method} && 2.6 \le S \le 3 \end{aligned} \qquad (4.3)$$

The respective minimum and maximum values of S are 1 and 3. The threshold values of 2 and 2.6 (instead of the evenly spaced values of 1.67 and 2.33) reflect a bias towards the lower cost option (i.e. the higher values delay the change to the more complex cooling option). Thus the value of 2 is based on all ‘levels’ being ‘medium’ and the value of 2.6 is based on ‘high’ part complexity and ‘narrow’ space availability (criteria placing severe limitations on manufacturability) with the remaining levels being ‘medium’ at this threshold.

4.5 Structural Analysis

The structural integrity of a mould is very important due to the large forces exerted on it during production. The cavity pressure in an injection mould can reach 600 bar or more. This is usually not a problem when conventional cooling is used, because the drilled channels remove relatively small amounts of material, thus leaving the structure of the mould virtually intact. When conformal cooling is used, however, this could become a problem. In both these cases a significant amount of material is often removed from the back of the mould closer to the cavity surface.

A number of software packages can be used to analyse the effect of the forces on the mould. Most of the larger CAD vendors supply embedded Finite Element Analysis (FEA) packages or modules. These embedded FEA modules operate mostly in the elastic stress/strain range, which is sufficient for checking purposes.

Some well established dedicated FEA packages, which are able to operate in the plastic, are:

- Nastran/Patran
- Abacus
- Cosmos

The CAD packages, which have either embedded FEA capabilities as standard or as an option, include:

- Pro Engineer
- Unigraphics
- Catia
- Autodesk Inventor
- Solidworks
- Solidedge

4.6 Illustrative Implementation of the Cooling Design Evaluation Model

4.6.1 Case study 1: Cup-shaped part

Description: Simple cup-shaped part (Figure 4.17)

Application: Packaging (+10,000 pieces per year)

Goal: acceptable part quality, and high part life cycle.

Decision matrix

The technique required to produce the cooling channels can be chosen by using the decision matrix shown in Table 4.1:

Part complexity is low, thus $Z_{11} = 1$

Space available for the cooling channels is medium, thus $Z_{22} = 2$

Quality requirement for the moulded part is medium, thus $Z_{32} = 2$

Production volume required is medium, thus $Z_{42} = 2$

Moulded product life cycle is long, thus $Z_{53} = 3$

Thus from equation (4.2)

$S = 1.72$

Therefore, the technique that should be used is the conventional cooling method.

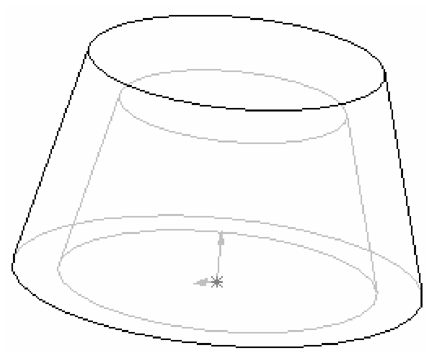

Figure 4.17: Example of a cup-shaped part

4.6.2 Case study 2: Cup-shaped part with different cavity diameters

Description: Cup-shaped part with different cavity diameters (see Figure 4.18)

Application: Packaging (+1,000,000 pieces per year)

Goal: acceptable part quality, and high part life cycle.

Decision matrix

The technique required to produce the cooling channels can be chosen by using the decision matrix shown in Table 4.1:

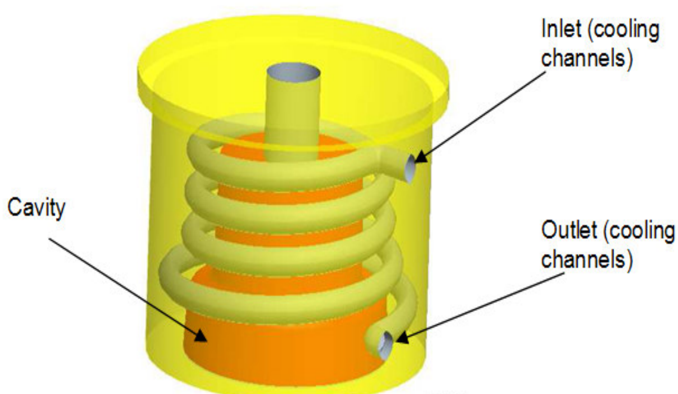

Figure 4.18: Spiral cooling channel in cavity with different diameters

Part complexity is medium, thus $Z_{12} = 2$

Space available for the cooling channels is medium, thus $Z_{22} = 2$

Quality requirement for the moulded part is medium, thus $Z_{32} = 2$

Production volume required is high, thus $Z_{43} = 3$

Moulded product life cycle is long, thus $Z_{53} = 3$

Thus from equation (4.2)

$S = 2.2$

Therefore, the technique that should be used is the conformal cooling method.

4.6.3 Case study 3: Sunglasses insert

Description: Sunglasses insert (see Figure 4.19)

Application: Personal article (+1,000,000 pairs per year)

Goal: High surface finish, and high part life cycle.

Decision matrix

The technique required to produce the cooling channels can be chosen by using the decision matrix shown in Table 4.1:

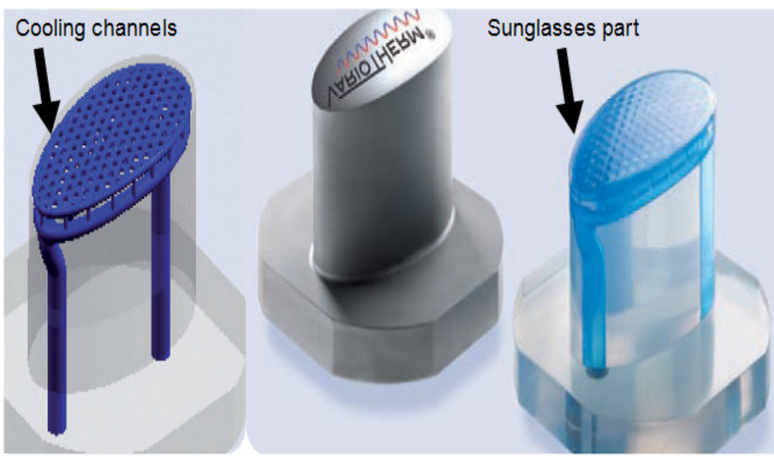

Figure 4.19: Sunglasses insert (LaserCusing, 2009)

Part complexity is high, thus $Z_{13} = 3$

Space available for the cooling channels is narrow, thus $Z_{23} = 3$

Quality requirement for the moulded part is high, thus $Z_{33} = 3$

Production volume required is high, thus $Z_{43} = 3$

Moulded product life cycle is long, thus $Z_{53} = 3$

Thus from equation (4.2)

$S = 3$

Therefore, the technique that should be used is the surface cooling method.

4.7 Summary

The methodology applicable to the mould design begins with the planning stage, to help the designer to determine the requirements that the mould must meet during its operational life cycle. The designer must consider all the factors that are critical to the mould design in order to produce the most desirable product, with acceptable cost, meeting the quality requirements.

There are many types of software on the commercial market today, such as Moldflow and Moldex3D that enable the analysis of the injection moulding process. The use of simulation in the product development process allows the designer to make most of the design changeable, at the lowest cost before manufacturing the mould.

AM technologies are currently allocated limited space in mould engineering textbooks. The most important advantage that those AM technologies provide for tool design and manufacture is extended freedom of cooling layout design, such as the conformal and surface cooling methods.

However, the manufacturing of conformal cooling and surface cooling channels with AM holds tremendous expectations, but also presents several challenges. The loose powder within the channels must be removed. This is a problem independent of the selected process. This presents also a constraint on the length and diameter of the channels, as well as a challenge in determining the point of completion of the powder removal operation. Porosity can also present serious challenges. There are some issues associated with the material properties of moulds produced by AM, such as hardness and toughness. As new materials are developed, this should improve.

The mould reliability is critical, and the structural integrity of the mould is important during the cooling design phase. There are some guidelines for the design of conventional drilled cooling layouts, but for more elaborate designs, such as conformal cooling, FEA must be used in order to ensure the reliability of the mould.

The new approach, namely proposing the use of a decision matrix to evaluate the injection moulded parts based on the manufacturing cost and the market needs, guides the designer in selecting the best cooling method required. In this way the mould designer can develop and evaluate different scenarios, taking in account cost and productivity.

5. COOLING DESIGN METHODOLOGY VALIDATION

This chapter describes the implementation of the methodology of the mould cooling design. Simulation was carried out to minimise the injection moulding parameters. The surface cooling method was also simulated.

The parameters of the injection moulding process obtained from the simulation were then used in the experimental work, which was carried out to validate the cooling design methodology developed in this study.

5.1 Moulded part

The case study used as an example was a Cutlery Drainer, a household product shown in Figure 5.1. The cutlery drainer is produced by USABCO, a plastic conversion company in the Western Cape, South Africa.

The cutlery drainer is produced from Polypropylene (PP). Bubbler cooling channels were used to cool the core side, and straight cooling channels were used to cool the cavity side.

The actual cycle time required to produce the cutlery drainer with the conventional cooling insert is 26 s: open and close time together is 6 s, cooling time is 12 s, packing time is 3.5 s, filling time is 3 s and ejection time is 1.5 s.

The goal was to reduce, as much as possible, the moulding cycle time while still maintaining the quality requirements.

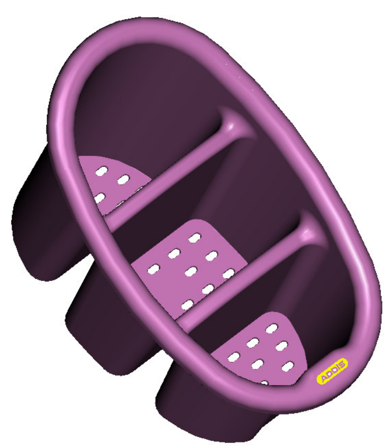

Figure 5.1: CAD model of cutlery drainer part

5.2 3D Digitising for Reverse Engineering

Reverse engineering (RE) is the process of creating a CAD model from an existing product. The process entails an object being digitised, and the data used in CAD software to generate a CAD model. Subsequently, the CAD model is used for manufacturing or other applications.

Reverse engineering is used where CAD models are unavailable, unusable, or insufficient for existing parts that must be duplicated or modified. The two key features in the RE chain are the 3D object digitisers and the surface reconstruction algorithms. Object digitisers can be classified into two broad categories: contact and non-contact (Schemenauer et al., 2002).

The 3D digitising and reconstruction of 3D shapes has numerous applications in areas that include manufacturing, virtual simulation, science, medicine and consumer marketing. Further related applications include, but are not limited to: tool making, product design and modification, design optimisation, rapid prototyping, mould repair, CNC-milling, and others (GOM, 2010).

The RE can be summarised in a few simple steps:

1. Part preparation
2. Digitising
3. Refining
4. Creating 3D CAD model
5. Verification of accuracy.

The RE design rules was discussed by (Dimitrov et al., 2004). These rules are:

1. Accuracy
2. Aesthetic requirements
3. Design for manufacturing rules
4. Use standard modelling features
5. Choose good datum features
6. Maintain continuity between surface
7. File size

The cutlery drainer core insert had to be prepared, in this case, for the RE of the external features. The reason for this was that the available 3D model could not be verified to be correct. Also, the core had been polished over its long period of usage, and thus had been worn down/distorted from the original, and therefore the need arose to compare the exact new geometry and dimensions with the old.

The part had to be set up in such a way that it could be optically scanned using a GOM 3D scanner/GOM camera (GOM, 2010). The advantage of using the GOM camera is due to the fact that it can create a point cloud of a surface very quickly, in essence speeding up the RE process. The GOM accuracy is in the tolerance band of 25-30 µm, while the CMM accuracy is 3 µm. The GOM method is suitable for RE of the cutlery drainer, because it is a cosmetic item, and the accuracy is not that critical to justify the use of the CMM.

Firstly, it had to be sprayed with a developer (white powder), to prevent glare from the GOM camera projector lamp.

Secondly, it had to be covered randomly with circular reference markers, as shown in Figure 5.2, to allow cross-reference from between shots (as long as at least 3 previous markers can be seen, a new shot can be taken).

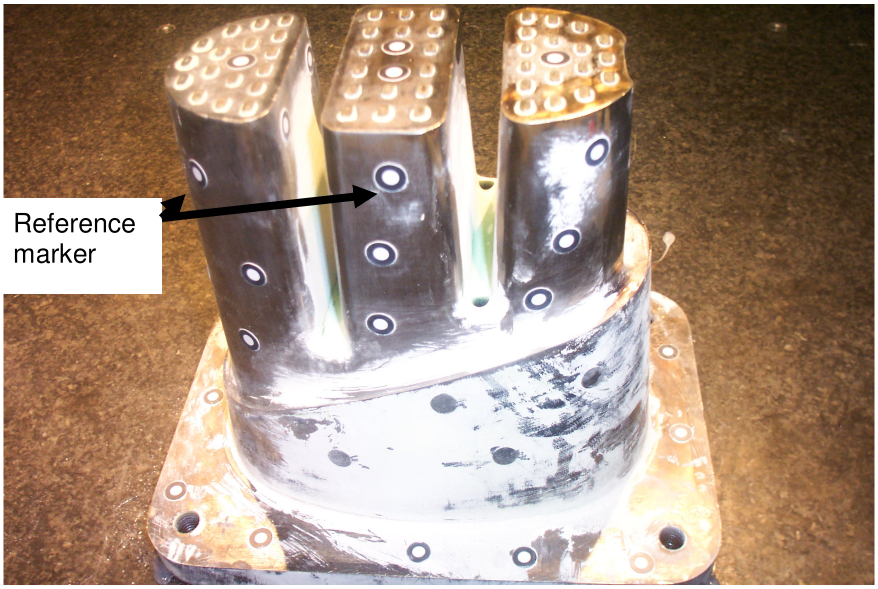

Figure 5.2: Cutlery drainer insert prepared for the GOM camera

The part was digitised using the GOM software. The scanned data was refined, and a basic 3D coordinate system set up.

The refined point cloud was exported as a STL file. The finer details, such as small holes and islands were measured on a Coordinate Measuring Machine (CMM), and exported as an .IGES file.

Delcam's CopyCAD was used to create surfaces on the point cloud. These surfaces were imported into Delcam's PowerShape, where the surfaces were refined, sharp edges and corners were created, and gaps were filled, until the model was seamless and watertight.

Thereafter, the CMM measurements were imported, and used to model the holes and small steps on top. The rectangular base of the cutlery insert was drawn. The surface model was converted to a solid part and merged with the base block, this was exported as an .IGES file, in solid form.

The GOM software was used again to check for accuracy of the RE model by importing the RE model and super-imposing it on the original scanned data. A full part inspection was then done to check for any surface deviations. Changes were corrected in PowerShape by editing the model as required. The process is repeated until a satisfactory model is generated.

5.3 Part Simulation

The cutlery drainer 3D CAD model that was created through RE was imported into the MPA Moldflow software for simulation.

5.3.1 Optimisation of injection moulding parameters

One of the first simulations that should be performed in Moldflow is the moulding window analysis (Shoemaker, 2006). The result enables the user to determine the optimal injection parameters, such as melt temperature, mould temperature, and injection time. The result of the cutlery drainer analysis (Figure 5.3) shows that a most favourable melt temperature of 241.1 ℃ should be used together with a mould temperature of 51.1 ℃, and that the injection time is 0.67 s.

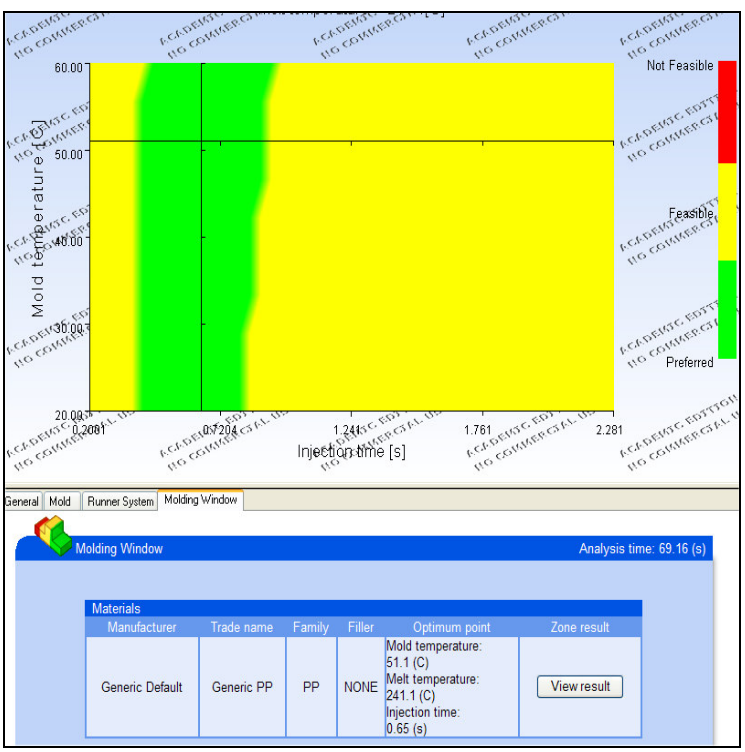

Figure 5.3: Moulding window result of the cutlery drainer

5.3.2 Minimising of filling time

The fill time result shows the path that the molten plastic takes through the part, and how long it takes to fill. In this result, all areas of the part that are filled at the same time are given the same colour contour.

The areas of the part that fill first are given a red contour, while those that fill last are blue. Areas of the part that fail to fill appear translucent (Shoemaker, 2006). Figure 5.4 shows the time for each stage of the component, as indicated by its colour. It shows that the time for the last area is 0.76 s.

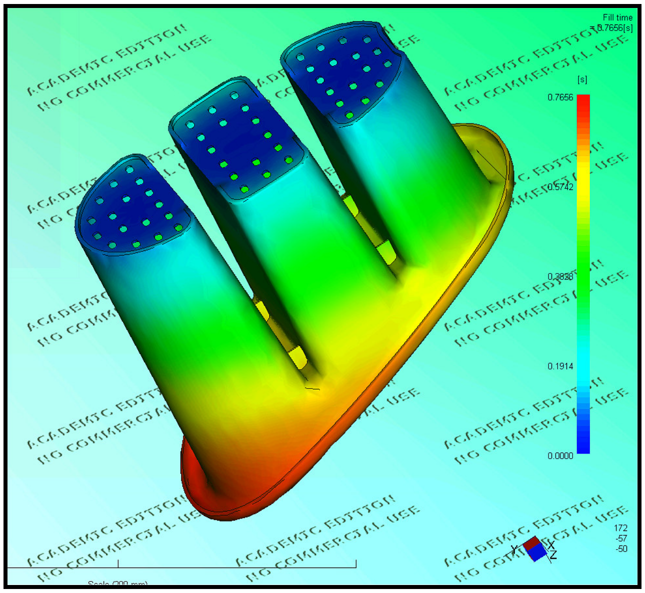

Figure 5.4: Injection time determined for the cutlery drainer part

5.3.3 Minimising of packing time

As discussed in the previous sections the packing time is the extra time required to fill more material into the mould to avoid shrinkage. The minimising of the packing time was achieved by weighing the part with different packing times, as tabullated in Table 5.1.

The packing time can be obtained when the part weight remains constant while changing the packing time. The results tabulated in Table 5.1 show that the minimum packing time is 2.5 s because after increasing the packing time to 3 s there is no change of the part weight.

Table 5.1: Minimizing the packing time

Exp no	Packing time (s)	Part weight (g)				
		Sample 1	Sample 2	Sample 3	Sample 4	Sample 5
Run 1	2	90	90	90	90	90
Run 2	2.5	95	95	95	95	95
Run 3	3	95	95	95	95	95

5.4 Cooling Channel Design

5.4.1 Determination of minimum cooling time

The most important injection moulding parameters pertaining PP that affect the injection moulding process are tabulated in Table 5.2. The melt temperature and the mould temperature were obtained from the Moldflow simulation.

Table 5.2: Optimum injection moulding parameters of PP (Shoemaker, 2006)

Parameters	Values	Units
Melting temperature (T_{melt})	241	℃
Mould temperature (T_m)	51.1	℃
Ejection temperature (T_e)	93	℃
Specific heat (C_p)	2.0934	kJ/kg/℃
Density (ρ_p)	$8.55\text{x}10^{-7}$	kg/mm^3

The experimental work was to be done at USABCO. The coolant supply from the chillier and the outside tower to the injection moulding machine are filled with water at temperatures (T_c) of 11 ℃ and 15 ℃, respectively.

The water parameters used to determine the minimum cooling time for the cutlery drainer are tabulated in Table 5.3.

Table 5.3: Water parameters used for the experimental work (Rees, 2002)

Parameters		Values	Unit
Reynolds number (R_e)		10000	-
Heat transfer coefficient (h_w)		10000	W/m^2 ℃
Viscosity (µ)	T_c = 10 ℃	$1.31\text{x}10^{-3}$	kg/m.s
	T_c = 15 ℃	$6.6\text{x}10^{-4}$	kg/m.s
Specific heat (C_c)		4.174	kJ/kg/℃

The volume (V_s) and the surface (A_s) of the cutlery drainer part are $0.0921\text{x}10^{+6}$ mm^3, $0.166\text{x}10^{+6}$ mm^2, respectively. These values were measured using the Pro-Engineer software.

The minimum cooling time considered possible to cool the cutlery drainer part was obtained by using equations (3.19) and (3.20):

Thus, from equation (3.19):

$$\tau_{Cooling\ .surface} = \frac{\rho V_s c_p}{hA_s}$$

$$\tau_{Cooling\ .surface} = \frac{8.55\,x10^{-7}\,(kg\ /\ mm^3)\,x0.0921\ x10^{+6}\,(mm^3)\,x2.0934\ (kJ\ /\ kg\ /\ °C)}{0.00001(\text{kJ}\ \ /\text{s.mm}^2.°\text{C})\ x0.166\text{x}10^{+6}\,(\text{mm}^2)} = 0.099\ \text{s}$$

And, from equation (3.20):

$$t_c = -\tau_{Cooling\ .surface}\,.\ln\left[\frac{T_e - T_c}{T_m - T_c}\right]$$

$$t_{cooling} = -0.099(s).\ln\left[\frac{(93-11)°\text{C}}{(241-11)°\text{C}}\right] = 0.1\ s \qquad \text{at } T_c = 11\ °\text{C}$$

$$t_{cooling} = -0.099(s).\ln\left[\frac{(93-15)°\text{C}}{(241-15)°\text{C}}\right] = 0.1\ s \qquad \text{at } T_c = 15\ °\text{C}$$

The strength of the proposed simple analysis vis a vie the new surface cooling technique now becomes apparent. While the analysis is approximate, it yields a benchmark, which can be used to evaluate the performance of a given injection moulding configuration.

Bearing in mind that the current cooling time is 12 s, this low value further suggests that a considerable improvement in cycle time is possible by the application of the AM technologies.

5.4.2 Evaluation of cooling channel layout

In order to design a desirable cooling method for the cutlery drainer the decision matrix was used (Table 5.4).

The part is cup-shaped with a deep core insert (Figure 5.5). The company produces about 35,000 pieces per year. They requested an improvement of mould cooling to reduce the injection cycle while still maintaining the quality requirements.

The part is of high complexity because the core is deep. The problem with the deep core insert is that it is difficult to manufacture an adequate cooling channel close to the top surface using the conventional cooling methods. With this type of mould the hottest spots are usually at the top surface of the core, in front of the gates.

The space at the top surfaces of the cutlery drainer is narrow for cooling channels with diameters > 3 mm, and therefore this component has a narrow space available for adequate cooling layout.

The quality requirements for this part do not demand precise dimensions as long as the shape is good. Therefore the quality of the part required is classified as a medium level.

The actual production volume is approximately 35,000 pieces per year, which is considered to be medium volume. However, the company's requirement was to reduce the injection moulding cycle time as much as possible to

- free the injection moulding machine for other products
- save on energy required per production unit
- free the operator for another job.

The cutlery drainer is a known product, thus the company considered to produce it with low manufacturing cost; therefore the product life cycle for the cutlery drainer is considered to be long.

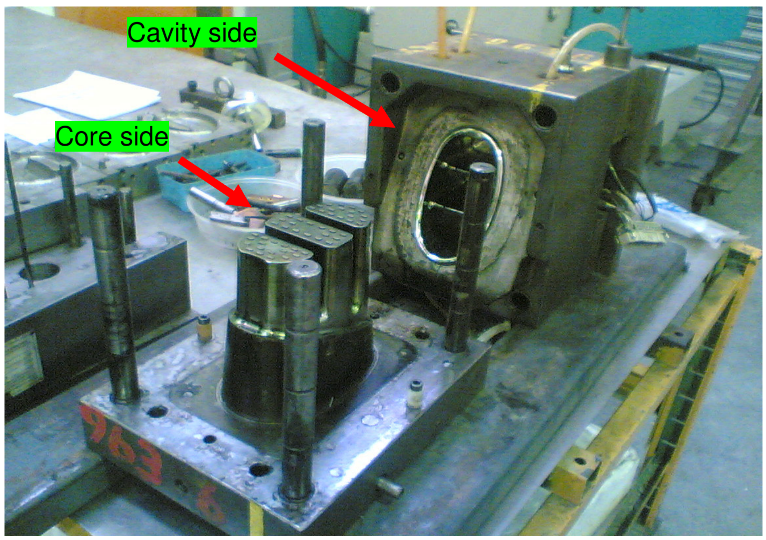

Figure 5.5: Cutlery drainer core and cavity

Table 5.4: A decision matrix used to determine the appropriate cooling method for the cutlery drainer insert

Criteria (Z)	Weight (W_e)	Levels		
Part complexity	0.34	Low	Medium	High
		1	2	3
Space available for the cooling channels	0.26	Wide	Medium	Narrow
		1	2	3
Quality requirement	0.20	Low	Medium	High
		1	2	3
Production volume	0.14	Low	Medium	High
		1	2	3
Product life cycle	0.06	Short	Medium	Long
		1	2	3

According to Table 5.4, and using equation (4.2), the output solution of the decision matrix for the cutlery drainer is:

S = (0.34 x 3) + (0.26 x 3) + (0.2 x 2) + (0.14 x 2) + (0.06 x 3) = 2.66

Therefore, the technique which should be used for such a part is the surface cooling method.

5.4.3 Design of surface cooling method

The cooling channels for the core insert of the cutlery drainer were designed with the honeycomb shape, with an approximate diameter of 2.5 mm and positioned 1.5 mm to the surface of the core insert, in order to obtain an optimum uniform cooling (Figure 5.6).

The honeycomb cooling channels connect with a number of vertical cooling channels with a diameter of 4 mm. These cooling channels are manufactured at all the core sections to obtain uniform cooling at the walls and to provide the required amount of coolant to the honeycomb cooling channels.

The vertical cooling channels are connected to the main cooling channels with a diameter of 12 mm and the branched cooling channels from the main cooling channels with a diameter of 8 mm. All the main cooling channels connect to one inlet channel and one outlet cooling channel to circulate the coolant in and out of the core insert.

It is very difficult, if not impossible to manufacture such a cooling layout using conventional methods, especially with the small cooling channels of diameters 2.5 mm and 1.5 mm close to the surface.

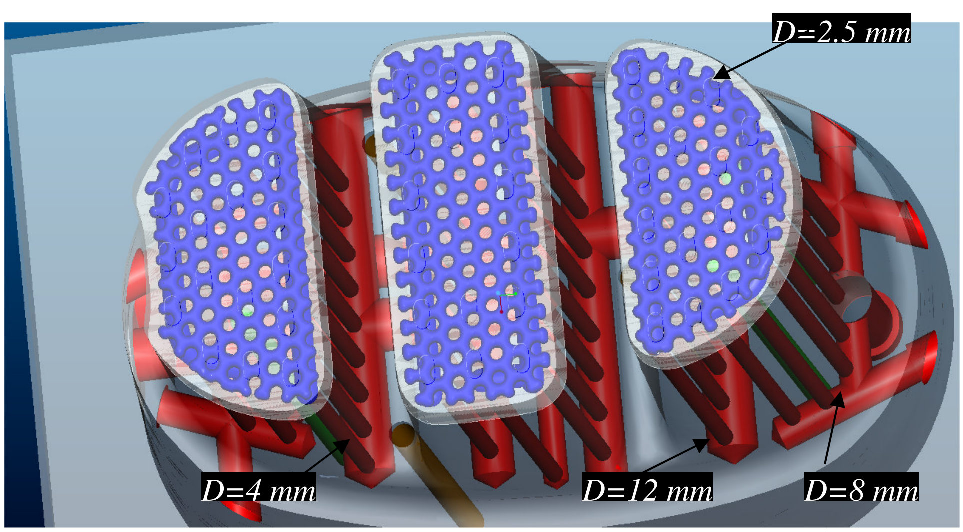

Figure 5.6: Surface cooling channels and diameters of the cutlery drainer insert

5.4.4 Determination of coolant flow rate required

For experimental purposes, the efficient cooling velocity that ensures a turbulent flow rate inside the cooling channels can be calculated using equation (5.1):

$$V = \frac{R_e.\nu}{D} \tag{5.1}$$

Different values of coolant velocities V would be obtained when changing the value of the coolant temperature. The kinematic viscosity ν of water has different values at different temperatures, as tabulated in Table 5.5:

Table 5.5: Kinematic viscosity values for pure water at different moulding temperature (Rees, 2002)

Temperature T_c (°C)	Kinematic viscosity ν (m^2/s)
10	1.3110×10^{-6}
15	1.5508×10^{-6}
20	1.0124×10^{-6}
40	0.6653×10^{-6}

<u>Conventional cooling channels</u>

Conventionally, the coolant water is circulated inside the core via a baffles system of diameter 10 mm, as can be seen in Figure 5.7.

$$V_1\,(T_c = 11\ °C \text{ and } D = 0.01\text{ m}) = \frac{10000\ x1.311\ x10^{-6}}{0.01} = 1.311\ m/s \tag{5.2}$$

$$V_2\,(T_c = 15\ °C \text{ and } D = 0.01\text{ m}) = \frac{10000\ x1.5508\ x10^{-6}}{0.01} = 1.5508\ m/s \tag{5.3}$$

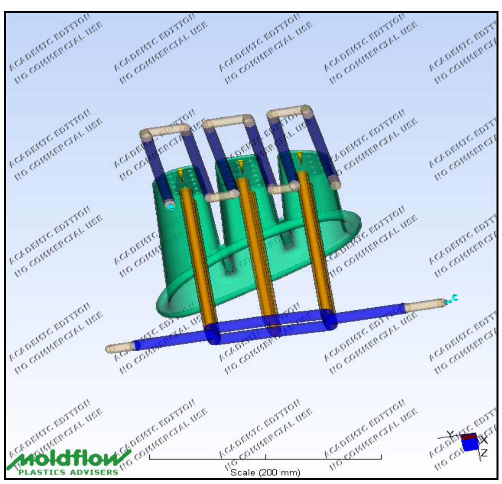

Figure 5.7: Cutlery drainer CAD model with conventional cooling method

The amount of cooling water required (FR) for one cooling channel can be calculated from equation (5.4).

$$FR = VxA_c \tag{5.4}$$

where V is the velocity and A_c is the cross-section of the cooling channels (πD^2).

$$FR_1 = V_1 x\pi D^2 = 1.311\,\pi(0.01)^2 = 0.0004\ m^3/s \approx 20.5l/\min \tag{5.5}$$

$$FR_2 = V_2 x\pi D^2 = 1.5508\ x\pi(0.01)^2 = 0.0005\ m^3/s \approx 25l/\min \tag{5.6}$$

As it can be seen from Figure 5.7, the cooling water entrance from the inlet is divided into two parallel channels, therefore the amount of cooling water required at the main inlet cooling channel is equal to twice the cooling flow rate required for one cooling channel.

$$FR_{1-inlet} = 20.5x2 = 41l/\min \tag{5.7}$$

$$FR_{2-inlet} = 25\ x2 = 50\,l/\min \tag{5.8}$$

Surface cooling channels

The coolant water is circulated through the core via one inlet connected with the main horizontal cooling channels with diameters of 12 mm and branched horizontal cooling channels with diameters of 8 mm (Figure 5.6).

All the horizontal cooling channels connected with the vertical cooling channels of diameters 4 mm provide the coolant (water) to the honeycomb cooling channels with diameters of about 2.5 mm at the top of the cutlery drainer close to the surface, at a distance of 1.5 mm.

Following the same procedure to ensure that the turbulent flow rate occurs throughout the honeycomb cooling channels with diameter of 2.5 mm, the effective velocities at different coolant temperatures can be calculated using equation (5.1), as follows:

$$V_1\,(T_c = 11\ ℃ \text{ and } D = 0.0025\text{ m}) = \frac{10000\ \ x1.311\ x10^{-6}}{0.0025} = 5.244\ m/s \tag{5.9}$$

$$V_2\,(T_c = 15\ ℃ \text{ and } D = 0.0025\text{ m}) = \frac{10000\ x1.5508\ \ x10^{-6}}{0.0025} = 6.2032\ m/s \tag{5.10}$$

Once again, cooling water FR required for one cooling channel with inlet and outlet can be calculated from equation (5.4).

$$FR_1 = V_1 x\pi D^2 = 5.244\ x\pi(0.0025)^2 = 0.0001\,m^3/s \approx 5.14\,l/\min \tag{5.11}$$

$$FR_2 = V_2 x\pi D^2 = 6.2032\,x\pi(0.0025)^2 = 0.00012\,m^3/s \approx 6.26l/\min \tag{5.12}$$

The number of cooling channels at the top of the cutlery drainer is assumed to be the sum of all the channels that have inlets and outlets that connected the vertical cooling channels together, which is about thirteen for each section. Therefore, the amount of the water that must enter the main inlet cooling channels can be calculated as follows:

$$FR_{1-inlet} = 5.14\,x13 = 66.8l/\min \tag{5.13}$$

$$FR_{2-inlet} = 6.25\,x13 = 81.25l/\min \tag{5.14}$$

5.5 Mould Cooling Simulation

It was not possible to simulate the surface cooling channels with the Moldflow software. Much time was spent on trying to simulate such cooling channels but all attempts failed.

The CAD model of the cutlery drainer insert was then sent to the Moldex3D Company to simulate the cooling channels (see Figure 5.8). However, owing the cost factor, it was difficult to carry out more simulation runs for the mould of the cutlery drainer using the optimisation parameters that were established in this study.

The parameters in the simulation were set up by a Moldex3D expert but are far from optimised. However, the results here obtained show that the Moldex3D software is capable of simulating such complex cooling channels.

The simulation was set up with the parameters as follows:

Part geometry

- Nominal thickness : 1.1 mm
- Length : 188 mm
- Width : 116 mm
- Height : 143 mm

Material (see Figure 5.8)

- Part material PP
- Mould insert material: Tool steel (1.2343)
- Mould base material: Tool steel (P20)

Process parameters

- Default cooling time: 20 s

Note: "It is obviously far more than needed. We will make a more precise prediction of the cooling time if further information is provided" (Moldex3D, 2005)

- Melt temperature: 230 °C
- Mould temperature: 40 °C
- Coolant temperature: 11 °C
- Coolant flow rate: 120 cm^3/s

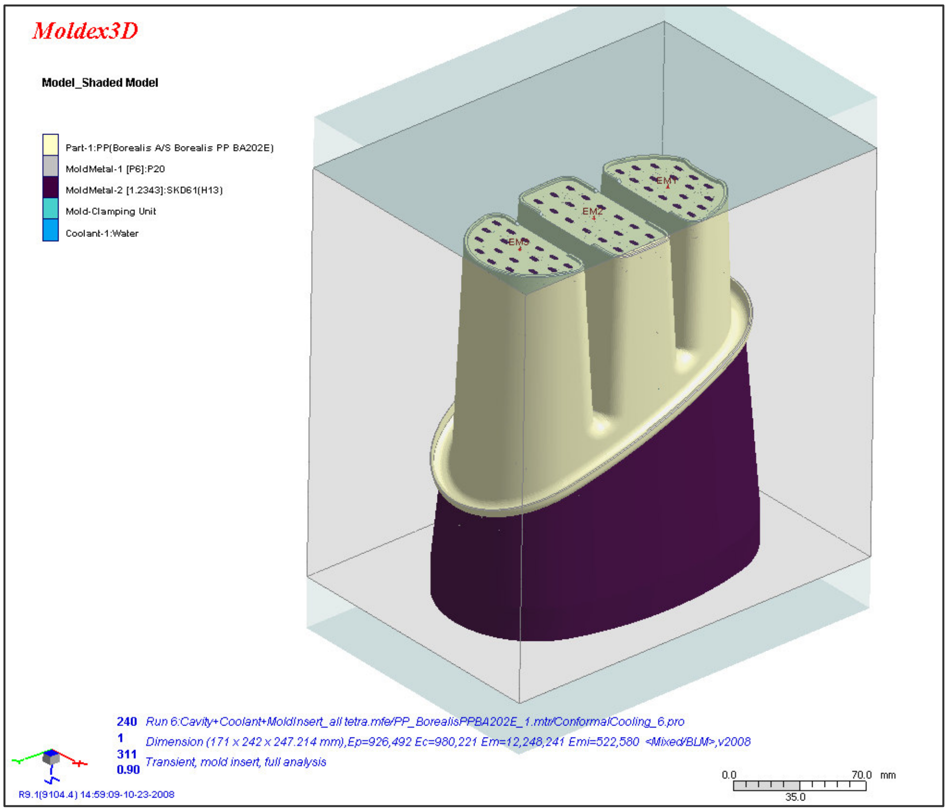

Figure 5.8: CAD model of the cutlery drainer insert using Moldex3D

The simulation took about 5 hrs to run. The results in Figure 5.9 show the temperature distribution on completion of cooling. The inner face of the part is almost completely cooled to the temperature of the coolant. This was due to the effect of the surface cooling system, which provides an extraordinarily efficient cooling.

The results in Figure 5.10 show the temperature of the coolant fluid. The heat is rapidly removed from the part, so the temperature of the coolant at the end of cooling is constant. The default cooling time is 20 s.

The results in Figure 5.11 show that 98% of the heat in the part is removed by the cooling system.

The results in Figure 5.12 show that the Reynolds number in the honeycomb section is almost 4,000 keeping the coolant in a turbulent phase.

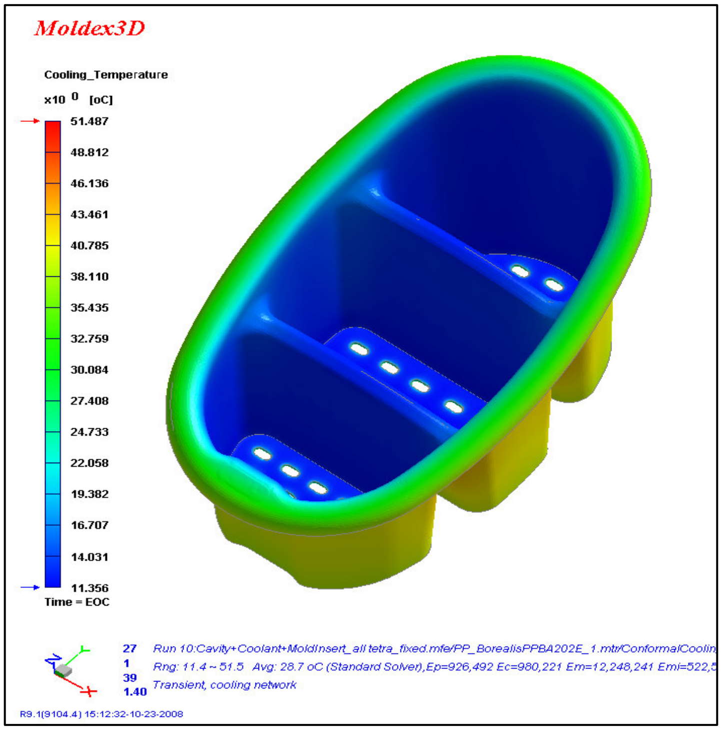

Figure 5.9: Temperature distribution using Moldex3D for the cutlery drainer part

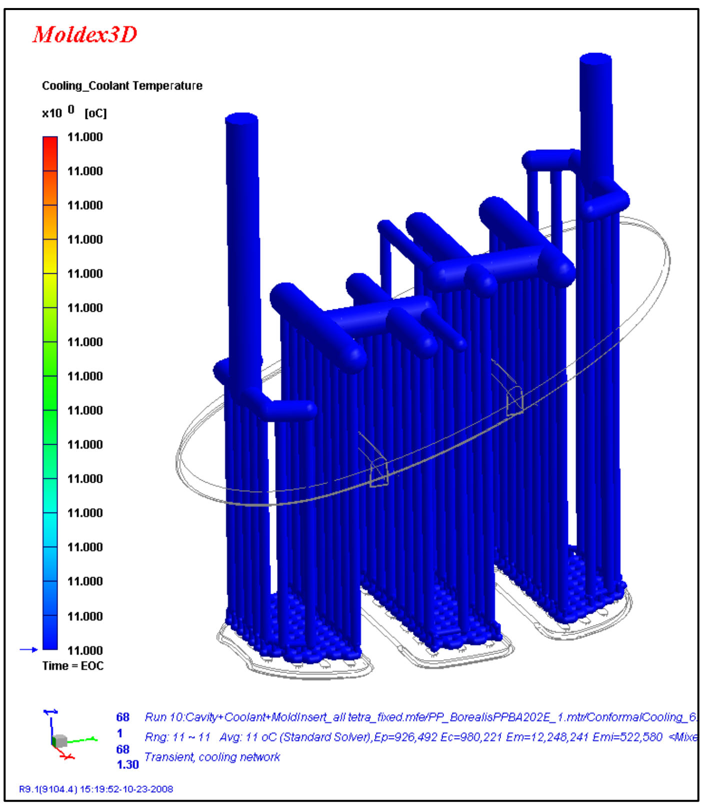

Figure 5.10: Coolant temperature using Moldex3D for the cutlery drainer part

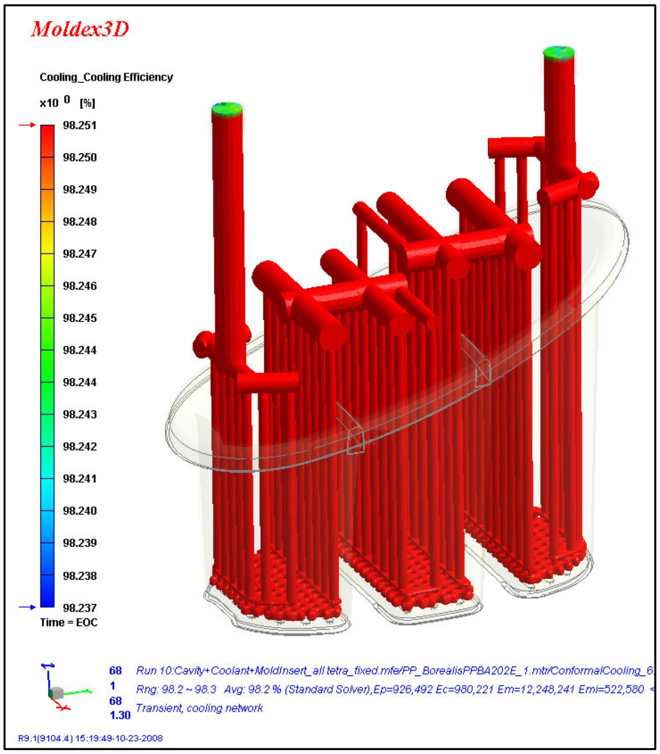

Figure 5.11: Coolant efficiency using Moldex3D for the cutlery drainer part

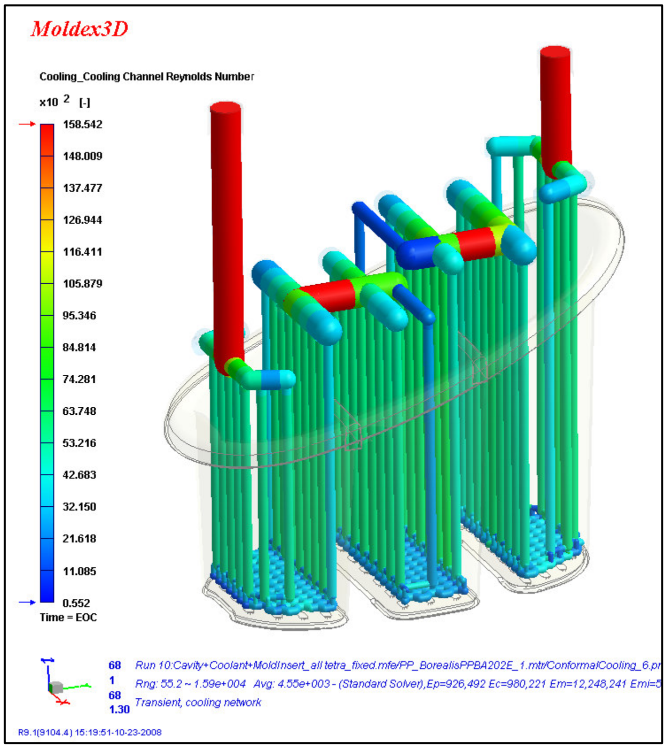

Figure 5.12: Reynolds number using Moldex3D for the cutlery drainer part

The results obtained from the cooling simulation of the cutlery drainer insert with the surface cooling method show that the use of the surface cooling method provides a uniform cooling and it efficiently removes all the heat absorbed from the molten material.

5.6 Manufacture of Surface Cooling Layout

The best way to cool the hottest spot of the cutlery drainer (top section in front of the gates) with uniform cooling and at acceptable cost was to use the hybrid method to manufacture the cooling configuration of the tooling insert.

The hybrid tooling method combines the use of drilling and milling with the advantage of the AM processes to produce cooling channels that cannot be created with drilling and milling alone.

Further advantages of using the hybrid tooling using the SLM include a reduction of production time, and saving in energy consumption.

Production time with the AM technique includes the following:

Powder deposition time

The powder depositioning time is proportional to the number of layers, and thus proportional to the built height.

Scanning time

The scanning time depends on the scan speed, scan spacing, and part dimensions.

File loading time

The file loading time depends on the part geometrical complexity, and the number of scan vectors.

Over the past decade the productivity of the AM technology has increased by a factor of 10 (Levy et al., 2003) due to higher feasible scan speeds, and with better part quality.

The production costs resulting from the use of the AM technology are mainly determined by the number of machine hours, and the material used.

The hybrid technique was used in this study, thus the cutlery drainer core was divided into two parts: the core base part and the top base part.

5.6.1 Manufacturing the core base with straight cooling channels

The base of the cutlery drainer was manufactured on a 5-axis High Speed Cutting (HSC) milling centre with drilled cooling channels as can be seen in Figure 5.13. The base was manufactured from the tool steel P20 material. The base was machined to the correct height of the parting line.

For the propose of producing the surface cooling method on the top of the cutlery drainer insert, the base was fabricated with an allowance of 0.3 mm.

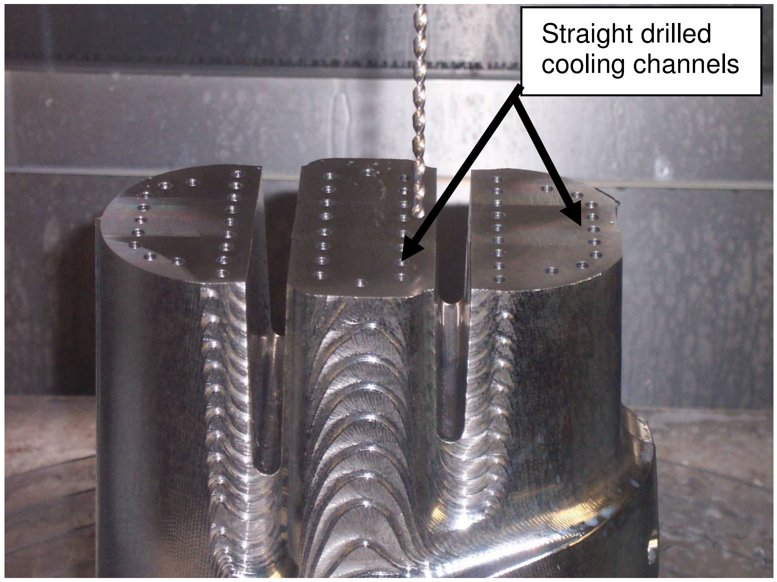

Figure 5.13: Base of cutlery drainer insert with straight cooling channels

5.6.2 Building surface cooling channels using the LaserCusing process

After producing the base insert with the vertical cooling channels the base part was placed on a LaserCusing M2 machine. Four main process parameters were selected for fabrication of the top section of the honeycomb cooling channels merged with the base of the cutlery drainer insert:

- laser power of 50 W
- layer thickness of 30 µm of about 400 slices
- scan pacing of 500 mm/s
- hatch spacing of 0.01 mm.

The starting plane of the base insert was set exactly levelled with the powder delivery system of the M2 machine. Then, in a single run, the remaining space in the build chamber was filled with tooling steel powder. The LaserCusing process was started after flushing the build chamber with nitrogen, while ensured a safe and controlled operation.

Thus the top section of the insert of about 10 mm height (Figure 5.14) was built with honeycomb cooling channels which were connected to the vertical cooling channels. The fabrication process of the top section took about 14 hours. The material used to build the top section was a tool steel powder 1.2709.

After the LaserCusing process was completed, the core insert was removed from the machine and unused powder removed from the internal cooling channels by using blowing air.

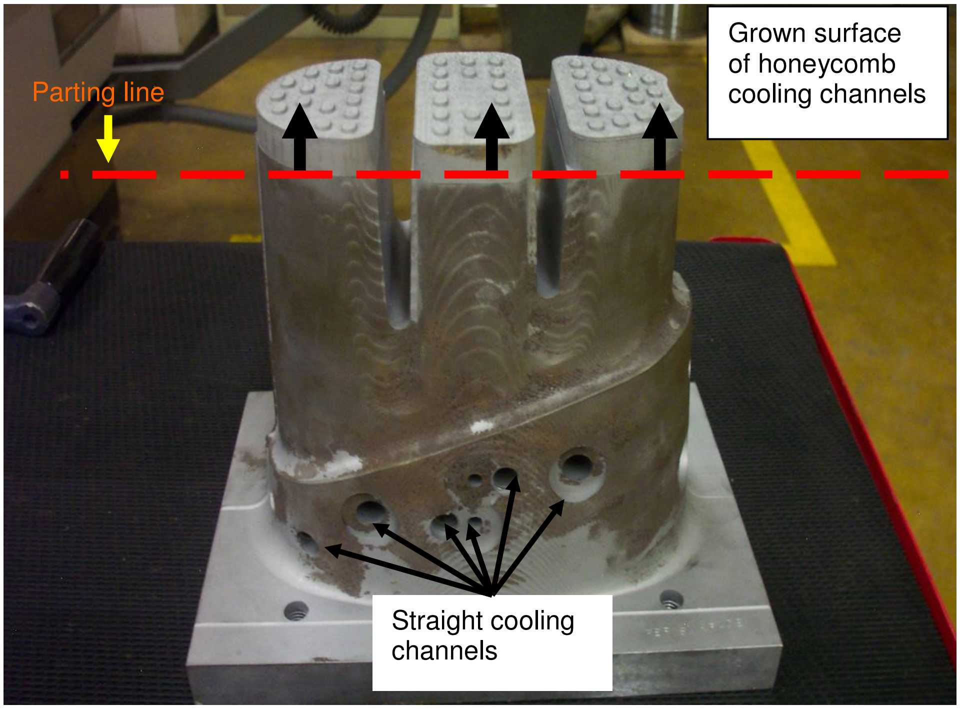

Figure 5.14: Cutlery drainer insert with grown honeycomb cooling channels

5.6.3 Manufacturing the deep slots

There is some limitation associated with using the HSM with parts that have deep slots or complex 3-D contours/profiles, as shown in the case of the cutlery drainer insert (Figure 5.15). Usually, the deep slots in the core would have to be machined using long, thin ball-nosed milling cutters, which would be prone to vibration, and result in poor surface finishes. This leads to more manual polishing, to eliminate the cutter marks. However, the risk of cutter breakage is high.

It is relatively easier to machine a copper electrode (Figure 5.16 and Figure 5.17) than to machine a deep slot into steel. The EDM process creates an advantage of securing a back-up for the process, if it is needed to be repeated, for example, during mould maintenance or for producing replicas of the same work piece.

The cutlery drainer insert was set parallel to the work table, and clamped in position by an electromagnet or mechanical clamps. The electrode was set relative to the cutlery drainer insert by alignment along the X, Y and Z axes, to position it parallel to the work table, perpendicular to the cutlery drainer insert, and simultaneously in the correct orientation to it, as well as in the correct position for the EDM process.

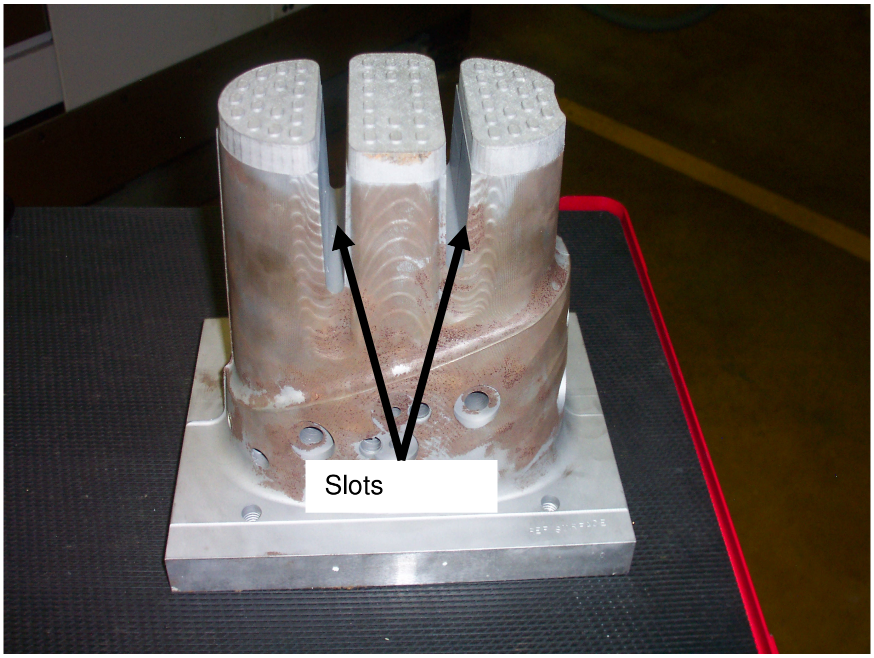

Figure 5.15: Slots in the cutlery drainer insert

Figure 5.16: Copper electrode used to machine the slots in the cutlery drainer

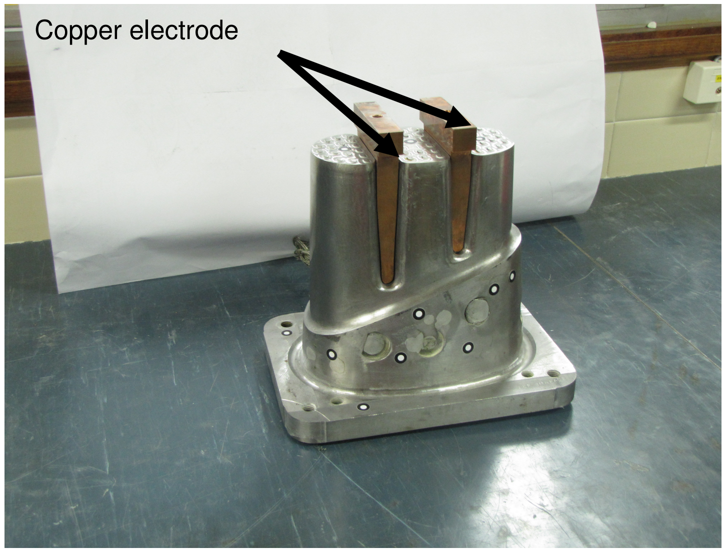

Figure 5.17: Cutlery drainer insert with copper electrodes

5.6.4 Surface finish

After building the top part with the honeycomb cooling channels for the cutlery drainer insert, the surface was quite rough. This is because metal powder particles are always obtained in the 'grey area', and these particles become loosely attached to the desired product. Post-processing was required; it involved milling, grinding, and even manual polishing. A total of 87 hours were depleted for machining the cutlery drainer insert including finishing programs, roughness, drilling the cooling channels.

5.6.5 Tool cost

The manufacturing cost of the cutlery drainer insert with the honeycomb cooling channels is presented in Table 5.6. It amounts to R 103,500.

Table 5.6: Manufacturing cost of the cutlery drainer insert with the honeycomb cooling channels

Process	Cost (Yadroitsev
Reverse engineering and 3D CAD modelling	5,500
Material (P20)	4,000
CAM programming	27,000
Milling, roughing, and drilling the straight cooling channels	18,000
LaserCusing (growing the honeycomb cooling channels)	22,000
EDM for removing the material from the deep slots	4,000
Polishing, assembly, and tryouts/trials	23,000
Total manufacturing cost	103,500

5.7 Design of Experiments (DOE)

Surface cooling layout was designed to increase productivity and improve moulded part quality. An experiment was designed to validate the proposed methodology in this work and determine its influence on the injection moulded part.

5.7.1 Factorial design of experiments

Statistically based DOE was first used in the early 1920s by Fisher in England. It was Fisher's idea that it is much better to vary all the factors simultaneously, in what he called a "factorial" design (Dowlatshahi, 2004).

The aim of experimental design is to minimise the number of experiments required to identify what causes are significantly related to important effects. This allows for a large number of variables to be studied and analysed just as easily and as economically as if only one variable was studied and analysed. Therefore, a decision was taken to carry out a full factorial experiment in the present study. The aim was to study the effect of the cooling layout, water temperature, and water flow rate on the injection moulded part.

There are therefore three controllable factors and, having two levels of the coolant temperature factor, two levels of the coolant flow rate factor, and five levels of the cooling cycle time factor the number of experiments was only 20 (2 x 2 x 5 = 20).

Other types of experiments such as the Taguchi and the fractional factorial are very useful when designing much bigger experiments. Since 20 experiments are not too many, a full factorial was applied.

The experiment was designed according to the calculated results from the previous sections 5.4.1 and 5.4.4. The selected variables in Table 5.7 were the settings generally used for process control.

The parameters setting values currently used for production at USABCO, and the parameters setting values used in the experiment work carried out in this study are tabulated in Table 5.7.

The values of injection time, injection pressure, and melting temperature were obtained by the simulation of the Moldflow in the previous sections 5.3.1, 5.3.2, and 5.3.3. All other values are adjusted by the machine operator.

The output of the experiment was the core insert temperature (℃) measured by thermocouples, and the deviation values (mm) of the parts from the CAD model were obtained using a Mitutoyo Bright 710 CMM.

The material used in the experiment for producing the cutlery drainer was PP.

Table 5.7: Production and experimental values of injection moulding setting

Parameters	Units	Production	Experimental
Injection time	s	3	1
Packing time	s	3.5	2.5
Opening/closing time	s	5.5	5.5
Cooling time	s	12	0 | 2 | 6 | 8 | 12
Ejection time	s	2	2
Melting temperature	°C	250	240
Coolant temperature	°C	11	11 | 15
Injection pressure	MPa	43	43

Table 5.8 shows the number of experimental runs with all the variables for the conventional cooling method that was used in the experimental work.

Table 5.8: Number of experiments with all levels in the conventional cooling method

Exp No	T_C (°C)	FR (l/min)	t_c (s)	Exp No	T_C (°C)	FR (l/min)	t_c (s)
C1	11	41	12	C11	15	41	12
C2	11	50	12	C12	15	50	12
C3	11	41	8	C13	15	41	8
C4	11	50	8	C14	15	50	8
C5	11	41	6	C15	15	41	6
C6	11	50	6	C16	15	50	6
C7	11	41	2	C17	15	41	2
C8	11	50	2	C18	15	50	2
C9	11	41	0	C19	15	41	0
C10	11	50	0	C20	15	50	0

Exp No: Experiment number FR: Flow rate

T_C: Water temperature t_c: Cooling time C: Conventional cooling method

Table 5.9 shows the number of experimental runs with all the variables for the surface cooling method that was used in the experimental work.

Table 5.9: Number of experiments with all levels in the surface cooling method

Exp No	T_C (℃)	FR (l/min)	t_c (s)	Exp No	T_C (℃)	FR (l/min)	t_c (s)
S1	11	67	12	S11	15	67	12
S2	11	81	12	S12	15	81	12
S3	11	67	8	S13	15	67	8
S4	11	81	8	S14	15	81	8
S5	11	67	6	S15	15	67	6
S6	11	81	6	S16	15	81	6
S7	11	67	2	S17	15	67	2
S8	11	81	2	S18	15	81	2
S9	11	67	0	S19	15	67	0
S10	11	81	0	S20	15	81	0

Exp No: Experiment number FR: Flow rate

T_C: Water temperature t_c: Cooling time S: Surface cooling method

5.7.2 Experimental setup

In order to measure the controllable factors described in the experimental design above, the following measuring equipment was required:

- The cooling time was set, and measured by the injection moulding machine's controller
- Flow meters were used to measure water flow
- Thermocouples were placed at specific points in both moulds, and a data logger was used to log the mould temperatures at 1 s intervals.

Thermocouples

The purpose of the thermocouples is to monitor the temperature of the mould throughout the entire experiment. The experimental thermal test involved the use of *K*-type thermocouples with diameter of 6 mm, length of 100 mm, and cable length of 1500 mm. The maximum measurement temperature was 300 ℃.

Some points were selected by means of inspection of the mould temperature. These points are illustrated in Figure 5.18.

Holes (diameter 6 mm) were drilled at these points, for the conventional core/cavity inserts from the outside of the core/cavity inserts to a depth of 5 mm, as close as possible to the surface.

A similar procedure was carried out for the surface cooling insert; the holes were drilled from the outside of the core insert to a depth of 5 mm from the surface cooling channels. Figure 5.19 illustrates how this was done for the surface cooling insert.

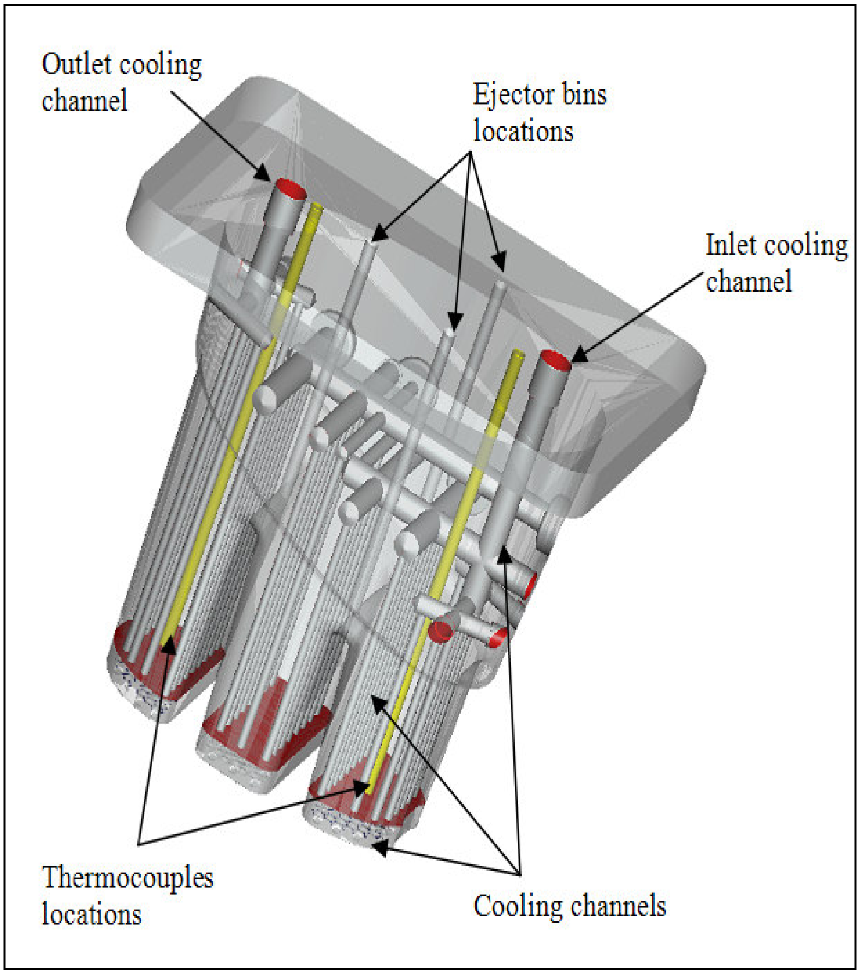

Figure 5.18: Locations of the thermocouples at the core of the cutlery drainer

Conductive grease (Figure 5.19) was inserted into the holes and the tip of the thermocouple was placed inside the conductive grease. The thermocouples were then glued in position with a strong thermally stable epoxy.

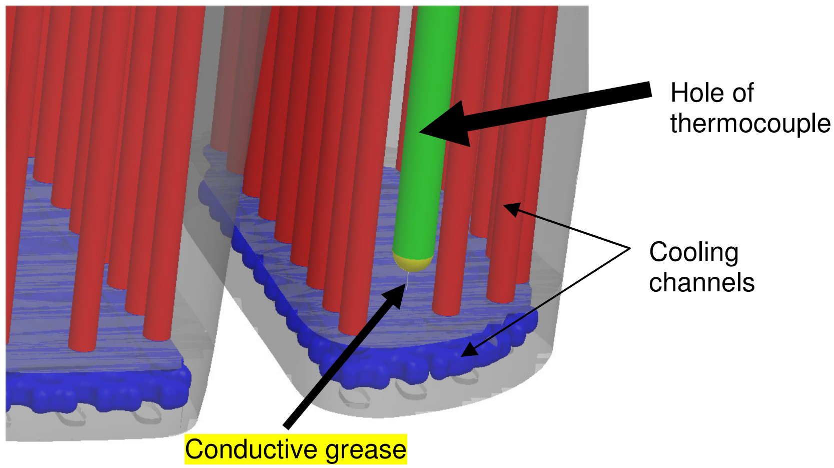

Figure 5.19: Drilled hole for thermocouple

5.7.3 Operation of the machine

The mould was installed into the injection moulding machine (Shuangma BLW358) (Figure 5.20). Ten to sixteen components were produced for each run, depending on the cooling time that was set in the machine for each run.

The coolant (water) circulated into the mould with two different temperatures from the chiller and the tower 11 °C and 15 °C, respectively. The coolant flow rate was controlled using a flow meter and stop watch.

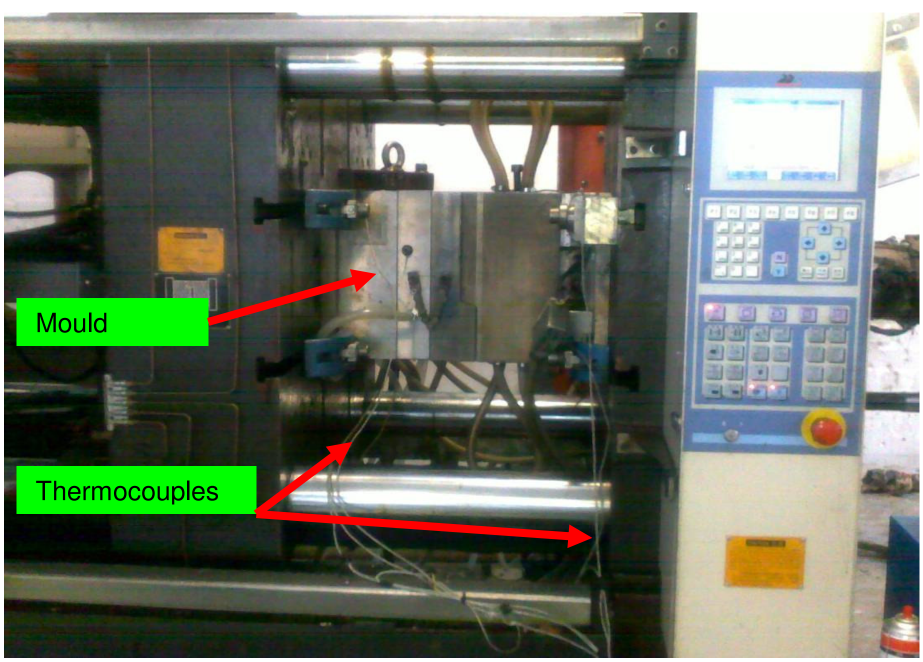

Figure 5.20: Installed mould in the injection moulding machine

6. RESULTS AND DISCUSSION

The capabilities of the different cooling layouts of the mould as well as the influence of the different variables on the production process were determined.

6.1 Mould-Wall Temperature Distribution

An infra red (IR) camera was used in this study to capture the temperature distributions around the cutlery drainer's insert. In a "dry run" two inserts were used. The conventional insert was constructed with traditional cooling channels (baffle) and the SLM insert was designed with a surface cooling insert (honeycomb channels) at the top (Figure 6.1).

The circulating water, which was set at 70 °C, was used to heat the inserts up to a higher temperature than the room temperature. This was done in order to show the speed of the heat transfer between the channels and the insert's surface. Keeping in mind that during the injection moulding cycle when chilled water is used, the cooling of the insert surface will occur. Figure 6.2 shows the temperature profile of the conventional cooling insert, with an average temperature of 30 °C at the three sections of the insert. It took about 23 s to reach this temperature.

Figure 6.3 shows the temperature profile of the surface cooling insert, with an average temperature of 40 °C. It took about 10 s to reach the temperature.

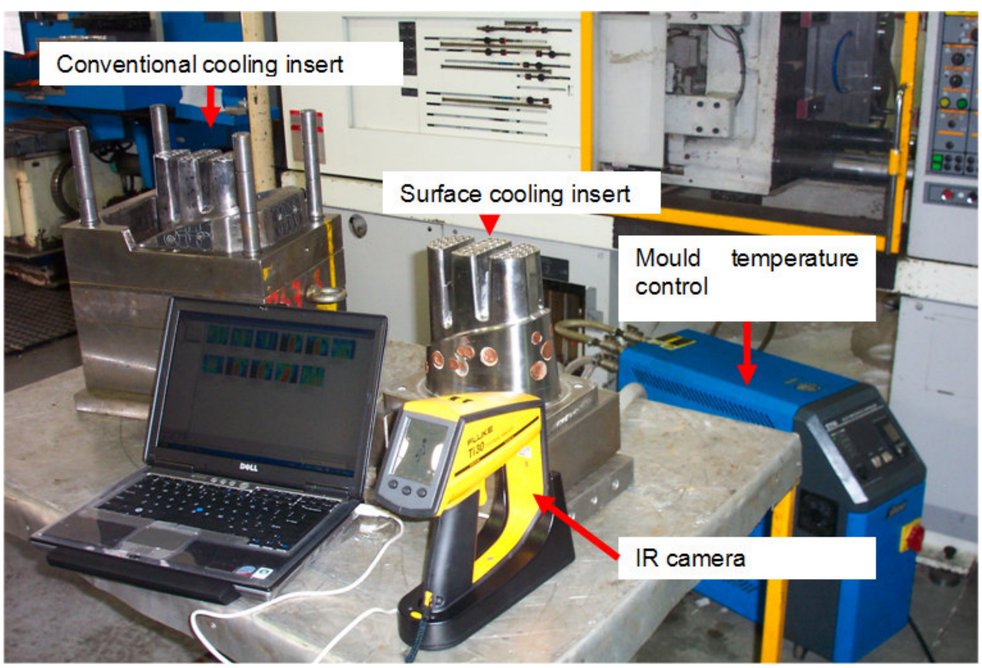

Figure 6.1: Set up used to determine mould wall temperature distribution

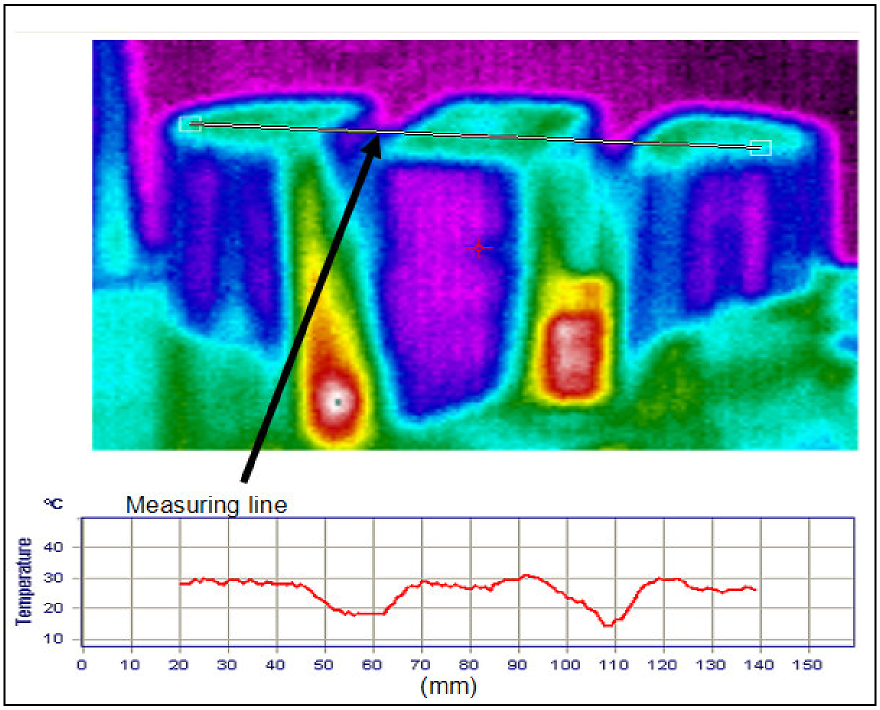

Figure 6.2: Temperature profile on the surface of the conventional cooling insert

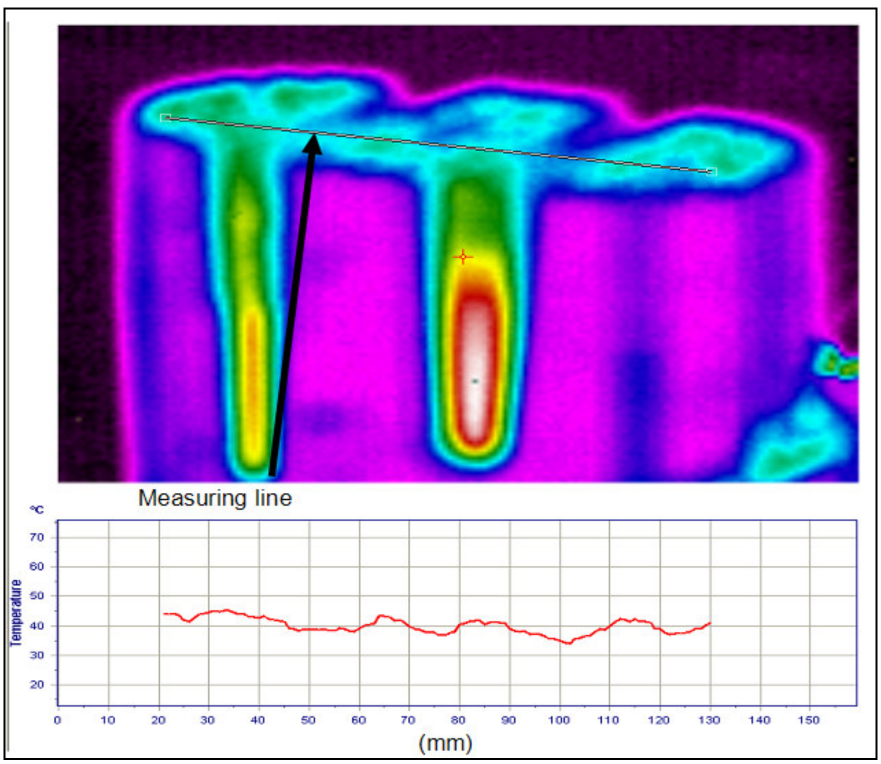

Figure 6.3: Temperature profile on the surface of the surface cooling insert

The results indicate that the insert with the honeycomb channels was able to heat up the surface of the cutlery drainer more quickly and efficiently. The surface cooling insert image showed a nearly uniform temperature distribution, which indicates better thermal management.

6.2 Mould Temperature Profile

Examples of some of the results of the mould temperature profile recorded during the experiment are plotted in Figure 6.4 and Figure 6.5. More results are shown in Appendix B.

Both moulds shown in the figures were exposed to the same conditions: a cooling time of 0 s was set on the machine, the water temperature was 15 ℃, and the water flow rate was low (41 *l/min* for the conventional cooling method and 67 *l/min* for the surface cooling method, which were determined in section 5.4.4).

It was observed that the mould in the surface cooling method reached a steady state condition after an approximate time of 60 s, while the mould in the conventional cooling method needed more time to stabilise (over 180 s).

Figure 6.4 shows that for one shot the temperature rises within 13 s and cools down within 6 s. This means that the mould needs extra time to cool down.

On the other hand, Figure 6.5 shows that for one shot the temperature rises within 8 s and cools down within 11 s. This means that the mould has sufficient time to cool down.

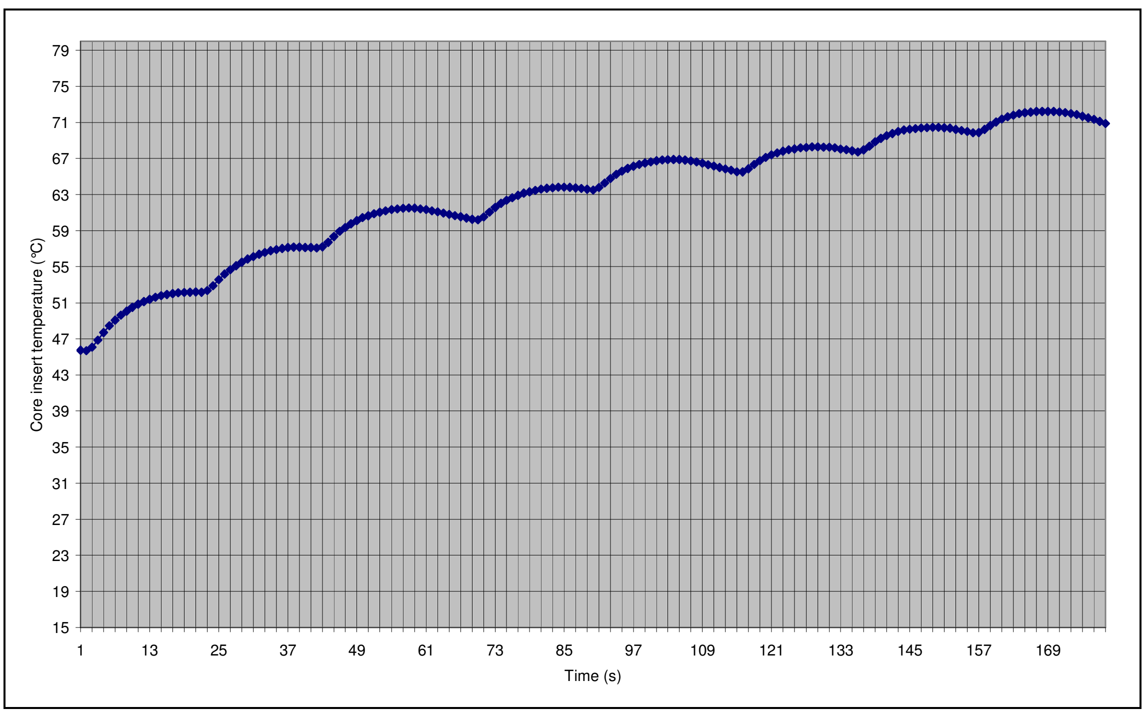

Figure 6.4: Temperature plot for conventional cooling method

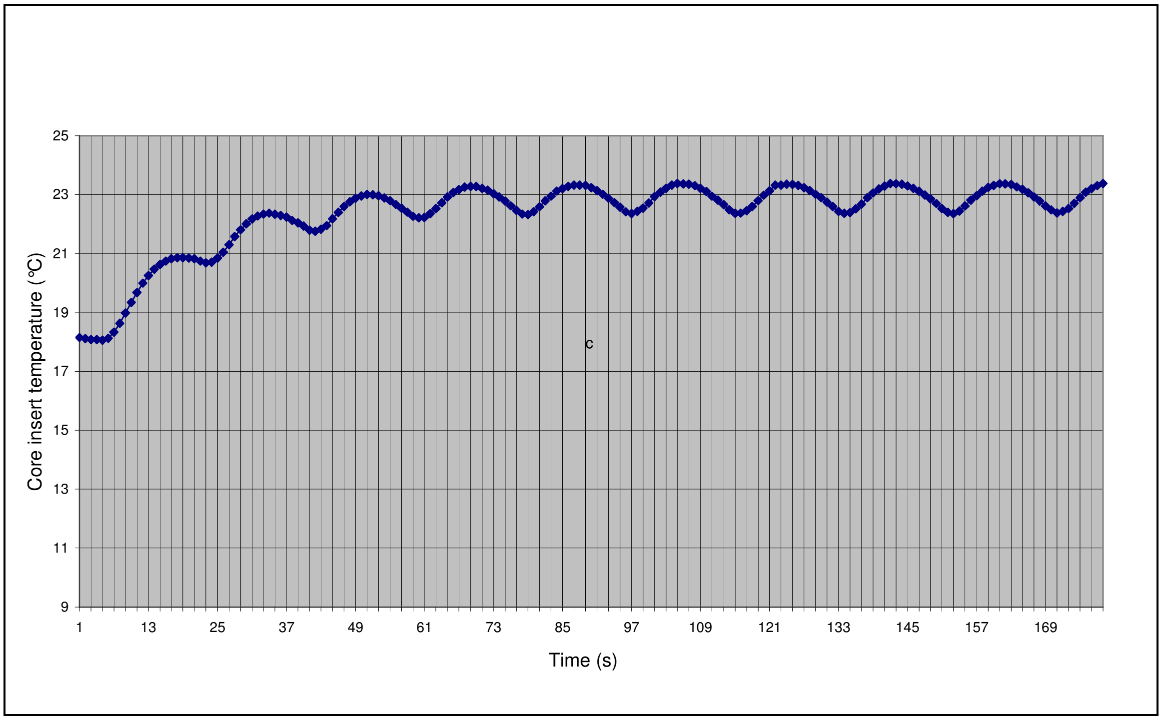

Figure 6.5: Temperature plot for surface cooling method

6.3 Mould Temperature Uniformity

Figure 6.6 and Figure 6.7 show the mean mould temperature that was recorded during the entire experiment involving both the conventional cooling mould and the surface cooling mould.

The result of the conventional cooling insert (Figure 6.6) shows that the core temperature at spot 2 has temperature of about 10 °C higher than the core temperature at the spot 1. This means that the temperature distribution within the conventional cooling method is uneven. Figure 6.6 also shows that the core side is hotter than the cavity side, which means that the part was ejected at high temperature, above 50 °C.

On the other hand, results in Figure 6.7 show that the surface cooling insert has a small difference in temperature of about 2 °C between spot 1 and spot 2 at the core side. This means that the distribution in the core is nearly uniform.

Figure 6.7 also shows that the core temperature in experiments No 11–20 is slightly higher than temperature in experiments No 1–10 due to the high temperature of the coolant that circulated through the core insert. This means that the surface cooling method is sensitive to the coolant temperature, unlike the conventional cooling method due to the long distance between the cooling channels and the cavity surface of the conventional cooling insert. This makes the cooling time longer of the conventional cooling insert than the cooling time of the surface cooling insert.

The figure also shows that the core is colder than the cavity, with a temperature difference of about 30 ℃, and thus the part is ejected at a temperature below 25 ℃. The core was cooled with surface cooling method for the whole experimental work.

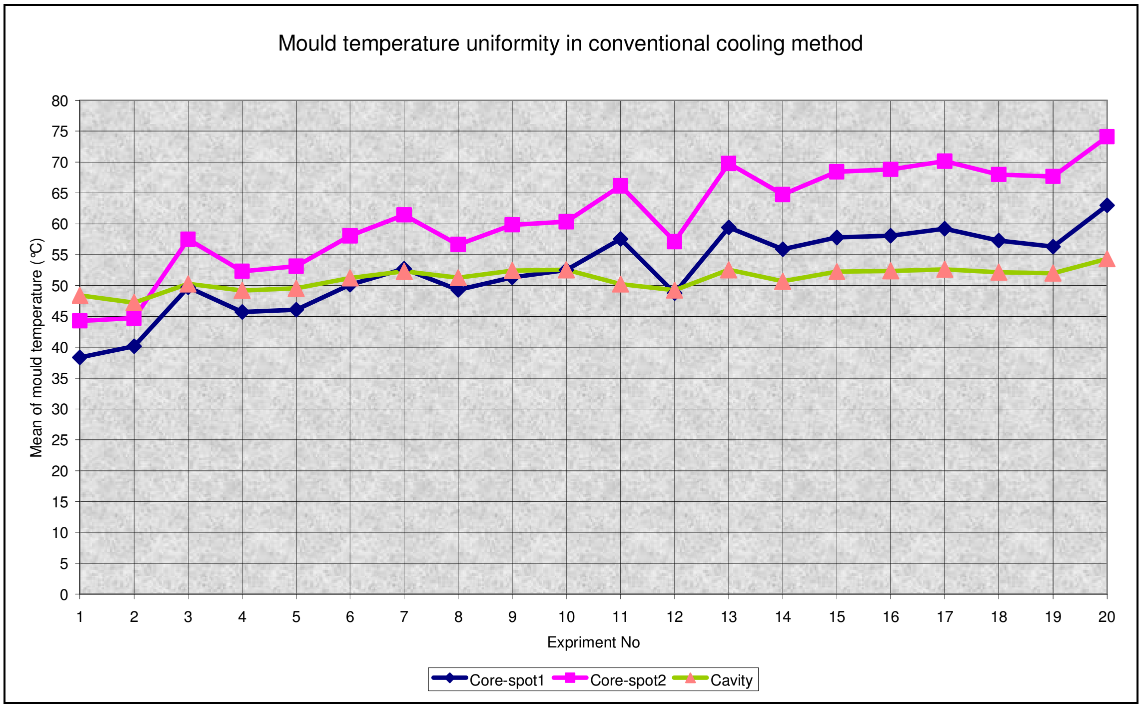

Figure 6.6: Mean of mould temperature for conventional cooling insert

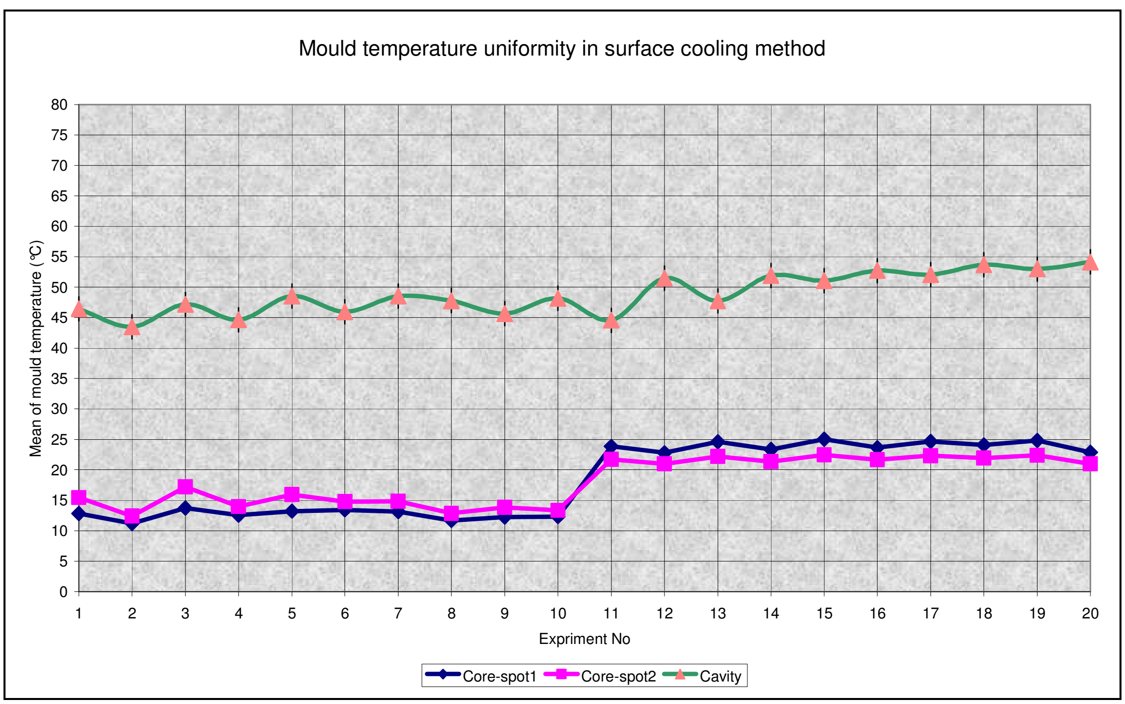

Figure 6.7: Mean of mould temperature for surface cooling insert

6.4 Quality Measurement

The capabilities of the different cooling layouts of the moulds as well as the influence of the different variables on the production process were determined. The method used to assess the quality of the produced cutlery drainer involved a comparison of the actual moulded component with its CAD model. The measurements were done on the CMM. The CMM was programmed to measure approximately 152 points on each produced part (some of the measurement points are shown in Figure 6.8).

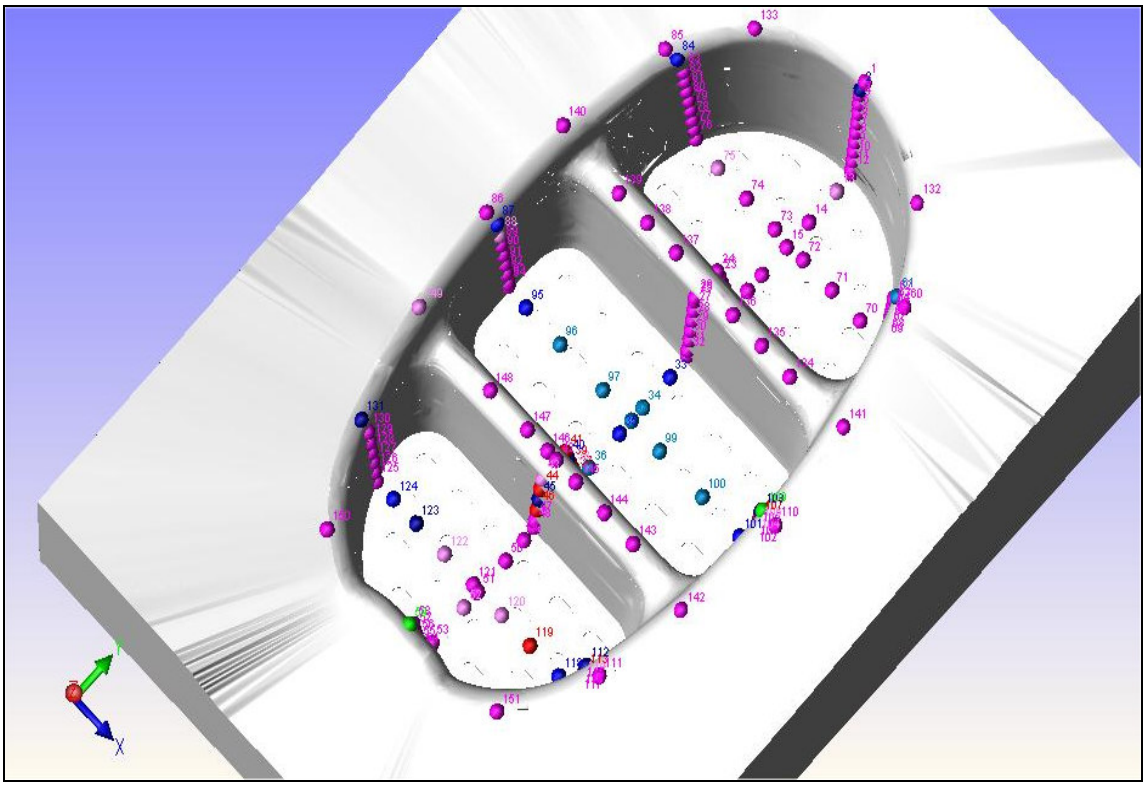

Figure 6.8: Selection of measured points on a sample cutlery drainer

The measurement data were analysed by the Two-Way Factorial Analysis of Variance (ANOVA) study (Dunn and Clarke, 1974), with confidence intervals of 0.95, using STATISTICA.

The ANOVA analysis was used to analyse the results obtained from the CMM with the factors method of cooling layouts (conventional and surface), cooling times (12, 8, 6, 2 and 0 s), coolant temperatures (11 ℃ and 15 ℃), and coolant flow rates (41 l/min and 50 l/min) for the conventional cooling layout, and (67 l/min and 81 l/min) for the surface cooling.

The ANOVA results in Table 6.1 show that no interactions are significant, and therefore, statistically, one may interpret the main effects directly.

The interactions of factors in the table would have differed significantly if the p-value was less than 0.05. (The p-value 0.05 is the significance level). The method differed significantly with a p-value of 0.000001 (F (1, 4) = 2807.5).

A comparison of the different cooling methods in the mean deviation can be seen in Figure 6.9. It is noticeable that the surface cooling method has a lesser mean deviation (0.18–0.24 mm) than the conventional cooling layout (0.26–0.41 mm). From a statistical point of view, the surface cooling method yields better quality parts than the conventional cooling method.

In Table 6.1 methods versus cooling time differ significantly (F (4, 4) = 34.270), with a p-value of 0.00237.

Table 6.1: Results from ANOVA showing the relationship between the controllable factors

	Univariate Tests of Significance for Mean deviation (Spreadsheet493 in results.stw) Sigma-restricted parameterization Effective hypothesis decomposition; Std. Error of Estimate: .0077421				
Effect	SS	Degr. of Freedom	MS	F	p
Intercept	3.092608	1	3.092608	51593.76	0.000000
Method	0.168289	1	0.168289	2807.55	0.000001
Coolant temperature (°C)	0.000571	1	0.000571	9.52	0.036748
Cooling time (sec)	0.022176	4	0.005544	92.49	0.000341
Coolant flow rate	0.000817	1	0.000817	13.63	0.020980
Method*Coolant temperature (°C)	0.000173	1	0.000173	2.89	0.164421
Method*Cooling time (sec)	0.008217	4	0.002054	34.27	0.002366
Coolant temperature (°C)*Cooling time (sec)	0.000503	4	0.000126	2.10	0.245535
Method*Coolant flow rate	0.000507	1	0.000507	8.45	0.043803
Coolant temperature (°C)*Coolant flow rate	0.000048	1	0.000048	0.80	0.421023
Cooling time (sec)*Coolant flow rate	0.000954	4	0.000239	3.98	0.104790
Method*Coolant temperature (°C)*Cooling time (sec)	0.000688	4	0.000172	2.87	0.165901
Method*Coolant temperature (°C)*Coolant flow rate	0.000001	1	0.000001	0.01	0.917337
Method*Cooling time (sec)*Coolant flow rate	0.000635	4	0.000159	2.65	0.184330
Coolant temperature (°C)*Cooling time (sec)*Coolant flow rate	0.001707	4	0.000427	7.12	0.041759
Error	0.000240	4	0.000060		

The sums of squares (SS) are shown in the first column of the data in Table 6.1, which are related to the effects. The next column lists the degree of freedom (DF) associated with the sum of squares. The next column in the ANOVA is the mean square: the SS divided by DF. The ratio of mean squares (MS_{model}/MS_{Error}) forms the F values. P is the p-value.

The difference between the cooling methods versus the cooling time can be seen in Figure 6.9: the mean deviation of the surface cooling method varies between 0.18 and 0.24 mm, while the mean deviation of the conventional cooling method differs between 0.26 and 0.41 mm. This means that the parts produced using the surface cooling method have less mean deviation than the parts produced using the conventional cooling method.

The interactions between the methods and coolant temperature do not differ significantly from each other, as noted in Figure 6.10: (F (1, 4) = 2.8888) with a p-value of 0.16442. However, the surface cooling method at the low and high coolant temperature has less deviation than the conventional cooling methods under the same coolant conditions.

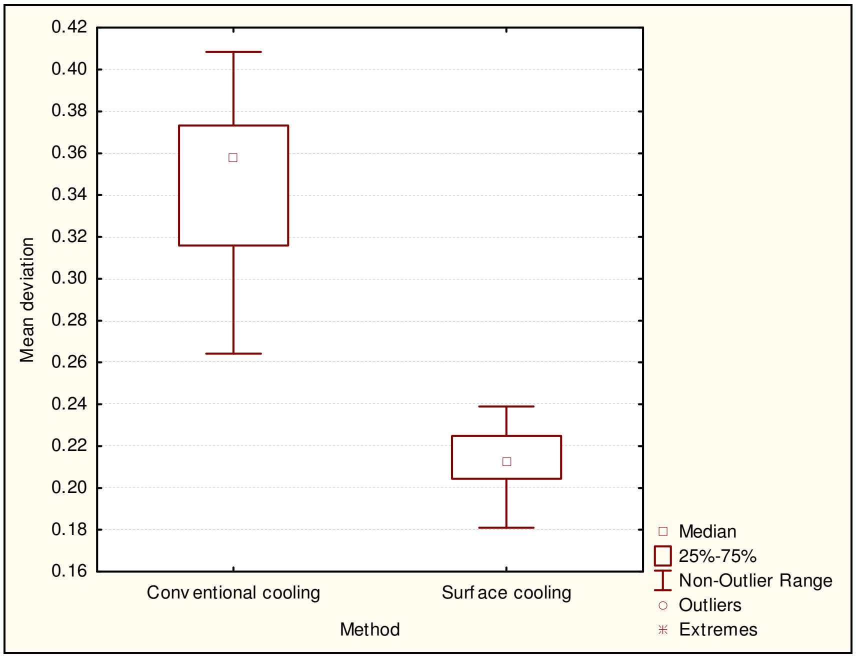

Figure 6.9: Statistical ANOVA result of values of cooling methods

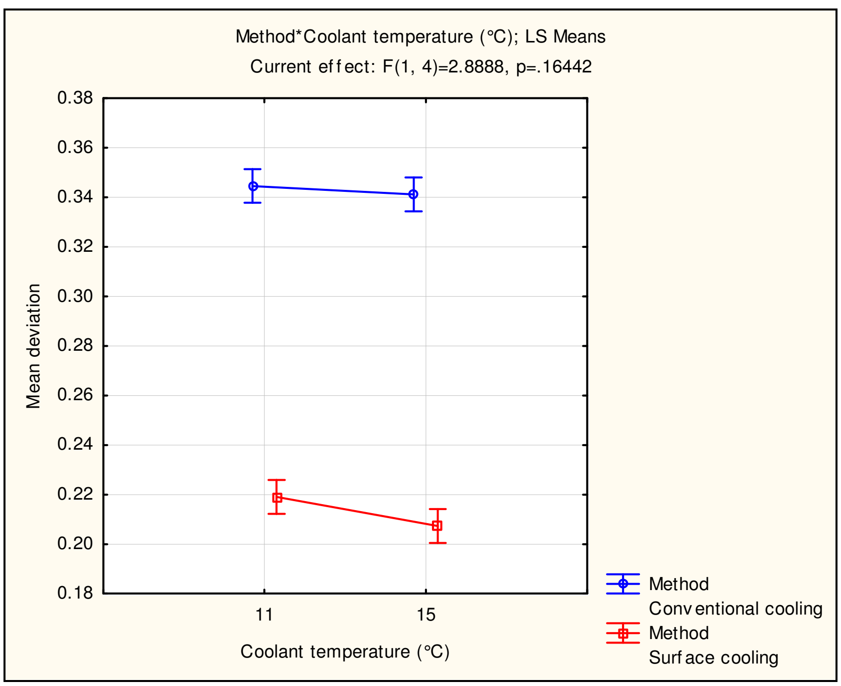

Figure 6.10: Statistical ANOVA result of values of coolant temperature against cooling methods

The method versus coolant flow rates differed significantly (F (1, 4) = 8.4515), with a p-value of 0.0438. However, the result in Figure 6.11 shows that there is no significant interaction between the conventional cooling method and the coolant flow rates with having same sign *a* for both high and low coolant flow rate.

On the other hand, the result in Figure 6.11 shows that there is significant interaction between the surface cooling method and the coolant flow rates with having different sings *b* and *c* for the low and high coolant flow rate, respectively. The higher the coolant flow rate for the surface cooling method the less mean deviation of the produced part.

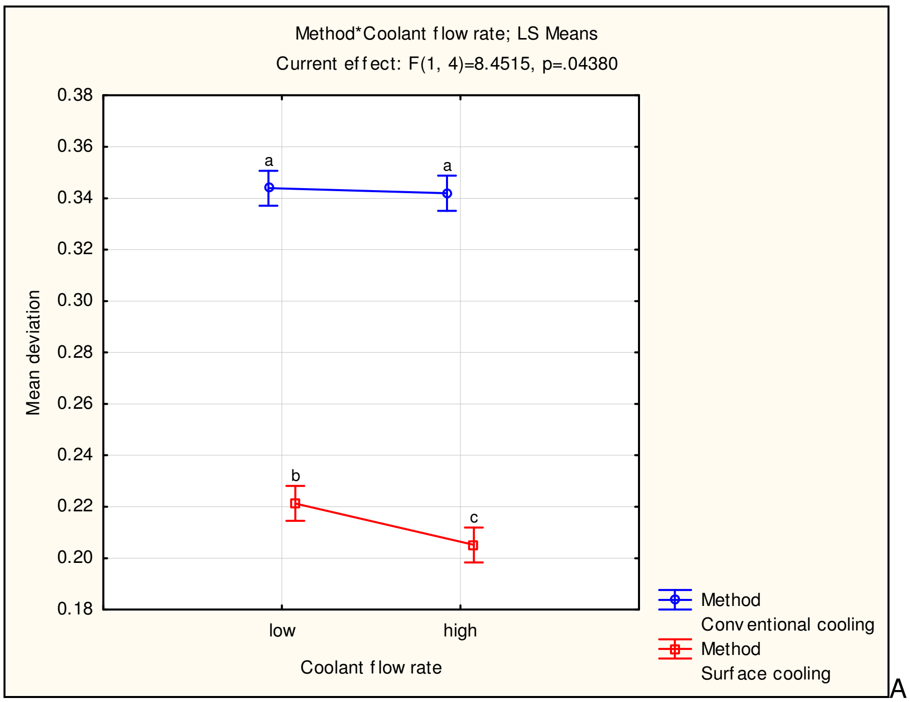

Figure 6.11: Statistical ANOVA result of values of coolant temperature

The extent of the deformation – the deviation from the CAD model - can be illustrated further by comparing the curves in Figure 6.12 to Figure 6.21. These figures are scatter plots of the total deviations between the CAD data and correlating measured points. The values on the Y-axis of each graph show the deviation from the CAD model, in millimetres. If the value is negative, it indicates that the measured point is deeper than in the CAD model.

Furthermore, by comparing the results in Figures 6.12 and 6.13, in the region of the point's number (33 to 43), (45 to 49), (71 to 75), and (84 to 98), a big difference in deviation between the surface cooling and conventional cooling method is noted. This means that the surface cooling method at cooling time of 12 s results in less deviation than the conventional cooling method.

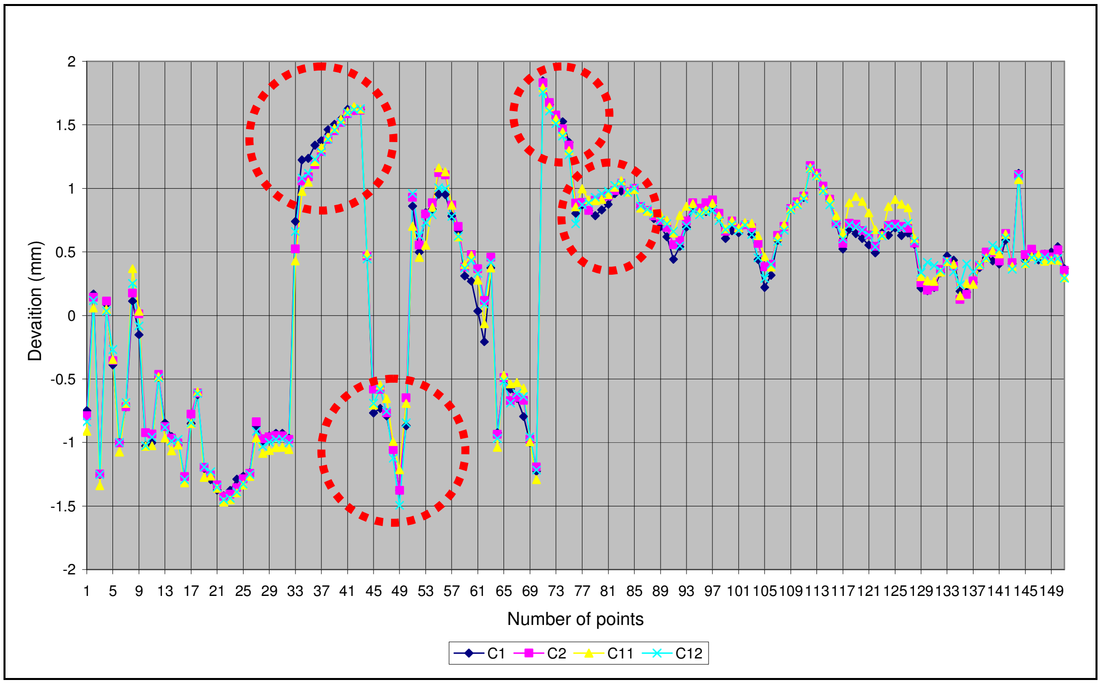

Figure 6.12: Deviation between CAD model and measured values of conventional cooling method (cooling time 12 s)

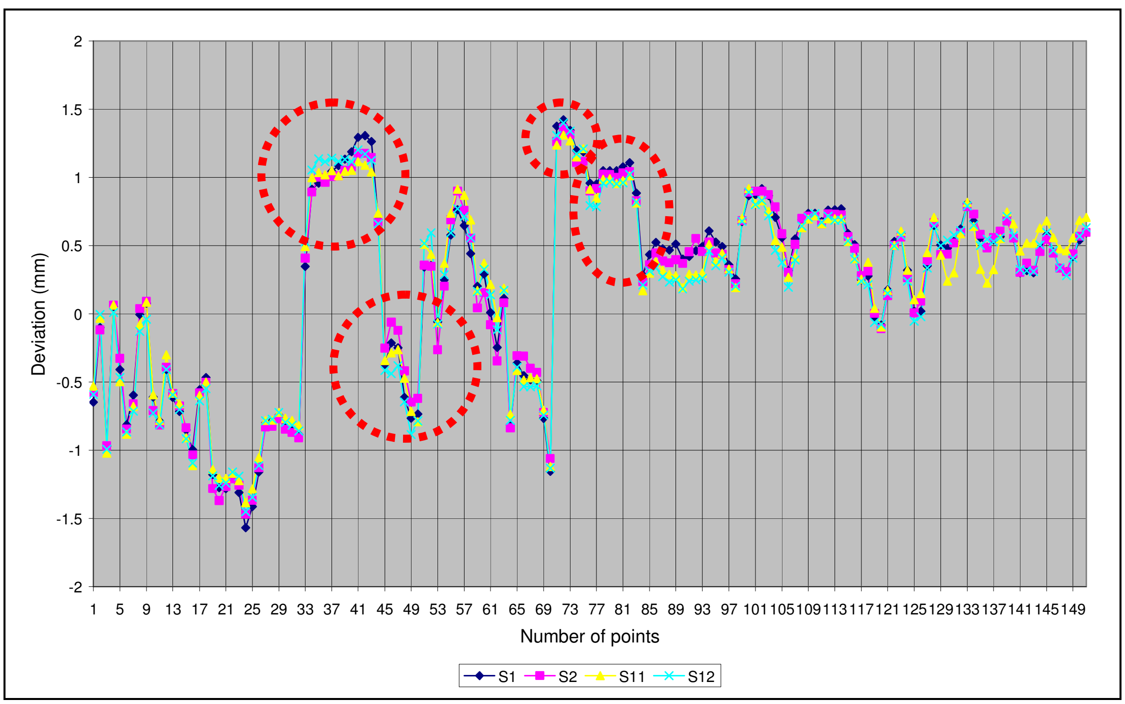

Figure 6.13: Deviation between CAD model and measured values of surface cooling method (cooling time 12 s)

At cooling time of 8 s, the comparison between the results in Figures 6.14 and 6.15, show that the surface cooling method results in less deviation than the conventional cooling method in the region of the point's number (33 to 43), (70 to 75), and (85 to 127).

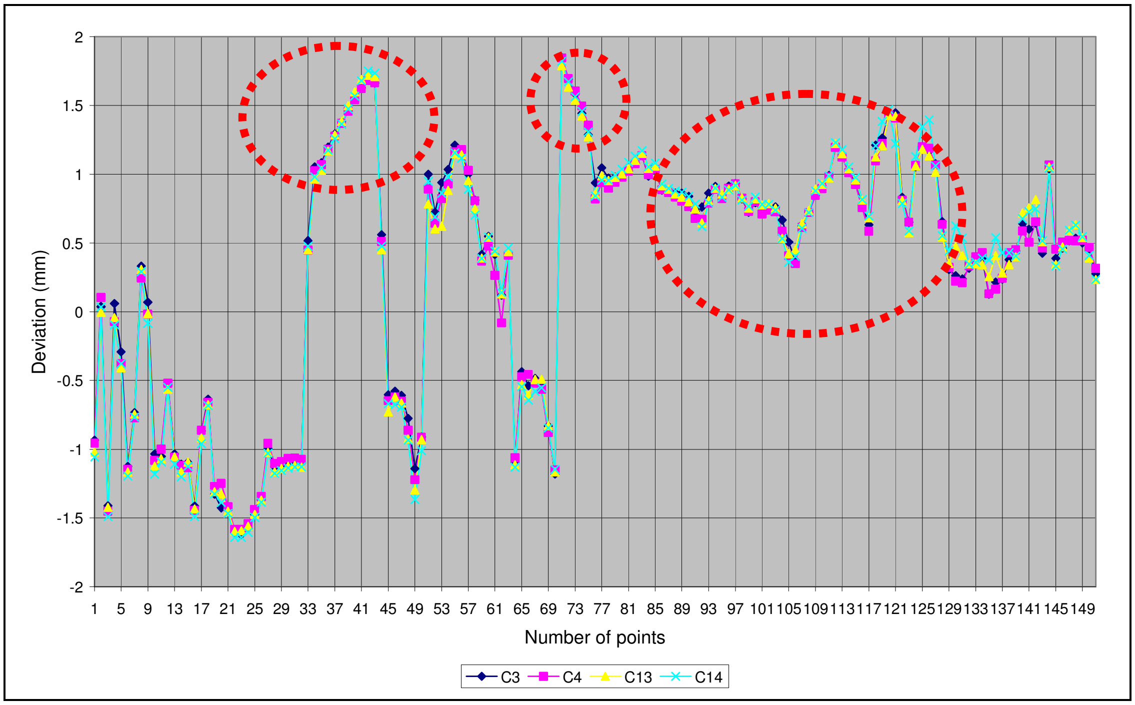

Figure 6.14: Deviation between CAD model and measured values of conventional cooling method (cooling time 8 s)

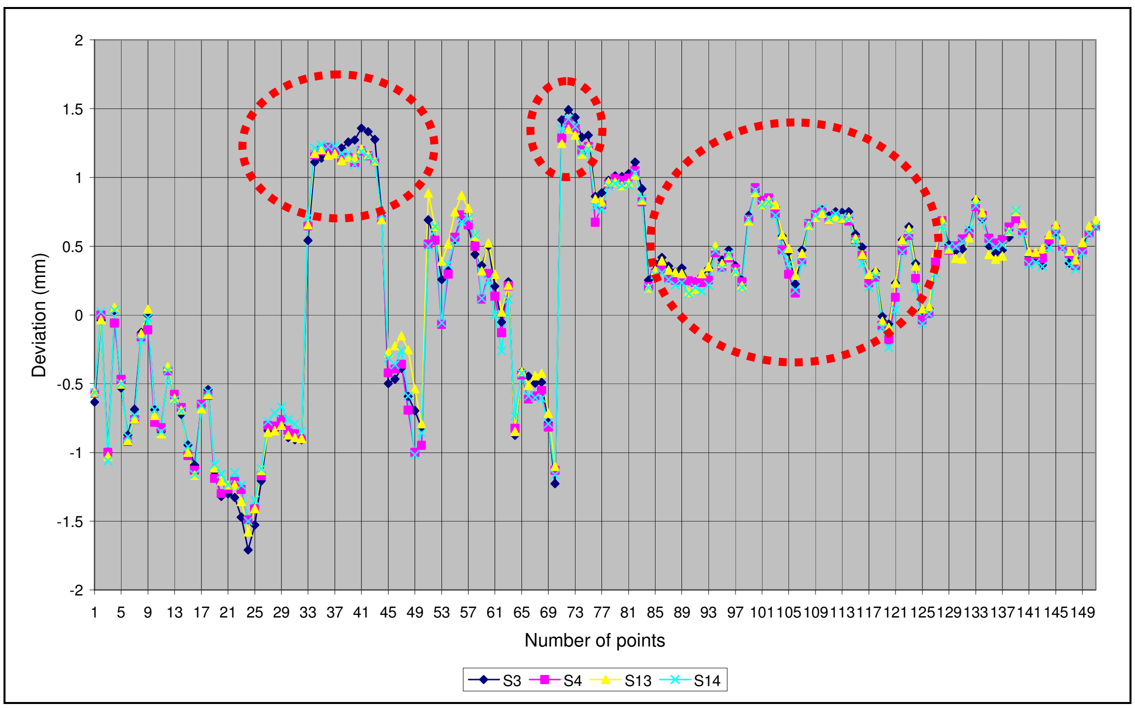

Figure 6.15: Deviation between CAD model and measured values of surface cooling method (cooling time 8 s)

For a cooling time of 6 s the results in Figures 6.16 and 6.17, show that the surface cooling method also results in less deviation than the conventional cooling method, particularly in the regions of the point's number (33 to 42), (45, 49), (50 to 61), and (85 to 129).

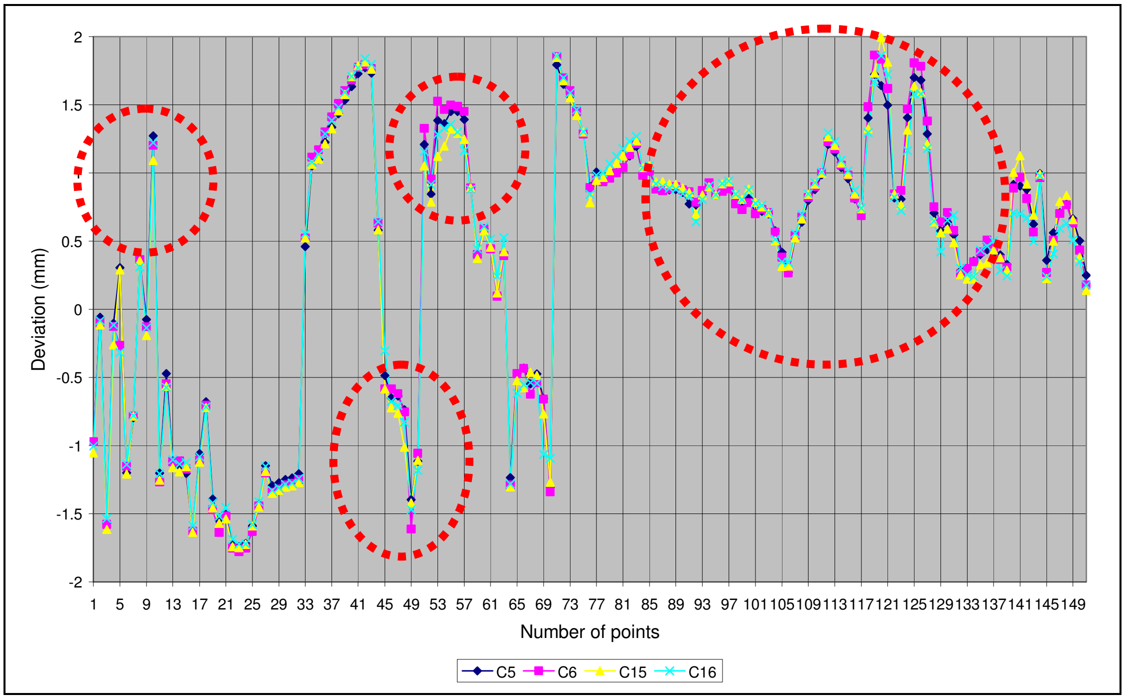

Figure 6.16: Deviation between CAD model and measured values of conventional cooling method (cooling time 6 s)

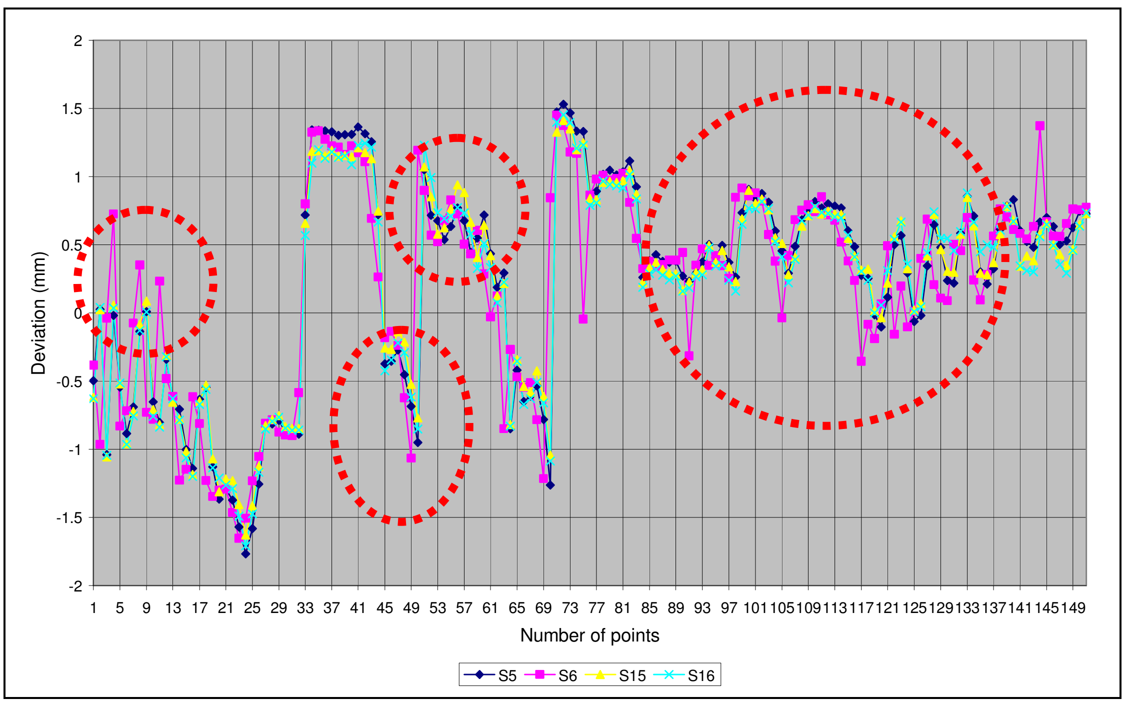

Figure 6.17: Deviation between CAD model and measured values of surface cooling method (cooling time 6 s)

The results in Figure 6.18 and 6.19 show that as the cooling time decreases as the difference in the deviation increases between the surface cooling and the conventional cooling method. The results in the figures show that the surface cooling results in less deviation than the conventional cooling method at the cooling time of 2 s, particularly in the region of the point's number (5 to 9), (45 to 49), (50 to 57), (70 to 105), and (118 to 128).

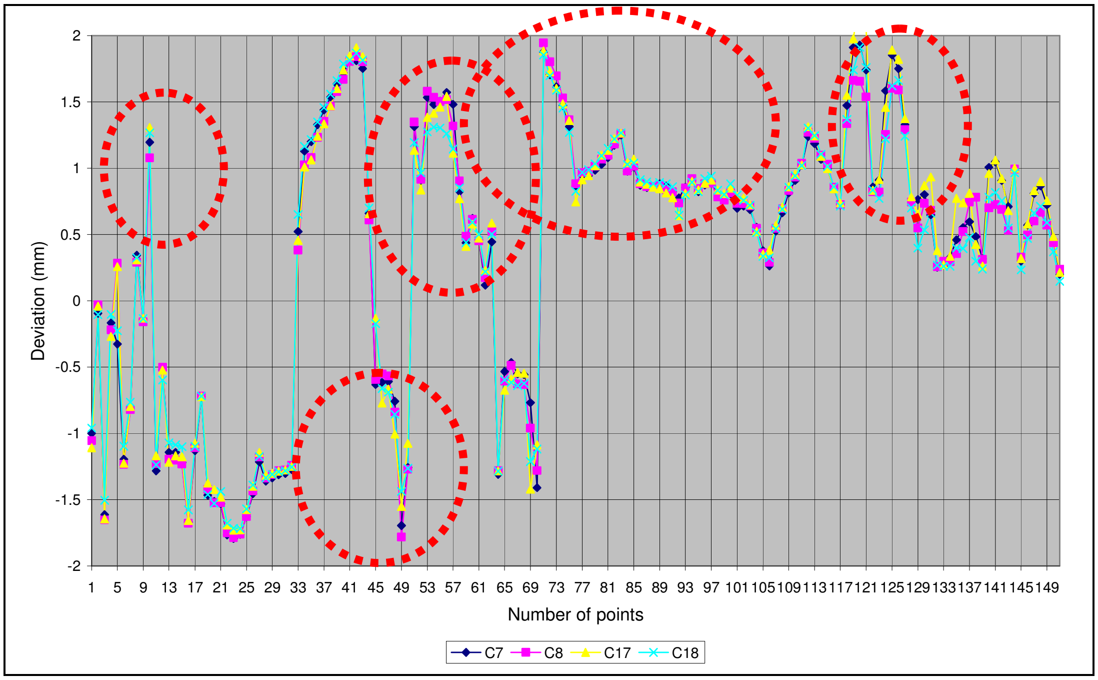

Figure 6.18: Deviation between CAD model and measured values of conventional cooling method (cooling time 2 s)

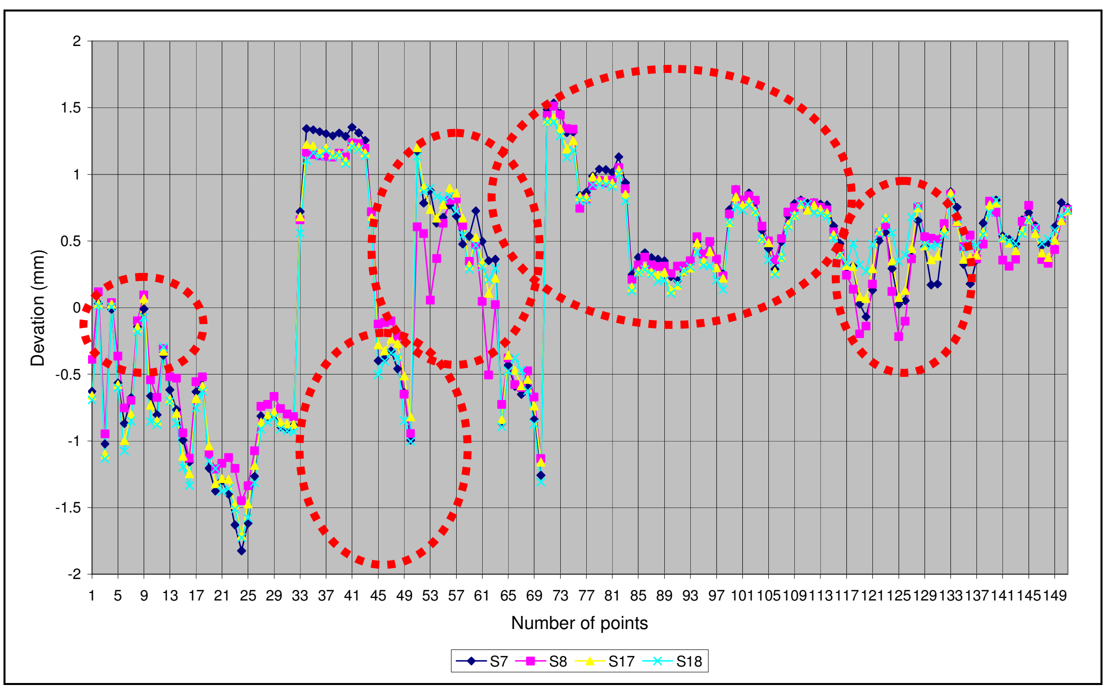

Figure 6.19: Deviation between CAD model and measured values of surface cooling method (cooling time 2 s)

Finally a cooling time of 0 s, a comparison of the deviation between the measured CAD and measured values of conventional and surface cooling is showing in Figures 6.20 and 6.21 respectively. With a cooling time of 0 s it is meant that 0 s is additionally required for cooling. The result is that there is no need for dedicated cooling after the injection and packing time. The produced parts using the surface cooling method have less mean deviation than the produced parts using the conventional cooling method. The differences in the deviation can be seen in the region of the point's number (7 to 10), (33 to 42), (45 to 49), (50 to 60), (85 to 97), and (118 to 126).

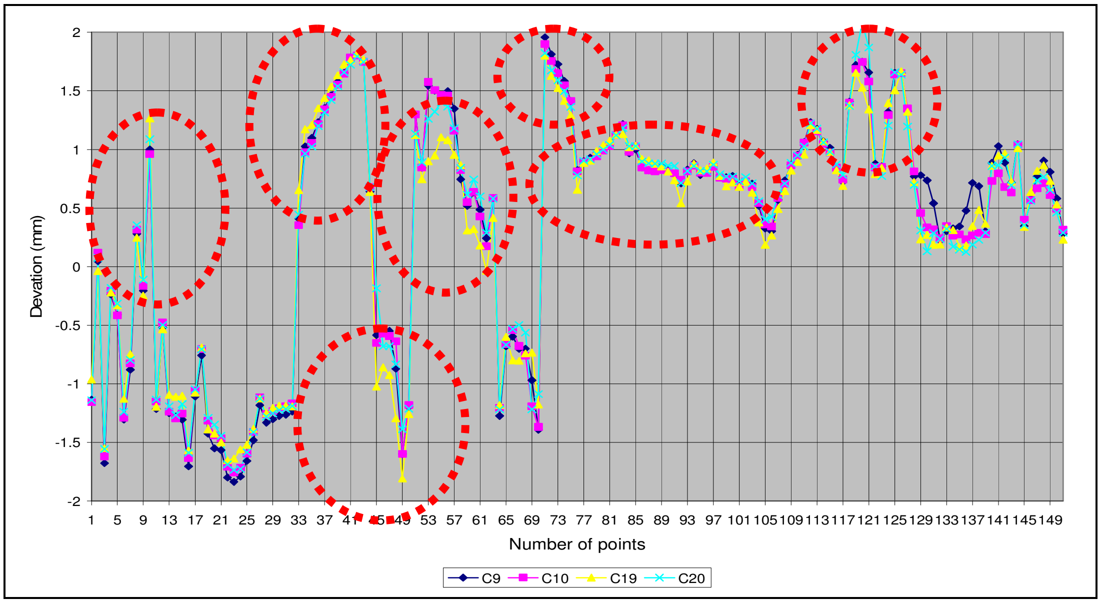

Figure 6.20: Deviation between CAD model and measured values of conventional cooling method (cooling time 0 s)

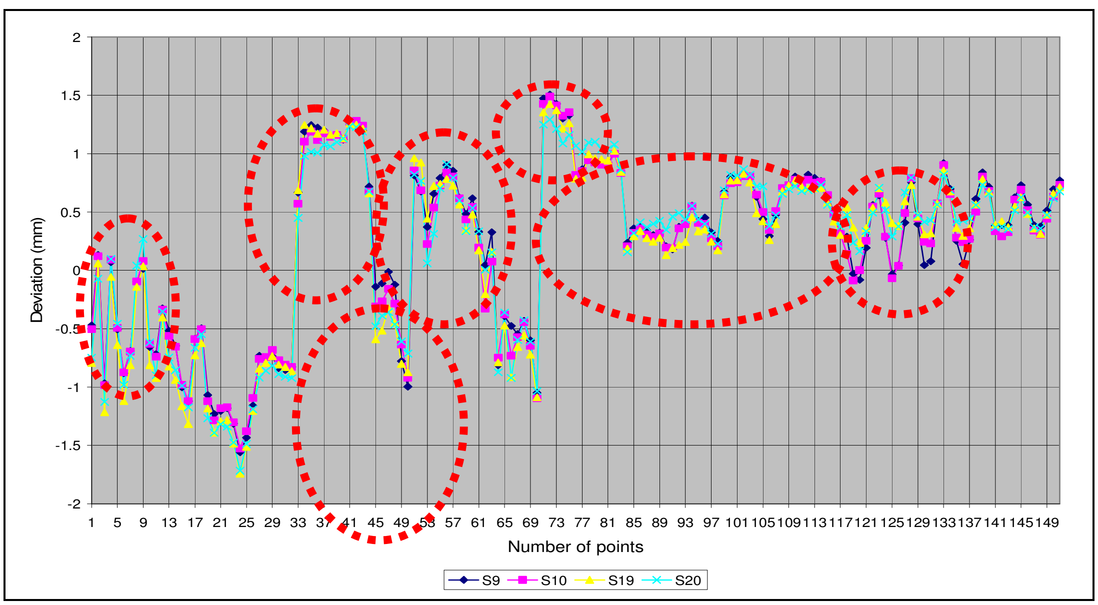

Figure 6.21: Deviation between CAD model and measured values of surface cooling method (cooling time 0 s)

Further investigations, using the mean deviation, show a clear difference when comparing the mean deviation of the surface cooling method and the mean deviation of the conventional cooling method. The comparisons are illustrated in Figure 6.23 to Figure 6.32. Measured zones are shown in Figure 6.22.

Results in Figure 6.24 show that the surface cooling method at 12 s cooling time results in less mean deviation than the conventional cooling method in Figure 6.23. Differences of deviations are clear in the regions S2, S3, S6 and B1.

In Figures 6.25 and 6.26, a comparison of the measured values at 8 s shows that the surface cooling method results in less mean deviation than the conventional cooling method, especially in the regions W3, S2, S3, S6 and B1.

For a cooling time of 6 s the results in Figures 6.27 and 6.28, show that the surface cooling method also results in less deviation than the conventional cooling method, particularly in the regions E2, W3, S2, S3, S6 and B1.

In Figures 6.29 and 6.30, the surface cooling method at a cooling time of 2 s has less mean deviation than in the case of conventional cooling method. The difference can clearly be distinguished at the regions E2, W2, W3, S2, S3, S6 and B1.

For a cooling time of 0 s, a comparison of the mean deviation between the measured CAD and measured values of conventional and surface cooling is shown in Figures 6.31 and 6.32 respectively. The produced parts using the surface cooling method have less mean deviation than the produced parts using the conventional cooling method. The differences in the deviation can be seen in the regions T1, E1, E2, W1, W2, W3, W5, S2, S3, S6 and B1.

Overall, the parts produced using the surface cooling method have better quality (less warpage and closer dimensions to the CAD model) than the parts produced using the conventional cooling method, at the same cooling time.

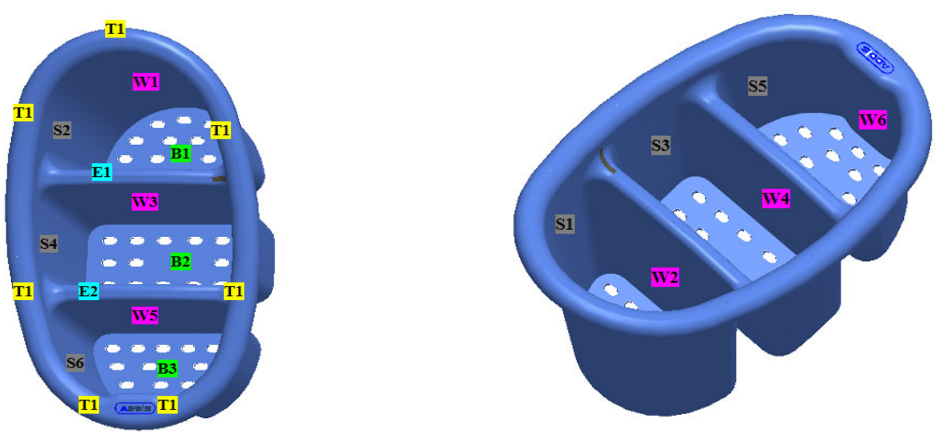

Figure 6.22: Zones where deviation values were measured on the produced parts

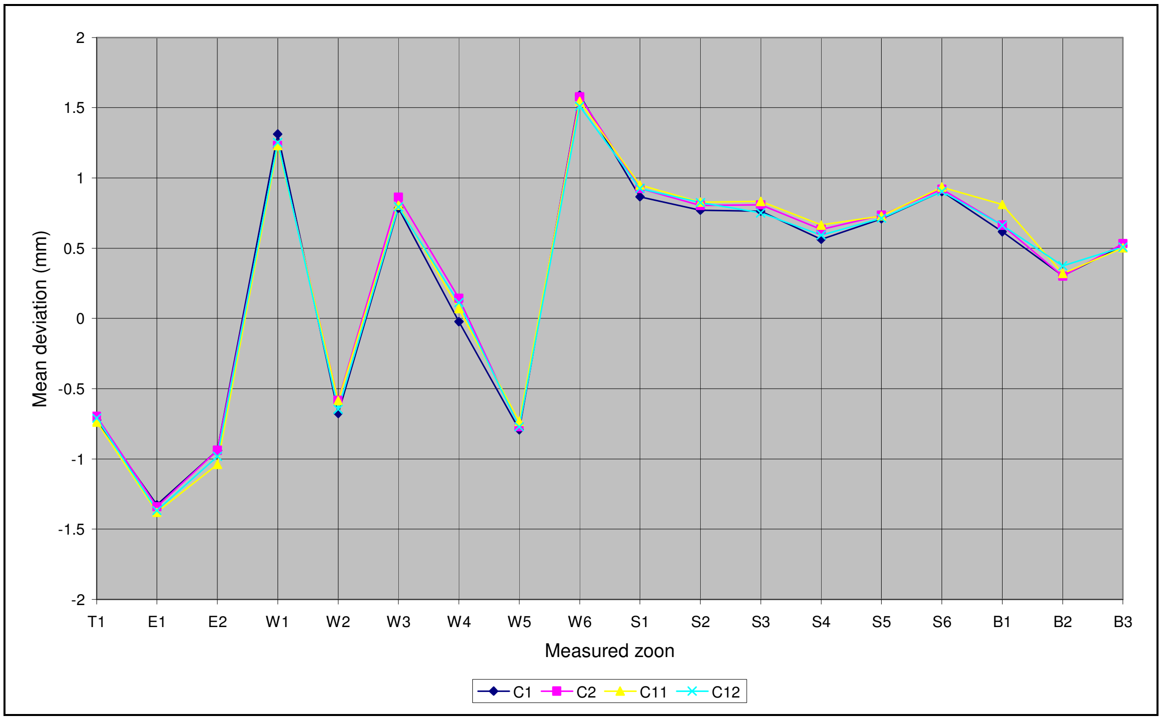

Figure 6.23: Mean deviation between CAD model and measured values of conventional cooling method (cooling time 12 s)

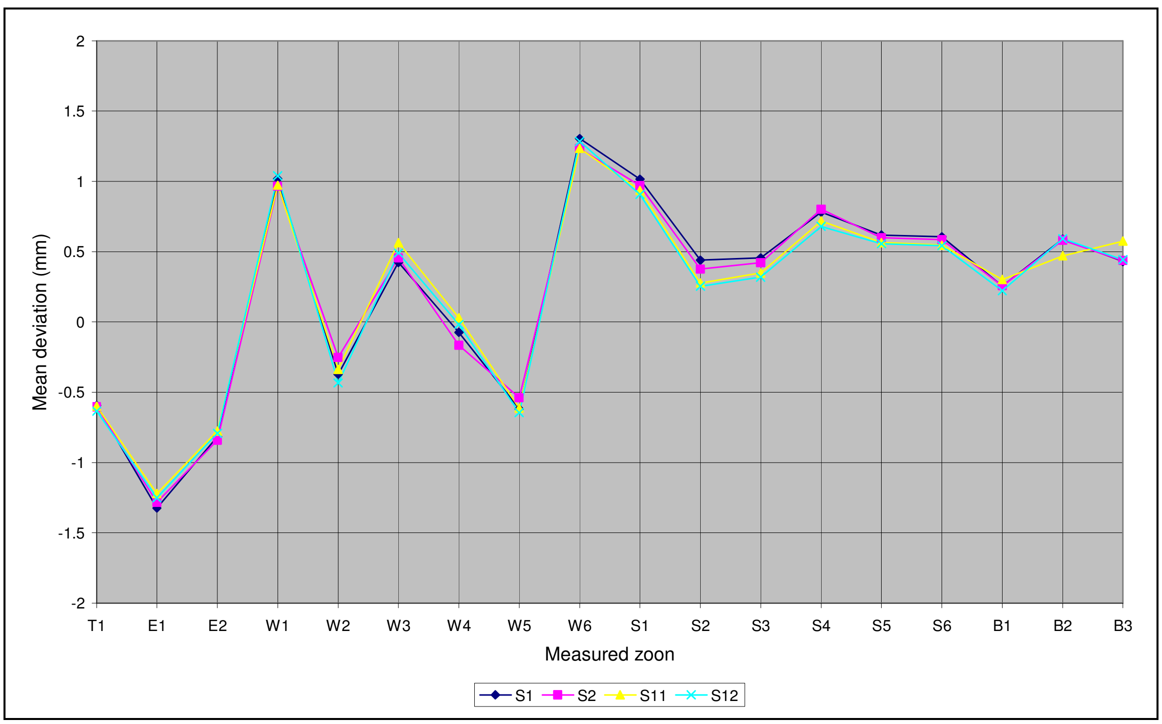

Figure 6.24: Mean deviation between CAD model and measured values of surface cooling method (cooling time 12 s)

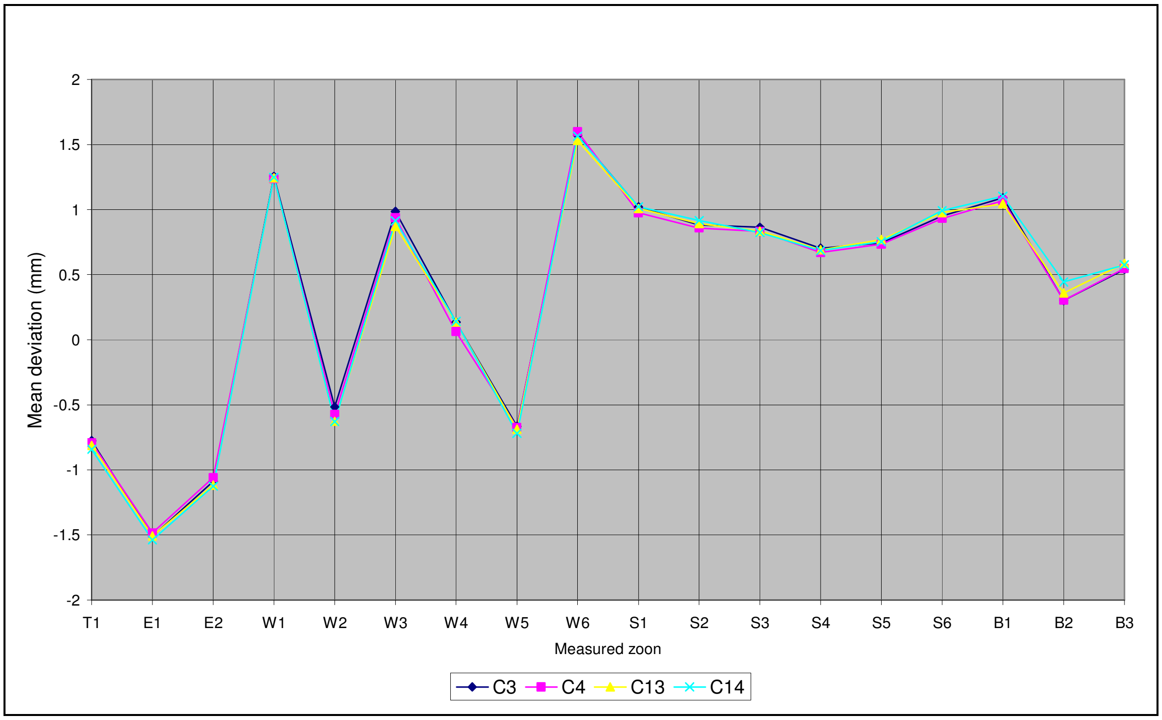

Figure 6.25: Mean deviation between CAD model and measured values of conventional cooling method (cooling time 8 s)

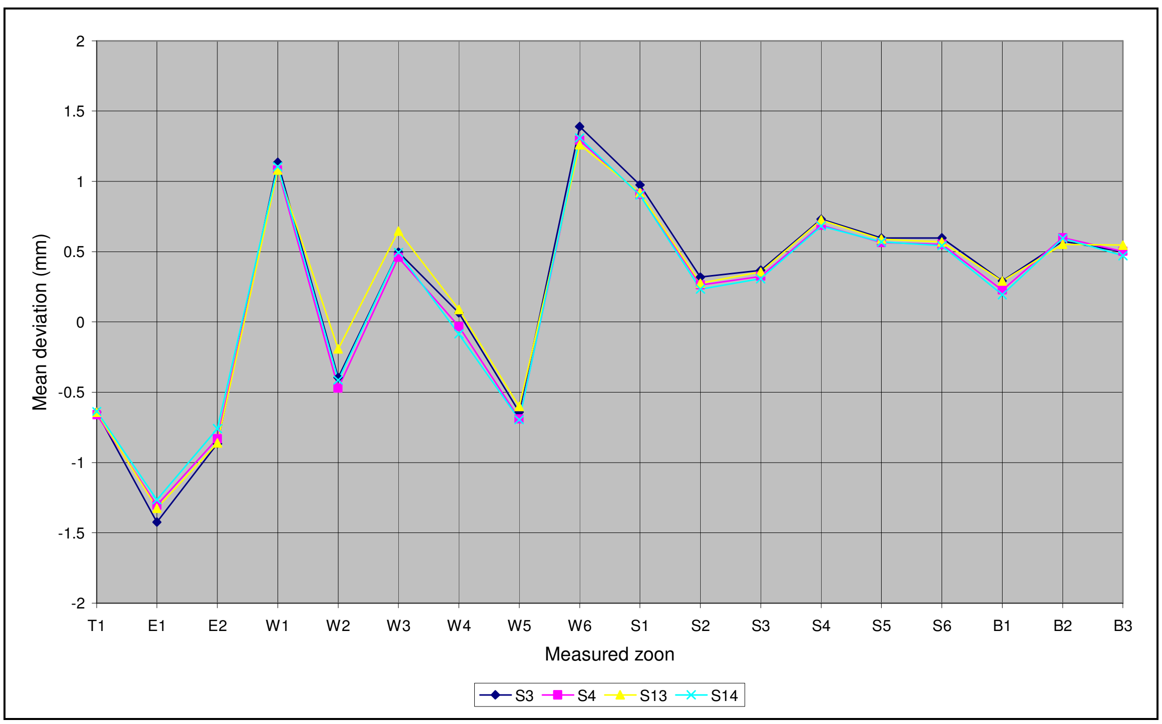

Figure 6.26: Mean deviation between CAD model and measured values of surface cooling method (cooling time 8 s)

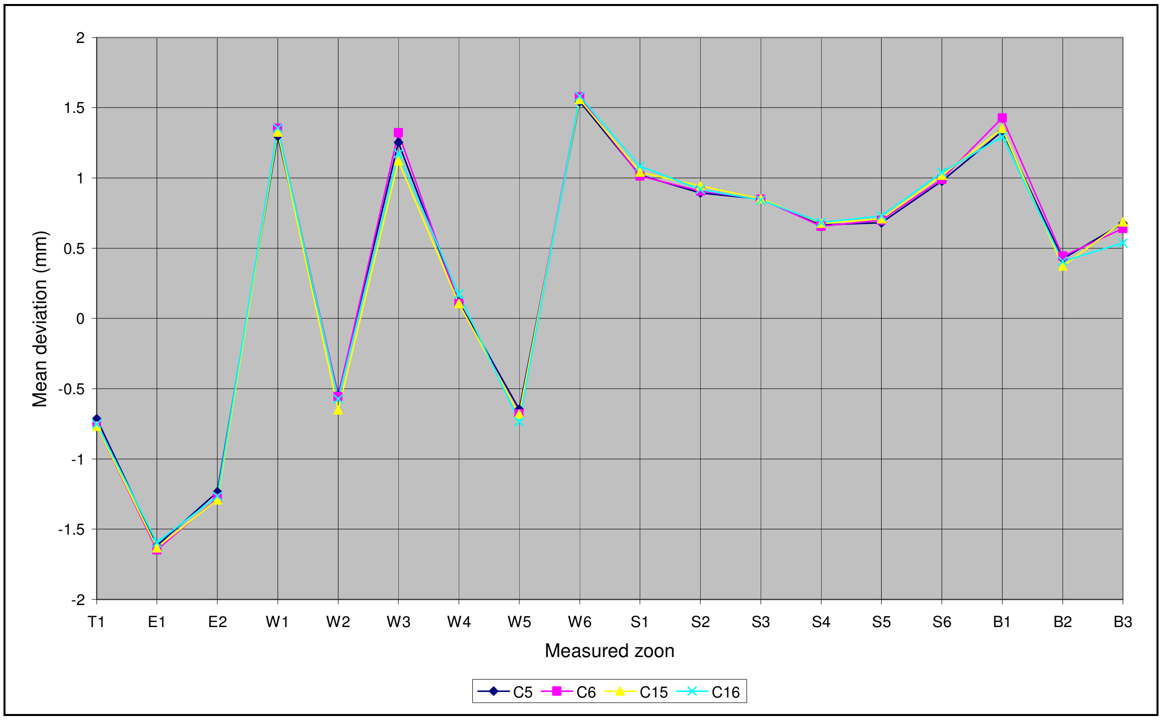

Figure 6.27: Mean deviation between CAD model and measured values of conventional cooling method (cooling time 6 s)

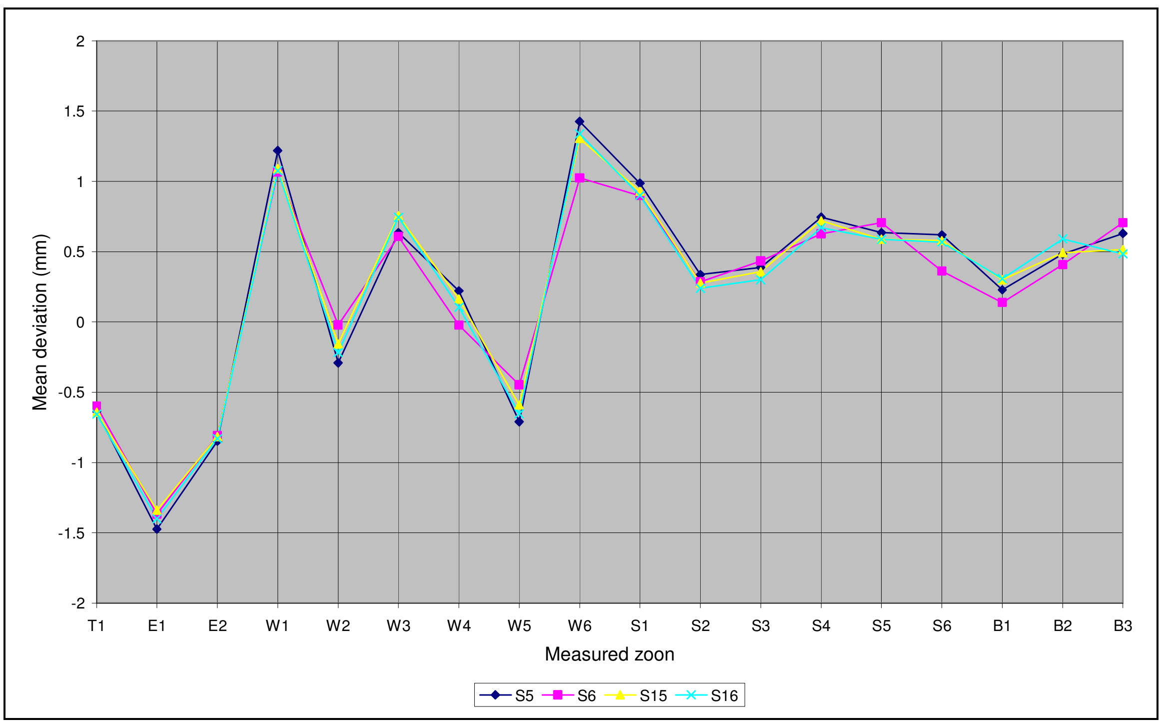

Figure 6.28: Mean deviation between CAD model and measured values of surface cooling method (cooling time 6 s)

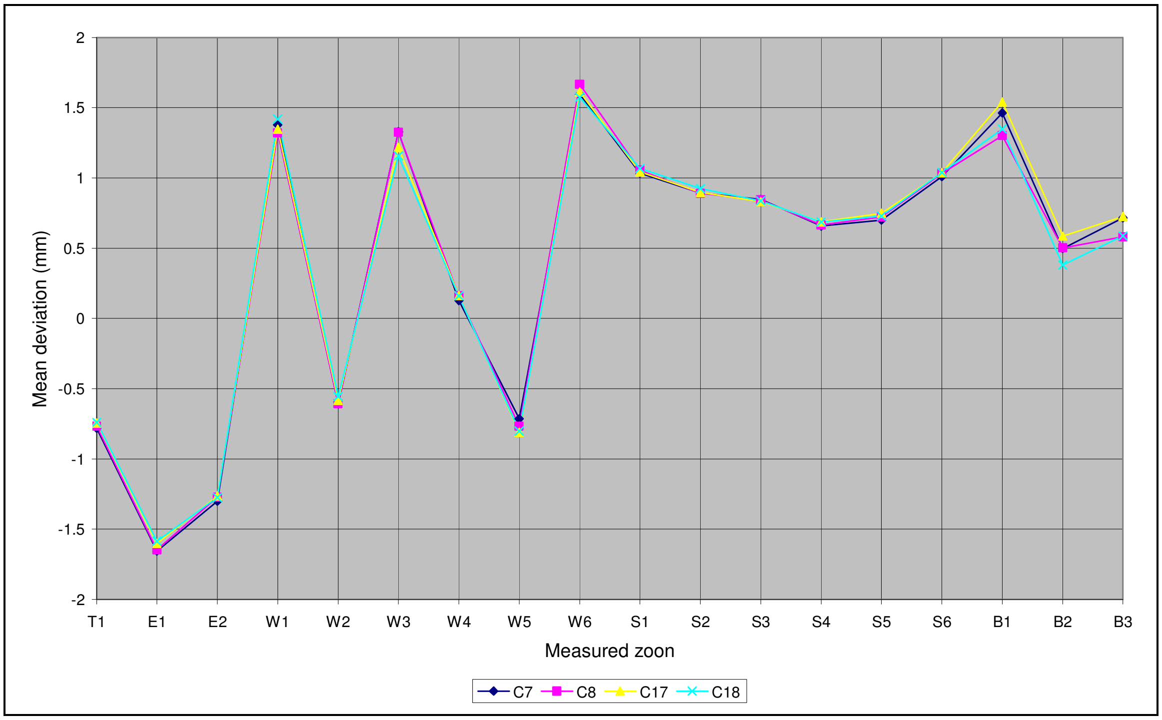

Figure 6.29: Mean deviation between CAD model and measured values of conventional cooling method (cooling time 2 s)

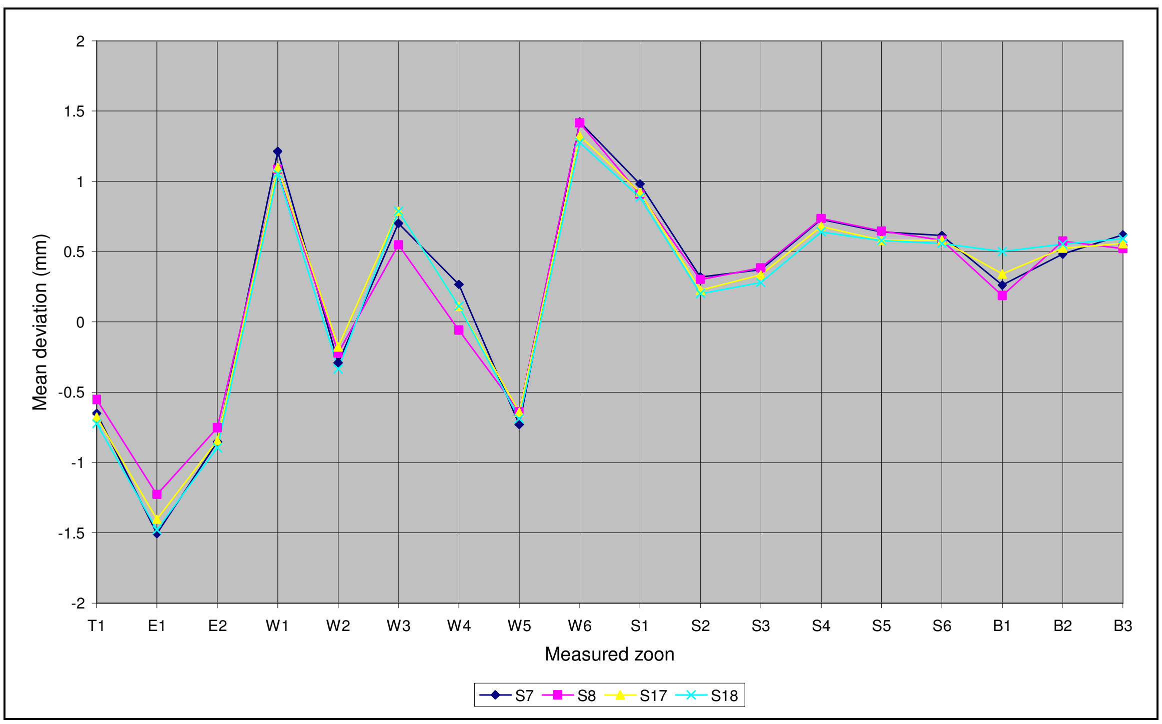

Figure 6.30: Mean deviation between CAD model and measured values of surface cooling method (cooling time 2 s)

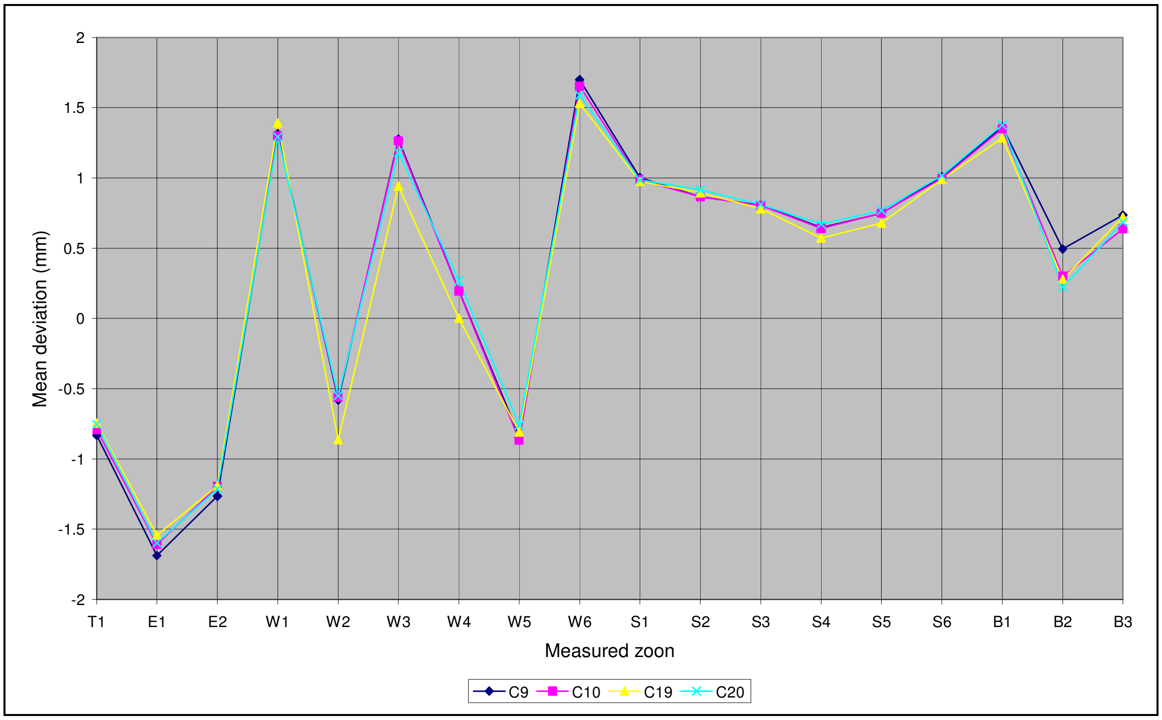

Figure 6.31: Mean deviation between CAD model and measured values of conventional cooling method (cooling time 0 s)

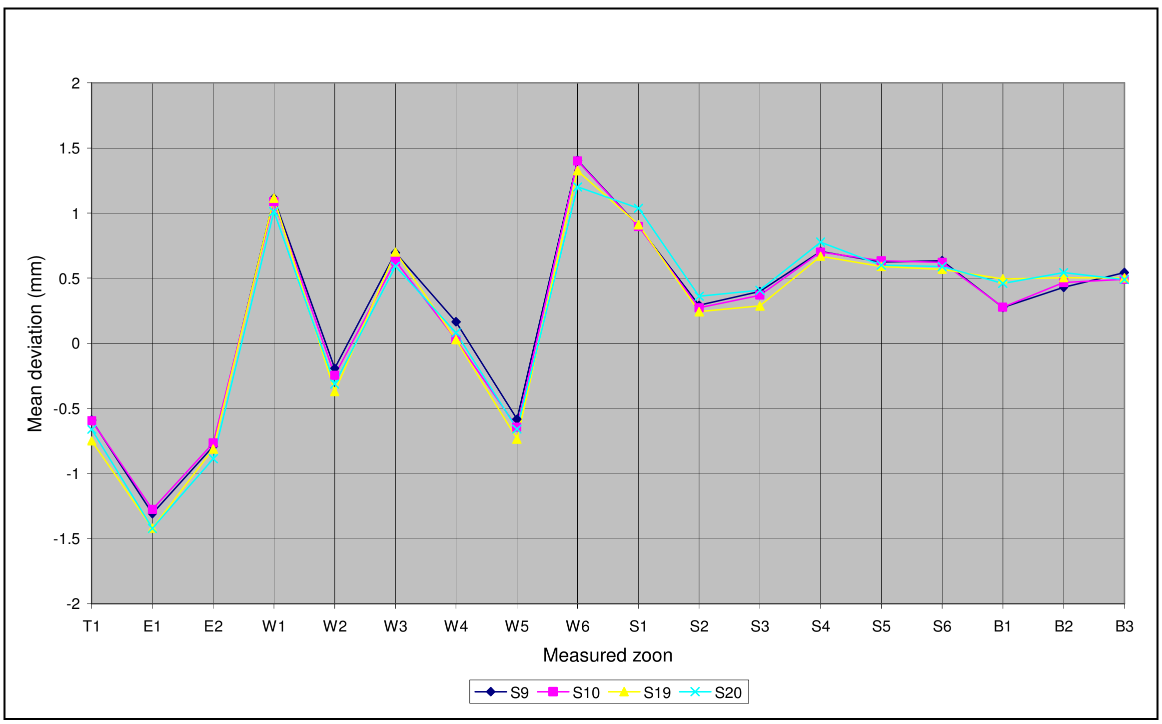

Figure 6.32: Mean deviation between CAD model and measured values of surface cooling method (cooling time 0 s)

6.5 Conclusive Remarks

The moulded parts produced using the surface cooling method have a lower mean deviation compared to the moulded parts produced using the conventional cooling method, at different cooling times of 0, 2, 6, 8 and 12 s (Figure 6.33).

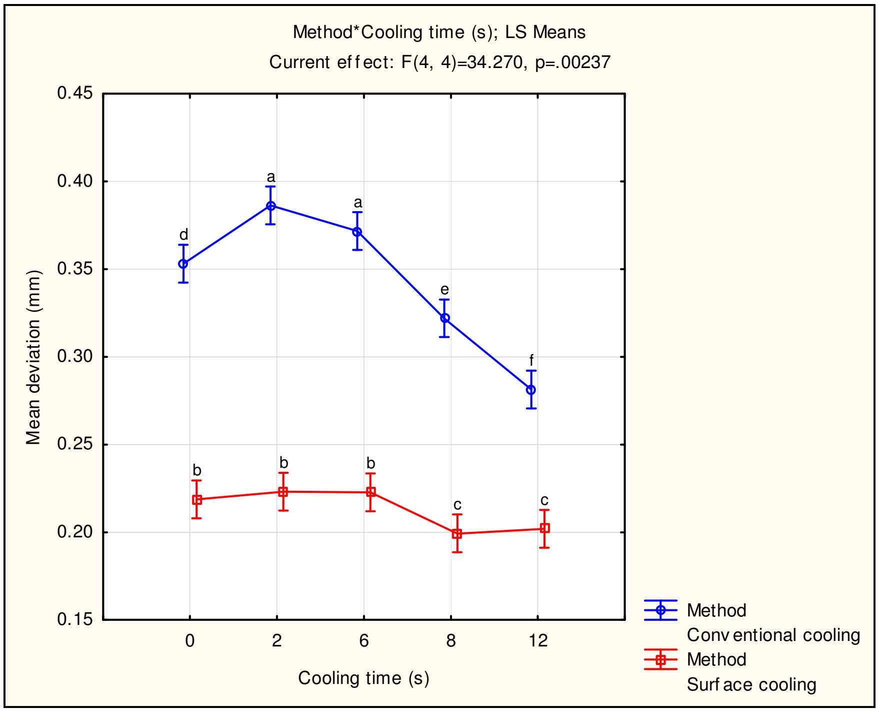

Figure 6.33: Statistical ANOVA result of cooling time against cooling methods

Figure 6.34 shows a comparison between the parts produced using the surface cooing method in cooling times of 6, 2 and 0 s, and parts produced using the conventional cooling method in 12 s. both methods used processing parameters: coolant temperature 11 ℃, water flow rate of 50 and 81 l/min for conventional and surface cooling method, respectively.

The results in Figure 6.34 show further that the part produced using the conventional cooling method in a cooling time of 12 s differs more from the CAD model than the parts produced using the surface cooling method in cooling times of 6, 2, and 0 s. Moreover, from the figure it can be seen that the moulded part produced using the surface cooling method in a cooling time of 6 s has the best quality among the alternatives tested.

Currently, the injection cycle time for producing the cutlery drainer using the conventional cooling method is 26 s, including cooling time of 12 s. However, the injection cycle time for producing the cutlery drainer using the surface cooling method during the experiments involving cooling times of 6, 2, and 0 s was 18 s. This was adjusted automatically in the injection moulding machine during the production due to the time needed for the accumulator pressure (hydraulic energy storage) of the machine to recharge, and also the time required to melt the material for the next shot.

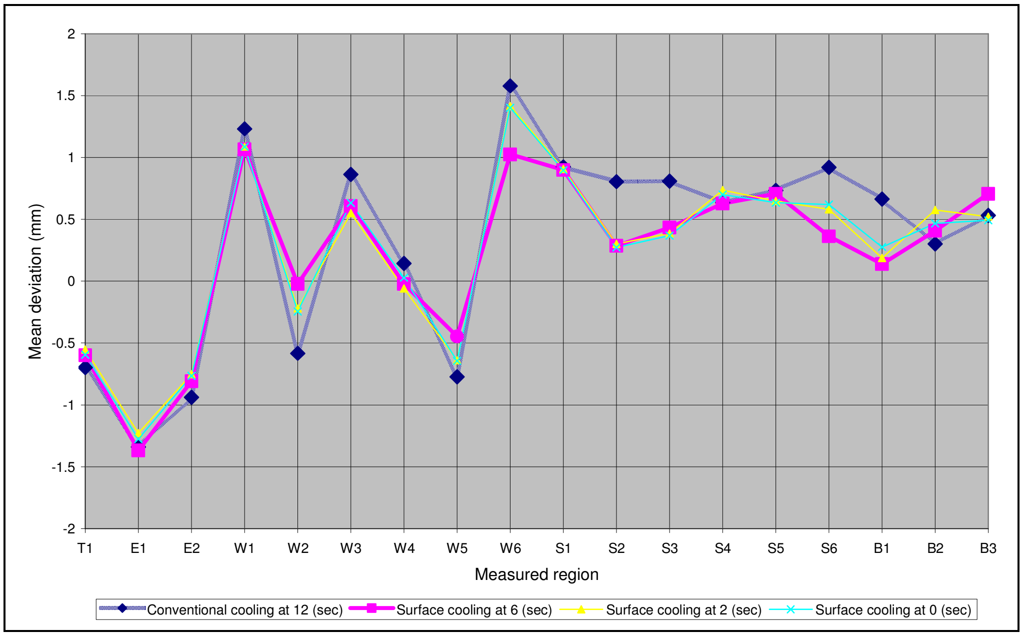

Figure 6.34: Quality measurement comparison between conventional cooling at cooling time 12 s and surface cooling at cooling times 6, 2 and 0 s

Thus the cycle time was reduced from 26 s to 18 s with good quality. That means that the implementation of the SLM technology in the cutlery drainer was a success. Therefore, the surface cooling layout has a significant impact on the cooling time, drastically influencing the total cycle time reduction by 30.78 %.

From the economic point of view, if a production year of 320 days is assumed, with production running 24 hours per day, then the free capacity on a single machine with a single cavity mould will be:

320 days X 24 h X 1 X 0.3078 improvement = 2363.9 hr

If an hourly rate of R 500 per hour is assumed for such a machine, then the additional available capacity for the machine would be equal to a value of R 1,181,950 annually.

Subtracting the manufacturing cost (R 103,500) (see Table 5.6) from the money saved as a free capacity (R 1,181,950), the company could make available additional capacity to the value of R 1,078,450 over the first year. From the second year onwards the free capacity could be valued at R 1,181,950 annually.

7. CONCLUSION AND RECOMMENDATIONS

7.1 Summary

It is clear that uniform cooling is the best way to improve the quality of plastic products and to increase productivity. It is also apparent that the currently available textbooks do not give the necessary attention to cooling, and are not up to date with the latest technologies and methods.

The FEA and CFD simulations are common praxis in tool design. These computer programs guide the tool designer by pointing out hotspots and stress concentrations. There are, however, also substantial limitations in their use. Much work still needs to be carried out in order to improve the user friendliness, compatibility with 3D computer modelling, true representation of the thermal process, as well as the affordability of these important aids.

A certain mathematical method, based on sound thermodynamic principles regarding heat transfer, already exists and can be used effectively in mould design. A coherent generic mathematical tool for surface cooling was developed in this research project. This was achieved using the lumped heat capacity method, which obliges the mould designer to design an adequate cooling channel layout to obtain the minimum cooling time possible for the moulded part.

The coolant mass flow rate required to remove the heat from the moulded part during the cooling time must first be determined, and then the coolant must be circulated through the cooling channels accordingly in order to achieve the maximum cooling efficiency.

Additive manufacturing technologies are becoming a more viable option for the manufacturing of moulds, comparing to the conventional methods. The design freedom related to these AM technologies is of remarkable importance. However, much systematic research and development work with regards to required material properties, process stability and reliability, as well as affordability must still be carried out.

In this study, a combination (hybrid tooling) of conventional methods and the SLM techniques for achieving optimum cooling configuration to reach maximum cooling performance at the lowest manufacturing cost was effectively used on the example of a cutlery drainer insert.

A new approach to evaluate the mould cooling design was successfully established using a decision matrix to guide the designer to select the best cooling layout for the injection moulded part based on part geometry, quality requirements, manufacturing cost, and market needs.

The main results of the experimental work were the following:

- The mould using the surface cooling method was able to remove the heat from the moulded part faster than the mould using the conventional cooling method

- The mould using the surface cooling method underwent a steady state temperature faster than the mould using the conventional cooling method
- The mould using the surface cooling method had uniform mould temperature distribution while the mould using the conventional cooling method had non-uniform mould temperature distribution
- The moulded parts produced using the surface cooling method had a lower mean deviation compared to the moulded parts produced using the conventional cooling method.

7.2 Conclusions

The objectives of this research were successfully achieved:

- A generic model was developed to predict the acceptable minimum cooling time required for the moulded part to meet the quality requirements. The generic model enables the designer to achieve the possible optimum productivity for the moulded part.
- A method for evaluating the cooling layout required for the mould part was successfully developed, based on an analysis of manufacturability and cost-effectiveness. This method leads the designer to choose the most suitable cooling layout for the moulded part.
- The improved cooling channels design (surface cooling method) enabled the production of the selected cutlery drainer with acceptable quality at a cycle time that was reduced by 30.78% from the current production cycle time. This improvement contributes directly to increasing the productivity compared to the conventional cooling method, resulting in a reduction of operational cost, saving in energy consumption, and freeing up the machine's capacity.

  The use of the surface cooling method resulted in the advantages offered by a decreased cycle time. If the cycle time improvements are expressed into monetary values then the available additional free capacity would be at a value of R 1,181,950 annually.
- Regarding the fouling that can occur with the honeycomb cooling channels, from the minerals in the water being deposited on the inside of the coolant channels or from corrosion and rusting of the steel, it is highly recommended that the cooling channels be regularly flushed with muriatic acid solution to eliminate the amount of mineral build up after and before each production run.

7.3 Future Work

Further research should be done on the injection moulding process, since the cooling time is now no longer the constraint determining the moulding cycle time. The total cycle time may now become dominated by the time needed for the accumulator pressure of the injection moulding machine to recharge or for the material plasticisation for each shot.

Software aids should be developed to enable the design of the cooling channel configuration such as conformal cooling or surface cooling for the moulded part based on the new design approach in order to determine the cooling cycle time required for the moulded part, and the evaluation of the cooling design method that was established in this research.

The design of the surface cooling method with parameters such as cooling channels diameters, possibility to produce different cooling channels shapes, and proper cooling channels position, needs further case studies.

Further investigations should be carried out with the existing software, such as Moldflow and Moldex3D, to simulate the conformal or surface cooling methods.

Taking the advantage of the capabilities of the AM methods for inserting sensors into the mould in order to use their signals (temperature, strain, stress etc) for an intelligent, self-controlling moulding process, need to be investigated.

The capabilities and the skills that the University of Stellenbosch have in the Global Competitiveness Centre in Engineering give confidence to establish a strong relationship with the Centre for Research and Technological Studies in Libya. This opportunity should be further explored in order to establish a fruitful collaboration of mutual benefit.

REFERENCES

ABE, F., OSAKADA, K., SHIOMI, M., UEMATSU, K. & MATSUMOTO, M. (2001) The manufacturing of hard tools from metallic powders by selective laser melting. *Journal of Materials Processing Technology* 111, 210-213.

AU, K. M. & YU, K. M. (2006) Variable radius conformal cooling channel for rapid tool. *Journal of Materials Science Forum* 532-533, 520-523.

AU, K. M. & YU, K. M. (2007) A scaffolding architecture for conformal cooling design in rapid plastic injection moulding. *Advanced Manufacture Technology* 34, 496-515.

BEAUMONT, J. P., NAGEL, R. & SHERMAN, R. (2002) *Successful injection moulding,* Munich, Hanser.

BERNARD, A. & FISCHER, A. (2002) New trends in rapid product development. *CIRP Annals - Manufacturing Technology* 51, 635-652.

BESTER, A. G. J. (2006) Investigation towards conformal cooling for blow moulding. *MSc thesis*. Department of Industrial Engineering. Stellenbosch University, Stellenbosch.

BOOTHROYD, G., DEWHURST, P. & KNIGHT, W. (2002) *Product design for manufacture and assembly,* New York, Dekker Inc.

BRATT, C. (2010). *Injection molding tools with conformal cooling systems*. Available: http://www.ccl.fraunhofer.org/working_areas/applications/e_injection_molding.php [2010, 25 June].

BRINKSMEIER, E., LEVY, G., MEYER, D. & SPIERINGS, A. B. (2010) Surface integrity of selective-laser-melted components. *CIRP Annal - Manufacturing Technology* 59, 601-606.

ÇENGEL & YUNUS, A. (2003) *Heat transfer: A practical approach* Boston, McGraw-Hill.

CUSTOMPARTNET [Online]. 2007. Available: http://www.custompartnet.com/wu/InjectionMolding [2010, 20 August].

DALGARNO, K. W. & STEWART, T. D. (2001) Manufacture of production injection mould tooling incorporating conformal cooling channels via indirect selective laser sintering. *ProQuest Science Journals* 215, 1323-1332.

DIMITROV, D., MOAMMER, A. & MABOGO, M. (2008) Thermal management of moulds and dies – state of the art and future perspectives. *3rd International Conference on Polymers and Mould Innovations.* Hogeschool, Genet.

DIMITROV, D., SCHREVE, K. & BARTEL, K. (2004) Analysis of current reverse engineering practice and possibilities for improvements to the process. Stellenbosch, South Africa, COMA ’04, International Conference on Competitive Manufacturing, 131-136.

DIMLA, D. E., CAMILOTTO, M. & MIAN, F. (2005) Design and optimisation of conformal cooling channels in injection moulding tools. *Journal of Materials Processing Technology* 164-165, 1294-1300.

DING, Y., LAN, H., HONG, J. & WU, D. (2004) An integrated manufacturing system for rapid tooling based on rapid prototyping. *Robotics and Computer-Integrated Manufacturing* 20, 281-288.

DOWLATSHAHI, S. (2004) An application of design of experiments for optimization. *Journal of Manufacturing Technology Management,* 15, 445-454.

DUNN, O. J. & CLARKE, V. A. (1974) *Applied statistics: Analysis of variance and regression,* New York, John Wiley and Sons.

EOS [Online]. 2009. Available: http://www.eos.info/en/applications/tooling/injection-moulding.html [2009, 15 July].

FERREIRA, J. C. & MATEUS, A. (2003) Studies of rapid soft tooling with conformal cooling channels for plastic injection moulding. *Journal of Materials Processing Technology* 142, 508-516.

GIBBONS, G. J. & HANSELL, R. G. (2005) Direct tool steel injection mould inserts through the Arcam EBM free-form fabrication process. *Assembly Automation* 25(4), 300-305.

GLOINN, T., HAYES, C., HANNIFFY, P. & VAUGH, K. (2007) FEA simulation of conformal cooling within injection moulds. *Manufacturing Research* 2(2), 162-170.

GOM [Online]. 2010. Available: http://www.gom.com [retrieved 2010, 12 October].

JARDAN [Online]. 2002. Available: http://www.jar.com/ [2010, 6 March].

KHAINGA, M. W., FUH, J. Y. H. & LU, L. (2001) Direct metal laser sintering for rapid tooling: Processing and characterisation of EOS parts. *Journal of Materials Processing Technology* 113, 269 -272.

KING, D. & TANSEY, T. (2002) Alternative materials for rapid tooling. *Journal of Materials Processing Technology* 121, 313-317.

KING, D. & TANSEY, T. (2003) Rapid tooling: Selective laser sintering injection tooling. *Journal of Materials Processing Technology* 132, 42-48.

KRUTH, J.-P., LEVY, G., KLOCKE, F. & CHILDS, T. H. C. (2007) Consolidation phenomena in laser and powder-bed based layered manufacturing. *CIRP Annals - Manufacturing Technology* 56, 730-759.

KRUTH, J.-P., MERCELIS, P. & VAN VAERENBERGH, J. (2005) Binding mechanisms in selective laser sintering and selective laser melting. *Rapid Prototyping Journal* 11, 26-36.

LASERCUSING [Online]. 2009. Available: http://www.lasercusing.nl [2009, 15 April].

LEVY, G., SCHINDEL, R. & KRUTH, J. P. (2003) Rapid manufacturing and rapid tooling with Layer Manufacturing (LM) technologies, state of the art and future perspectives. *CIRP Annal - Manufacturing Technology* 52, 589-609.

LI, C. G. & LI, C. L. (2008) Plastic injection mould cooling system design by the configuration space method. *Computer-Aided Design* 40, 334-349.

LI, C. L. (2001) A feature-based approach to injection mould cooling system design. *Computer-Aided Design* 33, 1073-1090.

LI, C. L., LI, C. G. & MOK, A. C. K. (2005) Automatic layout design of plastic injection mould cooling system. *Computer-Aided Design* 37, 645-662.

LIN, J. C. (2002) Optimum cooling system design of a free-form injection mould using an abductive network. *Materials Processing Technology* 120, 226-236.

MATSUMOTO, M., SHIOMI, M., OSAKADA, K. & ABE, F. (2002) Finite element analysis of single layer forming on metallic powder bed in rapid prototyping by selective laser processing. *International Journal of Machine Tools and Manufacture* 42, 61-67.

MENGES, G., MICHAELI, W. & MOHREN, P. (2000) *How to make injection molds,* Munich, Carl Hanser

MOAMMER, A. (2007) Investigation towards the impact of conformal cooling on the performance of injection moulds for the packaging industry. *MSc thesis*. Department of Industrial Engineering. University of Stellenbosch, Stellenbosch.

MOLDEX3D [Online]. 2005. Available: http://www.moldex3d.com [2009, 15 April].

MOLDFLOW (2005) *Moldflow plastics advisers training overview,* Moldflow Corporation.

MORROW, W. R., QI, H., KIM, I., MAZUMDER, J. & SKERLOS, S. J. (2007) Environmental aspects of laser-based and conventional tool and die manufacturing. *Journal of Cleaner Production* 15, 932-943.

MUMTAZ, K. A., ERASENTHIRAN, P. & HOPKINSON, N. (2008) High density selective laser melting of Waspaloy®. *Journal of Materials Processing Technology* 195, 77-87.

NORWOOD, A. J., DICKENS, P. M., SOAR, R. C., HARRIS, R., GIBBONS, G. & HANSELL, R. (2004) Analysis of cooling channels performance. *Computer Integrated Manufacturing* 17(8), 669-678.

NYLUND, C. & MEINANDER, K. (2005) The influence of heat transfer coefficient on cooling time in injection molding. *Heat Mass Transfer* 41, 428-431.

ÓDONNCHADHA, B. & TANSEY, A. (2004) A note on rapid metal composite tooling by selective laser sintering. *Journal of Materials Processing Technology* 153-154, 28-34.

OSAKADA, K. & SHIOMI, M. (2006) Flexible manufacturing of metallic products by selective laser melting of powder. *Journal of Machine Tools and Manufacture* 46, 1188-1193.

OSSWALD, T. A., TURNG, L.-S. & GRAMANN, P. J. (2002) *Injection Molding Handbook,* Munich, Carl Hanser.

PARK, S. J. & KWON, T. H. (1998) Optimal cooling system design for the injection molding process. *Polymer Engineering and Science* 38(9), 1450-1462.

POLI, C. (2001) *Design for manufacturing, a structured approach,* Boston, Butterworth Heinemann.

PYE, R. G. W. (2000) *Injection mould design,* New Delhi, Affiliated East-West Press.

RÄNNAR, L. E. (2003) Efficient cooling of FFF injection moulding tools with conformal cooling channels - an introductory analysis. Leiria, Portugal, Proceedings of the 1st International Conference on Advanced Research on Virtual and Rapid Prototyping,

RÄNNAR, L. E., GLAD, A. & GUSTAFSON, C. G. (2007) Efficient cooling with tool inserts manufactured by electron beam melting. *Journal of Rapid Prototyping* 13(3), 128-135.

REES, H. (2002) *Mould Engineering,* Munich, Carl Hanser.

ROLLE, K. C. (2000) *Heat and mass transfer,* New Jersey, Prentice-Hall,Inc.

RYDER, G., ION, B., GREEN, G., HARRISON, D. & WOOD, B. (2002) Rapid design and manufacture tools in architecture. *Automation in Construction* 11, 279- 290.

SACHS, E., WYLQMS, E., ALLEN, S., CIMA, M. & GUO, H. (2000) Production of injection molding tooling with conformal cooling channels using the three dimensional printing process. *Polymer Engineering and Science* 40(5), 1232-1247.

SAIFULLAH, A. B. M. & MASOOD, S. H. (2007) Optimum cooling channels design and thermal analysis of an injection moulded plastic part mould. *Materials Science Forum* 561-565, 1999-2002.

SCHEMENAUER, N., LI, L., PENG, X., ZENG, Y. & GU, P. (2002) A reverse engineering system for rapid manufacturing of complex objects. *Robotics and Computer Integrated Manufacturing* 18, 53-67.

SHARON (2009). *Construction Injection Molds Classification* Available: http://www.themouldinfo.com/search/label/Injection%20Mold [2010, 15 September].

SHOEMAKER, J. (2006) *Moldflow design guide,* Munich, Hanser.

SIMCHI, A. (2006) Direct laser sintering of metal powders: Mechanism, kinetics and microstructural features. *Materials Science and Engineering A* 428 148-158.

SIMCHI, A., PETZOLDT, F. & POHL, H. (2003) On the development of direct metal laser sintering for rapid tooling. *Journal of Materials Processing Technology* 141, 319-328.

SIMUFLOW [Online]. 2010. Available: http://www.gmsworks.com/simuflow.html [2010, 5 October].

SLM [Online]. 2008. Available: http://www.mtt-group.com/selective-laser-melting.html, [2009, 20 July].

SMITH, A. G., WROBLE, L. C., MCCALLA, B. A., ALLAN, P. S. & HORNSBY, P. R. (2008) A computational model for the cooling phase of injection moulding. *Journal of Materials Processing Technology* 195, 305-313.

STELSON, K. A. (2003) Calculating cooling times for polymer injection moulding. *Engineering Manufacture* 217, 709-713.

SUN, Y. F., LEE, K. S. & AYC, N. (2002) The application of U-shape milled grooves for cooling of injection moulds. *Engineering Manufacture* 216(12), 1561-1573.

TANG, L. Q., CHASSAPIS, C. & MANOOCHEHRI, S. (1997) Optimal cooling system design for multi-cavity injection molding. *Finite Elements in Analysis and Design* 26, 229-251.

TANG, S. H., KONG, Y. M., SAPUAN, S. M., SAMIN, R. & SULAIMAN, S. (2006) Design and thermal analysis of plastic injection mould. *Journal of Materials Processing Technology* 171, 259-267.

TRANSVALOR [Online]. 2006. Available: http://www.transvalor.com, [2010, 5 May].

VILLALON, A. V. (2005) Electron beam fabrication of injection mold tooling with conformal cooling channels. MSc thesis. Department of Industrial Engineering. North Carolina State University,

VOHA, P. (2005) *Milling catalogue and technical manual,* Pokolm Frastechnik GmbH & Co. KG/Voha-Tosec GmbH, Vollhartmetall-Werkzeuge.

WEIDENFELLER, B., HÖFER, M. & SCHILLING, F. R. (2005) Cooling behaviour of particle filled polypropylene during injection moulding process. *Composites Part A: Applied Science and Manufacturing* 36, 345-351.

WOHLERS, T. (2007) *Wohlers report, state of the industry, annual worldwide progress report,* Colorado, USA, Wohlers Associates Inc

WOHLERS, T. (2009) *Wohlers report, state of the industry, annual worldwide progress report,* Colorado, USA, Wohlers Associates Inc.

XU, X. (1999) Conformal cooling and rapid thermal cycling in injection molding with 3D printed tools. *Ph D thesis*. Mechanical engineering. Massachusetts Institute of Technology, Massachusetts.

XU, X., SACHS, E. & ALLEN, S. (2001) The design of conformal cooling channels in injection molding tooling. *Polymer Engineering and Science* 41(7), 1265-1279.

YADROITSEV, I., BERTRAND, P., LAGET, B. & SMUROV, I. (2007) Application of laser assisted technologies for fabrication of functionally graded coatings and objects for the international thermonuclear experimental reactor components. *Journal of Nuclear Materials* 362, 189-196.

ZHANG, Y., CHEN, Y., LI, P. & MALE, A. T. (2003) Weld deposition-based rapid prototyping: A preliminary study. *Journal of Materials Processing Technology* 135, 347-357.

ZHONG, M., LIU, W., NING, G., YANG, L. & CHEN, Y. (2004) Laser direct manufacturing of tungsten nickel collimation component. *Journal of Materials Processing Technology* 147, 167-173.

ZHU, H. H., LU, L. & FUH, J. Y. H. (2003) Development and characterisation of direct laser sintering Cu-based metal powder. *Journal of Materials Processing Technology* 140, 314-317.

Appendix A Material properties of different polymers

Table A1: Typical melt, mould, and ejection temperatures for various polymers (Shoemaker, 2006)

Polymer	Melt Temp (℃)			Mould Temp (℃)			Ejection Temp (℃)
	Min	*Rec.	Max	Min	*Rec.	Max	*Rec.
Acrylonitrile-Butadiene-Styrene (ABS)	200	230	280	25	50	80	88
Polyamide (PA12)	230	255	300	30	80	110	135
Polyamide (PA 6)	230	255	300	70	85	110	133
Polyamide (PA 66)	260	280	320	70	80	110	158
Polybutylene Terephthalates (PBT)	220	250	280	15	60	80	125
Polycarbonate (PC)	260	305	340	70	95	120	127
PC/ABS	230	265	300	50	75	100	117
PC/PBT	250	265	280	40	60	85	125
High Density Polyethylene (HDPE)	180	220	280	20	40	95	100
Low Density Polyethylene (LDPE)	180	220	280	20	40	70	80
Polyetherimid (PEI)	340	400	440	70	140	175	191
Polyethylene Terephthalate (Simchi et al.)	265	270	290	80	100	120	150
Glycol-modified PET; Copolyesters (PETG)	220	255	290	10	15	30	59
Polymethyl Methacrylate (PMMA)	240	250	280	35	60	80	85
Polyacetal or Polyoxymethylene (POM)	180	210	235	50	70	105	118
Polypropylene (PP)	200	230	280	20	50	80	93
Polypropylene Ether Blends (PPE/PPO)	240	280	320	60	80	110	128
Polystyrene (PS)	180	230	280	20	50	70	80
Polyvinyl Chloride (PVC)	160	190	220	20	40	70	75

*Rec. :Recommended

Appendix B Full experimental data

Table B 1: Injection cycle time recorded in the injection moulding machine during the experiment work

Exp No	T_c (°C)	t_c (s)	FR (l/min)	t_{cycle} (s)	Exp No	T_c (°C)	t_c (s)	FR (l/min)	t_{cycle} (s)
C1	11	12	41	26	S1	11	12	67	26
C2	11	12	50	26	S2	11	12	81	26
C3	11	8	41	22	S3	11	8	67	20
C4	11	8	50	22	S4	11	8	81	20
C5	11	6	41	20	S5	11	6	67	18
C6	11	6	50	20	S6	11	6	81	18
C7	11	2	41	20	S7	11	2	67	17
C8	11	2	50	20	S8	11	2	81	17
C9	11	0	41	20	S9	11	0	67	17
C10	11	0	50	20	S10	11	0	81	17
C11	15	12	41	26	S11	15	12	67	26
C12	15	12	50	27.6	S12	15	12	81	26
C13	15	8	41	23.7	S13	15	8	67	20
C14	15	8	50	22.6	S14	15	8	81	20
C15	15	6	41	22	S15	15	6	67	18
C16	15	6	50	20.6	S16	15	6	81	19
C17	15	2	41	20.5	S17	15	2	67	17
C18	15	2	50	20	S18	15	2	81	17
C19	15	0	41	20	S19	15	0	67	17
C20	15	0	50	20	S20	15	0	81	17

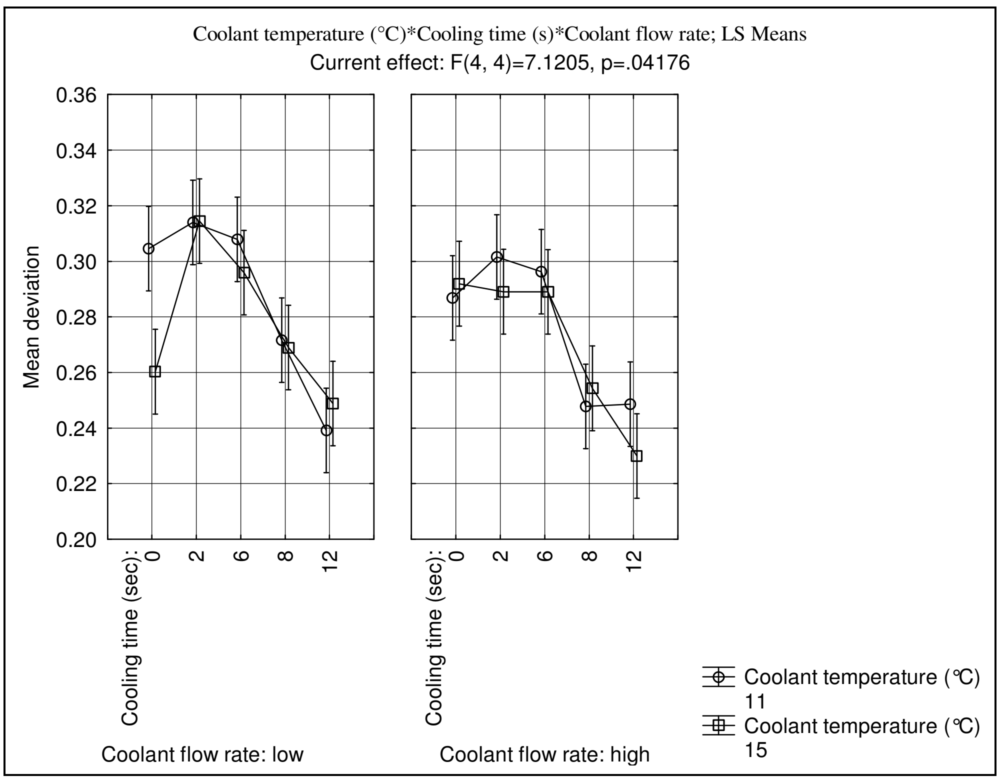

Figure B 1: Statistical ANOVA result of cooling time and coolant flow rate against coolant temperature

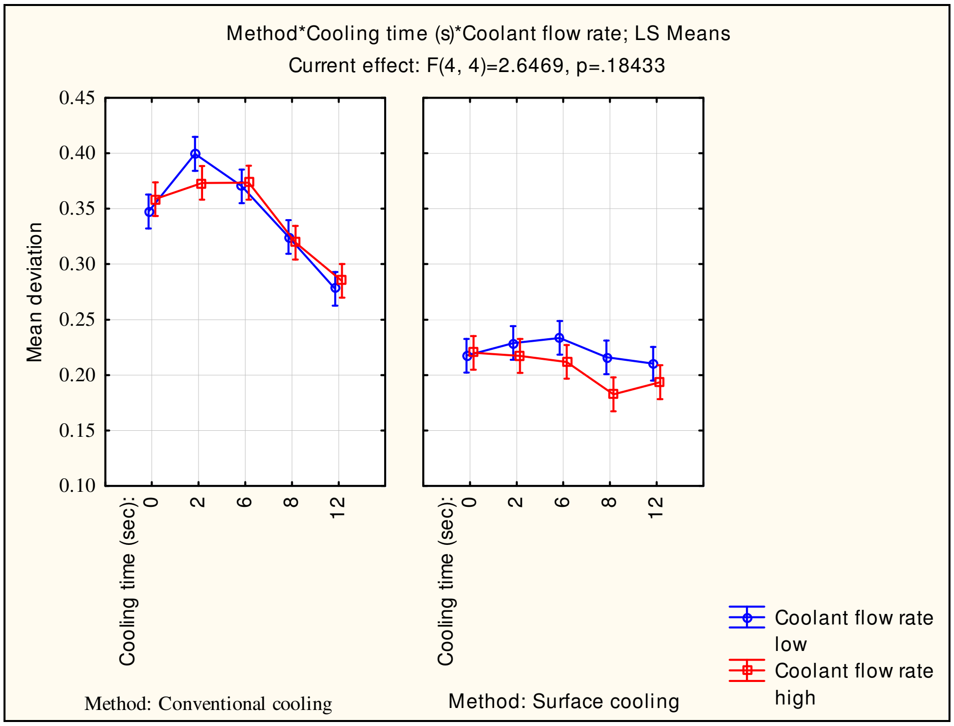

Figure B 2: Statistical ANOVA result of cooling time and coolant flow rate against methods

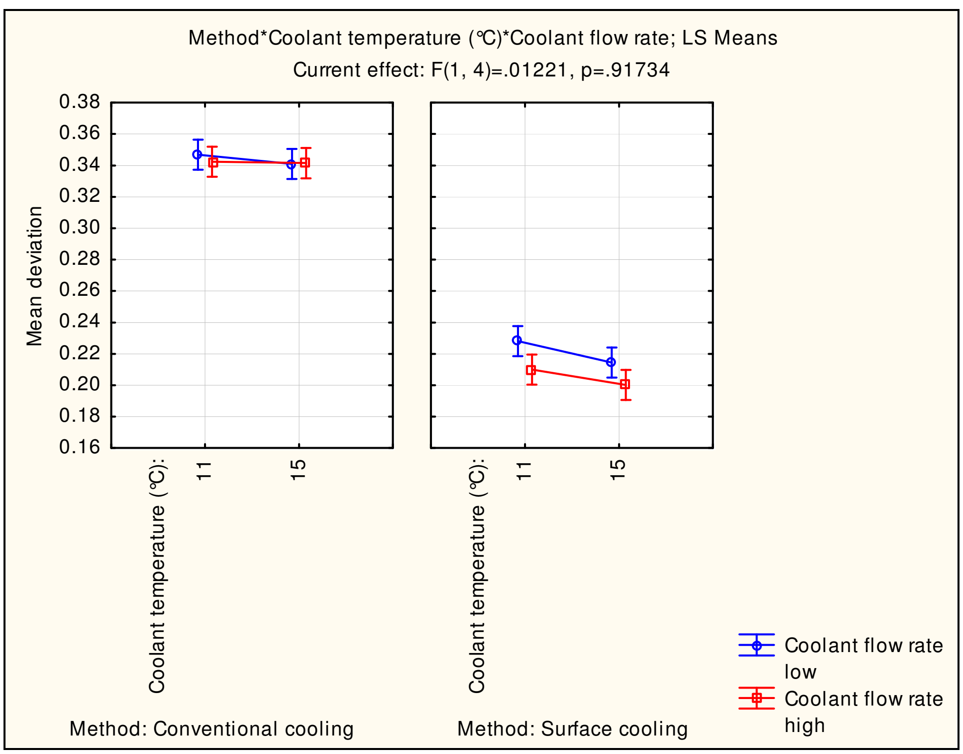

Figure B 3: Statistical ANOVA result of coolant temperature and coolant flow rate against methods

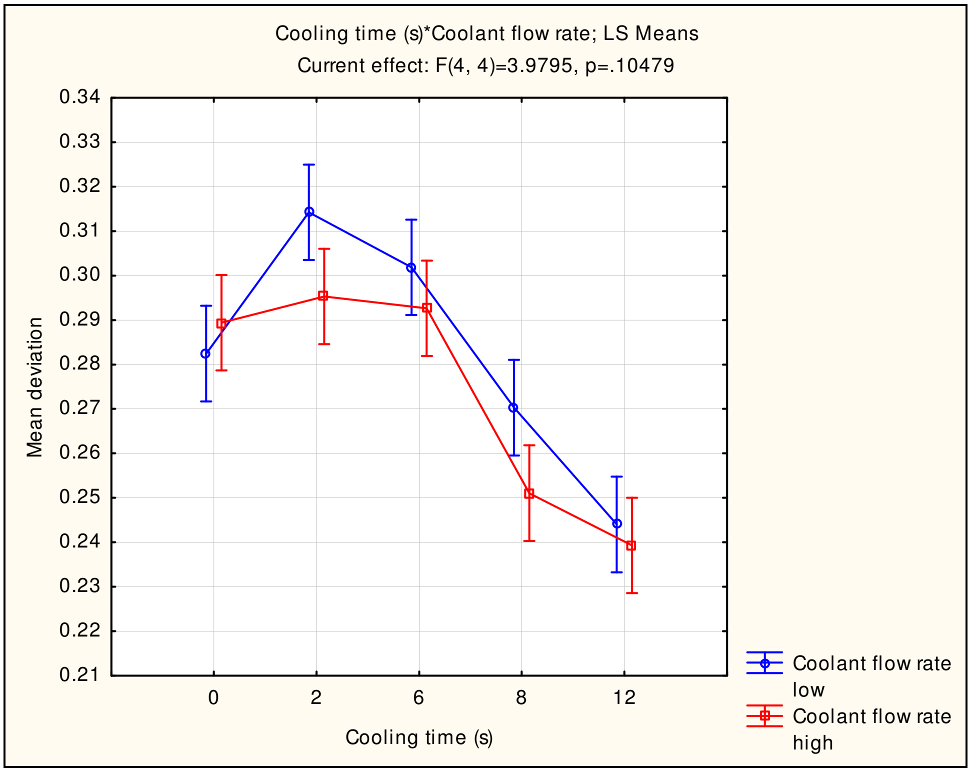

Figure B 4: Statistical ANOVA result of coolant flow rate against cooling time

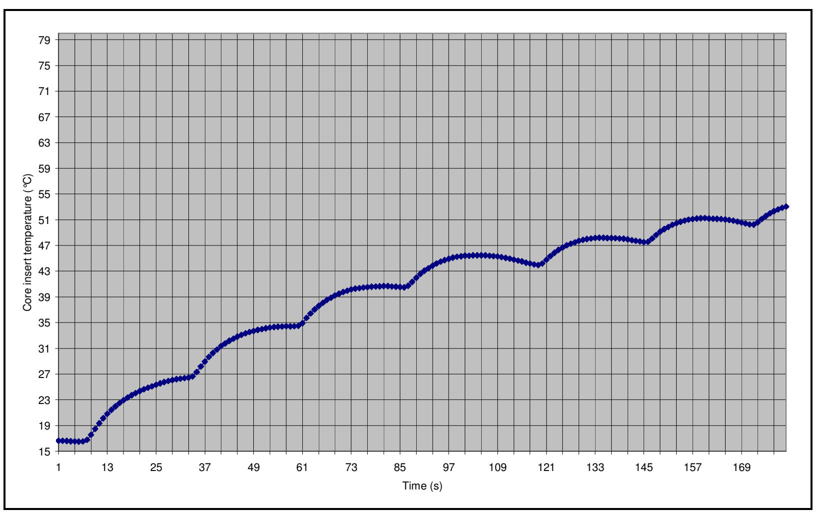

Figure B 5: Temperature plot for conventional cooling method: cooling time 12 s, coolant temperature 11℃, and coolant flow rate 41 l/min

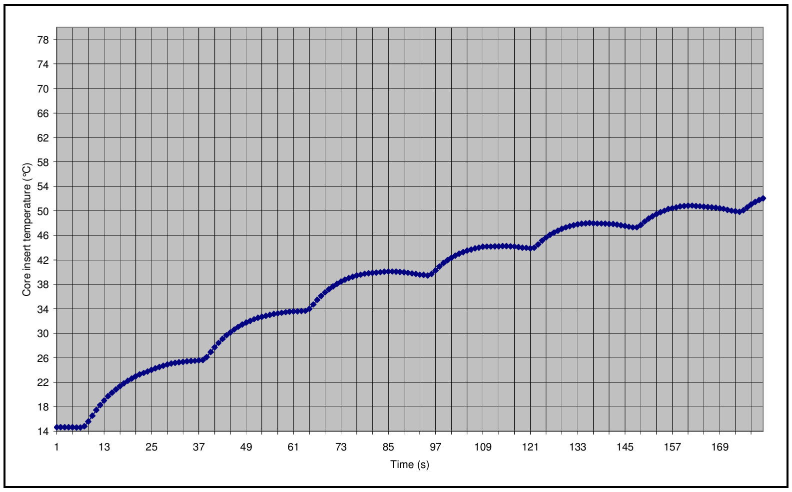

Figure B 6: Temperature plot for conventional cooling method: cooling time 12 s, coolant temperature 11°C, and coolant flow rate 50 l/min

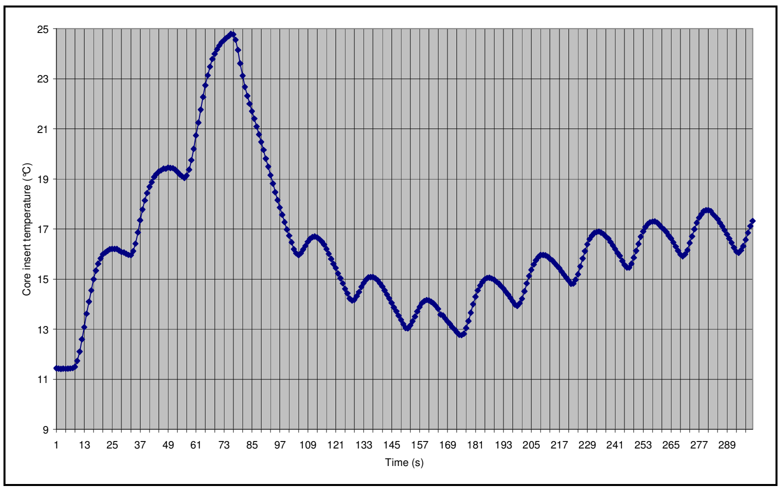

Figure B 7: Temperature plot for surface cooling method: cooling time 12 s, coolant temperature 11°C, and coolant flow rate 67 l/min

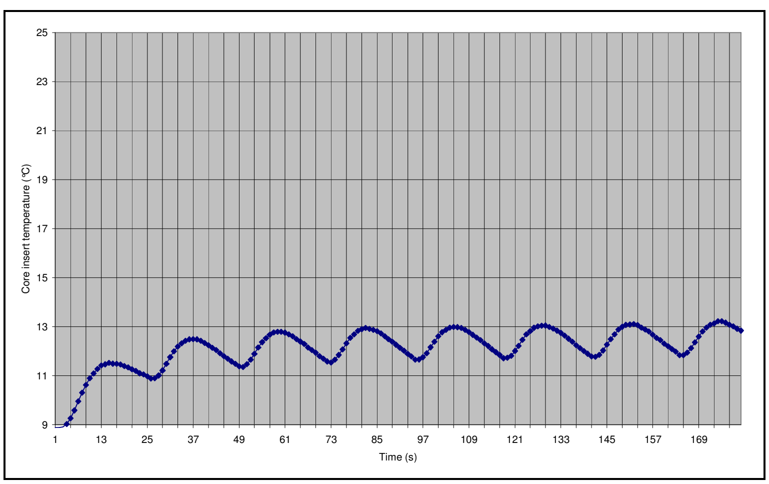

Figure B 8: Temperature plot for surface cooling method: cooling time 12 s, coolant temperature 11°C, and coolant flow rate 81 l/min

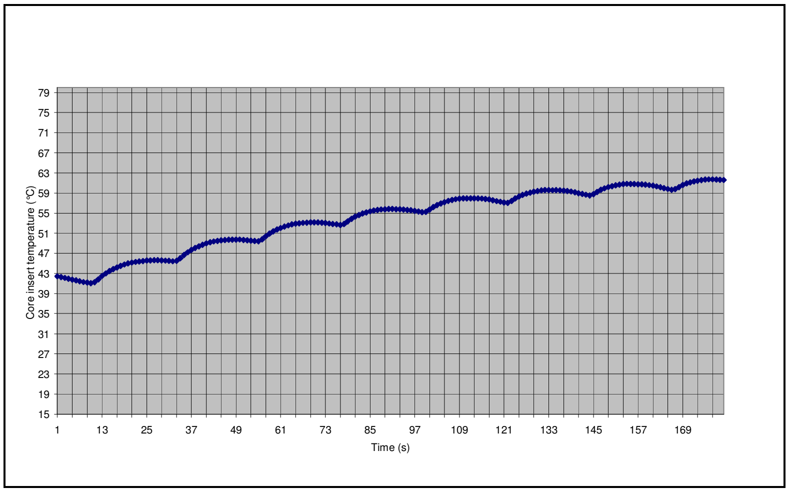

Figure B 9: Temperature plot for conventional cooling method: cooling time 8 s, coolant temperature 11℃, and coolant flow rate 41 l/min

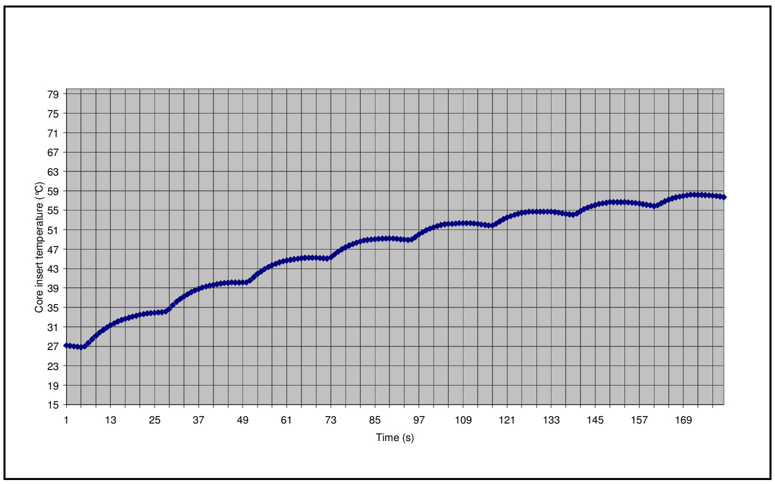

Figure B 10: Temperature plot for conventional cooling method: cooling time 8 s, coolant temperature 11℃, and coolant flow rate 50 l/min

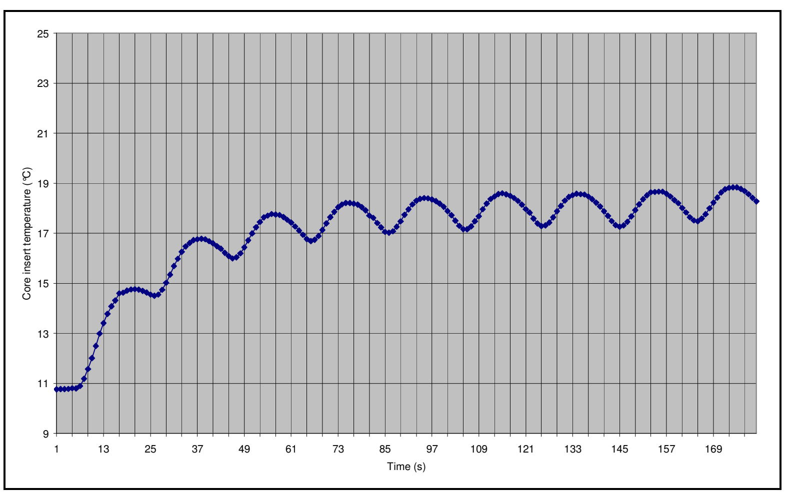

Figure B 11: Temperature plot for surface cooling method: cooling time 8 s, coolant temperature 11℃, and coolant flow rate 67 l/min

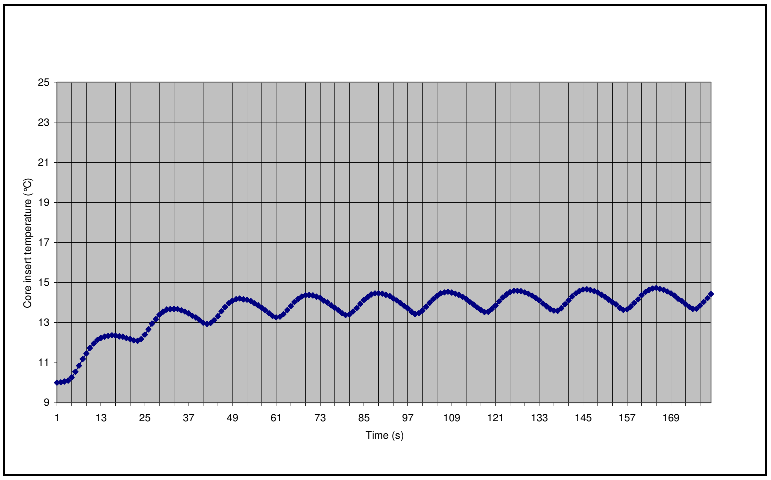

Figure B 12: Temperature plot for surface cooling method: cooling time 8 s, coolant temperature 11℃, and coolant flow rate 81 l/min

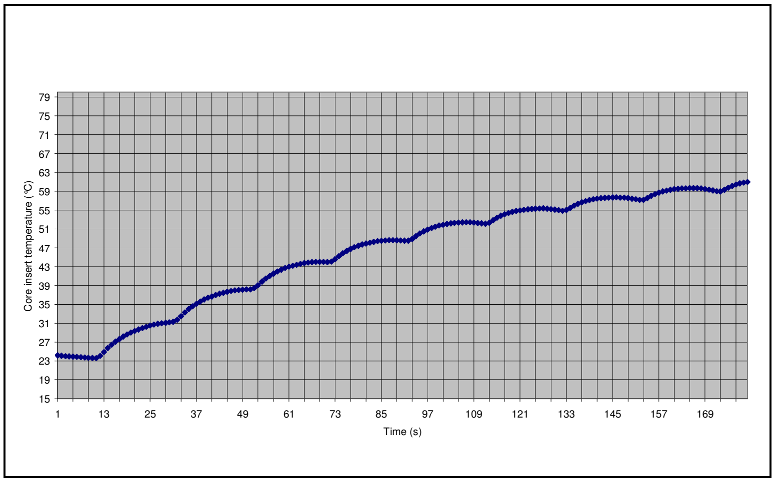

Figure B 13: Temperature plot for conventional cooling method: cooling time 6 s, coolant temperature 11℃, and coolant flow rate 41 l/min

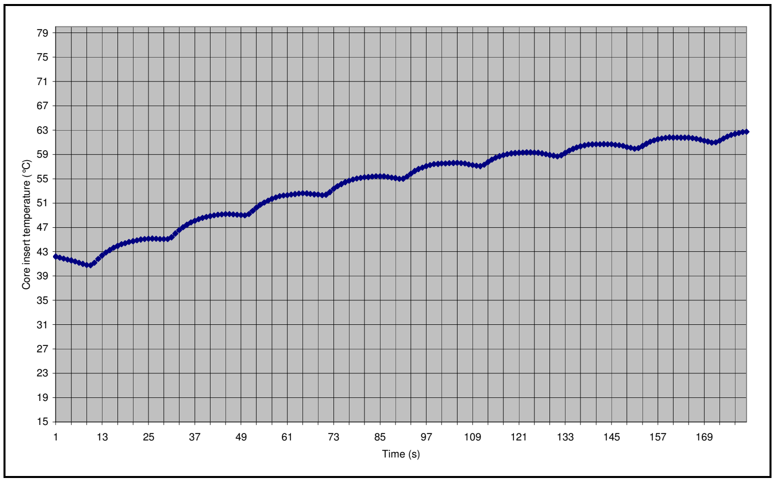

Figure B 14: Temperature plot for conventional cooling method: cooling time 6 s, coolant temperature 11℃, and coolant flow rate 50 l/min

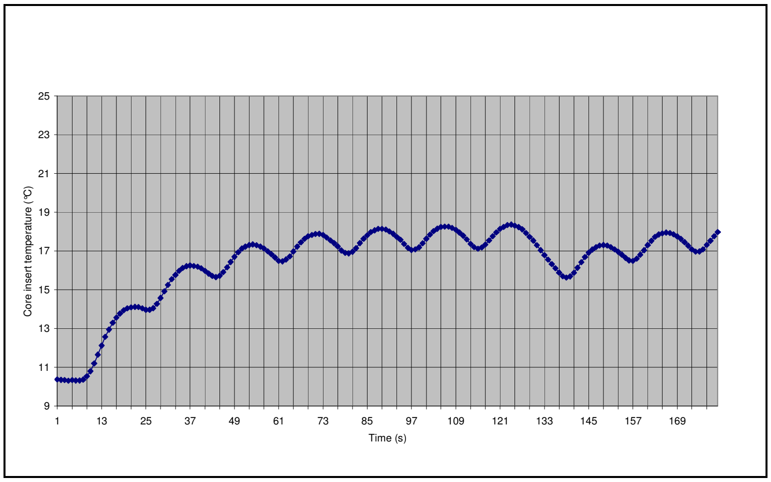

Figure B 15: Temperature plot for surface cooling method: cooling time 6 s, coolant temperature 11°C, and coolant flow rate 67 l/min

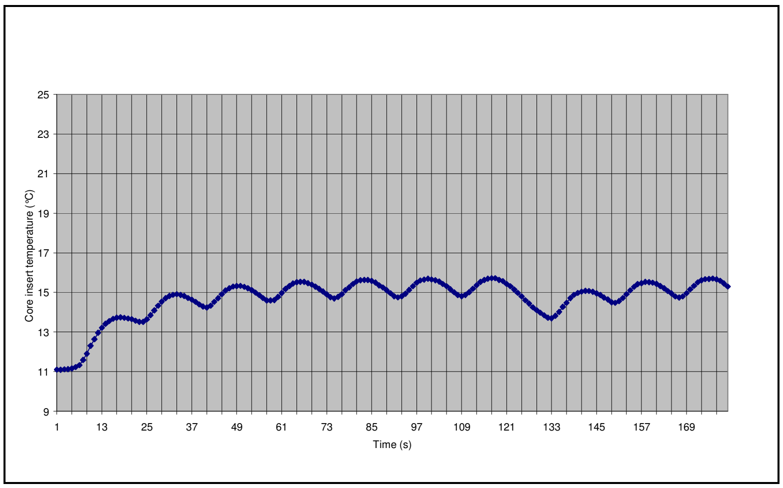

Figure B 16: Temperature plot for surface cooling method: cooling time 6 s, coolant temperature 11°C, and coolant flow rate 81 l/min

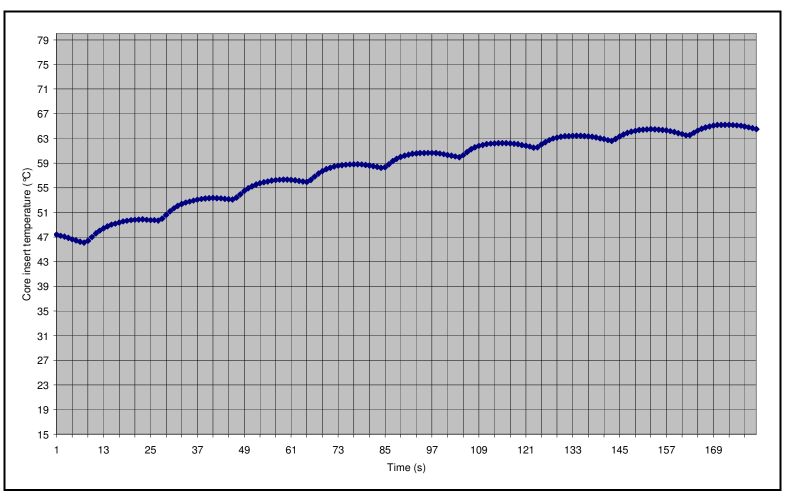

Figure B 17: Temperature plot for conventional cooling method: cooling time 2 s, coolant temperature 11°C, and coolant flow rate 41 l/min

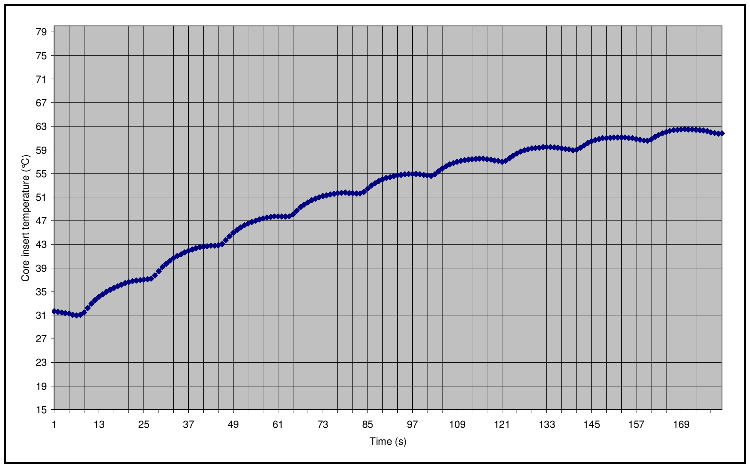

Figure B 18: Temperature plot for conventional cooling method: cooling time 2 s, coolant temperature 11°C, and coolant flow rate 50 l/min

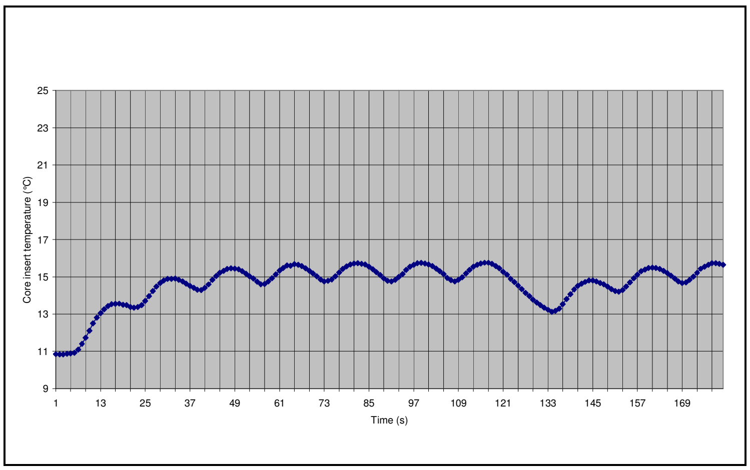

Figure B 19: Temperature plot for surface cooling method: cooling time 2 s, coolant temperature 11°C, and coolant flow rate 67 l/min

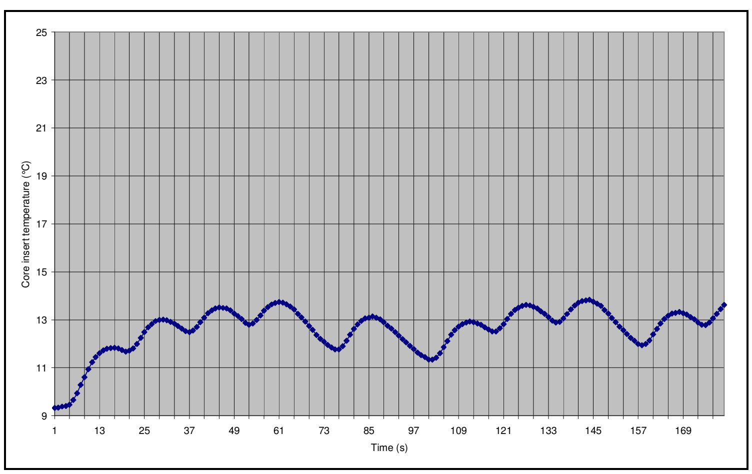

Figure B 20: Temperature plot for surface cooling method: cooling time 2 s, coolant temperature 11°C, and coolant flow rate 81 l/min

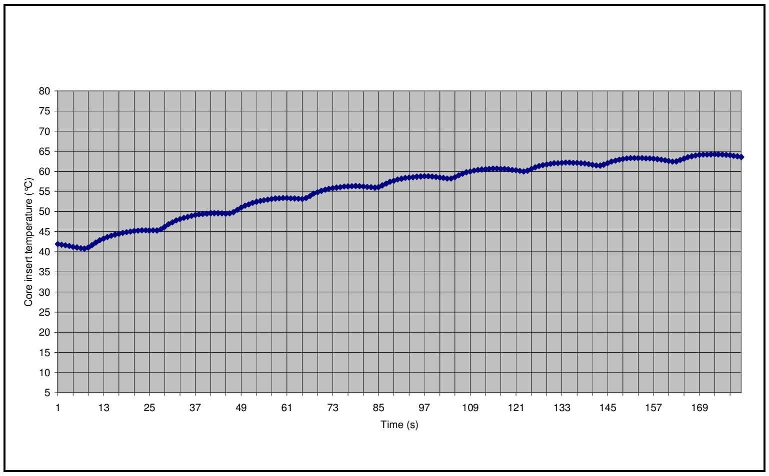

Figure B 21: Temperature plot for conventional cooling method: cooling time 0 s, coolant temperature 11°C, and coolant flow rate 41 l/min

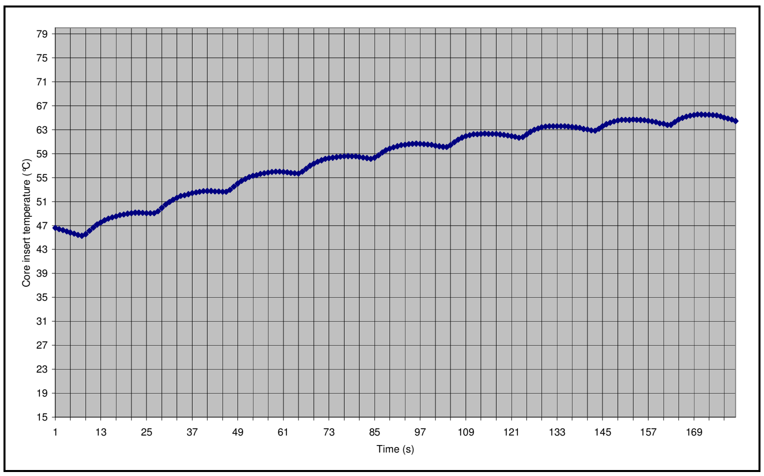

Figure B 22: Temperature plot for conventional cooling method: cooling time 0 s, coolant temperature 11°C, and coolant flow rate 50 l/min

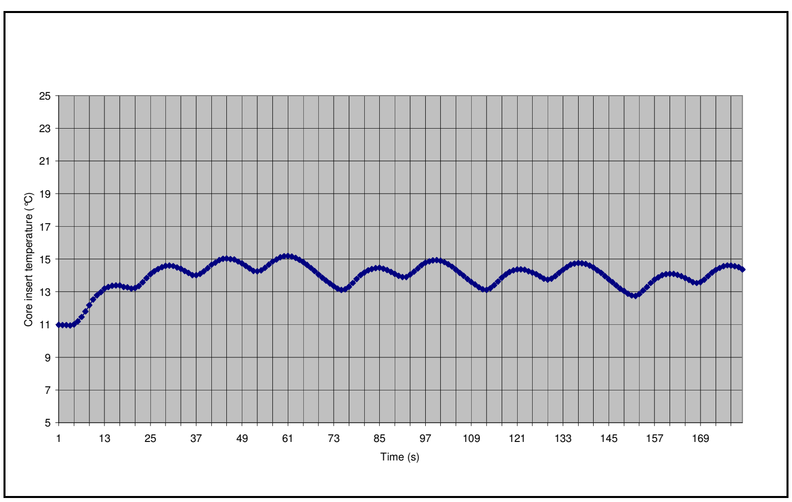

Figure B 23: Temperature plot for surface cooling method: cooling time 0 s, coolant temperature 11°C, and coolant flow rate 67 l/min

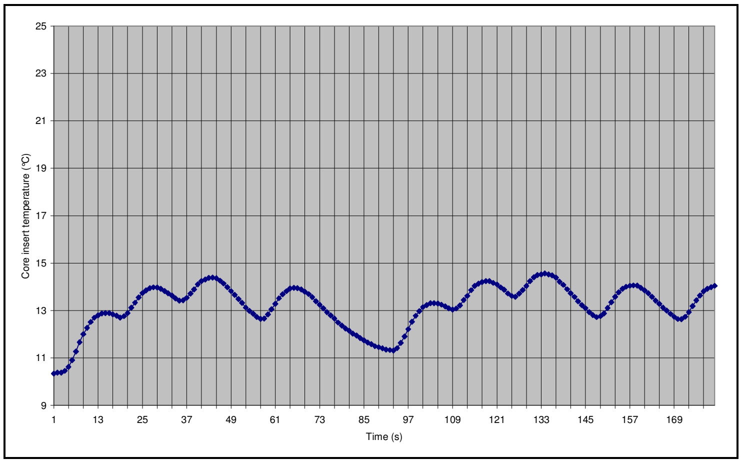

Figure B 24: Temperature plot for surface cooling method: cooling time 0 s, coolant temperature 11°C, and coolant flow rate 81 l/min

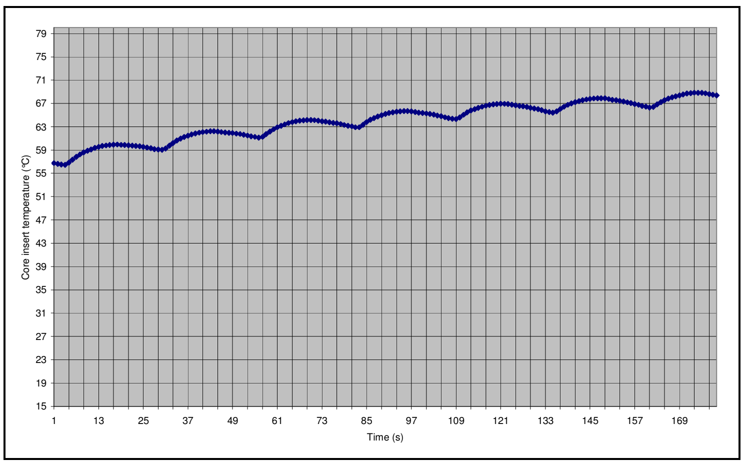

Figure B 25: Temperature plot for conventional cooling method: cooling time 12 s, coolant temperature 15°C, and coolant flow rate 41 l/min

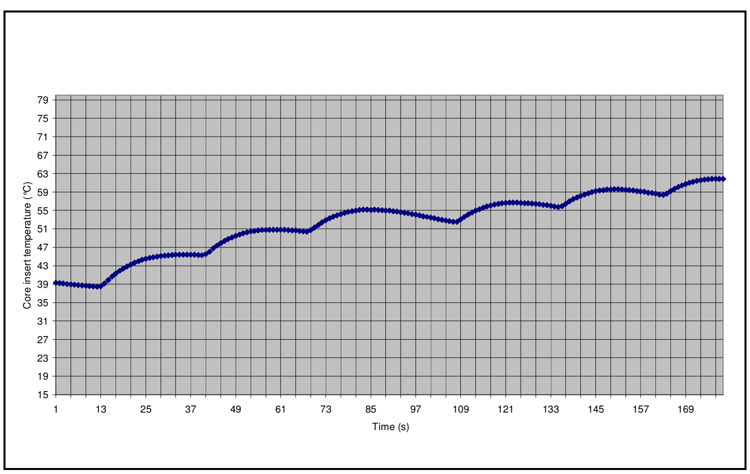

Figure B 26: Temperature plot for conventional cooling method: cooling time 12 s, coolant temperature 15°C, and coolant flow rate 50 l/min

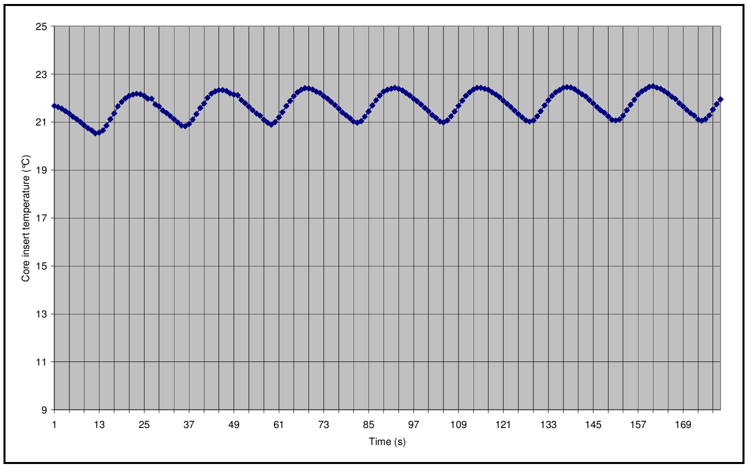

Figure B 27: Temperature plot for surface cooling method: cooling time 12 s, coolant temperature 15 °C, and coolant flow rate 67 l/min

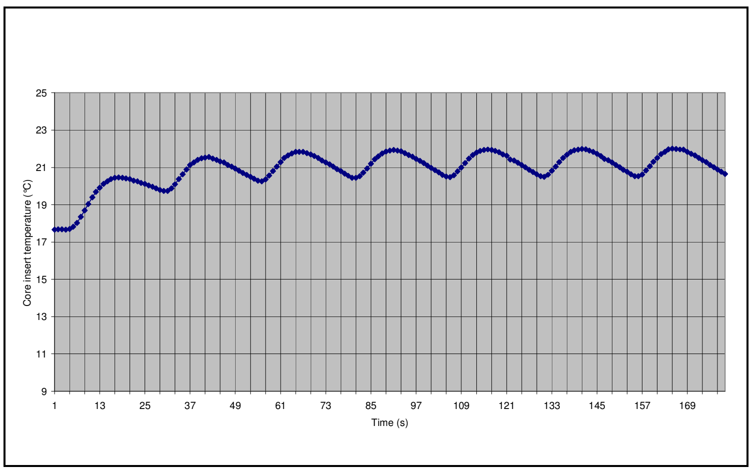

Figure B 28: Temperature plot for surface cooling method: cooling time 12 s, coolant temperature 15 °C, and coolant flow rate 81 l/min

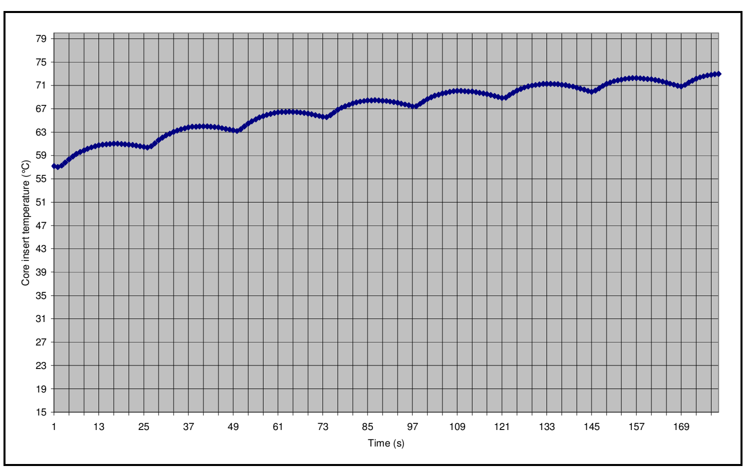

Figure B 29: Temperature plot for conventional cooling method: cooling time 8 s, coolant temperature 15 °C, and coolant flow rate 41 l/min

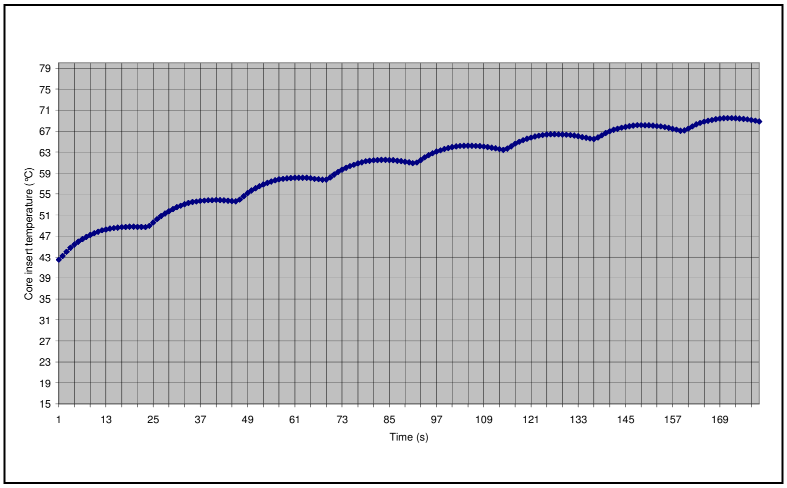

Figure B 30: Temperature plot for conventional cooling method: cooling time 8 s, coolant temperature 15 °C, and coolant flow rate 50 l/min

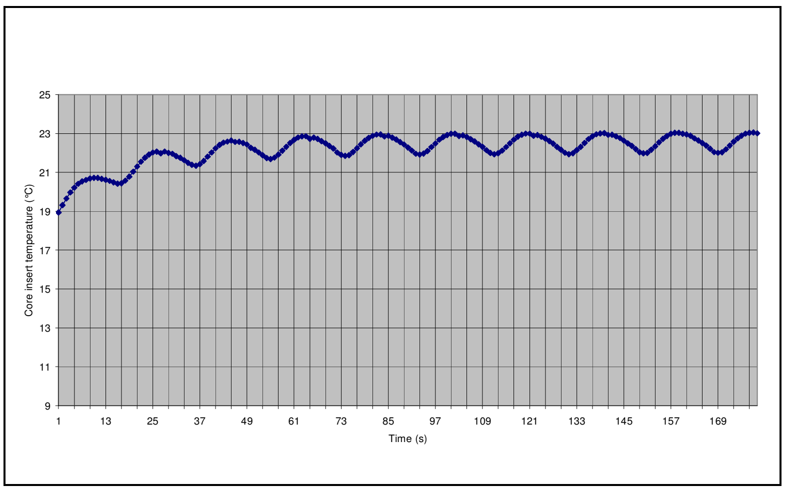

Figure B 31: Temperature plot for surface cooling method: cooling time 8 s, coolant temperature 15 °C, and coolant flow rate 67 l/min

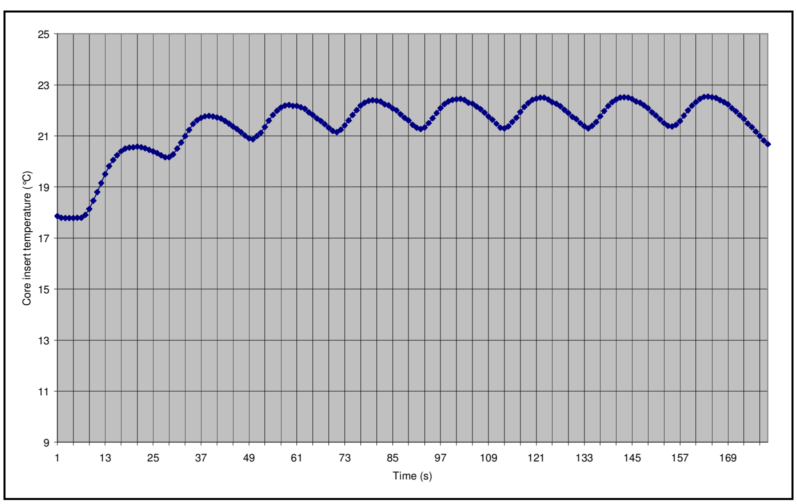

Figure B 32: Temperature plot for surface cooling method: cooling time 8 s, coolant temperature 15 °C, and coolant flow rate 81 l/min

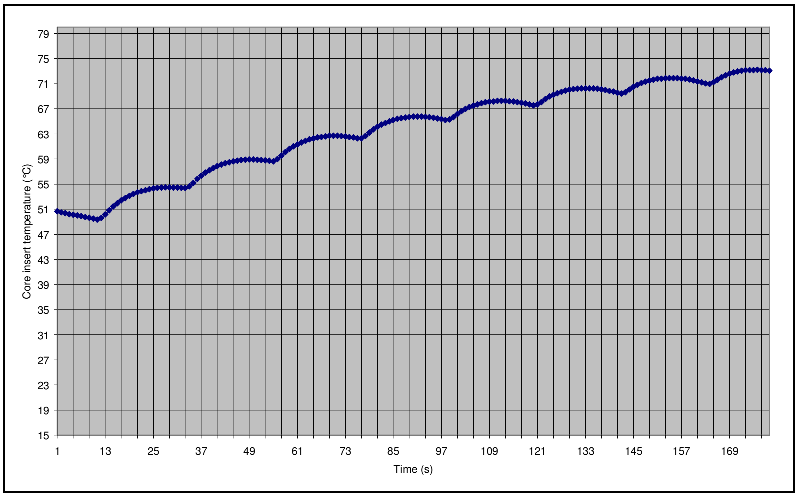

Figure B 33: Temperature plot for conventional cooling method: cooling time 6 s, coolant temperature 15 °C, and coolant flow rate 41 l/min

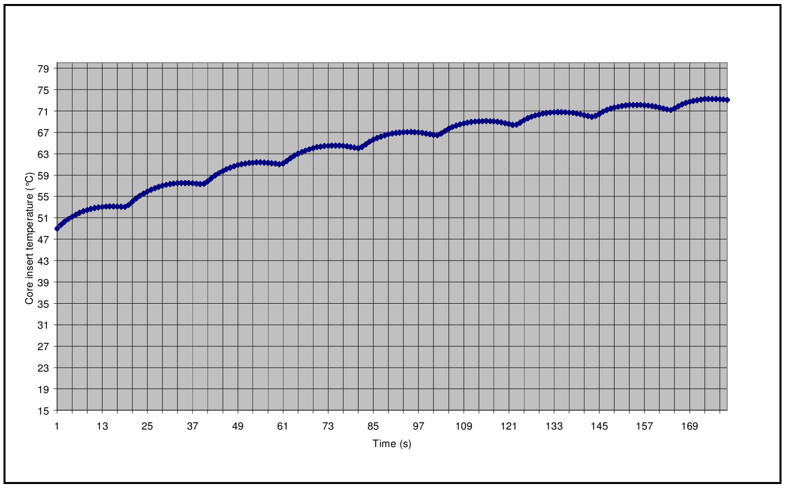

Figure B 34: Temperature plot for conventional cooling method: cooling time 6 s, coolant temperature 15 °C, and coolant flow rate 50 l/min

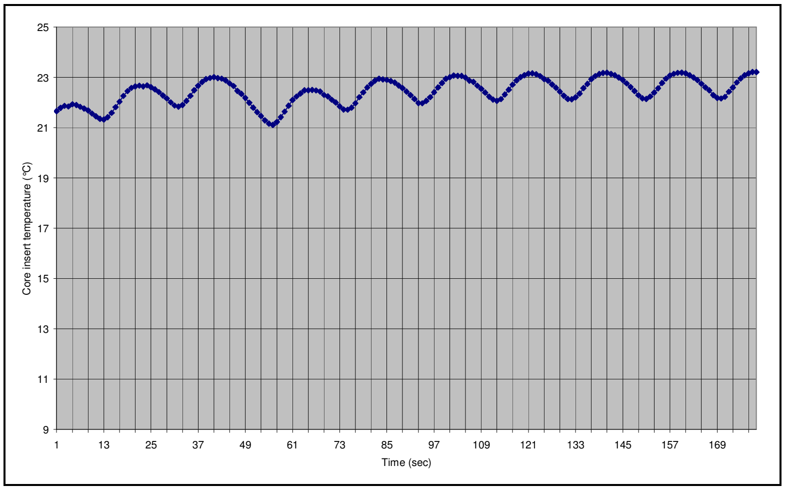

Figure B 35: Temperature plot for surface cooling method: cooling time 6 s, coolant temperature 15 °C, and coolant flow rate 67 l/min

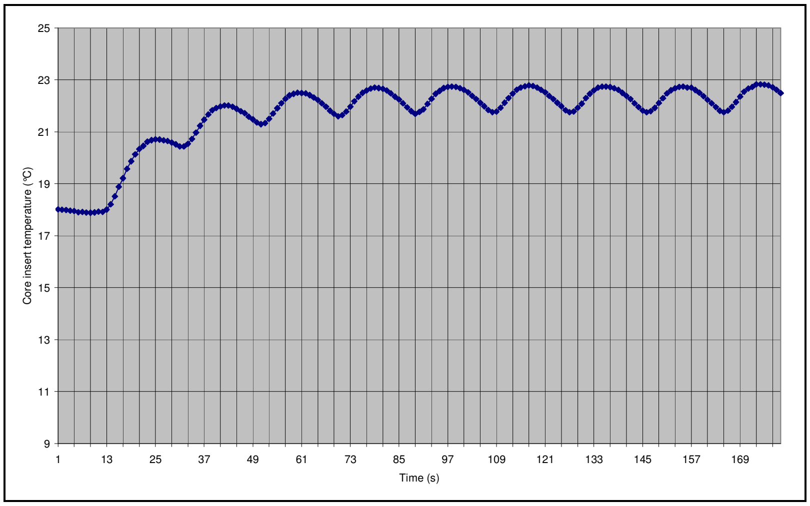

Figure B 36: Temperature plot for surface cooling method: cooling time 6 s, coolant temperature 15 °C, and coolant flow rate 81 l/min

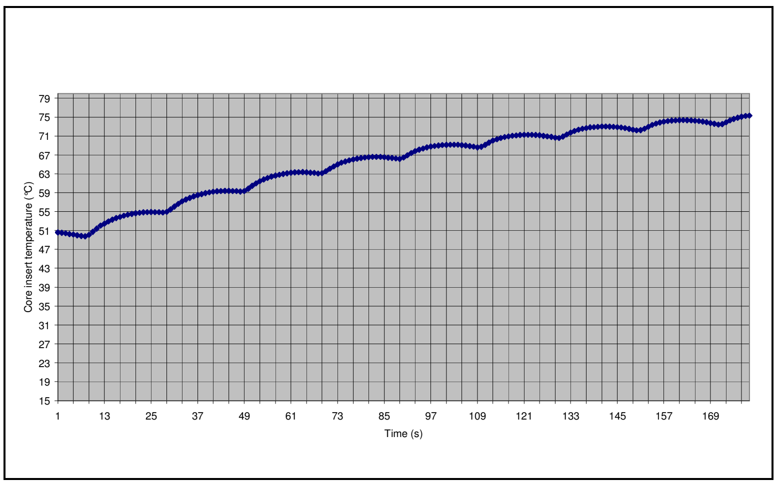

Figure B 37: Temperature plot for conventional cooling method: cooling time 2 s, coolant temperature 15 °C, and coolant flow rate 41 l/min

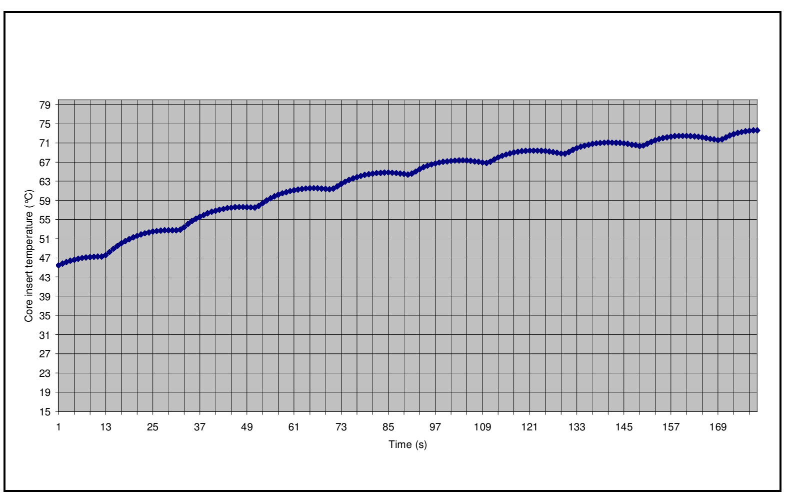

Figure B 38: Temperature plot for conventional cooling method: cooling time 2 s, coolant temperature 15 °C, and coolant flow rate 50 l/min

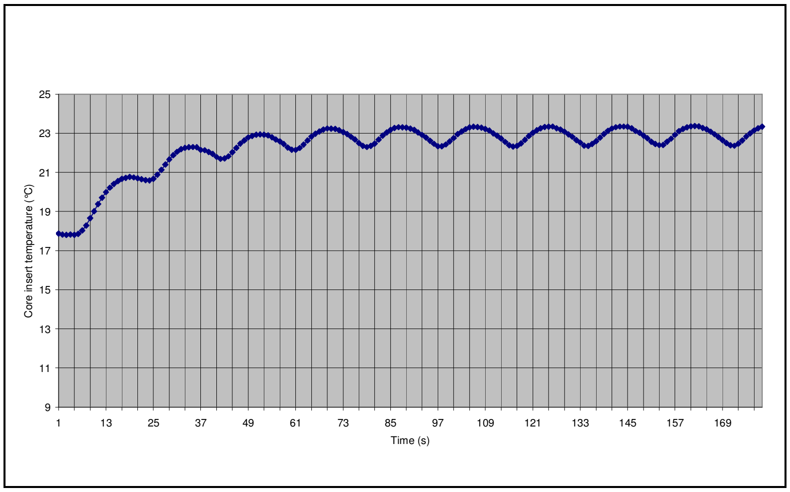

Figure B 39: Temperature plot for surface cooling method: cooling time 2 s, coolant temperature 15 °C, and coolant flow rate 67 l/min

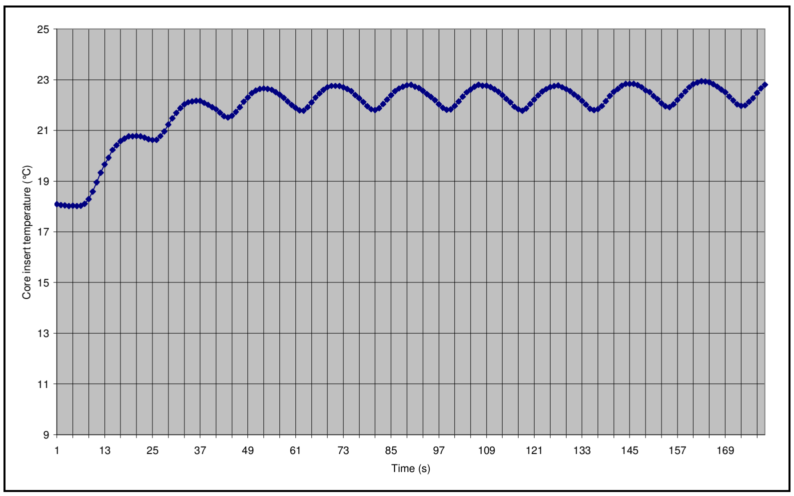

Figure B 40: Temperature plot for surface cooling method: cooling time 2 s, coolant temperature 15 °C, and coolant flow rate 81 l/min

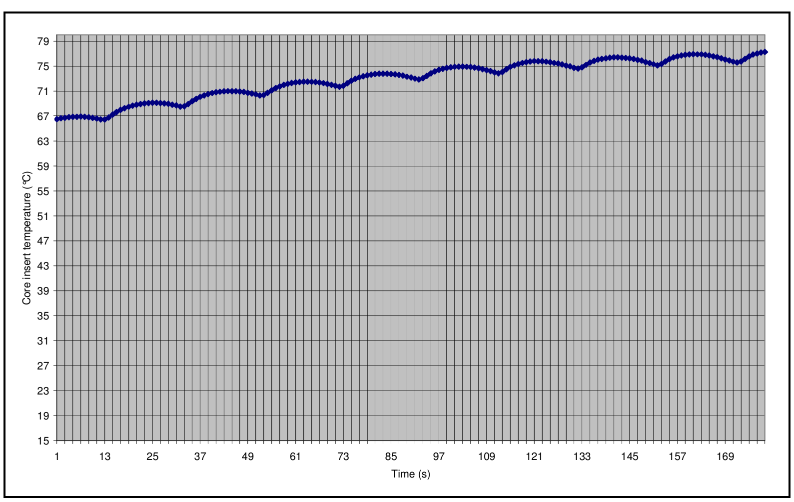

Figure B 41: Temperature plot for conventional cooling method: cooling time 0 s, coolant temperature 15 °C, and coolant flow rate 50 l/min

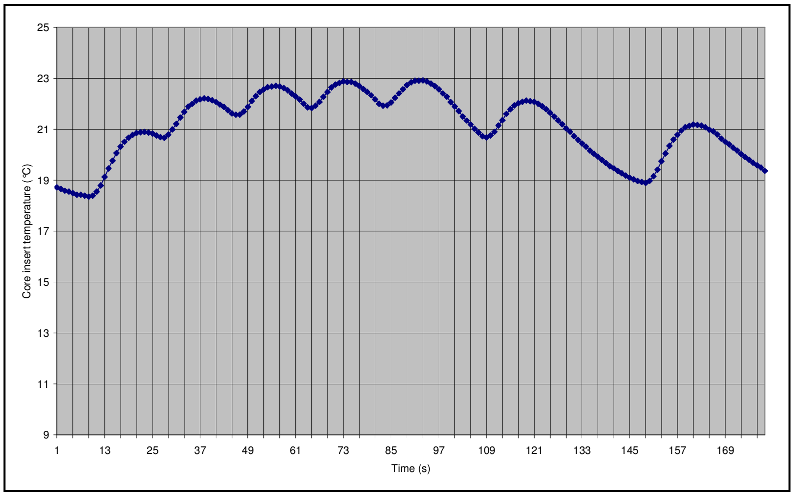

Figure B 42: Temperature plot for surface cooling method: cooling time 0 s, coolant temperature 15 °C, and coolant flow rate 81 l/min

Table B2: Measured deviation values of cutlery drainer produced by using conventional cooling insert

Cn1	Cn2	Cn3	Cn4	Cn5	Cn6	Cn7	Cn8	Cn9	Cn10
-1.549	-1.588	-1.735	-1.757	-1.78	-1.772	-1.8	-1.856	-1.935	-1.955
-0.059	-0.277	-0.283	-0.353	-0.341	-0.279	-0.278	-0.419	-0.391	-0.445
0.423	0.257	0.253	0.226	0.25	0.315	0.328	0.223	0.225	0.175
0.436	0.29	0.283	0.269	0.297	0.368	0.399	0.281	0.297	0.255
0.539	0.385	0.398	0.38	0.423	0.499	0.527	0.432	0.432	0.416
0.576	0.489	0.493	0.478	0.534	0.61	0.638	0.553	0.552	0.54
0.662	0.585	0.582	0.57	0.634	0.709	0.737	0.667	0.663	0.649
0.704	0.653	0.662	0.659	0.734	0.802	0.834	0.778	0.776	0.753
0.745	0.72	0.75	0.741	0.832	0.88	0.918	0.869	0.853	0.846
0.823	0.787	0.829	0.823	0.926	0.973	1.009	1.005	0.985	0.984
0.814	0.811	0.889	0.881	0.972	0.993	1.01	1.042	1.01	1
0.821	0.815	0.863	0.865	0.932	0.965	0.952	1.003	0.959	0.948
-0.334	-0.331	-0.24	-0.289	-0.221	-0.167	-0.14	-0.191	-0.159	-0.123
-0.122	-0.075	0.412	0.298	0.602	0.684	0.672	0.537	0.608	0.598
-0.156	-0.082	0.464	0.423	0.923	1.063	1.11	0.861	0.921	0.886
-0.195	-0.132	0.631	0.63	0.84	1.034	1.128	0.855	0.948	0.946
-0.246	-0.166	0.648	0.607	0.697	0.818	0.941	0.738	0.856	0.78

Table B2: (continued)

-0.308	-0.255	0.033	0.011	0.016	0.043	0.057	0.021	0.078	0.046
-1.567	-1.381	-1.403	-1.447	-1.287	-1.384	-1.433	-1.395	-1.384	-1.451
-1.532	-1.383	-1.377	-1.419	-1.45	-1.386	-1.415	-1.354	-1.366	-1.372
-1.591	-1.566	-1.408	-1.452	-1.436	-1.419	-1.41	-1.368	-1.348	-1.392
-1.856	-1.858	-1.577	-1.662	-1.537	-1.553	-1.559	-1.639	-1.67	-1.438
-2.177	-2.176	-1.942	-2.022	-2.197	-2.413	-2.497	-2.582	-2.398	-2.399
-1.669	-1.449	-1.711	-1.714	-1.915	-1.857	-2.059	-2.072	-1.997	-1.981
0.06	0.129	0.199	0.092	0.407	0.526	0.513	0.549	0.499	0.498
-0.302	-0.245	-0.076	-0.158	0.043	0.153	0.109	0.115	0.044	0.045
0.009	-0.002	0.14	0.023	0.585	0.724	0.733	0.781	0.743	0.776
0.036	0.087	0.235	0.13	0.56	0.664	0.68	0.734	0.702	0.706
0.155	0.322	0.412	0.362	0.651	0.698	0.705	0.703	0.651	0.666
0.15	0.306	0.378	0.379	0.651	0.687	0.772	0.718	0.696	0.659
-0.018	0.068	0.201	0.229	0.592	0.65	0.681	0.518	0.547	0.361
-0.131	-0.101	0.011	0.006	0.094	0.088	0.023	0.103	-0.055	0.024
-0.584	-0.543	-0.494	-0.477	-0.226	-0.161	-0.037	-0.252	-0.019	-0.343
-0.606	-0.601	-0.538	-0.578	-0.164	-0.092	0.001	-0.065	-0.064	-0.466
-0.579	-0.572	-0.561	-0.589	-0.255	-0.223	-0.153	-0.118	-0.259	-0.481
-0.464	-0.438	-0.485	-0.465	-0.519	-0.54	-0.548	-0.544	-0.579	-0.559
-0.49	-0.42	-0.383	-0.431	-0.413	-0.398	-0.362	-0.314	-0.282	-0.251
-0.53	-0.322	-0.251	-0.323	-0.209	-0.21	-0.18	-0.186	-0.166	-0.164
-0.765	-0.431	-0.385	-0.535	-0.354	-0.358	-0.339	-0.348	-0.314	-0.371
-1.007	-0.683	-0.679	-0.882	-0.695	-0.704	-0.683	-0.625	-0.558	-0.626
-0.424	-0.342	-0.387	-0.391	-0.389	-0.407	-0.357	-0.277	-0.216	-0.215
-1.723	-1.736	-1.897	-1.863	-2.036	-2.089	-2.111	-2.083	-2.073	-2.005
-1.297	-1.288	-1.237	-1.274	-1.271	-1.273	-1.335	-1.406	-1.48	-1.461
-1.378	-1.472	-1.338	-1.257	-1.233	-1.234	-1.266	-1.289	-1.397	-1.343
-1.452	-1.444	-1.286	-1.321	-1.347	-1.424	-1.352	-1.428	-1.501	-1.477
-1.595	-1.467	-1.32	-1.366	-1.274	-1.339	-1.357	-1.432	-1.5	-1.56

Table B2: (continued)

-1.803	-1.773	-1.631	-1.68	-1.455	-1.46	-1.57	-1.762	-1.769	-1.992
-2.027	-1.991	-1.98	-1.95	-2.105	-2.139	-2.211	-2.081	-2.193	-2.168
-0.371	-0.303	-0.159	-0.213	0.115	0.088	0.206	-0.1	0.085	-0.069
-0.396	-0.371	-0.2	-0.295	0.103	0.168	0.248	-0.076	0.227	-0.003
-0.208	-0.154	-0.155	-0.146	0.078	0.011	0.107	-0.111	0.088	-0.122
-0.392	-0.385	-0.374	-0.337	-0.175	-0.235	-0.09	-0.269	-0.082	-0.169
0.318	0.308	0.239	0.268	0.195	0.164	0.188	0.193	0.244	0.24
1.046	1.031	1.05	1.045	0.993	1.052	1.076	1.145	1.157	1.099
0.861	0.875	0.891	0.895	0.85	0.897	0.904	1.002	1.012	0.954
0.753	0.776	0.783	0.805	0.76	0.802	0.814	0.896	0.927	0.851
0.725	0.669	0.643	0.696	0.627	0.649	0.674	0.728	0.784	0.747
0.562	0.541	0.487	0.555	0.489	0.486	0.513	0.565	0.613	0.613
-0.63	-0.657	-0.762	-0.696	-0.861	-0.901	-0.895	-0.831	-0.753	-0.681
-2.051	-2.048	-2.212	-2.252	-2.367	-2.378	-2.414	-2.454	-2.476	-2.42
-0.712	-0.687	-0.741	-0.873	-0.905	-0.926	-0.968	-1.02	-1.038	-1.006
0.004	0.084	0.137	0.021	0.098	0.091	0.063	0.081	0.023	0.012
0.07	0.089	0.247	0.138	0.207	0.146	0.147	0.167	0.1	0.092
0.027	0.026	0.171	0.1	0.14	0.134	0.144	0.177	0.13	0.105
-0.014	0.107	0.179	0.141	0.166	0.16	0.184	0.216	0.17	0.141
0.031	0.124	0.189	0.178	0.201	0.199	0.229	0.268	0.209	0.19
0.074	0.139	0.223	0.223	0.238	0.237	0.279	0.298	0.246	0.229
0.157	0.183	0.282	0.276	0.323	0.333	0.374	0.382	0.337	0.324
0.178	0.241	0.337	0.335	0.394	0.413	0.449	0.46	0.415	0.405
-0.15	-0.17	-0.15	-0.148	0.007	0.07	0.111	0.019	0.057	0.051
-0.17	-0.092	0.254	0.265	0.605	0.669	0.783	0.454	0.52	0.492
-0.11	-0.082	0.401	0.399	0.898	1.007	1.053	0.802	0.853	0.839
-0.171	-0.099	0.37	0.389	0.879	0.981	0.95	0.791	0.852	0.851
-0.153	-0.116	0.276	0.266	0.487	0.579	0.527	0.491	0.527	0.548
-0.24	-0.232	-0.145	-0.165	-0.093	-0.049	-0.047	-0.056	-0.03	0.012

Table B2: (continued)

0.174	0.172	0.187	0.197	0.187	0.18	0.177	0.179	0.166	0.179
0.2	0.2	0.229	0.235	0.212	0.213	0.209	0.216	0.2	0.225
0.05	0.057	0.085	0.087	0.095	0.081	0.07	0.081	0.046	0.046
0.027	0.025	0.069	0.066	0.072	0.069	0.053	0.06	0.023	0.022
-0.039	-0.018	0.062	0.033	0.074	0.083	0.058	0.059	0.031	0.013
-0.1	-0.052	0.063	0.005	0.078	0.097	0.082	0.071	0.054	0.024
-0.181	-0.108	0.04	-0.036	0.057	0.074	0.065	0.037	0.022	0.012
-0.358	-0.243	-0.07	-0.123	-0.028	0.06	0.024	0.021	-0.007	-0.004
-1.189	-1.154	-1.091	-1.179	-0.496	-1.066	-1.128	-0.517	-1.211	-1.215
-1.798	-1.804	-1.926	-1.947	-1.999	-1.953	-1.996	-2.034	-2.105	-2.089
-1.519	-1.519	-1.533	-1.572	-1.595	-1.586	-1.617	-1.622	-1.678	-1.626
-0.686	-0.623	-0.468	-0.555	-0.446	-0.438	-0.457	-0.51	-0.52	-0.484
-0.258	-0.211	-0.038	-0.128	-0.036	-0.015	-0.025	-0.062	-0.089	-0.059
-0.105	-0.057	0.062	-0.01	0.04	0.071	0.056	0.051	0.028	0.011
0.057	0.086	0.112	0.089	0.105	0.125	0.106	0.12	0.082	0.062
0.013	0.044	0.049	0.024	0.037	0.04	0.024	0.045	-0.018	0.002
0.018	0.086	0.113	0.097	0.088	0.063	0.073	0.081	0.015	-0.002
0.06	0.109	0.133	0.131	0.109	0.082	0.1	0.086	0.061	0.05
-0.031	0.002	0.021	0.025	-0.003	-0.026	0	-0.017	-0.036	-0.041
-0.332	-0.376	-0.4	-0.401	-0.501	-0.502	-0.534	-0.502	-0.496	-0.453
-0.366	-0.412	-0.41	-0.372	-0.447	-0.452	-0.474	-0.504	-0.474	-0.535
-0.611	-0.675	-0.672	-0.67	-0.399	-0.379	-0.34	-0.444	-0.456	-0.526
-0.616	-0.633	-0.584	-0.636	-0.364	-0.294	-0.248	-0.277	-0.322	-0.567
-0.539	-0.527	-0.562	-0.557	-0.391	-0.351	-0.205	-0.057	-0.085	-0.534
-0.423	-0.406	-0.421	-0.371	-0.401	-0.434	-0.316	-0.019	-0.114	-0.512
-0.348	-0.302	-0.359	-0.35	-0.471	-0.492	-0.484	-0.489	-0.499	-0.522
-0.193	-0.139	-0.078	-0.072	-0.058	-0.07	-0.033	-0.041	-0.038	-0.051
-0.133	-0.058	-0.007	0	0.011	-0.018	0.007	0.014	-0.025	-0.053
-0.149	-0.114	-0.076	-0.089	-0.096	-0.1	-0.103	-0.065	-0.103	-0.117

Table B2: (continued)

-0.087	-0.088	-0.056	-0.063	-0.082	-0.068	-0.085	-0.069	-0.071	-0.073
-0.161	-0.111	-0.037	-0.074	-0.102	-0.092	-0.112	-0.086	-0.092	-0.121
-0.359	-0.235	-0.134	-0.214	-0.226	-0.236	-0.246	-0.255	-0.28	-0.257
-0.579	-0.417	-0.293	-0.393	-0.382	-0.418	-0.422	-0.44	-0.473	-0.441
-0.951	-0.786	-0.731	-0.817	-0.876	-0.929	-0.94	-0.96	-1.004	-0.965
-1.827	-1.723	-1.834	-1.881	0.47	0.402	0.395	0.277	0.2	0.161
-1.801	-1.732	-1.853	-1.799	-2.003	-2.068	-2.084	-2.03	-2.016	-1.951
-0.484	-0.397	-0.426	-0.451	-0.53	-0.536	-0.538	-0.511	-0.498	-0.458
-0.211	-0.171	-0.169	-0.186	-0.28	-0.262	-0.273	-0.253	-0.231	-0.215
-0.105	-0.101	-0.077	-0.079	-0.162	-0.126	-0.137	-0.106	-0.065	-0.094
0.041	0.042	0.048	0.046	-0.002	0.02	0.014	0.032	0.069	0.065
0.085	0.095	0.097	0.094	0.078	0.098	0.107	0.134	0.154	0.145
0.128	0.14	0.191	0.18	0.184	0.199	0.224	0.236	0.263	0.257
-0.368	-0.321	-0.412	-0.344	-0.442	-0.531	-0.502	-0.472	-0.453	-0.4
-0.311	-0.28	-0.338	-0.294	-0.238	-0.293	-0.229	-0.305	-0.223	-0.233
-0.363	-0.327	-0.283	-0.283	-0.092	-0.099	0.009	-0.2	-0.031	-0.132
-0.318	-0.319	-0.266	-0.284	-0.028	-0.034	0.066	-0.132	0.104	-0.089
-0.3	-0.338	-0.299	-0.28	-0.137	-0.169	-0.077	-0.231	0.009	-0.19
-0.259	-0.283	-0.341	-0.332	-0.297	-0.368	-0.338	-0.364	-0.218	-0.307
-0.432	-0.446	-0.525	-0.485	-0.551	-0.623	-0.601	-0.563	-0.519	-0.486
0.359	0.379	0.398	0.395	0.409	0.427	0.439	0.471	0.432	0.42
0.303	0.319	0.336	0.326	0.353	0.375	0.385	0.425	0.375	0.355
0.206	0.217	0.217	0.212	0.238	0.256	0.267	0.296	0.268	0.246
0.111	0.115	0.143	0.124	0.158	0.182	0.198	0.229	0.215	0.172
-0.078	-0.072	-0.015	-0.044	0.01	0.014	0.045	0.055	0.04	0.043
-0.278	-0.235	-0.168	-0.214	-0.098	-0.115	-0.077	-0.076	-0.078	-0.057
-1.288	-1.263	-1.332	-1.321	-1.272	-1.348	-1.321	-1.302	-1.32	-1.275
-1.646	-1.675	-1.834	-1.858	-1.914	-1.919	-1.945	-1.995	-2.049	-2.038
-1.752	-1.764	-1.908	-1.918	-1.948	-1.912	-1.945	-2.004	-2.08	-2.095

Table B2: (continued)

-2.174	-2.132	-2.219	-2.218	-2.305	-2.316	-2.331	-2.324	-2.366	-2.265
-2.22	-2.224	-2.407	-2.385	-2.525	-2.553	-2.567	-2.553	-2.599	-2.509
-2.176	-2.206	-2.421	-2.383	-2.543	-2.58	-2.594	-2.588	-2.636	-2.557
-2.089	-2.155	-2.376	-2.342	-2.518	-2.553	-2.564	-2.562	-2.591	-2.516
-2.065	-2.086	-2.273	-2.239	-2.391	-2.43	-2.429	-2.429	-2.458	-2.395
-2.037	-2.044	-2.169	-2.145	-2.232	-2.245	-2.254	-2.236	-2.281	-2.209
-1.818	-1.804	-1.896	-1.937	-2.005	-1.973	-2.019	-2.033	-2.104	-2.054
-2.067	-2.069	-2.215	-2.245	-2.415	-2.429	-2.469	-2.479	-2.505	-2.433
-1.65	-1.577	-1.667	-1.662	-1.859	-1.91	-1.932	-1.909	-1.908	-1.859
-1.672	-1.638	-1.795	-1.758	-1.948	-2.001	-2.016	-1.979	-1.982	-1.915
-1.794	-1.771	-1.928	-1.905	-2.094	-2.143	-2.16	-2.138	-2.131	-2.058
-1.748	-1.756	-1.917	-1.889	-2.072	-2.119	-2.137	-2.112	-2.103	-2.033
-1.726	-1.744	-1.901	-1.867	-2.049	-2.09	-2.113	-2.082	-2.074	-2.007
-1.727	-1.747	-1.897	-1.864	-2.039	-2.079	-2.103	-2.078	-2.062	-1.993
-1.766	-1.774	-1.899	-1.875	-2.008	-2.05	-2.075	-2.043	-2.036	-1.966
-1.424	-1.411	-1.437	-1.459	-1.478	-1.504	-1.525	-1.52	-1.558	-1.504
-2.004	-1.994	-2.128	-2.072	-2.193	-2.271	-2.267	-2.224	-2.225	-2.114
-2.092	-2.054	-2.226	-2.049	-2.348	-2.437	-2.315	-2.325	-2.35	-2.24
Cn11	Cn12	Cn13	Cn14	Cn15	Cn16	Cn17	Cn18	Cn19	Cn20
-1.711	-1.638	-1.819	-1.857	-1.854	-1.806	-1.909	-1.76	-1.763	-1.939
-0.37	-0.14	-0.35	-0.324	-0.276	-0.247	-0.345	-0.15	-0.146	-0.357
0.177	0.28	0.166	0.181	0.263	0.28	0.208	0.365	0.372	0.164
0.25	0.318	0.228	0.245	0.3	0.335	0.262	0.416	0.408	0.223
0.41	0.428	0.37	0.374	0.413	0.485	0.44	0.548	0.551	0.399
0.519	0.486	0.487	0.459	0.525	0.583	0.534	0.658	0.638	0.516
0.602	0.585	0.584	0.565	0.654	0.682	0.669	0.758	0.735	0.622
0.673	0.658	0.699	0.676	0.776	0.792	0.8	0.86	0.832	0.739
0.743	0.72	0.798	0.769	0.906	0.909	0.941	0.986	0.926	0.857
0.806	0.794	0.888	0.88	0.987	0.97	1.047	1.014	0.961	0.922

Table B2: (continued)

0.844	0.819	0.92	0.951	1.013	1.036	1.109	1.067	1.018	0.993
0.823	0.828	0.91	0.935	0.959	0.994	1.042	1.015	0.966	0.948
-0.316	-0.356	-0.349	-0.323	-0.219	-0.157	-0.145	-0.101	-0.163	-0.122
0.087	-0.088	0.325	0.407	0.523	0.496	0.749	0.567	0.577	0.572
0.135	-0.1	0.408	0.585	0.933	0.867	1.176	0.939	0.854	1.007
0.097	-0.129	0.628	0.671	1.194	1.057	1.491	1.111	0.727	1.279
0.006	-0.166	0.622	0.422	1.012	0.922	1.254	0.959	0.541	1.07
-0.125	-0.259	0.009	-0.013	0.043	0.021	0.033	0.035	-0.012	0.057
-1.504	-1.491	-1.529	-1.469	-1.385	-1.106	-0.933	-0.973	-1.822	-0.984
-1.348	-1.38	-1.42	-1.475	-1.524	-1.476	-1.572	-1.462	-1.66	-1.48
-1.454	-1.553	-1.464	-1.495	-1.564	-1.506	-1.468	-1.49	-1.725	-1.478
-1.792	-1.924	-1.725	-1.733	-1.812	-1.629	-1.808	-1.657	-2.095	-1.633
-2.013	-2.294	-2.096	-2.166	-2.22	-2.27	-2.352	-2.238	-2.608	-2.188
-1.493	-1.644	-1.731	-1.812	-1.91	-1.985	-1.877	-2.064	-2.058	-2.011
-0.098	0.159	-0.017	0.15	0.252	0.357	0.334	0.393	0.322	0.333
-0.343	-0.172	-0.197	-0.108	-0.014	0.115	0.035	0.165	-0.053	0.091
-0.249	-0.069	-0.178	0.06	0.322	0.483	0.584	0.474	0.098	0.462
0.05	-0.008	0.083	0.182	0.395	0.527	0.614	0.51	0.148	0.522
0.361	0.205	0.349	0.355	0.522	0.554	0.661	0.503	0.304	0.601
0.331	0.198	0.343	0.316	0.49	0.499	0.74	0.46	0.278	0.566
0.069	-0.021	0.153	0.091	0.447	0.365	0.314	0.344	0.153	0.379
-0.181	-0.178	-0.052	-0.098	0.091	0.077	-0.031	0.051	0.066	0.041
-0.494	-0.463	-0.449	-0.358	-0.238	-0.379	-0.147	-0.404	-0.567	-0.493
-0.526	-0.381	-0.326	-0.174	-0.211	-0.149	0.069	-0.265	-0.529	-0.669
-0.532	-0.407	-0.392	-0.264	-0.313	-0.11	0.133	-0.141	-0.613	-0.515
-0.458	-0.446	-0.451	-0.455	-0.548	-0.501	-0.421	-0.532	-0.612	-0.563
-0.399	-0.427	-0.41	-0.412	-0.427	-0.358	-0.392	-0.361	-0.493	-0.186
-0.328	-0.367	-0.259	-0.257	-0.226	-0.194	-0.223	-0.207	-0.479	-0.056
-0.522	-0.468	-0.365	-0.358	-0.346	-0.286	-0.329	-0.301	-0.62	-0.199

Table B2: (continued)

-0.864	-0.711	-0.67	-0.662	-0.682	-0.559	-0.57	-0.581	-0.836	-0.511
-0.428	-0.384	-0.363	-0.337	-0.378	-0.275	-0.215	-0.299	-0.384	-0.22
-1.837	-1.768	-1.914	-1.931	-2.104	-2.081	-2.084	-2.085	-1.982	-2.018
-1.272	-1.316	-1.331	-1.345	-1.325	-1.418	-1.475	-1.397	-1.399	-1.467
-1.339	-1.49	-1.406	-1.444	-1.375	-1.354	-1.392	-1.416	-1.599	-1.332
-1.327	-1.414	-1.293	-1.379	-1.263	-1.338	-1.341	-1.441	-1.603	-1.297
-1.373	-1.438	-1.291	-1.354	-1.288	-1.342	-1.348	-1.425	-1.54	-1.363
-1.795	-1.754	-1.63	-1.645	-1.568	-1.865	-2.222	-2.013	-1.534	-2.017
-2.092	-2.016	-1.965	-1.947	-2.069	-1.894	-1.888	-1.919	-1.975	-1.886
-0.291	-0.249	-0.083	-0.124	0.203	-0.095	0.16	-0.02	0.061	0.058
-0.315	-0.279	-0.044	-0.074	0.325	-0.101	0.261	0.016	0.147	0.064
-0.161	-0.19	0.017	-0.05	0.116	-0.129	0.122	-0.046	0.165	0.13
-0.415	-0.436	-0.291	-0.284	-0.11	-0.302	-0.121	-0.252	-0.074	-0.106
0.27	0.3	0.254	0.243	0.19	0.179	0.199	0.164	0.212	0.244
0.991	0.956	0.989	1.023	1.045	1.057	1.086	1.054	0.999	1.021
0.841	0.808	0.833	0.872	0.875	0.896	0.926	0.896	0.828	0.874
0.747	0.709	0.738	0.764	0.75	0.786	0.802	0.788	0.723	0.79
0.643	0.611	0.625	0.658	0.623	0.663	0.685	0.653	0.614	0.696
0.499	0.465	0.473	0.507	0.5	0.502	0.558	0.471	0.492	0.563
-0.741	-0.683	-0.805	-0.765	-0.916	-0.884	-0.842	-0.905	-0.837	-0.726
-2.139	-2.053	-2.224	-2.29	-2.415	-2.335	-2.445	-2.306	-2.349	-2.355
-0.751	-0.766	-0.843	-0.897	-1.062	-0.916	-1.07	-0.904	-1.02	-0.982
0.055	-0.079	0.057	0.042	-0.018	0.042	-0.055	0.025	-0.143	-0.021
0.197	0.072	0.19	0.157	0.146	0.182	0.112	0.167	0.084	0.102
0.11	0.086	0.155	0.157	0.166	0.2	0.143	0.189	0.102	0.116
0.102	0.13	0.176	0.192	0.217	0.265	0.218	0.233	0.187	0.159
0.114	0.16	0.202	0.237	0.27	0.32	0.299	0.294	0.237	0.198
0.152	0.179	0.239	0.287	0.323	0.376	0.334	0.35	0.275	0.239
0.21	0.223	0.3	0.333	0.388	0.432	0.423	0.42	0.326	0.32

Table B2: (continued)

0.26	0.237	0.351	0.373	0.433	0.468	0.464	0.467	0.33	0.383
-0.17	-0.174	-0.225	-0.212	-0.034	-0.078	0.113	-0.029	0.041	-0.028
0.057	-0.096	0.261	0.328	0.513	0.363	0.659	0.422	0.595	0.404
0.112	-0.099	0.382	0.547	0.835	0.778	1.091	0.82	0.706	0.858
0.076	-0.11	0.332	0.595	0.789	0.779	1.021	0.862	0.865	0.839
0.047	-0.075	0.214	0.261	0.412	0.376	0.573	0.441	0.52	0.396
-0.194	-0.215	-0.255	-0.247	-0.16	-0.154	-0.017	-0.1	-0.079	-0.104
0.17	0.169	0.242	0.253	0.238	0.24	0.241	0.227	0.219	0.228
0.191	0.203	0.259	0.281	0.254	0.255	0.269	0.238	0.232	0.228
0.044	0.061	0.116	0.131	0.133	0.119	0.096	0.114	0.118	0.097
0.02	0.036	0.09	0.099	0.135	0.097	0.078	0.097	0.106	0.081
0.008	-0.002	0.056	0.08	0.119	0.086	0.055	0.083	0.077	0.08
-0.008	-0.05	0.033	0.071	0.115	0.08	0.045	0.092	0.056	0.08
-0.053	-0.079	0	0.038	0.088	0.047	0.012	0.083	0.01	0.062
-0.152	-0.138	-0.053	-0.017	0.056	0.031	-0.022	0.059	-0.061	0.06
-1.147	-1.068	-1.207	-1.179	-0.511	-1.118	-0.544	-1.027	-1.131	-1.116
-1.874	-1.798	-1.966	-1.995	-2.01	-1.939	-2.026	-1.898	-1.928	-2.039
-1.491	-1.487	-1.546	-1.567	-1.584	-1.581	-1.599	-1.566	-1.545	-1.596
-0.431	-0.547	-0.492	-0.509	-0.444	-0.49	-0.493	-0.476	-0.553	-0.447
-0.012	-0.253	-0.154	-0.182	-0.107	-0.16	-0.158	-0.155	-0.26	-0.087
0.06	-0.094	0.01	-0.006	0.038	0.005	0.01	-0.001	-0.073	0.015
0.079	0.022	0.098	0.1	0.097	0.104	0.101	0.093	0.077	0.06
0.012	-0.008	0.056	0.033	0.039	0.039	0.037	0.023	0.022	0.016
0.029	0.013	0.09	0.087	0.119	0.122	0.087	0.121	0.037	0.012
0.082	0.027	0.118	0.119	0.134	0.14	0.11	0.14	0.089	0.071
-0.016	-0.054	0.027	0.011	0.042	0.045	0.036	0.033	-0.028	-0.012
-0.377	-0.369	-0.451	-0.44	-0.58	-0.548	-0.53	-0.541	-0.465	-0.478
-0.398	-0.456	-0.458	-0.411	-0.578	-0.562	-0.465	-0.541	-0.488	-0.63
-0.645	-0.559	-0.545	-0.423	-0.475	-0.368	-0.028	-0.402	-0.635	-0.654

Table B2: (continued)

-0.548	-0.394	-0.392	-0.261	-0.46	-0.338	-0.062	-0.408	-0.619	-0.674
-0.556	-0.455	-0.518	-0.371	-0.367	-0.298	0.011	-0.322	-0.454	-0.612
-0.4	-0.402	-0.457	-0.372	-0.423	-0.516	-0.375	-0.502	-0.317	-0.57
-0.346	-0.349	-0.4	-0.395	-0.515	-0.557	-0.539	-0.561	-0.435	-0.511
-0.119	-0.123	-0.047	-0.032	0.007	0.005	0.009	0	-0.114	-0.03
-0.054	-0.087	0.021	0.035	0.081	0.074	0.05	0.081	-0.081	-0.032
-0.112	-0.131	-0.023	-0.02	-0.016	-0.023	-0.013	-0.004	-0.121	-0.072
-0.07	-0.088	-0.014	-0.02	-0.051	-0.037	-0.027	-0.042	-0.076	-0.037
-0.075	-0.163	-0.046	-0.06	-0.095	-0.092	-0.076	-0.08	-0.169	-0.089
-0.173	-0.346	-0.267	-0.267	-0.299	-0.286	-0.279	-0.286	-0.422	-0.243
-0.339	-0.509	-0.378	-0.44	-0.486	-0.452	-0.449	-0.466	-0.615	-0.397
-0.766	-0.882	-0.813	-0.885	-0.992	-0.937	-0.932	-0.935	-1.047	-0.911
-1.829	-1.825	-1.923	-1.98	0.29	0.422	0.507	0.466	0.464	0.286
-1.825	-1.757	-1.87	-1.892	-2.053	-2.006	-1.97	-2.038	-1.996	-1.933
-0.419	-0.399	-0.35	-0.398	-0.484	-0.457	-0.419	-0.476	-0.534	-0.376
-0.182	-0.218	-0.159	-0.194	-0.277	-0.244	-0.232	-0.256	-0.307	-0.187
-0.089	-0.13	-0.064	-0.079	-0.138	-0.107	-0.095	-0.11	-0.155	-0.091
0.042	0.031	0.092	0.079	0.042	0.046	0.059	0.056	0.019	0.085
0.082	0.072	0.126	0.132	0.118	0.129	0.154	0.141	0.092	0.15
0.144	0.12	0.173	0.188	0.198	0.207	0.225	0.219	0.155	0.225
-0.391	-0.392	-0.456	-0.468	-0.574	-0.562	-0.482	-0.568	-0.46	-0.445
-0.336	-0.344	-0.329	-0.345	-0.301	-0.395	-0.223	-0.33	-0.165	-0.237
-0.322	-0.362	-0.21	-0.206	-0.01	-0.208	0.03	-0.139	0.016	-0.064
-0.373	-0.343	-0.167	-0.17	0.035	-0.171	0.099	-0.087	0.065	-0.033
-0.364	-0.36	-0.262	-0.255	-0.143	-0.291	-0.045	-0.212	-0.069	-0.146
-0.365	-0.352	-0.409	-0.392	-0.417	-0.453	-0.316	-0.431	-0.269	-0.338
-0.502	-0.506	-0.565	-0.565	-0.661	-0.626	-0.586	-0.653	-0.57	-0.51
0.363	0.354	0.424	0.431	0.465	0.492	0.512	0.501	0.407	0.422
0.303	0.297	0.35	0.379	0.402	0.43	0.442	0.445	0.367	0.377

Table B2: (continued)

0.194	0.18	0.24	0.254	0.272	0.292	0.289	0.305	0.266	0.26
0.116	0.072	0.158	0.176	0.19	0.214	0.197	0.212	0.176	0.179
-0.017	-0.079	0.011	0.017	0.044	0.071	0.045	0.059	0.024	0.073
-0.152	-0.198	-0.115	-0.106	-0.062	-0.06	-0.063	-0.086	-0.112	-0.017
-1.283	-1.291	-1.364	-1.349	-1.365	-1.373	-1.324	-1.399	-1.334	-1.297
-1.764	-1.681	-1.854	-1.908	-1.963	-1.904	-2.018	-1.873	-1.895	-1.992
-1.864	-1.79	-1.966	-2.002	-1.994	-1.937	-1.97	-1.886	-1.911	-2.065
-2.16	-2.152	-2.251	-2.267	-2.338	-2.253	-2.281	-2.238	-2.299	-2.243
-2.268	-2.25	-2.399	-2.442	-2.542	-2.488	-2.492	-2.478	-2.452	-2.487
-2.251	-2.238	-2.393	-2.441	-2.549	-2.523	-2.532	-2.517	-2.437	-2.534
-2.195	-2.189	-2.36	-2.404	-2.524	-2.521	-2.529	-2.519	-2.359	-2.526
-2.133	-2.127	-2.275	-2.296	-2.389	-2.38	-2.375	-2.37	-2.32	-2.383
-2.067	-2.052	-2.17	-2.186	-2.25	-2.21	-2.2	-2.19	-2.183	-2.212
-1.82	-1.775	-1.893	-1.926	-1.955	-1.926	-1.977	-1.901	-1.903	-1.973
-2.117	-2.091	-2.234	-2.291	-2.436	-2.388	-2.459	-2.378	-2.368	-2.387
-1.65	-1.644	-1.719	-1.76	-1.921	-1.883	-1.876	-1.9	-1.875	-1.848
-1.763	-1.712	-1.824	-1.829	-1.991	-1.953	-1.945	-1.975	-1.925	-1.926
-1.886	-1.83	-1.965	-1.976	-2.151	-2.128	-2.119	-2.136	-2.049	-2.079
-1.862	-1.797	-1.941	-1.955	-2.13	-2.109	-2.103	-2.111	-2.006	-2.052
-1.839	-1.776	-1.923	-1.936	-2.106	-2.084	-2.086	-2.089	-1.988	-2.024
-1.836	-1.773	-1.918	-1.929	-2.096	-2.076	-2.078	-2.083	-1.986	-2.014
-1.854	-1.802	-1.931	-1.928	-2.073	-2.043	-2.051	-2.054	-1.993	-1.989
-1.399	-1.415	-1.477	-1.483	-1.521	-1.516	-1.524	-1.52	-1.491	-1.505
-2.073	-1.993	-2.109	-2.125	-2.259	-2.221	-2.177	-2.263	-2.189	-2.091
-2.064	-2.029	-2.124	-2.188	-2.372	-2.319	-2.225	-2.329	-2.225	-2.148

Table B3: Measured deviation values of cutlery drainer produced by using surface insert

Sn1	Sn2	Sn3	Sn4	Sn5	Sn6	Sn7	Sn8	Sn9	Sn10
-0.649	-0.577	-0.634	-0.57	-0.498	-0.384	-0.629	-0.39	-0.472	-0.505
-0.101	-0.118	-0.037	-0.001	0.025	-0.965	0.032	0.12	0.131	0.12

Table B3: (continued)

-0.971	-0.969	-0.998	-0.999	-1.04	-0.039	-1.023	-0.948	-0.967	-0.985
0.052	0.062	0.032	-0.059	-0.019	0.725	-0.013	0.036	0.07	0.091
-0.41	-0.328	-0.53	-0.469	-0.546	-0.832	-0.567	-0.365	-0.507	-0.494
-0.814	-0.845	-0.875	-0.921	-0.886	-0.718	-0.87	-0.753	-0.881	-0.874
-0.598	-0.659	-0.687	-0.761	-0.69	-0.075	-0.675	-0.697	-0.69	-0.696
-0.005	0.038	-0.127	-0.161	-0.136	0.351	-0.145	-0.1	-0.097	-0.095
0.077	0.092	-0.002	-0.109	0.009	-0.731	-0.01	0.096	0.013	0.081
-0.61	-0.711	-0.691	-0.782	-0.653	-0.781	-0.663	-0.542	-0.657	-0.63
-0.787	-0.817	-0.848	-0.819	-0.804	0.233	-0.805	-0.674	-0.719	-0.742
-0.409	-0.392	-0.404	-0.407	-0.341	-0.482	-0.357	-0.309	-0.325	-0.337
-0.613	-0.584	-0.604	-0.577	-0.628	-0.613	-0.616	-0.518	-0.519	-0.561
-0.717	-0.675	-0.723	-0.674	-0.708	-1.228	-0.766	-0.529	-0.646	-0.656
-0.851	-0.835	-0.946	-1.023	-1.002	-1.148	-0.994	-0.941	-1.002	-0.98
-0.996	-1.035	-1.092	-1.13	-1.141	-0.616	-1.159	-1.131	-1.122	-1.121
-0.556	-0.581	-0.661	-0.652	-0.634	-0.813	-0.633	-0.557	-0.586	-0.588
-0.468	-0.504	-0.544	-0.587	-0.548	-1.231	-0.528	-0.52	-0.497	-0.505
-1.179	-1.282	-1.141	-1.19	-1.129	-1.347	-1.206	-1.103	-1.069	-1.122
-1.275	-1.37	-1.321	-1.299	-1.366	-1.3	-1.377	-1.211	-1.231	-1.286
-1.283	-1.267	-1.301	-1.267	-1.291	-1.293	-1.298	-1.17	-1.206	-1.18
-1.205	-1.211	-1.329	-1.211	-1.374	-1.466	-1.399	-1.125	-1.18	-1.172
-1.309	-1.257	-1.471	-1.27	-1.57	-1.653	-1.631	-1.207	-1.313	-1.303
-1.568	-1.468	-1.709	-1.49	-1.767	-1.507	-1.826	-1.45	-1.56	-1.527
-1.414	-1.368	-1.527	-1.41	-1.583	-1.233	-1.618	-1.338	-1.433	-1.379
-1.159	-1.129	-1.207	-1.17	-1.257	-1.055	-1.266	-1.075	-1.159	-1.094
-0.801	-0.832	-0.842	-0.803	-0.819	-0.811	-0.814	-0.742	-0.732	-0.76
-0.785	-0.825	-0.838	-0.809	-0.815	-0.786	-0.821	-0.727	-0.752	-0.743
-0.743	-0.769	-0.807	-0.763	-0.788	-0.876	-0.802	-0.667	-0.74	-0.684
-0.829	-0.848	-0.892	-0.839	-0.877	-0.897	-0.893	-0.758	-0.837	-0.769
-0.853	-0.871	-0.91	-0.864	-0.898	-0.9	-0.908	-0.799	-0.854	-0.81

Table B3: (continued)

-0.886	-0.909	-0.909	-0.9	-0.891	-0.585	-0.883	-0.82	-0.828	-0.828
0.346	0.407	0.543	0.649	0.719	0.799	0.721	0.659	0.666	0.57
0.914	0.892	1.112	1.165	1.342	1.324	1.343	1.166	1.189	1.102
0.956	0.999	1.139	1.196	1.339	1.334	1.335	1.15	1.244	1.189
1.002	0.963	1.173	1.219	1.334	1.274	1.321	1.141	1.224	1.115
1.045	1.005	1.2	1.187	1.329	1.224	1.305	1.133	1.2	1.174
1.085	1.01	1.214	1.141	1.302	1.214	1.289	1.129	1.154	1.145
1.134	1.052	1.257	1.146	1.307	1.16	1.311	1.158	1.166	1.161
1.187	1.075	1.274	1.109	1.308	1.225	1.285	1.13	1.122	1.125
1.293	1.173	1.358	1.193	1.364	1.174	1.354	1.236	1.252	1.269
1.306	1.175	1.333	1.158	1.314	1.11	1.312	1.231	1.233	1.28
1.262	1.145	1.276	1.115	1.256	0.692	1.256	1.194	1.197	1.24
0.69	0.669	0.747	0.695	0.72	0.263	0.715	0.72	0.717	0.676
-0.371	-0.253	-0.498	-0.422	-0.375	-0.183	-0.399	-0.125	-0.14	-0.309
-0.214	-0.062	-0.468	-0.394	-0.355	-0.135	-0.38	-0.113	-0.112	-0.266
-0.249	-0.122	-0.388	-0.358	-0.272	-0.239	-0.326	-0.1	-0.014	-0.16
-0.614	-0.419	-0.593	-0.693	-0.453	-0.623	-0.46	-0.215	-0.122	-0.286
-0.765	-0.648	-0.696	-0.999	-0.686	-1.065	-0.638	-0.65	-0.778	-0.636
-0.736	-0.62	-0.82	-0.948	-0.951	1.193	-0.994	-0.945	-0.996	-0.92
0.342	0.356	0.692	0.516	1.048	0.897	1.166	0.607	0.812	0.856
0.355	0.348	0.544	0.544	0.714	0.569	0.784	0.555	0.675	0.686
-0.061	-0.265	0.258	-0.069	0.676	0.521	0.878	0.055	0.372	0.224
0.247	0.202	0.32	0.297	0.537	0.677	0.634	0.368	0.655	0.538
0.576	0.689	0.549	0.566	0.634	0.828	0.678	0.632	0.791	0.726
0.761	0.899	0.72	0.727	0.769	0.725	0.769	0.806	0.902	0.835
0.646	0.758	0.648	0.655	0.676	0.504	0.687	0.814	0.851	0.804
0.441	0.553	0.44	0.5	0.443	0.431	0.477	0.615	0.623	0.616
0.201	0.041	0.36	0.116	0.549	0.604	0.536	0.346	0.483	0.437
0.292	0.154	0.502	0.301	0.719	0.285	0.727	0.473	0.618	0.544

Table B3: (continued)

0.01	-0.08	0.209	0.136	0.432	-0.03	0.497	0.046	0.331	0.193
-0.247	-0.346	-0.052	-0.129	0.187	0.124	0.352	-0.505	0.045	-0.328
0.113	0.079	0.241	0.211	0.293	-0.85	0.363	0.022	0.327	0.075
-0.814	-0.837	-0.876	-0.826	-0.85	-0.269	-0.869	-0.726	-0.814	-0.75
-0.362	-0.308	-0.413	-0.437	-0.422	-0.47	-0.433	-0.379	-0.394	-0.377
-0.454	-0.312	-0.446	-0.613	-0.651	-0.546	-0.591	-0.579	-0.477	-0.732
-0.485	-0.4	-0.496	-0.59	-0.61	-0.512	-0.652	-0.599	-0.547	-0.573
-0.491	-0.431	-0.489	-0.55	-0.536	-0.784	-0.598	-0.474	-0.433	-0.445
-0.767	-0.723	-0.782	-0.817	-0.782	-1.215	-0.84	-0.671	-0.6	-0.647
-1.157	-1.061	-1.226	-1.131	-1.262	0.843	-1.259	-1.134	-1.051	-1.096
1.374	1.261	1.419	1.285	1.474	1.449	1.487	1.442	1.472	1.425
1.422	1.361	1.492	1.395	1.53	1.374	1.535	1.511	1.506	1.488
1.343	1.314	1.437	1.357	1.466	1.179	1.46	1.446	1.427	1.413
1.196	1.11	1.292	1.2	1.333	1.17	1.314	1.344	1.302	1.324
1.187	1.117	1.308	1.226	1.33	-0.046	1.317	1.338	1.33	1.354
0.957	0.9	0.862	0.674	0.861	0.862	0.841	0.744	0.788	0.816
0.95	0.917	0.889	0.801	0.89	0.98	0.865	0.815	0.868	0.849
1.049	1.022	0.979	0.954	1.017	1.009	0.987	0.915	0.951	0.944
1.049	1.019	1.011	0.993	1.046	0.974	1.039	0.953	0.916	0.926
1.049	0.999	1.006	0.979	1.011	0.985	1.036	0.936	0.923	0.904
1.076	1.032	1.027	0.995	1.035	1.024	1.016	0.958	0.901	0.899
1.107	1.042	1.111	1.048	1.115	0.81	1.132	1.05	1.007	0.998
0.885	0.827	0.917	0.824	0.924	0.545	0.937	0.892	0.835	0.834
0.284	0.235	0.254	0.207	0.259	0.324	0.247	0.211	0.236	0.206
0.433	0.358	0.373	0.305	0.383	0.376	0.378	0.321	0.358	0.321
0.524	0.444	0.418	0.335	0.426	0.336	0.412	0.377	0.379	0.36
0.476	0.385	0.354	0.267	0.377	0.355	0.375	0.321	0.344	0.308
0.467	0.373	0.313	0.251	0.369	0.387	0.364	0.308	0.302	0.285
0.512	0.395	0.341	0.255	0.379	0.386	0.35	0.31	0.322	0.315

Table B3: (continued)

0.402	0.368	0.249	0.249	0.268	0.442	0.233	0.256	0.207	0.195
0.421	0.454	0.242	0.237	0.232	-0.316	0.201	0.311	0.18	0.189
0.461	0.552	0.284	0.235	0.292	0.349	0.268	0.313	0.372	0.359
0.493	0.457	0.338	0.254	0.373	0.469	0.338	0.351	0.402	0.396
0.607	0.525	0.476	0.452	0.503	0.348	0.496	0.531	0.554	0.55
0.525	0.444	0.399	0.348	0.407	0.421	0.393	0.403	0.422	0.405
0.493	0.437	0.471	0.415	0.495	0.346	0.491	0.495	0.451	0.397
0.358	0.322	0.357	0.336	0.371	0.254	0.355	0.363	0.325	0.276
0.255	0.219	0.253	0.24	0.263	0.847	0.253	0.239	0.251	0.207
0.676	0.683	0.724	0.694	0.734	0.915	0.735	0.702	0.671	0.642
0.866	0.889	0.899	0.925	0.905	0.858	0.888	0.884	0.802	0.746
0.873	0.897	0.829	0.833	0.834	0.88	0.801	0.808	0.777	0.755
0.916	0.899	0.848	0.851	0.874	0.82	0.86	0.84	0.822	0.806
0.865	0.873	0.779	0.739	0.811	0.573	0.793	0.806	0.798	0.806
0.707	0.783	0.574	0.473	0.601	0.379	0.581	0.611	0.629	0.648
0.557	0.585	0.46	0.295	0.456	-0.038	0.445	0.499	0.441	0.498
0.315	0.303	0.224	0.16	0.29	0.421	0.289	0.359	0.293	0.346
0.55	0.508	0.472	0.402	0.488	0.683	0.494	0.519	0.475	0.508
0.692	0.699	0.661	0.665	0.682	0.754	0.691	0.717	0.696	0.705
0.738	0.714	0.734	0.731	0.766	0.792	0.78	0.751	0.726	0.728
0.738	0.716	0.765	0.745	0.815	0.741	0.808	0.794	0.805	0.776
0.676	0.658	0.721	0.686	0.768	0.85	0.785	0.744	0.746	0.742
0.759	0.732	0.751	0.718	0.799	0.719	0.789	0.786	0.821	0.776
0.761	0.73	0.747	0.7	0.783	0.679	0.778	0.754	0.791	0.752
0.769	0.725	0.751	0.684	0.77	0.518	0.771	0.734	0.766	0.76
0.59	0.566	0.587	0.548	0.603	0.38	0.612	0.568	0.636	0.643
0.506	0.48	0.493	0.432	0.486	0.237	0.481	0.407	0.499	0.479
0.248	0.28	0.255	0.234	0.274	-0.356	0.257	0.243	0.299	0.314
0.275	0.312	0.316	0.275	0.254	-0.085	0.312	0.138	0.288	0.14

Table B3: (continued)

-0.021	0.003	-0.01	-0.076	-0.015	-0.19	0.026	-0.197	-0.03	-0.087
-0.082	-0.109	-0.066	-0.182	-0.105	0.066	-0.068	-0.14	-0.082	0.001
0.174	0.132	0.233	0.128	0.115	0.491	0.132	0.176	0.194	0.251
0.53	0.501	0.546	0.467	0.498	-0.157	0.502	0.56	0.56	0.547
0.587	0.561	0.642	0.578	0.567	0.196	0.565	0.615	0.642	0.655
0.319	0.263	0.375	0.263	0.293	-0.103	0.293	0.121	0.278	0.288
0.019	0.006	0.033	-0.036	-0.063	0.012	0.024	-0.219	-0.034	-0.068
0.017	0.093	0.046	0.009	-0.02	0.399	0.053	-0.103	0.041	0.039
0.352	0.387	0.409	0.386	0.345	0.686	0.382	0.367	0.408	0.49
0.647	0.669	0.683	0.685	0.646	0.207	0.653	0.756	0.753	0.788
0.505	0.433	0.512	0.471	0.479	0.108	0.457	0.53	0.396	0.443
0.481	0.437	0.467	0.502	0.237	0.088	0.171	0.52	0.044	0.245
0.529	0.518	0.478	0.553	0.217	0.503	0.177	0.51	0.078	0.23
0.62	0.596	0.611	0.592	0.583	0.455	0.582	0.63	0.574	0.572
0.808	0.784	0.835	0.787	0.854	0.699	0.871	0.85	0.917	0.903
0.677	0.729	0.701	0.722	0.71	0.24	0.754	0.641	0.699	0.652
0.559	0.581	0.502	0.557	0.299	0.096	0.325	0.458	0.252	0.279
0.487	0.482	0.448	0.524	0.209	0.281	0.178	0.544	0.052	0.241
0.541	0.559	0.472	0.549	0.322	0.563	0.357	0.367	0.262	0.269
0.565	0.605	0.564	0.638	0.613	0.762	0.634	0.477	0.611	0.502
0.714	0.679	0.734	0.701	0.785	0.703	0.791	0.799	0.839	0.805
0.554	0.553	0.629	0.612	0.832	0.611	0.807	0.715	0.714	0.68
0.301	0.303	0.427	0.388	0.603	0.582	0.539	0.356	0.382	0.334
0.315	0.369	0.409	0.439	0.523	0.543	0.512	0.31	0.388	0.292
0.3	0.32	0.362	0.411	0.481	0.634	0.478	0.362	0.385	0.328
0.465	0.456	0.522	0.544	0.666	1.371	0.658	0.648	0.625	0.606
0.576	0.545	0.606	0.623	0.698	0.669	0.713	0.767	0.729	0.691
0.451	0.445	0.516	0.498	0.633	0.563	0.616	0.594	0.561	0.515
0.334	0.333	0.378	0.444	0.503	0.56	0.465	0.361	0.385	0.341

Table B3: (continued)

0.31	0.307	0.378	0.359	0.526	0.654	0.487	0.332	0.376	0.305
0.42	0.439	0.481	0.473	0.624	0.762	0.608	0.436	0.512	0.441
0.54	0.568	0.623	0.597	0.747	0.756	0.789	0.652	0.695	0.63
0.594	0.596	0.652	0.648	0.726	0.775	0.754	0.736	0.771	0.731
Sn11	Sn12	Sn13	Sn14	Sn15	Sn16	Sn17	Sn18	Sn19	Sn20
-0.531	-0.593	-0.562	-0.564	-0.621	-0.628	-0.66	-0.693	-0.792	-0.748
-0.033	-0.005	-0.036	0.022	0.023	0.04	0.029	0.013	0.06	-0.073
-1.022	-0.994	-1.028	-1.062	-1.057	-1.045	-1.1	-1.135	-1.216	-1.127
0.062	0.01	0.055	0.035	0.057	0.035	0.027	0.005	-0.057	0.098
-0.498	-0.468	-0.502	-0.498	-0.523	-0.515	-0.577	-0.602	-0.639	-0.457
-0.884	-0.868	-0.912	-0.887	-0.961	-0.964	-0.998	-1.076	-1.12	-0.981
-0.678	-0.714	-0.757	-0.73	-0.723	-0.757	-0.8	-0.85	-0.813	-0.732
-0.08	-0.13	-0.136	-0.186	-0.086	-0.129	-0.146	-0.184	-0.142	0.04
0.084	-0.041	0.04	-0.022	0.087	0.005	0.069	-0.073	0.035	0.269
-0.595	-0.728	-0.732	-0.689	-0.709	-0.759	-0.732	-0.856	-0.812	-0.618
-0.783	-0.815	-0.865	-0.848	-0.82	-0.84	-0.849	-0.879	-0.921	-0.898
-0.301	-0.41	-0.375	-0.403	-0.312	-0.322	-0.328	-0.298	-0.403	-0.353
-0.583	-0.594	-0.606	-0.619	-0.656	-0.628	-0.692	-0.703	-0.825	-0.747
-0.661	-0.703	-0.692	-0.699	-0.779	-0.787	-0.792	-0.868	-0.94	-0.855
-0.908	-0.916	-0.998	-0.957	-1.018	-1.064	-1.115	-1.198	-1.163	-0.989
-1.114	-1.094	-1.166	-1.159	-1.186	-1.201	-1.247	-1.336	-1.317	-1.174
-0.599	-0.64	-0.683	-0.66	-0.647	-0.672	-0.683	-0.754	-0.728	-0.663
-0.499	-0.549	-0.578	-0.559	-0.531	-0.561	-0.59	-0.629	-0.624	-0.547
-1.142	-1.187	-1.112	-1.088	-1.072	-1.138	-1.037	-1.152	-1.184	-1.267
-1.205	-1.258	-1.207	-1.157	-1.314	-1.213	-1.321	-1.208	-1.392	-1.391
-1.206	-1.241	-1.237	-1.235	-1.218	-1.264	-1.284	-1.38	-1.293	-1.317
-1.168	-1.16	-1.236	-1.146	-1.231	-1.289	-1.288	-1.359	-1.283	-1.341
-1.224	-1.192	-1.356	-1.238	-1.408	-1.492	-1.478	-1.512	-1.484	-1.475
-1.386	-1.45	-1.579	-1.501	-1.631	-1.71	-1.71	-1.727	-1.744	-1.717

Table B3: (continued)

-1.285	-1.346	-1.409	-1.347	-1.417	-1.475	-1.473	-1.58	-1.513	-1.487
-1.054	-1.114	-1.131	-1.117	-1.127	-1.169	-1.185	-1.314	-1.206	-1.19
-0.783	-0.785	-0.856	-0.774	-0.828	-0.851	-0.859	-0.911	-0.842	-0.919
-0.78	-0.772	-0.842	-0.713	-0.783	-0.797	-0.809	-0.86	-0.792	-0.859
-0.724	-0.724	-0.804	-0.669	-0.755	-0.767	-0.784	-0.827	-0.736	-0.816
-0.767	-0.796	-0.873	-0.761	-0.833	-0.845	-0.862	-0.911	-0.808	-0.89
-0.783	-0.818	-0.892	-0.791	-0.847	-0.861	-0.875	-0.926	-0.829	-0.912
-0.819	-0.859	-0.899	-0.845	-0.847	-0.86	-0.877	-0.933	-0.863	-0.923
0.491	0.527	0.655	0.707	0.655	0.568	0.682	0.559	0.687	0.449
0.997	1.053	1.174	1.214	1.185	1.098	1.223	1.106	1.245	0.981
1.035	1.137	1.204	1.237	1.19	1.197	1.213	1.162	1.217	1.016
1.018	1.113	1.16	1.225	1.152	1.134	1.161	1.136	1.17	1.007
1.048	1.139	1.172	1.23	1.191	1.181	1.198	1.176	1.205	1.076
1.01	1.116	1.124	1.176	1.148	1.139	1.149	1.134	1.162	1.063
1.045	1.13	1.147	1.173	1.155	1.153	1.154	1.145	1.174	1.098
1.052	1.113	1.14	1.095	1.146	1.087	1.101	1.08	1.131	1.13
1.115	1.201	1.208	1.187	1.211	1.229	1.223	1.209	1.26	1.233
1.089	1.171	1.166	1.153	1.175	1.242	1.205	1.188	1.247	1.228
1.038	1.124	1.119	1.121	1.13	1.214	1.162	1.138	1.216	1.19
0.738	0.658	0.693	0.725	0.747	0.665	0.677	0.62	0.66	0.676
-0.342	-0.417	-0.271	-0.314	-0.258	-0.426	-0.279	-0.504	-0.591	-0.479
-0.287	-0.44	-0.224	-0.362	-0.269	-0.345	-0.324	-0.402	-0.516	-0.388
-0.264	-0.38	-0.152	-0.259	-0.138	-0.22	-0.236	-0.34	-0.324	-0.357
-0.471	-0.646	-0.255	-0.59	-0.214	-0.292	-0.27	-0.372	-0.449	-0.463
-0.716	-0.887	-0.538	-1.017	-0.524	-0.618	-0.513	-0.847	-0.8	-0.61
-0.792	-0.786	-0.793	-0.857	-0.769	-0.853	-0.819	-1.005	-0.875	-0.713
0.508	0.516	0.886	0.5	1.071	1.229	1.2	1.132	0.961	0.819
0.436	0.593	0.645	0.644	0.851	0.991	0.905	0.87	0.924	0.765
-0.065	-0.076	0.39	-0.056	0.576	0.734	0.738	0.897	0.442	0.061

Table B3: (continued)

0.37	0.286	0.517	0.367	0.625	0.692	0.671	0.835	0.722	0.313
0.736	0.592	0.748	0.542	0.763	0.709	0.773	0.817	0.742	0.704
0.913	0.769	0.87	0.679	0.938	0.772	0.897	0.837	0.782	0.91
0.868	0.712	0.777	0.703	0.881	0.735	0.86	0.724	0.727	0.793
0.687	0.555	0.572	0.584	0.664	0.58	0.672	0.542	0.564	0.597
0.17	0.162	0.32	0.119	0.405	0.325	0.318	0.287	0.346	0.337
0.371	0.327	0.523	0.254	0.644	0.508	0.527	0.469	0.479	0.533
0.215	0.138	0.296	0.003	0.419	0.332	0.34	0.306	0.172	0.336
-0.029	-0.117	0.022	-0.262	0.123	0.073	0.108	0.21	-0.204	0.006
0.188	0.171	0.216	0.113	0.215	0.225	0.221	0.296	0.16	0.153
-0.739	-0.783	-0.849	-0.738	-0.82	-0.831	-0.842	-0.894	-0.788	-0.875
-0.417	-0.394	-0.412	-0.424	-0.344	-0.356	-0.357	-0.476	-0.474	-0.361
-0.488	-0.535	-0.512	-0.589	-0.541	-0.672	-0.472	-0.377	-0.915	-0.922
-0.47	-0.536	-0.442	-0.602	-0.582	-0.63	-0.586	-0.47	-0.655	-0.597
-0.478	-0.529	-0.424	-0.606	-0.424	-0.511	-0.539	-0.623	-0.557	-0.429
-0.707	-0.744	-0.715	-0.791	-0.612	-0.659	-0.737	-0.875	-0.721	-0.611
-1.12	-1.131	-1.102	-1.163	-1.042	-1.088	-1.16	-1.31	-1.088	-1.035
1.237	1.307	1.247	1.357	1.326	1.398	1.402	1.394	1.354	1.248
1.309	1.398	1.351	1.425	1.409	1.453	1.427	1.393	1.424	1.294
1.266	1.339	1.307	1.371	1.348	1.396	1.34	1.289	1.372	1.212
1.15	1.171	1.171	1.185	1.195	1.209	1.192	1.126	1.214	1.087
1.212	1.207	1.227	1.207	1.248	1.23	1.254	1.181	1.261	1.161
0.912	0.793	0.845	0.786	0.839	0.788	0.835	0.807	0.785	1.066
0.847	0.784	0.822	0.768	0.831	0.807	0.83	0.801	0.794	1.016
0.984	0.957	0.968	0.938	0.957	0.966	0.981	0.921	0.995	1.095
0.99	0.967	0.967	0.956	0.963	0.94	0.959	0.925	0.959	1.102
0.955	0.952	0.939	0.944	0.958	0.931	0.958	0.925	0.951	1.038
0.975	0.96	0.961	0.944	0.97	0.915	0.935	0.907	0.94	1.039
1.012	1.019	1.017	1.032	1.044	1.014	1.034	1.005	1.023	1.077

Table B3: (continued)

0.812	0.82	0.836	0.849	0.869	0.836	0.85	0.799	0.842	0.862
0.168	0.211	0.197	0.199	0.221	0.187	0.154	0.124	0.187	0.156
0.297	0.314	0.324	0.293	0.332	0.287	0.274	0.261	0.292	0.319
0.382	0.337	0.393	0.307	0.371	0.316	0.301	0.286	0.337	0.411
0.318	0.271	0.326	0.258	0.318	0.275	0.269	0.252	0.277	0.37
0.289	0.233	0.31	0.218	0.29	0.242	0.243	0.198	0.246	0.399
0.279	0.249	0.301	0.235	0.286	0.268	0.264	0.205	0.278	0.425
0.191	0.181	0.165	0.156	0.167	0.158	0.131	0.107	0.131	0.346
0.291	0.238	0.188	0.2	0.225	0.183	0.167	0.179	0.191	0.461
0.284	0.248	0.299	0.173	0.296	0.265	0.272	0.277	0.218	0.491
0.297	0.259	0.351	0.218	0.315	0.279	0.298	0.305	0.242	0.435
0.508	0.46	0.503	0.468	0.494	0.478	0.487	0.418	0.452	0.552
0.383	0.351	0.373	0.34	0.371	0.341	0.349	0.315	0.335	0.438
0.442	0.408	0.433	0.44	0.458	0.349	0.419	0.313	0.35	0.398
0.328	0.303	0.319	0.315	0.337	0.238	0.3	0.205	0.245	0.313
0.191	0.202	0.212	0.201	0.23	0.159	0.22	0.134	0.171	0.229
0.699	0.678	0.684	0.699	0.69	0.65	0.638	0.642	0.652	0.686
0.916	0.892	0.89	0.904	0.898	0.767	0.832	0.758	0.768	0.816
0.81	0.8	0.803	0.803	0.802	0.761	0.768	0.73	0.772	0.813
0.828	0.832	0.835	0.821	0.834	0.817	0.796	0.771	0.826	0.867
0.75	0.718	0.801	0.724	0.756	0.764	0.722	0.716	0.753	0.819
0.537	0.465	0.582	0.456	0.551	0.523	0.52	0.512	0.489	0.718
0.487	0.376	0.483	0.372	0.509	0.411	0.486	0.357	0.422	0.719
0.266	0.195	0.287	0.181	0.28	0.22	0.273	0.248	0.261	0.379
0.415	0.393	0.447	0.381	0.407	0.392	0.38	0.375	0.397	0.473
0.631	0.642	0.653	0.661	0.636	0.675	0.624	0.607	0.677	0.657
0.693	0.705	0.711	0.72	0.713	0.718	0.695	0.688	0.726	0.695
0.718	0.733	0.74	0.773	0.765	0.78	0.775	0.781	0.77	0.722
0.658	0.672	0.691	0.704	0.725	0.737	0.733	0.776	0.715	0.678

Table B3: (continued)

0.697	0.714	0.715	0.737	0.746	0.73	0.768	0.712	0.703	0.688
0.696	0.684	0.703	0.713	0.724	0.704	0.737	0.706	0.704	0.703
0.698	0.688	0.71	0.698	0.721	0.697	0.712	0.684	0.707	0.731
0.531	0.534	0.557	0.532	0.547	0.57	0.549	0.521	0.579	0.562
0.404	0.4	0.439	0.374	0.418	0.409	0.404	0.394	0.419	0.475
0.253	0.238	0.295	0.201	0.314	0.303	0.316	0.333	0.302	0.374
0.377	0.213	0.318	0.281	0.321	0.239	0.31	0.482	0.542	0.475
0.039	-0.064	-0.044	-0.091	0.016	-0.002	0.082	0.32	0.366	0.238
-0.097	-0.079	-0.088	-0.238	-0.035	0.055	0.069	0.274	0.234	0.164
0.17	0.15	0.233	0.037	0.218	0.31	0.293	0.476	0.363	0.336
0.503	0.497	0.547	0.455	0.559	0.538	0.573	0.559	0.536	0.496
0.605	0.575	0.623	0.585	0.675	0.665	0.673	0.662	0.703	0.708
0.32	0.238	0.355	0.207	0.322	0.359	0.349	0.562	0.58	0.516
0.104	-0.055	0.043	-0.066	0.022	0.009	0.077	0.345	0.406	0.289
0.146	-0.022	0.06	0.007	0.07	0.044	0.129	0.397	0.38	0.378
0.447	0.336	0.451	0.304	0.417	0.44	0.444	0.678	0.592	0.668
0.707	0.643	0.69	0.649	0.722	0.741	0.749	0.762	0.732	0.794
0.43	0.499	0.48	0.497	0.464	0.547	0.462	0.474	0.459	0.474
0.238	0.54	0.411	0.497	0.305	0.545	0.36	0.46	0.308	0.415
0.299	0.577	0.407	0.535	0.298	0.456	0.387	0.472	0.315	0.429
0.586	0.61	0.562	0.621	0.576	0.597	0.584	0.547	0.572	0.564
0.817	0.791	0.839	0.796	0.846	0.878	0.859	0.815	0.855	0.82
0.639	0.65	0.743	0.687	0.638	0.663	0.646	0.669	0.677	0.686
0.325	0.498	0.439	0.535	0.292	0.449	0.363	0.444	0.363	0.416
0.225	0.547	0.406	0.496	0.28	0.499	0.38	0.476	0.296	0.426
0.323	0.528	0.429	0.511	0.368	0.48	0.394	0.464	0.36	0.443
0.551	0.558	0.607	0.608	0.574	0.609	0.567	0.549	0.564	0.559
0.745	0.713	0.751	0.761	0.78	0.78	0.771	0.712	0.781	0.733
0.658	0.572	0.662	0.591	0.679	0.671	0.788	0.804	0.676	0.655

Table B3: (continued)

0.46	0.327	0.459	0.368	0.341	0.344	0.523	0.524	0.389	0.368
0.518	0.315	0.457	0.382	0.417	0.309	0.485	0.499	0.421	0.373
0.516	0.31	0.482	0.353	0.382	0.301	0.427	0.478	0.37	0.353
0.629	0.505	0.583	0.488	0.576	0.557	0.573	0.554	0.546	0.513
0.679	0.596	0.654	0.6	0.655	0.648	0.662	0.656	0.626	0.625
0.557	0.465	0.544	0.485	0.499	0.495	0.557	0.599	0.483	0.493
0.475	0.338	0.464	0.369	0.43	0.353	0.41	0.479	0.358	0.37
0.461	0.28	0.4	0.335	0.347	0.29	0.378	0.516	0.312	0.358
0.555	0.408	0.526	0.451	0.467	0.458	0.507	0.582	0.475	0.474
0.685	0.567	0.646	0.589	0.646	0.635	0.653	0.686	0.657	0.618
0.707	0.63	0.688	0.641	0.728	0.735	0.726	0.728	0.712	0.677